

9 Doctoral thesis,

EMISSION CROSS-SECTION MEASUREMENTS
OF LOW ENERGY Het JONS WITH
C17. Br 7. 12 REACTIONS.

DISSERTATION

(14) DS/PH/76-2/(Kenneth E./S	Siegenthaler USAF
1 Sep 76	1 1334	12p.

NTIS DOC MILITIKO UNICED	White Section
JUSTIFICATION	
£Y	
	AVAILABILITY CODES

Approved for public release; distribution unlimited.

012225

EMISSION CROSS-SECTION MEASUREMENTS OF LOW ENERGY He IONS WITH Cl₂, Br₂, I₂ REACTIONS

DISSERTATION

Presented to the Faculty of the School of Engineering of the Air Force Institute of Technology

Air University
in Partial Fulfillment of the
Requirements for the Degree of
Doctor of Philosophy

by

Kenneth E. Siegenthaler, B.S., M.S.
Major USAF

August 1976 pee 1473

Approved for public release; distribution unlimited.

EMISSION CROSS-SECTION MEASUREMENTS OF LOW ENERGY He IONS WITH C12, Br2, I2 REACTIONS

by

Kenneth E. Siegenthaler, B.S., M.S.
Major USAF

Approved:

Deorge Chairman
Chairman
23 Maria

Robert J Hongholl 23 Aus 76

Ma Garanden. 23 Aug 76.

Emert a. Darko 24 Aug 76.

Accepted.

JSRzemieniecki Dean, School of Engineering

Preface

This dissertation was made possible by the generosity and cooperation of many people. I would like to first thank my wife, Phyllis, and son, John, for their understanding and encouragement during this period. I wish to express my gratitude to Dr. Thomas O. Tiernan for the opportunity to work in one of the finest research environments in the Air Force at the Aerospace Research Laboratories (ARL), Wright-Patterson AFB OH. Special thanks are due Dr. B. Mason Hughes for his advice and technical assistance, Mr. Dean Miller for his technical assistance, Dr. E. Grant Jones for his advice and encouragement, and Dr. Darrel Hopper for the use of his computer search program. Sincere thanks are given to my AFIT advisors, Dr. George John and Dr. Robert Hengehold, for their advice, encouragement and guidance.

I wish to thank the Air Force Materials Laboratory for providing me with support for my analysis of this research after the disestablishment of ARL. I thank Mr. John Dryen for his expert drawing of the figures in this dissertation. A final debt of gratitude is owed to Mrs. Jane Manemann for typing this dissertation.

Contents

Prefa	ce	•	٠	٠	٠	٠	٠	•		•	•	•			٠	•	•				٠	•		•	٠	٠	ii
List	of	Fi	gu	ıre	s	•		٠		•	•	•				•	•			•	٠	٠	•	•	•	•	v
List	of	Ta	ıb1	es	3	٠	•				•	•			•	٠	•			•	•	•	•			•	
Abstr	act	ŧ	•			•	٠	•			•	•			•		•				•	•	•	٠		٠	xii
ı.	Iı	ntı	od	luc	t	io	n			•	•					٠				•	•	•		٠	٠	٠	1
II.	E	сре	ri	me	n	ta	l	In	S	tr	un	ıe:	nt	a	ti	.01	n	aı	nd	c	al	i	br	at:	i 01	n	10
		E	mi	. 5 5	ii	on	C	ro	5	s	Se	c	ti	.0	ns												10
		A	ng	aı	- 21	tu	5																				13
		1	pp	06	+	G		S	v	e t	-																16
			100	6		C.		+ 0	7	•	-					•	•					•					16
			ac	·ut	1111	0	, 3		ш		•	•	_ •	-	٠.	:				•		•	•	•	•	•	
			ar																								20
			on																								21
			ns																								
		8	370	r	ım	R	ge	io	n																		28
		.1	/UV	1	n	st	ru	me	n	t	Ca	1	ib	r	at	i	on			•			٠				34
III.	E	сре	ri	m e	ent	ta	l i	Pr	0	ce	du	ır	es														41
		E	dim	101	le	cu	la	r-	R	ea	ct	i	OI		De	t	er	mi	in	at	ic	n					41
		E	mi	SS	i	n	W	av	e	le	nø	t	h	D	et	e	rm	ir	12	t i	OF						45
			ro																								
																											47
			ra	III S	. 1 .		.0	II &		E	пе		g 1	. 6	5	•	•			•	•	•	•	•	•	•	47
IV.	Da	ıta	A	na	11)	15	is	•				1													٠	٠	49
		1	in		Te	101	.+	i f	1	- 9	+ 1	0															51
			ur																								55
		E	rr	01	. 1	In	11	ys	1:	5	•								•				•			•	60
				Re	11	t	LV	e	Cı	ro	55		Se	C	ti	01	ns										61
				Ab)50	110	ıt	e	Cı	ro	55		Se	C	ti	01	n s			•					•	•	62
v.	CI	110	ri	ne	,																						63
		1	nt	T	di	101	· i	on																			63
	*		ре																	•							64
		-	ro	-			.:	.:	_	P	•	-	_:		'n.				_	:-							64
		,	TO	55		96	CL	10	n	C	ne	1	gy		иe	P	en	ae	n	Ce		·u	rv.	55			
			.in												•												72
		F	ur	th	1e1	. 1	An	al	y:	si	S	•					•			•	•		•	•	•	•	73
VI.	B1	on.	in	e	•					•					•	•	•			•	٠	•			•	•	86
					٠.																						86
			nt								•	•	•							•		•	•				
		S	pe	ct	T	1				•																	86

		Cr	os	s S	e	ct	ioi	1	En	er	gy	D	ер	enc	lei	nce	. (Cui	cve	95			86
		Li	ne	Id	e	nti	if:	LC	at:	io	n												99
		Fu	rt	her		Ana	a1;	y s	is	٠	٠	•		•	•	٠	•	٠	•	٠	٠	٠	100
VII.	Iod	lin	e	•	•		•	•	•	•	•	٠	·	•		٠		٠	٠	٠	٠	•	112
		In	tr	odu	ıc	tic	on																112
				tra																			112
		Cr	os	s S	e	ct:	io	n i	En	er	gy	D	ep	end	le	nce	3 (Cu	rve	95			112
				Id																			. 130
				her																			130
VIII.	Coi	ncl	us	ior	l .		•		٠	•	٠	٠	٠		•		•	•	•			•	134
Biblio	gra	aph	у		•	•	•	-					•	٠		•	٠	•	٠	٠	•	•	141
Append	lix	A	•	٠			٠	٠		•	•	•	٠	٠	٠	٠	٠				٠		147
Append	lix	В		•	٠	•			٠	٠	٠	٠	•	٠		•	٠		٠	•			181
Append	lix	С			•		٠				٠		٠		٠		•		٠	٠	٠	•	208
Vita																							285

List of Figures

Figure		Page
1	Typical Examples of Possible Potential Energy Curves in Charge Transfer Processes	5
2	Typical Example of Pseudo-Crossings of Potential Energy Curves in Charge Transfer Processes	7
3	Experimental Apparatus	14
4	Block Diagram of the Target Gas System .	18
5	Block Diagram of the Vacuum System	19
6	Configurations Used for Target Gas Pressure Calibration	22
7	Target Gas Pressure Calibration Using Air	23
8	Target Gas Pressure Calibration Using Xenon	24
9	Possible Ion Paths of Measured and Unmeasured Ions Available for Excitation of Atoms/Molecules in Collision Chamber .	26
10	The 400 nm to 870 nm Instrument Function $[F(\lambda)]$ Calibration Setup	29
11	Geometric Diagram of Monochromator	30
12	Instrument Function $[F(\lambda)]$ from 400 nm to 870 nm	35
13	VUV Instrument Function $[F(\lambda)]$ from 80 nm to 125 nm	37
14	VUV Instrument Function $[F(\lambda)]$ from 120 nm to 185 nm Using EMR LiF Window Detector	39
15	VUV Instrument Function $[F(\lambda)]$ from 120 nm to 185 nm Using EMR MgF ₂ Window Detector	40
16	Cl ₂ Target Gas Pressure Dependence	42
17.	Br 2 Target Gas Pressure Dependence	43

Figure		Page
18	I Target Gas Pressure Dependence	44
19	Computer Listing of Allowed Transitions Matching Observed Lines	53
20	Computer Listing of Allowed Transitions Matching Observed Lines Plus Other Allowed Transitions from the Same Upper Energy Levels	54
21	High Resolution Spectra of 100 eV He ⁺ Cl ₂	
	Reaction in 95 nm to 122 nm Region	65
22	Low Resolution Spectra of 100 eV He ⁺ Cl ₂ Reaction in 100 nm to 145 nm Region	66
23	High Resolution Spectra of 100 eV He +	
23	Cl ₂ Reaction in 117 nm to 140 nm Region .	67
24	High Resolution Spectra of 100 eV He + C1 ₂ Reaction in 720 nm to 795 nm Region .	68
25	High Resolution Spectra of 100 eV He^{\dagger} + Cl_2 Reaction in 795 nm to 865 nm Region .	69
26	The Energy Dependence of the Emission Cross Sections of Selected VUV Lines from	
	the He ⁺ + Cl ₂ Reaction	70
27	The Energy Dependence of the Emission Cross Sections of Selected Lines from the	
	He ⁺ + Cl ₂ Reaction	71
28	C1 I Term Diagram for 100 eV He ⁺ + C1 ₂ Reaction	78
29	Comparison of C1 I Emission Cross Sections and Direct Formation Cross	
	Sections as a Function of the Energy Levels of the Cl I Atom	82
30	High Resolution Spectra of 100 eV He ⁺ + Br ₂ Reaction in 85 nm to 159 nm Region .	87
31	Low Resolution Spectra of 100 eV He ⁺ + Br ₂ Reaction in 110 nm to 170 nm Region .	88
32	High Resolution Spectra of 100 eV He + + Br. Reaction in 130 nm to 160 nm Region .	89

Figure		Page
33	High Resolution Spectra of 100 eV He ⁺ + Br ₂ Reaction in 440 nm to 485 nm Region .	90
34	High Resolution Spectra of 100 eV He^+ + Br_2 Reaction in 630 nm to 755 nm Region .	91
35	High Resolution Spectra of 100 eV He + Br Reaction in 775 nm to 880 nm Region .	92
36	The Energy Dependence of the Emission Cross Sections of Selected VUV Lines from the He ⁺ + Br ₂ Reaction	93
37	The Energy Dependence of the Emission Cross Sections of the 447.5 nm and	
	478.2 nm Lines from the He ⁺ + Br ₂ Reaction	94
38	The Energy Dependence of the Emission Cross Sections of Selected Visible Lines	
	from the He ⁺ + Br ₂ Reaction	95
39	The Energy Dependence of the Emission Cross Sections of Selected Lines from the	
	He + Br ₂ Reaction	96
40	The Energy Dependence of the Emission Cross Section of the 827.3 nm Line from	
	the He ⁺ + Br ₂ Reaction	97
41	The Energy Dependence of the Emission Cross Sections of Selected Infrared Lines	
	from the He + Br 2 Reaction	98
42	Br I Term Diagram for 100 eV + Br 2 Reaction	104
43	Comparison of Br I Emission Cross Sections and Direct Formation Cross Sections as a Function of the Energy Levels of the Br I Atom	108
44	High Resolution Spectra of 100 eV He ⁺ + I ₂ Reaction in 98 nm to 124 nm Region	113
45	Low Resolution Spectra of 100 eV He + + I. Reaction in 110 nm to 190 nm Region .	114

Figure		Page
46	High Resolution Spectra of 100 eV He^+ + I_2 Reaction in 114 nm to 150 nm Region .	115
47	High Resolution Spectra of 100 eV He^+ + I_2 Reaction in 150 nm to 185 nm Region .	116
48	High Resolution Spectra of 100 eV He^+ + I_2 Reaction in 410 nm to 495 nm Region .	117
49	High Resolution Spectra of 100 eV He^+ + I_2 Reaction in 510 nm to 650 nm Region .	118
50	High Resolution Spectra of 100 eV He^+ + I_2 Reaction in 650 nm to 720 nm Region .	119
51	High Resolution Spectra of 100 eV He^+ + I_2 Reaction in 720 nm to 800 nm Region .	120
52	High Resolution Spectra of 100 eV He^+ + I_2 Reaction in 800 nm to 870 nm Region .	121
53	The Energy Dependence of the Emission Cross Sections of Selected VUV Lines from	122
54	the He ⁺ + I ₂ Reaction	122
	178.23 nm Lines from the He ⁺ + I ₂ Reaction	123
55	The Energy Dependence of the Emission Cross Section of the 145.78 nm Line from	
	the He ⁺ + I ₂ Reaction Using Various Detectors	124
56	The Energy Dependence of the Emission Cross Section of the 183.00 nm Line from	
	the He ⁺ + I ₂ Reaction Using Various Detectors	125
57	The Energy Dependence of the Emission Cross Sections of Selected Visible Lines	
58	from the He ⁺ + I ₂ Reaction	126
3.0	Cross Sections of Selected Lines from	127

Figure		Page
59	The Energy Dependence of the Emission Cross Sections of the 723.8 nm and	
	747.0 nm Lines from the He [†] + I ₂ Reaction	128
60	The Energy Dependence of the Emission Cross Sections of Selected Infrared Lines	
	from the He ⁺ + I ₂ Reaction	129
61	Comparison of the Energy Levels of the Halogen Atoms and Ions Available for Population Exclusively by the Energy	137
	Released in Thermal Charge Transfer	13/

List of Tables

Table		Page
Ι.	Symbols Used in the Derivation of the Emission Cross Section σ	11
II	Detector and Grating Combinations	17
111	Symbols Used in the Derivation of the Visible Instrument Function $F(\lambda)$	32
IV	Summary of 100 eV He ⁺ + Cl ₂ Reaction	
	Transitions Selected by the Computer Search Program	74
V	Cl I Transition Assignments for the	
	100 eV He ⁺ + Cl ₂ Reaction	75
VI	Emission and Cascading Cross Sections for	
	C1 I States Observed in the 100 eV He ⁺ + C1 ₂ Reactions	80
VII	Relative Transition Probabilities for Selected Cl I Transitions in the 700 nm to 870 nm Region	84
VIII	Summary of 100 eV He ⁺ + Br ₂ Reaction	
	Allowed Transitions Selected by the Computer Search Program	101
IX	Br I Transition Assignments for the 100 eV	
	He ⁺ + Br ₂ Reaction	102
x	Emission and Cascading Cross Sections for	
	Br I States Observed in 100 eV He + Br 2 Reaction	106
XI	Relative Transition Probabilities for Selected Br I Transitions in 700 nm to 870 nm Region	110
XII	Summary of 100 eV He ⁺ + I ₂ Reaction	
	Allowed Transitions Selected by the Computer Search Program	131

Table		Page
XIII	Summary of 100 eV He ⁺ /Halogen Emission Cross Sections	135
XIV	Summary of Results of 100 eV He ⁺ /Halogen Investigation in 60 nm to 870 nm Spectral Region	136
xv	Luminescence from the Reaction 100 eV $He^+ + Cl_2 \rightarrow He + Cl^+ + Cl + Energy$.	148
XVI	Luminescence from the Reaction 100 eV $He^+ + Br_2 \rightarrow He + Br^+ + Br + Energy$	182
XVII	Luminescence from the Reaction 100 eV He ⁺ + I ₂ \rightarrow He + I ⁺ + I + Energy	209

Abstract

The cross sections for production of emission lines in the 60 nm to 870 nm region were measured for the collision of 100 eV $He_{\perp}^{(+)}$ ions with $Cl_2^{(-)}$, $Br_2^{(-)}$, and $I_2^{(-)}$. These cross section measurements were made with an ion beam apparatus. Only emissions from transitions from excited electronic states with lifetimes shorter than a usec were measured. The dependence of the cross sections on the kinetic energy of the He ions between 2 to 170 eV was determined by use of the more intense emission lines. The total cross section obtained for emissions between 90 nm and 870 nm for chlorine is 5.0 A2; of this, 3.8 A² is for emission in the VUV region. Emissions from excited neutral chlorine atoms account for at least 85% of the total cross section. Of the cross section for production of emission from excited neutral chlorine atoms, 80% is caused by direct excitation with the remainder resulting from cascading. The total cross section obtained for emissions between 80 nm and 870 nm for bromine is 14.9 A²; of this, 11.9 A² is for emission in the VUV region. Emissions from excited neutral bromine atoms account for at least 85% of the total cross section. Of the cross section for production of emission from excited neutral bromine atoms, 75% is caused by direct excitation with the remainder resulting from cascading. The total cross section obtained for emissions between 100 nm and 870 nm for iodine is 15.9A2; of this, 14.4 A^2 is for emissions in the VUV region. The proportion of the total cross section for the production of emissions

from singly-ionized iodine atoms is much larger than for either the chlorine or bromine reactions. In all three systems dissociative charge transfer appears to be the predominant reaction process for the production of emissions in the 60 nm to 870 nm spectral region.

EMISSION CROSS-SECTION MEASUREMENTS OF LOW ENERGY He tons with C12, Br2, I2 REACTIONS

I. Introduction

The study of ion-neutral collisions has mushroomed in recent years (Refs 13, 23 and 46). One area of interest in this field is the examination of the emission spectra produced by the excited product species formed in ion-neutral collisions. These studies yield information about the internal energy states of the products of such reactions. This is the type of information needed to better understand the collision mechanisms and the nature of the potential surface for the intermediate complex involved in the low energy collision process. In the experiment discussed in this thesis, examination of the emission spectra of the reactions is used to study the excited states produced by low energy He ions interacting with three of the halogens; chlorine, bromine, and iodine. The results produce a more complete understanding of ion-neutral collision processes in general, with possible applications in the design of more efficient plasma and/or laser systems. For example, the competing processes in the helium iodine laser might be more fully understood (Ref 62).

The study of the emission spectra produced in low energy ion-beam experiments is a relatively new area of investigation. The main reason that little interest was shown in the early studies of these processes was that experimentalists

tended to explain these interactions in terms of Massey's adiabatic hypothesis (Ref 44:261). This adiabatic hypothesis predicted very low radiative cross sections at ion energies below 10 keV. It was considered a startling result when a number of experiments resulted in very large cross sections for low energy ion-neutral collisions (Refs 5, 8, 9, 24, 39, 53, 65, and 69). Massey's hypothesis was of course only a crude approximation and it assumed that the energy levels of the colliding particles did not change as the particles approached each other. Such a treatment makes no allowance for a change in the electron structure during the collision process. At high ion energies where the collision interaction time is very short, this assumption yields good results. At low energies where the interaction time is much longer, the assumption is not valid.

The early studies reporting large cross sections for low energy ion reactions were conducted by Pretzer, et al. (Ref 53), Stebbins, et al. (Ref 65), Lippeles and Novick (Ref 39), Jaecks, et al. (Ref 24), Dworetsky, et al. (Ref 9), Dworetsky and Novick (Ref 8), DeHeer, et al. (Ref 5), and Tolk, et al. (Ref 69). Most of these studies used a system which focused an ion beam on a rare gas target in a collision chamber. The collision chamber was mated to a monochromator or a photon detector with filters. These studies were limited to total emissions within the bandwidth of the filtering system or within narrow spectral region scans. Some of the ion beams in these studies were produced by a modified high energy ion

beam apparatus which was able to go down only to 300 eV.

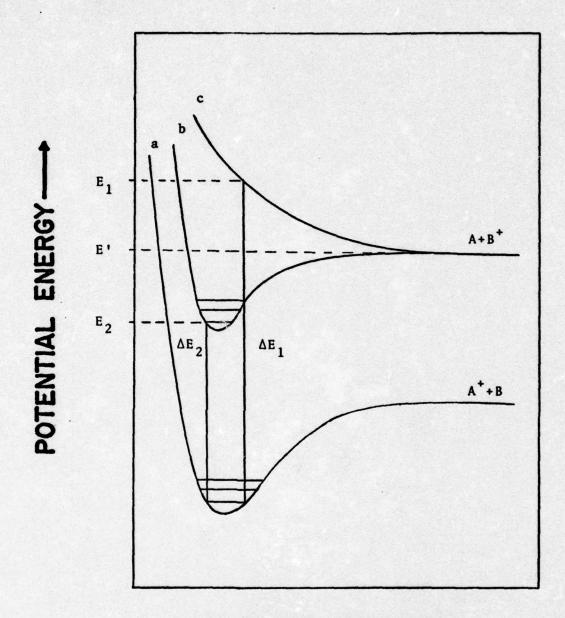
The first low energy (0 - 170 eV) studies over a wide spectral region (50 nm to 870 nm) were reported by Hughes, Jones, and Tiernan (Refs 18, 19, 20, and 28). Their apparatus was designed for optimal performance in the 100 eV ion energy region. The ability to observe resolved spectral lines from 50 to 870 nm enabled the investigation of a wide range of electronic transitions. This provided a capability to examine the effects of cascading in relation to the direct formation of specific energy states.

This type of apparatus has many advantages over other methods of studying low energy ion-neutral reactions, such as afterglows and discharges. The latter plasma studies are usually difficult to interpret in detail because of the several concurrent reaction processes which may yield radiation (ion-neutral collisions, electron-ion recombination, neutral-neutral collisions, etc.). In addition it is difficult to determine the effect of the electric field in the plasma on the emissions seen, particularly in the VUV region. In the ion beam apparatus the pressures are sufficiently low to allow only bimolecular ion-neutral collisions to occur. The collision chamber can also be shielded to minimize electric fields in the reaction region.

One disadvantage of such an ion beam apparatus is that it can observe transitions only from energy states with lifetimes less than 10^{-6} sec. Metastable energy states with longer lifetimes are not observed.

To obtain an insight into the detailed mechanisms of ion-neutral reactions involving excited electronic states, it is useful to use the theoretical concept of potential energy surfaces (Ref 34:19-45). For two particle reactions these are called potential energy curves. These curves are obtained by plotting the potential energy of the combined two particle system as a function of the distance between the two particles, as illustrated in Fig. 1. Various potential energy curves are obtained depending on the energy states of the two particles. Thus, as the electronic energy states of the two particles are varied, various other curves results (Refs 15 and 45).

Curve (a) in Fig. 1 represents the potential energy of a two particle system consisting of an ion, A^+ , and a neutral particle, B. At large distances A^+ and B exist as separate particles, each in the ground state. Curve (b) represents a bonding state of A (now a neutral particle) and B^+ (now an ion). Curve (c) represents an antibonding state of A and B^+ . At large distances A and B^+ exist as separate particles, each in the ground state. When A and B^+ are in the potential well of the bonding state described by curve (b), A and B^+ exist as a bound complex $(AB)^+$. E' in Fig. 1 is the energy required for the charge transfer reaction A^+ + B + A + B + to occur. If there is a surplus of energy in the reaction A^+ + B + A + B + the process is designated as an exothermic process. This is illustrated in Fig. 1 by the transition, with an energy change of ΔE_1 , from curve (a) to the upper antibonding state repre-



DISTANCE BETWEEN PARTICLES

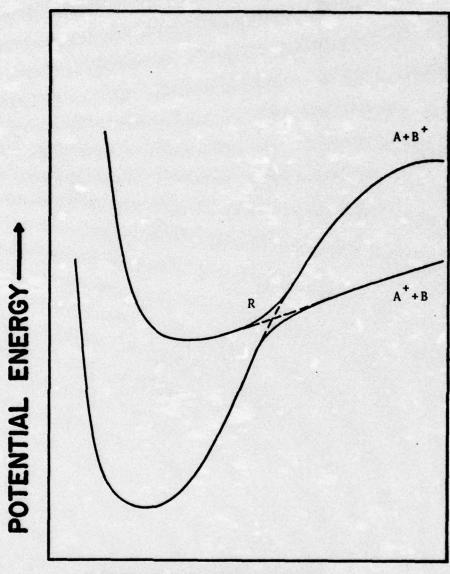
Fig. 1. Typical Examples of Possible Potential Energy Curves in Charge Transfer Process.

sented by curve (c). The surplus of energy is equal to $E_1 - E'$. If there is not enough energy available for the reaction $A^+ + B + A + B^+$ to occur, then the process is designated as an endothermic process. This is illustrated in Fig. 1 by the transition, with an energy change of ΔE_2 , from curve (a) to the upper bonding state at a potential energy value on curve (b) below E'. In this case the addition of a quantity of energy equal to $E' - E_2$ is required for the reaction $A^+ + B + A + B^+$ to occur.

It can be seen that if the charge transfer process results in the production of product species in excited states, the detection of the emissions produced by the decaying transitions to lower energy levels can be used to identify the product species produced in the charge transfer process.

This method of investigation has the advantage that not only the product species is identified, but the actual excited energy levels of the product species are also determined.

In the actual charge transfer process, there are many curves describing the possible energy states. The curve shapes are generally more complex than the idealized curves shown in Fig. 1. In the more complex system the particles are most likely to exchange energy in their collision process when the potential energies actually cross as indicated by the dashed curves in Fig. 2. Another region of high probability of energy exchange is where the curves come very close together, nearly crossing, as for example in region R of the solid curves in Fig. 2. These are called pseudo-crossings.



DISTANCE BETWEEN PARTICLES

Fig. 2. Typical Example of Pseudo-Crossings of Potential Energy Curves in Charge Transfer Processes.

If a third particle is added to the system, a third dimension is added to the theoretical collision model and potential energy surfaces are formed.

The most promising theory proposed to explain the large cross sections for radiation emission from ion-neutral interactions at low ion energies is the pseudo-crossing of these potential energy surfaces (Refs 1, 59, 60 and 73). One of the primary needs for the formulation of better theoretical models is more experimental data from a number of different systems. This was one of the incentives for performing the experiment presented in this thesis.

The potential of charge transfer processes as an excitation mechanism for laser systems has only recently been considered. In some systems, the charge transfer process releases several electron volts of energy, which is available for excitation of the product species. Helium-metal-vapor lasers are some of the systems where charge transfer is very important. One of the most extensive studies to assess the importance of charge transfer in relation to the competing Penning ionization process for the He-Cd and He-Zn ion laser systems has been accomplished by G. Collins (Ref 4). On the basis of this study, Collins has proposed several new raregas-metal-vapor laser systems emitting lines in the region between 200 nm and 400 nm which use charge transfer as the primary pumping mechanism. (NOTE: Penning ionization is the process of producing excited ions and free electrons by the collision of an excited metastable atom and a neutral

atom. For the He-Cd system this is described by the relationship $He(2^3S) + Cd \rightarrow (Cd^+)^* + He + e^-.)$

Later, C. B. Collins, et al. proposed that very high efficiency lasers of from 50 to 10% in the visible region could be constructed using charge transfer pumping mechanisms (Refs 3 and 50). The He^+ formed by electron impact in a plasma is the pumping ion in most rare-gas-metal-vapor laser systems. C. Collins, et al. proposed a system which promises to approach the theoretical limit of one photon out for every He^+ ion formed in the plasma. Their studies of a He_2^+ - N_2 laser system lasing at 427.8 nm are very promising.

The afterglow studies by Shay, et al. of the sixteen iodine ion laser lines indicate that charge transfer is the primary source of excitation for the upper levels of the helium iodine ion laser (Ref 63).

The interest in a better understanding of ion-neutral collision processes, coupled with the possible application of the results of such studies to the design of more efficient plasma and/or laser systems, prompted the present studies in which a low energy ion beam experiment has been utilized to investigate He⁺/halogen systems.

II. Experimental Instrumentation and Calibration

This chapter begins with a discussion of the cross sections being measured. The remainder of the chapter describes the experimental instrumentation used to obtain the necessary data for determining these cross sections. The calibration of the instrument is also discussed.

Emission Cross Sections

Throughout this thesis the term emission cross section or cross section means the cross section for production of a given emission line by the reaction of He⁺ ions with the target molecule. Due to instrument limitations, this cross section includes only emissions attributed to transitions from electronic energy states with lifetimes of less than a µsec. Excited product species move out of the focal point of the monochromator in about a µsec. Nonradiative decay processes and radiation from long lived states (greater than a µsec) are neglected. Whenever a cross section other than the emission cross section of an individual emission line is referenced, the type of cross section will be explicitly described.

A derivation of the relations for calculating the emission cross section, σ , from data measured in this experiment illustrates the parameters necessary for obtaining the cross sections. The derivation is for the monochromator whose diagram is shown in Fig. 11. The source is the exit slit of the collision chamber. The symbols used in the derivation are defined in Table I.

Table I

σ	Emission Cross Section (cm ² /neutral particle)
n	Number of target gas particles in radiating volume
N _A	Avogadros number
N _R	Number of photons per second recorded by SSRI Photon Counter
N _S	Number of photons per second striking the grating
N _T	Total number of radiating particles in the radiating volume of the collision chamber
V	Volume of target gas radiating (cm ³)
S _{CH}	Collision chamber exit slit height (cm)
S _{CW}	Collision chamber exit slit width (cm)
2	Distance between collision chamber entrance and exit slits (cm)
S _{DW}	Slit width of detector (Monochromator exit slit width) (cm)
D	Linear Dispersion (cm of wavelength/cm of detector slit)
dλ	Wavelength interval focused on detector slit (cm)
f	Flux of He ⁺ ions (ions/sec-cm ²)
I	He ⁺ ion-beam current incident on the collision volume (amps)
F(λ)	Instrument function
$^{\Omega}\mathbf{g}_{\perp}$	Solid angle subtended by grating when parallel to the plane of the collision chamber exit slit (ster)
Y	Horizontal angle of rotation of the grating from parallel to the plane of the collision chamber exit slit (see Fig. 10)
р .	Pressure of target gas
R _o	Ideal Gas constant
T _o	Temperature of target gas(°K)
е	Charge of an electron (coulomb)

The number of photons striking the grating per second in the wavelength interval d λ (where d λ - DS_{DW}) is

$$N_{S} = \frac{N_{R}}{F(\lambda)} \tag{1}$$

Assuming isotropic radiation from the excited atoms, ions, or molecules in the collision chamber, the total number of photons radiated into a sphere [4π steradians solid angle] can be shown to be

$$\frac{4\pi}{\Omega_{g_{\perp}}} \frac{N_{R}}{\cos \gamma} = N_{T}$$
 (2)

The radiating volume has the dimensions $S_{CH} \times S_{CW} \times \ell$. But also

$$N_{T} \equiv nf\sigma$$
 (3)

where by the ideal gas law

$$n = \frac{PVN_A}{R_O T_O} \tag{4}$$

and f can be expressed as

$$f = \frac{I}{S_{CH} \times S_{CW} \times e}$$
 (5)

Therefore

$$\sigma = \frac{N_T}{nf} = \frac{4\pi R_o T_o N_R}{P \ell N_A I \Omega_{g_i} F(\lambda)}$$
 (6)

Equation (6) illustrates that in order to obtain accurate cross sections the instrument must be carefully calibrated for accurate measurements of the target gas pressure P, the ion current I, and the instrument function $F(\lambda)$. The remainder of this chapter is devoted to describing the instrumentation used to measure these quantities and the calibration of the instrument.

Apparatus

The measurements in this study were made on an instrument originally designed and constructed by the Gaseous Excitation and Ionization Processes Group at the Aerospace Research Laboratories (ARL) (Refs 19, 20 and 21). The apparatus consists of a single-focusing mass spectrometer with a conventional electron bombardment ion source coupled to a 1-meter vacuum ultraviolet monochromator [McPherson Model 225 (see Fig. 3)]. The mass spectrometer is used to select singly-ionized helium ions and accelerate them to 170 eV (lab) translational energy. Typical helium ion currents in the collision chamber were 0.1 nanoamps with the 0.1 mm slit used for high resolution scans, and 1.0 nanoamps with the 1 mm slit used for low resolution scans.

The decelerating lens is a four element electrostatic slot lens which decreases the translational energy of the ions from 170 eV to the desired interaction energy. The beam interaction energy can be varied from 2 eV to 170 eV, and the energy resolution of the beam is on the order of

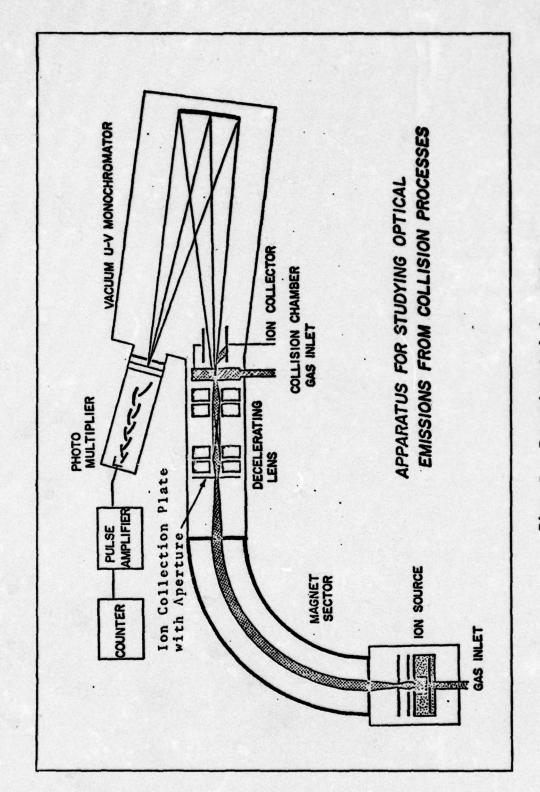


Fig. 3. Experimental Apparatus.

21 eV. The electrostatic lens also focuses the ions at the point in the collision chamber which is the entrance focal point of the monochromator. The collision chamber and the electrostatic lens were designed to minimize the penetration of electric and magnetic fields into the collision region.

The target gas in the collision chamber was at room temperature and was considered to be at thermal equilibrium for the experiments reported here. Typical target gas pressures ranging from 2 to 4 mTorr were maintained in the collision region by using differential pumping. Typical pressures in the monochromator during an experiment were in the 1 x 10⁻⁶ Torr region.

The emissions from radiative transitions of excited product species were directly observed with the scanning monochromator. The only optical element in the scanning monochromator is the concave blazed grating. The resolved spectrum is focused on the detector at the exit slit of the monochromator. The signal from the detector was measured by an SSRI photon counting system (Ref 64). The output of the SSRI photon counter was either visually observed and recorded or recorded directly on a strip chart recorder. Various combinations of detectors and gratings were used in investigating emission in the wavelength region from 50 nm to 870 nm.

In this experiment, the combinations of detectors and gratings used limit the detection of emission lines to those

radiative transitions produced by reaction cross sections greater than 1×10^{-17} cm². In some spectral regions the instrument can measure radiation arising from reactions with excitation cross sections as low as 7×10^{-19} cm². The detector and grating combinations used in these measurements are shown in Table II.

Target Gas System

The target gas pressure is controlled by a Granville Phillips Automatic Pressure Controller and an MKS Baratron Capacitance Pressure Meter (see Fig. 4). Several manual valves are positioned to allow entry of the target gas into the storage bottle, or to pump out the storage bottle and source lines with a 2" CVC oil vapor diffusion pump attached to a Model 1400 Welch mechanical forepump (25 liter/minute pumping speed).

Vacuum System

The vacuum in the instrument is maintained by two 4" and one 6" oil diffusion pumps and one 500 liters/minute mechanical forepump (see Fig. 5). The pumping systems include a pneumatic actuated gate valve, a liquid nitrogen cooled trap, and the oil diffusion pump. The 4" Norton pumps, Model 0183, maintain the vacuum in the ion source and at the electrostatic collision chamber region. The 6" diffusion pump, (CVC Model PAS-63C), maintains the vacuum in the monochromator. All three diffusion pumps are connected to a 500 liter/minute mechanical forepump, Welch Model 1397.

Table II

Detector and Grating Combinations

Detector	Grating (995.4 mm Concave Radius)	Wavelength Region
RCA C31034A Photomultiplier Cooled with Dry Ice to -78°C GaAs Photocathode UV-Transmitting Glass Window	Bausch & Lomb #2662-1-1 700 nm Blazed Wavelength 300 Grooves/mm Aluminum Coated BSC2 Glass	300 nm to 870 nm
EMR 541F-08-18-03900 Photomultiplier SN 15245 CsTe Photocathode LiF Window	Bausch & Lomb #2571-5-3 200 nm Blazed Wavelength 600 Grooves/mm MgF ₂ Overcoated Aluminum on BSC2 Glass	105 nm to 350 nm
EMR 541F-08-18-03900 Photomultiplier SN 15245 CsTe Photocathode LiF Window	Bausch & Lomb #2478-19-6-1 90 nm Blaxed Wavelength 600 Grooves/mm Platinum Coated BSC2 Glass	105 nm to 190 nm
EMR 541F-09-18-03900 Photomultiplier SN 17891 CsTe Photocathode MgF ₂ Window	Bausch & Lomb #2571-5-3 200 nm Blazed Wavelength 600 Grooves/mm MgF ₂ Overcoated Aluminum on BSC2 Glass	115 nm to 350 nm
EMR 541F-09-18-03900 Photomultiplier CsTe Photocathode MgF ₂ Window	Bausch & Lomb #2478-19-6-1 90 nm Blazed Wavelength 600 Grooves/mm Platinum Coated BSC2 Glass	115 nm to 190 nm
Bendix CEM-4028 Channeltron Photon Counter Tube	Bausch & Lomb #2478-19-6-1 90 nm Blazed Wavelength 600 Grooves/mm Platinum Coated BSC2 Glass	50 nm to 130 nm

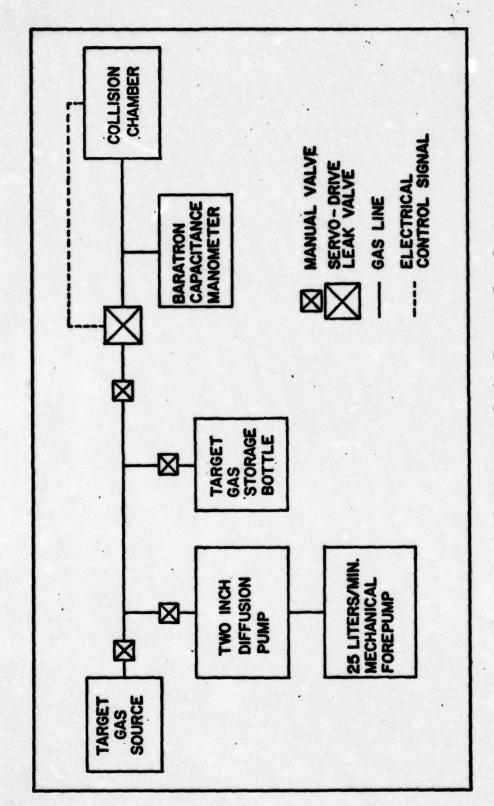


Fig. 4. Block Diagram of the Target Gas System.

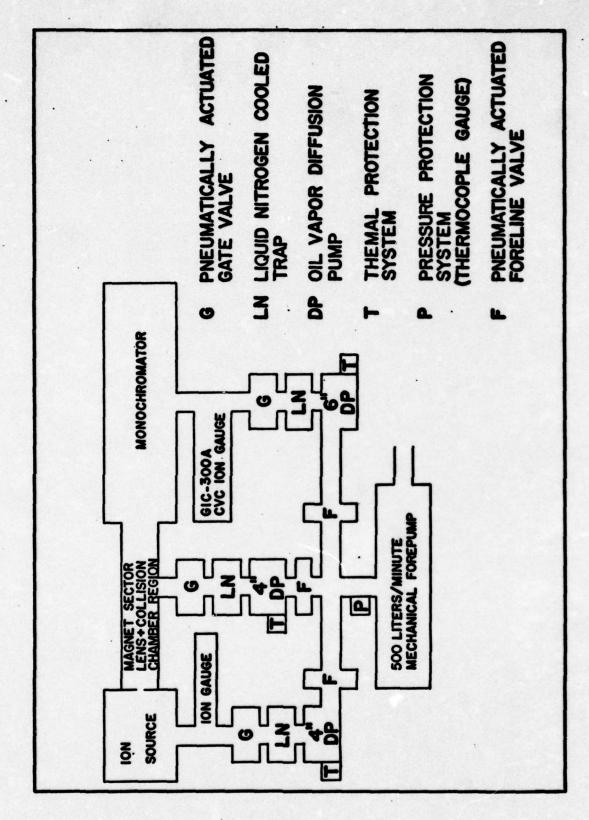


Fig. 5. Block Diagram of the Vacuum System.

Typical pressures in the monochromator with no gas in the collision chamber are in the 5×10^{-7} Torr region. With a 3 mTorr target gas pressure in the collision chamber, the monochromator pressure is about 1×10^{-6} Torr. Typical pressure readings on the ionization gauge near the ionization chamber are 4×10^{-7} Torr with no helium in the ionization chamber and 1.5×10^{-5} Torr while performing an experiment with helium in the ionization chamber.

Several protection systems are used to prevent damage to the diffusion pumps. An automatic system for filling the traps with liquid nitrogen insures that the traps are always cooled. An automatic system which will close all of the gate valves and shut off the diffusion pumps is actuated when (1) the ion gauge near the ion source detects high pressure, or (2) the thermocouple gauge near the forepump detects high pressure, or (3) there is an electrical power failure. Each diffusion pump also has a thermal protection system such that if the temperature of that pump becomes too high the pump will shut off.

Target-Gas Pressure Calibration

The pressure of the target gas in the collision chamber was controlled by differential pumping and by regulation of the inflow of gas. The gas input was measured and regulated by an MKS Baratron capacitance manometer and the pressure controller. Since the Baratron is located several inches from the chamber the pressure measured by the Baratron gauge

needed correction to obtain the true value of the pressure in the collision chamber. To determine this factor, a calibration experiment was performed.

The correction factors were obtained by comparison of the pressures measured by the Baratron gauge in two different configurations as shown in Figs. 6a and 6b. Figure 6a is that of the experiment and Fig. 6b is with the gauge at the end of a 1/8" tube projecting into the center of the collision chamber. The pressure readings, obtained for air and xenon, are plotted in Figs. 7 and 8 against the pressure at the mouth of the six-inch diffusion pump. A CVC ion gauge (GIC-300A) was used to measure these pressures where the diffusion pump enters the monochromator. As can be seen by inspection of the figures, it is evident that deviations occur at pressures above 4 mTorr. Since there is no significant difference between the calibration for air (atomic weight of 28) and xenon (atomic weight of 131), it is assumed that this calibration is also valid for chlorine, bromine and iodine.

Ion Beam Current Calibration

Following each cross section measurement, the ion beam current was calibrated to determine an upper limit on the uncertainty of measuring the current of the helium ion beam which enters the collision chamber. The purpose of this ion beam calibration was to determine the efficiency of collection of ions passing through the collision chamber at

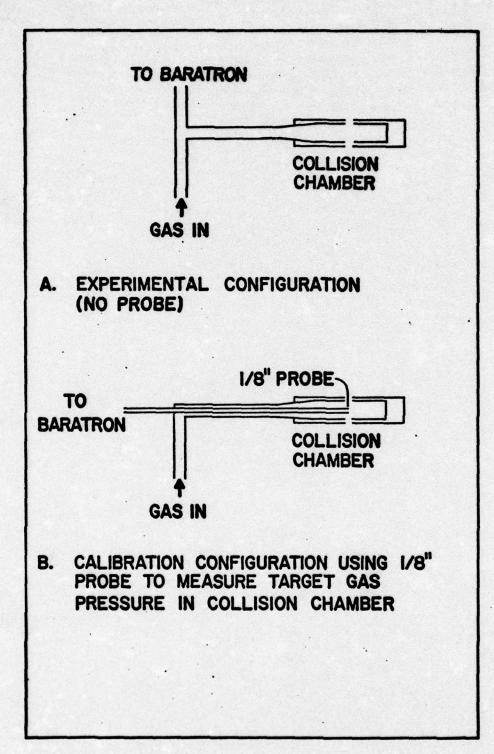


Fig. 6. Configurations Used for Target Gas Pressure Calibration.

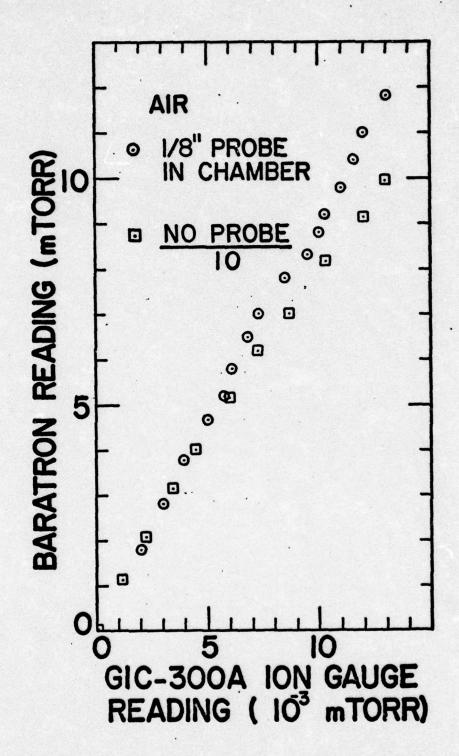
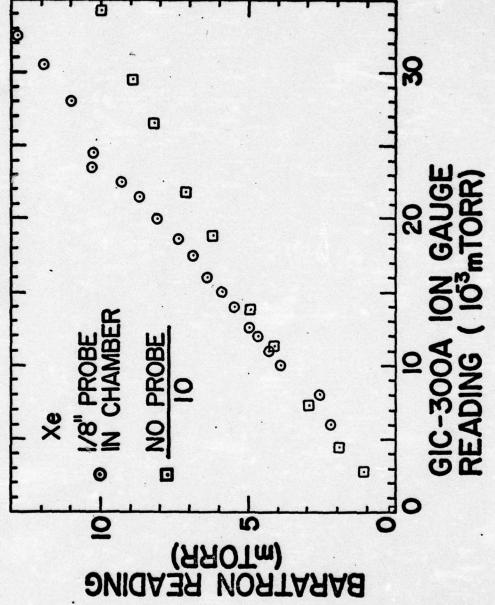


Fig. 7. Target Gas Pressure Calibration Using Air.



the ion collector in the monochromator [on the exit side of the collision chamber (see Fig. 9)]. This calibration was performed with no target gas in the collision chamber.

The calibration consisted of three measurements of the current. The difference between the first two, i_1 - i_2 , is a measure of the number of helium ions which passed through the aperture in the ion collection plate at the entrance to the electrostatic lens (see Fig. 3). The currents i_1 and i_2 were obtained with the ion beam deflected to one side of the aperture and aligned with the aperture respectively. The third current i_3 was measured at the ion collector at the exit of the collision chamber. The quantity i_1 - i_2 - i_3 is a measure of the number of helium ions which passed through the entrance sperture of the electrostatic lens, but did not exit the collision chamber.

A typical set of values for i_1 , i_2 , and i_3 are approximately 1.3 nA, 0.6 nA, and 0.7 nA respectively. This suggests that for these conditions very few ions which enter the electrostatic lens (i_1-i_2) fail to exit from the collision chamber. When i_1 was increased to 2 nanoamps the i_3 value decreased to about 70% of the i_1-i_2 value. Examination of the collision chamber after this experiment revealed an ion burn spot completely encircling the entrance slit. The total area of the ion burn spot is nearly equal to the area of the entrance slit. It appears that as the ion beam current is increased, the divergent characteristics of ion beam (space charge effects) cause more and more of the ions to ultimately

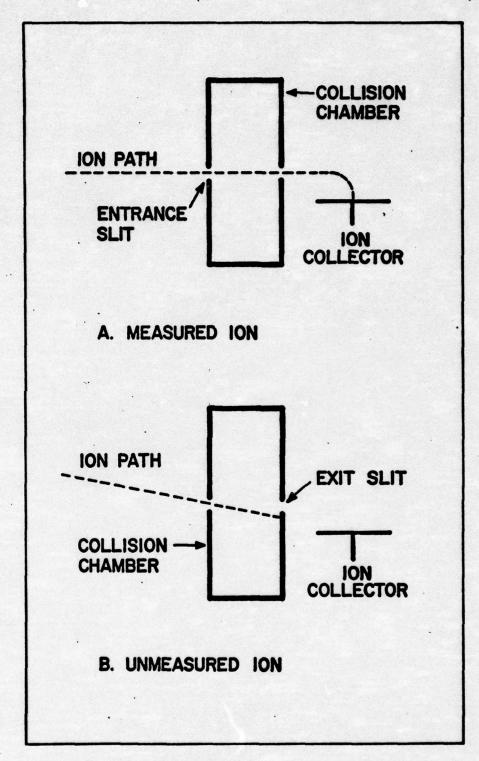


Fig. 9. Possible Ion Paths of Measured and Unmeasured Ions Available for Excitation of Atoms/Molecules in Collision Chamber.

collide with the entrance wall of the collision chamber. At ion energies of 2 to 5 eV, this divergence of the beam and the weaker focusing characteristics of the lens reduce the transmission through the collision chamber to about 50%.

This calibration shows that for i_3 values of 0.7 nA at 100 eV the ion beam current measured at the ion collector on the exit side of the collision chamber is an accurate measure of the ions which are available for excitation in the reaction region of the collision chamber. The He⁺ ion currents recorded at this ion collector with no target gas in the chamber are the values used in the cross section calculations for the experiments reported here. Typical He⁺ ion flux through the collision chamber during this experiment was 6 x 10^{10} ions/sec-cm² (10 nanoamps/cm²).

It should be noted that for experiments at ion energies above 110 eV the cross section measurements are probably lower than the actual values. This is due to the fact that at energies above 110 eV the ion beam is not efficiently collected with the potentials used on the ion collector. (This potential could not be increased without a major modification to the apparatus.) Therefore, energy dependence measurements at energies above 110 eV were made by tuning the beam at 100 eV, where accurate ion collection measurements can be made. (This is the ion current value used in the cross section calculations.) Then the deceleration voltage was adjusted to the desired value for the experiment. The deceleration voltage adjustment tends to defocus the

ion beam to some degree, resulting in the calculated cross sections being smaller than the actual cross sections. Thus the error in the cross section values probably increases as the energy is increased from 100 eV to 170 eV (see Figs. 26, 27, 36 to 41 and 53 to 60). This error is estimated to be as large as 50% at 170 eV.

Instrument Calibration for 400 nm to 870 nm Region

In the 400 nm to 870 nm region the instrument function $F(\lambda)$ was determined by using a calibrated tungsten light source (Ref 33). The calibration arrangement is shown in Fig. 10. This calibration was based on the black body radiation law from a gray body (Ref 31:126) and the law of conservation of radiance in an elementary beam (Ref 31:134). The instrument function $F(\lambda)$ is defined as

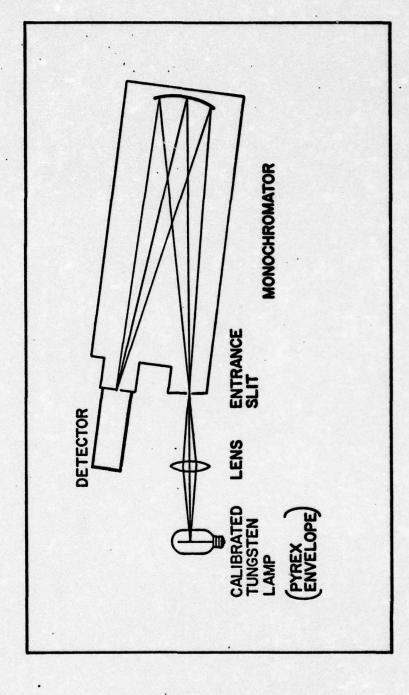
$$F(\lambda) \equiv \frac{Q}{P_{\lambda}}$$
 (7)

where

Q = Counts/sec recorded on the SSRI photon counter converted to power (watts)

 P_{λ} = Spectral power incident on the grating (watts)

The calibration procedure was as follows. First the image of the tungsten filament is focused on the entrance slit of the monochromator. Then the image in the slit is treated as a source for the monochromator. Referring to Fig. 11 one can see that a differential area of the grating perpendicular, to a line from the source is



The 400 nm to 870 nm Instrument Function [F(λ)] Calibration Setup. Fig. 10.

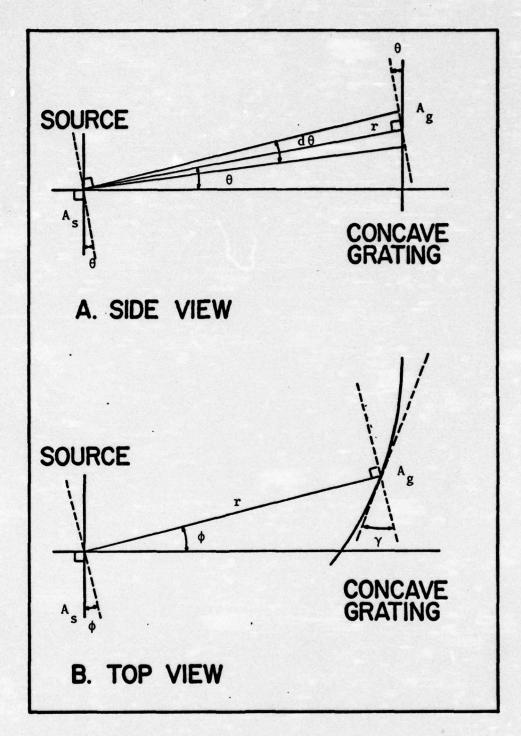


Fig. 11. Geometric Diagram of Monochromator.

$$dA_{g_i} = (rd\phi)(r \cos \theta d\theta)$$
 (8)

where the symbols are explained in Table III. A similar differential area of the source perpendicular to a line from a point on the grating is

$$dA_{s_{\perp}} = dA_{s} \cos \theta \cos \phi \qquad (9)$$

The differential solid angle subtended by dA_{g} at the source is

$$d\Omega = \frac{dA_{g_1}}{r^2} = \cos \theta d\theta d\phi \qquad (10)$$

The differential spectral power d^2P_{λ} from the source that is incident on the grating is

$$d^{2}P_{\lambda} = L_{\lambda}dA_{s_{\perp}}d\Omega \qquad (11)$$

Therefore the total spectral power is

$$P_{\lambda} = L_{\lambda}A_{s} \int \int A_{g} \cos^{2} \theta d\theta \cos \phi d\phi = L_{\lambda}A_{s}\Phi$$
 (12)

where

$$\Phi = \int \int A_g \cos^2 \theta d\theta \cos \phi d\phi$$

Now

$$L_{\lambda} = T_{\lambda_{\text{pyrex}}} T_{\lambda_{\text{Lens}}} \varepsilon_{\lambda_{\text{Tungsten}}} L_{\lambda}^{BB}$$
 (14)

and assuming the source is a Lambert emitter

. Table III

Symbols Used in the Derivation of the Visible Instrument Function $F(\lambda)$

h	Plancks constant
c	Velocity of light
k	Boltzmann's constant
λ	Wavelength
T	Temperature °K
R	Radiant Emittance (watts/cm ²)
P	Power (watts)
r.	Radiance (watts/ster-cm ²)
$R_{\lambda}, P_{\lambda}, L_{\lambda}$	Spectral Radiant Emittance, Spectral Power and Spectral Radiance
R_{λ}^{BB} , P_{λ}^{BB} , L_{λ}^{BB}	Spectral Radiant Emittance of a Blackbody, etc.
τ _λ	Spectral transmittance
ελ	Spectral emissivity
Q	Counts/sec of SSRI Photon Counter (Photons/sec)
As	Area of source (cm ²)
Ag	Area of grating (cm ²)
Ω	Solid angle (ster)
θ	Vertical angle between normal to source and a line to a point on the grating
φ	Horizontal angle between normal to source and a line to a point on the grating
Υ	Horizontal angle of rotation of the grating from parallel to source
r	Distance from source to a point on the grating

$$L_{\lambda}^{BB} = \frac{R_{\lambda}^{BB}}{\pi} \tag{15}$$

where

$$R_{\lambda}^{BB} = \frac{c_1}{\lambda^5} \frac{1}{\begin{bmatrix} c_2/\lambda T & 1 \end{bmatrix}} d\lambda \tag{16}$$

with

$$C_1 = 2\pi c^2 h \tag{17}$$

$$C_2 = \frac{hc}{k} \tag{18}$$

The total spectral radiance incident on the grating is

$$L_{\lambda} = T_{\lambda_{\text{pyrex}}} T_{\lambda_{\text{Lens}}} \varepsilon_{\lambda_{\text{Tungsten}}} \frac{C_{1}}{\pi \lambda^{5}} \frac{1}{\begin{bmatrix} C_{2}/\lambda T \\ e \end{bmatrix}} d\lambda \qquad (19)$$

The energy of one photon
$$= \frac{hc}{\lambda}$$
 (20)

Therefore the photons/sec incident on the grating as a result of the total spectral power is

$$P_{\lambda}(\text{photons/sec}) = \frac{T_{\lambda_{\text{pyrex}}}^{T_{\lambda_{\text{Lens}}} \epsilon_{\lambda_{\text{Tungsten}}}^{C_{1} \lambda d \lambda A_{s} \Phi}}{hc\pi\lambda^{5} \left[e^{C_{2}/\lambda T} - 1\right]}$$
(21)

The instrument function $F(\lambda)$ is defined as

$$F(\lambda) \equiv \frac{Q}{P_{\lambda}} \tag{7}$$

Therefore

$$F(\lambda) = \frac{Q\lambda^4 \left[e^{hc/k\lambda T} - 1\right]}{2cT_{\lambda_{\text{Pyrex}}} T_{\lambda_{\text{Lens}}} \epsilon_{\lambda_{\text{S}}}^{A_{\text{S}}} \Phi d\lambda}$$
(22)

The resulting instrument function from 400 nm to 870 nm is shown in Fig. 12.

VUV Instrument Calibration

The calibration of gratings in the VUV region is a difficult task. The only experts whom the author was able to locate with the capability to accomplish this type of calibration are located at the Naval Research Laboratories (NRL), and this is not readily available to people outside of NRL (Ref 22). Bausch and Lomb, the company which manufactured the grating, does not routinely calibrate gratings at less than 200 nm (Ref 54). In addition, grating reflectance changes over a period of time, and absolute calibrations would therefore change. In view of these considerations it was decided to use the measurements of an emission line for which radiative cross section data is available as a calibration standard. The use of a known reaction as a standard has the advantages of eliminating the need for periodic absolute calibration of the system, since the calibration of the grating can be checked at any time by merely observing the standard reaction. The experimental arrangement is in no way disturbed, and the grating need not be removed.

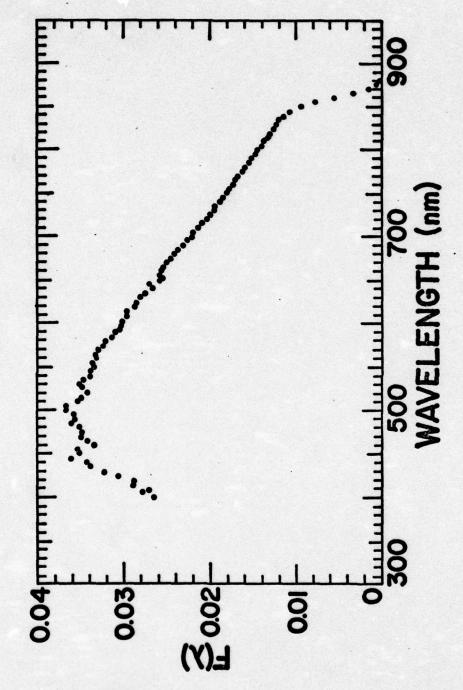


Fig. 12. Instrument Function $[F(\lambda)]$ from 400 nm to 870 nm.

In the VUV region, the instrument function was calibrated by measuring the cross section for the L_{α} hydrogen line (121.6 nm from the reaction of 100 eV He⁺ with H₂. A value of 0.60 x 10^{-16} cm² was used as a reference standard. This value was obtained in other studies using the same apparatus (Ref 21). This value for the L_{α} hydrogen line from the reaction of 100 eV He⁺ with H₂ is in good agreement with Dunn's value of 0.52 x 10^{-16} cm² for the L_{α} hydrogen line from the reaction of 120 eV He⁺ with H₂ (Refs 6 and 7).

A profile of the 90 nm blazed platinum grating was obtained by consideration of the following factors: (a) the measured reflectance curves from similar gratings (Ref 14), (b) the theoretical reflectance curve for blazed gratings (Ref 31:342-347), and (c) the reflectance curves for platinum (Refs 61 and 71). The reflectivity profile was assumed constant between 88.9 nm and 121.6 nm because the reflectivity of platinum increases from 88.9 nm to 121.6 nm (Ref 71:67), while the theoretical blaze reflectance decreases by approximately the same amount. The 88.9 nm line is the shortest wavelength line detected in this experiment. assumed reflectivity profile was multiplied by the published spectral response of the Bendix Channeltron (Ref 26) to obtain the instrument function profile from 88.9 nm to 121.6 This instrument function profile was then normalized to the calibrated value of the L hydrogen line at 121.6 mm (see Fig. 13).

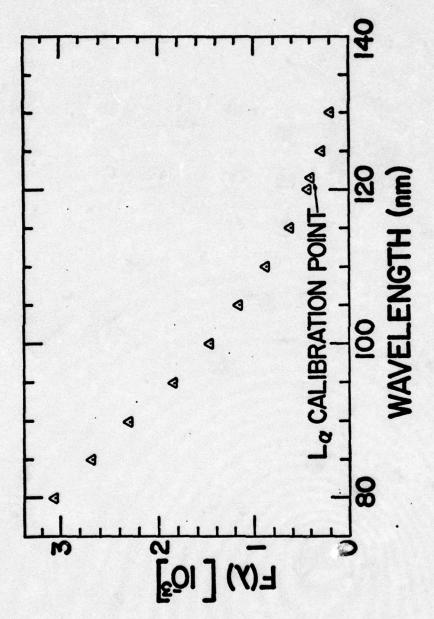
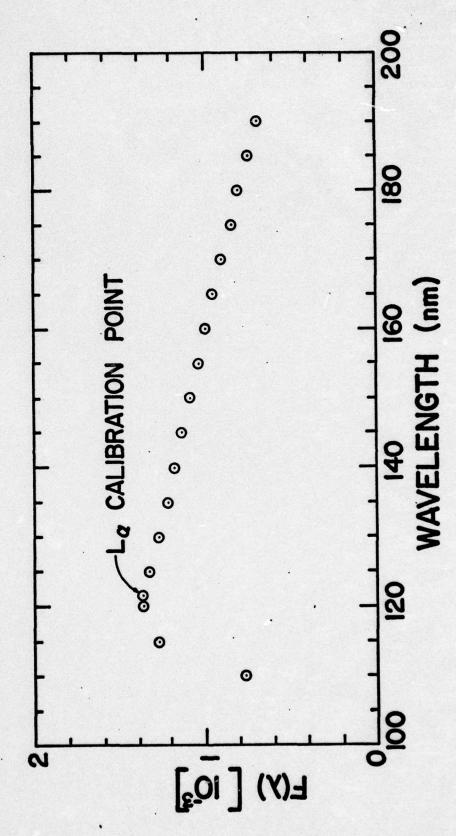


Fig. 13. VUV Instrument Function $[F(\lambda)]$ from 80 nm to 125 nm.

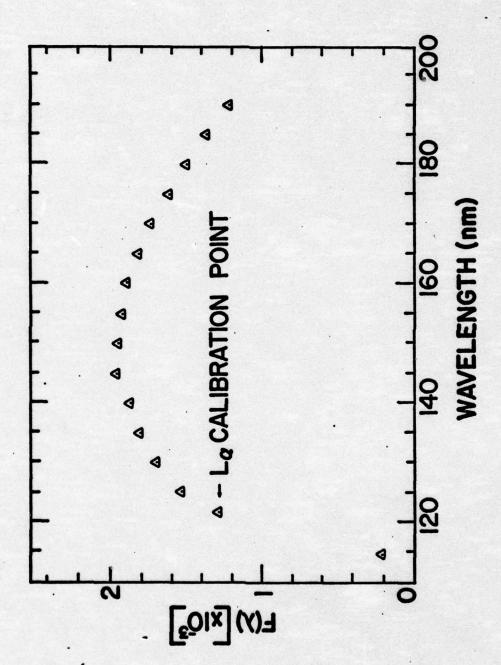
After examining a number of blazed grating calibrated reflectance curves for the VUV (Ref 14), and comparing them to the theoretical curve, the reflectivity profile between 121.6 nm and 183.0 nm was assumed to decreased by one-half linearly. This reflectivity profile was multiplied by the factory calibrated spectral response of the EMR photomultiplier to obtain the instrument function profile for the 121.6 nm to 183.0 nm region. This instrument function profile was then normalized to the calibrated value of the L_{α} hydrogen line at 121.6 nm (see Figs. 14 and 15).

This total instrument function calibration results in an instrument function profile that is calibrated at the 121.6 nm point and is less accurate at the extreme ends, the maximum error being at 183.0 nm. Due to the possible variation of the actual reflectivity profile of the platinum grating from the theoretical profile, this error could be as large as a factor of four. The uncertainty of this profile is taken into account in citing the accuracy of the cross section measurements in this region.

Other detector and grating combinations were used to investigate the 190 nm to 400 nm spectral region. Since no emissions were observed in this region, the instrument functions in the 190 nm to 400 nm spectral region are not discussed in this report.



VUV Instrument Function $[F(\lambda)]$ from 120 nm to 185 nm Using EMR LiF Window Detector. Fig. 14.



VUV Instrument Function [F(λ)] from 120 nm to 185 nm Using EMR MgF 2 Window Detector. Fig. 15.

III. Experimental Procedures

Bimolecular-Reaction Determination

The purpose of the He +/halogen experiment is to study bimolecular ion neutral collisions. Before performing the experiment it is necessary to determine the maximum pressure at which the experiment can be performed while avoiding the occurrence of multiple collisions. This information is obtained by positioning the monochromator on an intense line from the reaction, and obtaining the response for various pressures of the target gas. Next a plot is made of the response as a function of target gas pressure. As long as the plot is linear, single collision events are occurring (Ref 49:278-282); whereas when the curve becomes nonlinear, multiple events are occurring. The resulting pressure dependence curves for the $\mathrm{He}^+/\mathrm{Cl}_2$, Br_2 , I_2 reactions at 100 eV are shown in Figs. 16, 17 and 18. The Cl, and Br, curves become nonlinear at about 4 mTorr. The I_2 curve extends only to 2 mTorr because that is the vapor pressure of I, in the instrument at room temperature.

The linear portions of the curves in Figs. 16, 17 and 18 are also an indication that the effect of any secondary electrons generated in or near the collision region are negligible. If these secondary electrons were significant, the reaction would be a higher order process, and there would not be a linear region. If any secondary electrons are generated, they probably have low energies in the 1 eV to 12 eV region (Ref 29:276). Because of the shielding of the colli-

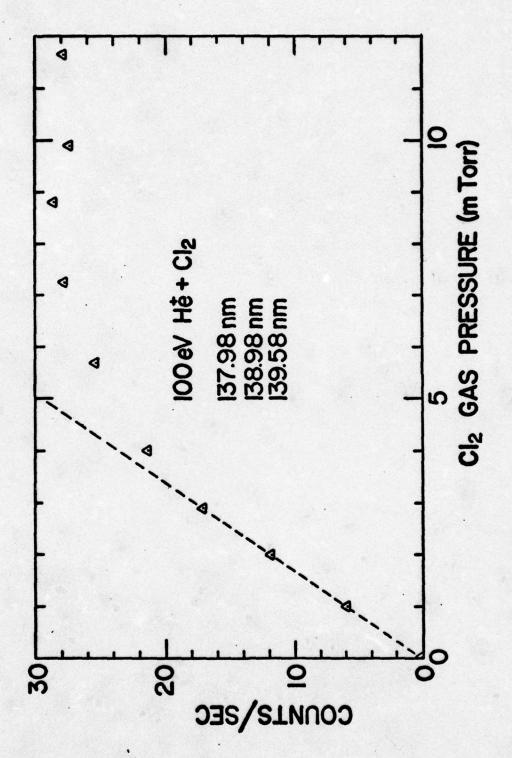
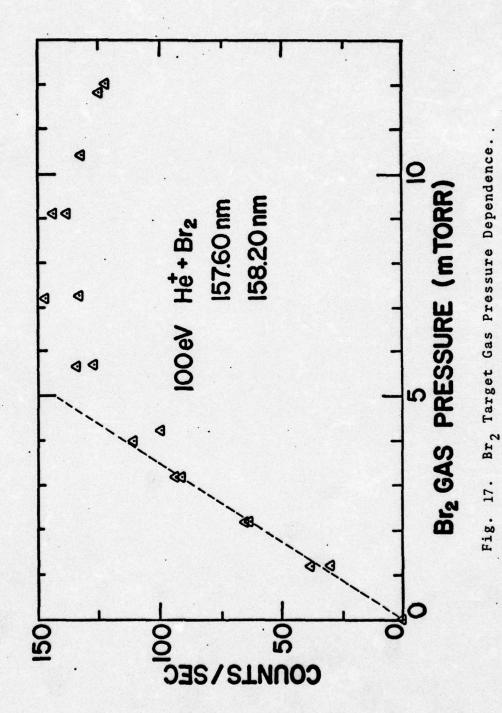


Fig. 16. Cl₂ Target Gas Pressure Dependence.



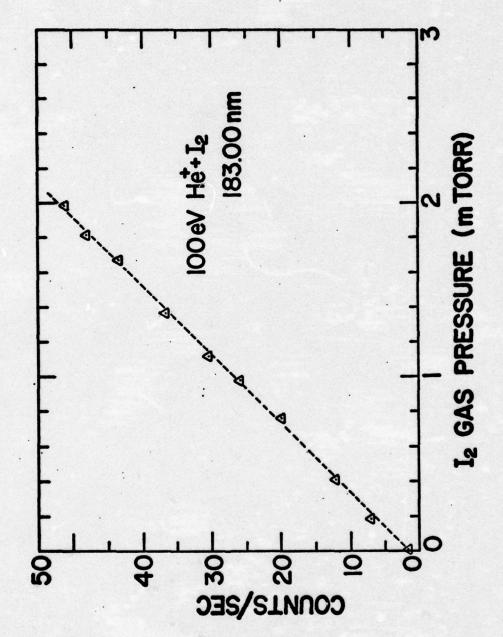


Fig. 18. I2 Target Gas Pressure Dependence.

sion chamber, the experimental collision region is in a field-free environment. The generation of any secondary electrons would generally be outside of the collision region. If any secondary electrons are generated by the collision of He⁺ ions with the edges of the entrance slit of the collision chamber, they would be quickly collected by the positively charged plate of the electrostatic lens. If they are generated at the ion collector in the monochromator on the exit side of the collision chamber (see Fig. 3), the low energy electrons would be repelled by the ion collector plate toward the opposite plate. Even if an electron collided with a halogen molecule in this region, the emission from the excited product species would occur so far from the focal point of the monochromator that it would not be focused on the exit slit of the monochromator.

Emission Wavelength Determination

The proper detector and grating for the wavelength region to be investigated (see Table II) are installed prior to an experiment. Initially, the 1 mm slit chamber was installed and the detector slit was set at 1 mm. A central image scan was performed to obtain the correction to be applied to the monochromator readings. A low resolution scan was then taken of the complete wavelength region to be studied. The low resolution half-width-at-half-maximum (HWHM) values were generally ± 1.5 nm in the VUV and 3.0 nm in the visible. Next, the 0.1 mm slit chamber was installed and the detector slit was set at 0.1 nm (some scans were

performed with larger exit slit settings). Another central image scan was performed to obtain a new monochromator reading correction. A high resolution scan was then taken of the regions of particular interest in which peaks were observed in the low resolution scan. The high resolution HWHM values were generally \pm 0.3 nm from 80 nm to 120 nm, \pm 0.1 nm from 120 nm to 400 nm and \pm 0.5 nm from 400 nm to 860 nm.

The uncertainties $\Delta\lambda_0$ of the measured wavelengths λ_0 were determined by a combination of the accuracy of the counter reading on the monochromator, the resolution of the instrument for the given grating and slit combination used for the scan, and the shape of the peak being evaluated. Usually $\Delta\lambda_0$ was given the value of the half-width-at-half-maximum of the observed peak plus the uncertainty of the counter reading of the monochromator.

The ion beam was focused for the experiment by varying the magnetic field in the mass spectrometer until the maximum number of ions entered the electrostatic lens systems. The voltage on the electrostatic lens was then varied until the maximum number of ions were collected at the ion collector inside the monochromator (see Fig. 3). This procedure for tuning the instrument assures that the ion beam is properly focused at the collision region which is located at the focal point of the monochromator, regardless of the He⁺ ion translational kinetic energy. This procedure is particulary important when measurements are taken at various ion energies as described in the next section. The ion beam is very

sensitive to even minute adjustments. The 100 eV He⁺ ion beam was the most stable beam, as well as having the largest number of ions incident on the collision region which could be accurately measured. Therefore, the 100 eV He⁺ ion beam was used for most spectral scans.

Cross Section Measurements at Various Translational Energies

In order to obtain data which would aid in determining if a specific emission line was produced by an endothermic or exothermic process, the cross section of a specific emission line was measured at various He⁺ ion translational energies. To obtain this data the following procedure was used.

With the 1 mm collision chamber slit installed and a 1 mm detector slit setting, the monochromator was positioned on one of the most intense peaks. Then the ion translational energy was adjusted to a specific setting and many readings were manually recorded. For example, ten 20-sec readings at 100 eV were recorded. Then the ion translational energy was adjusted to 0 eV at which energy no ions are transmitted into the collision chamber and ten more 20 sec readings were taken to obtain the background. The average of the background readings was subtracted from the average of the 100 eV readings. This process was repeated for the translational energy values of 2, 5, 10, 15, 20, 30, 40, 50, 60, 70, 80, 90, 100, 110, 120, 130, 140, 150, 160, and 170 eV. Typical energy dependence plots are seen in Figs. 26, 27, 36 through 41, and 53 through 60.

It is important to measure a background reading with the ion translational energy adjusted to 0 eV. Because of differential pumping, there is a flow of target gas through the collision chamber entrance slit into the electrostatic lens region. Collisions of the ion beam with the target gas in this region (where the effective energy is higher than at the collision chamber) also produces radiation. Typical background corrections were on the order of 30% in the VUV region and 45% in the visible region. In the near infra-red region from 700 nm to 870 nm there was also a significant amount of blackbody radiation from the ion source, causing corrections on the order of 65%.

IV. Data Analysis

In this chapter the general outline of the data analysis used for all three systems will be explained. The next three chapters will discuss the results of the data analysis of that particular system. It must be remembered that the limitations of the experimental apparatus dictate that only emissions from energy states with lifetimes of 10⁻⁶ sec or less will be observed. Therefore metastable states of the product species will not be identified in this analysis.

When a 100 eV He^{\dagger} ion beam collides with Cl_2 , Br_2 , or I_2 , the following possibilities exist:

Collision

Reactants Product Species

100 eV He⁺ +
$$X_2$$
 + He⁺ + X_2 * (1)

He +
$$(X_2^+)^*$$
 (2)

$$He^{+} + X_{2}^{+}$$
 (3)

$$He^* + X + X^+$$
 (4)

He +
$$X^* + X^+$$
 (5)

He + X +
$$(X^+)^*$$
 (6)

$$He^+ + X + X^+$$
 (7)

where * represents an excited atom/molecule/ion
X represents Cl, Br, or I

If reactions (1) or (2) are significant, molecular emission lines should be observed. Upon examination of the experimental spectra none of the reported emissions for $C1_2$, $C1_2^+$, Br_2 , Br_2^+ , I_2 , or I_2^+ were present (Refs 16, 27, and 51). Consequently, it is assumed that molecular emissions are insignificant in this experiment. Reaction (3) will be examined in the <u>Further Analysis</u> section of this chapter.

In the cases of Cl_2 , Br_2 , I_2 all of the charge transfer processes, reactions (4), (5) and (6), are exothermic by a much greater amount than the dissociation energy of the (X_2^+) molecule. The overall processes (including dissociation) for the three systems, when both He^+ and X_2 are at thermal energies, are exothermic as indicated

$$He^+ + C1_2 \rightarrow He + C1^+ + C1 + 9.09 \text{ eV}$$
 (8)

$$He^+ + Br_2 + He + BR^+ + Br + 10.77 \text{ eV}$$
 (9)

$$He^+ + I_2 \rightarrow He + I^+ + I + 12.58 \text{ eV}$$
 (10)

Therefore there is a large amount of energy available in the charge transfer process for excitation of neutral atoms or atomic ions.

Reaction (7) is not considered significant. The observed emission lines are still present at He⁺ ion energies of less than 10 eV. This is not enough energy to account for molecular dissociation and excitation of the neutral halogen atom to the excited energy levels detected in this experiment.

Line Identification

The experimental data obtained was in the form of low and high resolution spectra (see Figs. 21 through 25, 30 through 35, and 44 through 52), and measured emission cross section energy dependence curves (see Figs. 26, 27, 36 through 41, and 53 through 60). The analysis of the data began with an examination of the high resolution spectra to determine the observed peak center wavelengths (λ_0) . Then using the instrument function for each λ_0 , all of the observed peak intensities were normalized. By use of the measured cross section values of the more intense peaks as references, each observed wavelength was assigned a partial emission cross section value. Next the observed wavelength λ_0 values with a search interval of $\pm \Delta \lambda_0$ were matched (using a computer search program developed by Dr. Darrell Hopper (Ref 17) with allowed transitions between the energy levels of He I (Ref 42), C1 I (Ref 55), C1 II (Ref 56), Br I (Ref 68), Br II (Ref 58), I I (Refs 30 and 48), and I II (Ref 41). The selection criteria used in the search program were

- 1. $\Delta J = \pm 1$, 0 where 0 \Rightarrow 0
- 2. Change of parity
- 3. $\pm \Delta\lambda_0$ from observed peak center wavelength λ_0 These criteria are valid for LS, JJ or any intermediate type of coupling (Ref 36:271). The complete listings of transitions which meet these criteria are given in Tables XV, XVII, and XVII in Appendices A, B, and C.

The computer identification program can be used in various modes. In the search mode the program applies any or all of the selection criteria listed above to match the wavelengths of allowed transitions to the measured wavelengths λ_0 (see computer output in Fig. 19). For convenience in this discussion, these allowed transitions which meet the above criteria are called A type transitions. Included in this computer output is information as to the electronic configurations, the energy levels, and the J values of both the upper and lower energy states of each allowed A type transition. It also states the wavelength of each allowed A type transition and how closely it matches with the measured wavelength λ_0 . The program can indicate the endothermicity of a particular A type transition for the given reaction. [Note it is not programmed to do this on the output in Fig. 19.]

The computer identification program can also be used in a mode where it will not only list the allowed A type transitions whose wavelengths match the measured wavelength λ_0 , but also lists all of the allowed transitions from the populated upper energy state of the selected A type transition (see Fig. 20). For convenience these additionally listed transitions are called B type transitions. The electron configurations, energy levels, and J values are listed for all the lower energy levels of these B type transitions. In each case the wavelength for the allowed B type transition is listed.

Computer Listing of Allowed Transitions Matching Observed Lines, Fig. 19.

HATCHING O				-						-	-	-				
	MATCHING OF OASERVED TRANSITION	RANS	A SWUITE	DNISIA	S APISING FROM IMPACT OF AN	ICT OF		בר חבר מבסא	200							
ON CL? GAS!	1521+3H 15	•	+ CL2(X1SI+)		HE (*) +	בורונרג	בנו לפו בנו לפו	STABCH	SEABCH OF	# E						
					+ (52)+3H	פרינים	(6)-10 + (+)+10		SEARCH OF	OF CLII						
HICH RESOL	MIGH RESOLUTION DATA								-	,						
HATCH .	1 09554	UZAZ	OBSERVED TRANSITI	ON 10	ITTON TO BE MATCHED	:	7414.00 ±	\$ 5.00		ANGSTROMS WITHIN	WITHIN	2.00		ANGSTE OMS .	CASCADED	
LOWER STATE	LOMER STATE LOMER STATE LOMER STATE	PES	IGNATION			USPE &	UPPER STATE	ISUELI	. D. D.	UPPER STATE -NYMERECOMEIGURAIIOMJ.LEXELKEVI	NO	רבאבו	1725	ENDOTH.	OIFFERENCES (4)	OIFFERENCES (A) SAME
MATCHES FOR HE I	S FOR HE I	:														i
5	. I 10 ol															
	47571 at 1701	57	9	5.5	9.9214	13.	304	304 (30) 40200	a7 000	042		10.5932	1932	19.593	7416.15	51.5
-	6757(ci) 701	45	40	2.5	4.9214	W > 0	L' PODIL.	STEN FR	HOU WOO	PROPULATER FROM UPPER LIVEL		HITH	13 WITH A TORNSTITON OF	TION OF	7416.15	7416.15 A155T204S
	454141144	rs.	40	1.5	8.9471	491	E PCPULATED	ATED FA	10 - OF	FROW UPPER LEVEL		WITH	TRANSI	TO VOIT	1719.71	SHUSSTROMS
	מסר (בם) לכלים	5	40		9.000	> 1	Theoa 3	ATEN CL	3df1 WU	DODOLATEN COOM UPPER LEVEL		MITH E	TOANSITION T		7926.82	A45512045
	259(45)963	2	2:		9.50	144	POPIN ATEN	בוביו בי	oof word			HILL	TEANSITION		4415.37	SHC 2155AV
15.	15207(01)701	2 0	250		10.6521	160	Tilaua :	TOURTED FROM UPPER [140 FOX	PER LEVEL		13 KITH K T2	NCILIZNET 12.	12. 325	7412.91	ENSSTRONS -1.03
	002 501	305		1.5	0.00.0	N 484	E BOOULATED	Da Call	egow upper	JEE LEVEL	15	16P WITH A	T TRANSIT		1935.94	SHCCLSSAV
2.	000 501	306		5.	1001.		E POPULATED		FPON UPP	UPPER LEVEL	L 16P	WITH !	A TRANSITION	TION OF	1014.97	ANGOTROMS
•	6000 (a£) 501	40		1.5	14. 1044				CEUM 1100	PER LEVEL	1 158	MITH B	TRANSIT.	TEON DE	6147.54	AUGET204S
5. 3	שטר (שם ורם רם ו	4.3	663		10.1156	Bu ASM			adn woes	Appen Livel	L 15F	MITH A	TRENSIFION	TION OF	4233.25	£45572745
	שנים ומו ומושו	63	404	1.5	10.4745	**	E PAPILATES			TENET aldan	L 168	WITH I	1 TRANSTITION	1174 DF	6701.25	2 MC = 1 . 2 . 4
10.	ונספונט ואסדום	40	404		11.4997	444	F POPULATED		FUND 19PF	JOURS LIVEL	116.	WITH !	WELLETION	11.04 OF	57.93.92	245574045
	uccuttat) tat	0,	200	1.5	19.6 169	444	E POPULATEN				1 164	WITH A	TRAUSITION		6935.09	ANSSTED 4S
12.	102ch(31) 338	40	500	5.	19.5686	MAY A	E Proul ATEN		FROM UPP	UPPER LEVEL	1 166	WITH	MCITISHAGT A	TION OF	7067.36	SMOCESSAN
17. 4	bo2chld1)hd1	4	002	1.5	10.5012	MAY	E POPULATED		FROM UPP			WITH	A TPANSITION		7150.51	ANGSTROMS
	usadalds las	4	650	1.5	10.6794	. AV.	E POSILATED			UPPER LEVEL	168	WITH A	TPANSITION		7313.79	ANGSTROYS
	15207(41)765	9	152		10.4521	E 49%	E POPULATES		EBON UPPER	-	166	WITH A	MOITISPAST A	TION OF	7412.31	AVSSTROMS
*	TATCHES FOUND															

Computer Listing of Allowed Transitions Matching Observed Lines Plus Other Allowed Transitions from the Same Upper Energy Levels. Fig. 20.

Cory available to DDC does not permit fully legible reproduction.

Further Analysis

Up to this point, the analysis described is firmly based on instrument resolution and quantum mechanical selection rules. Further considerations require the introduction of various assumptions.

An examination of Tables XV, XVI, and XVII reveals a number of lines which could be assigned to allowed He I transitions. It is noticed that these transitions are all in the 400 nm to 870 nm region and are between the higher He I energy levels. If these transitions do originate from He I, then transitions from these upper levels to the ground state should also be observed, but in fact, none are detected. This situation prevails in all of the results from studies of reactions of He^+ with Cl_2 , Br_2 , and I_2 , as well as for reactions of He with H2, Ar, Kr, and Xe, studied by Hughes, Jones, and Tiernan (Refs 18, 10, 20, 21 and 28). Also all lines observed which could be assigned to He I transitions can also be assigned to other processes. All of the processes leading to the He I transitions in the upper levels are highly endothermic (in the neighborhood of 15 eV), and the energy dependence curves obtained for emission lines which might originate from He I all have thresholds below 10 eV. For these several reasons, the author assumes that no significant He I transitions [reactions (3) and (4)] are actually observed in the present experiments.

If a light-emission experiment were performed in a field-free environment the ratio of the actual intensities

of the transitions from a particular energy state should be the same as the ratio of the theoretical A factors (transition probabilities) for the respective transitions from that particular energy state. The He + /halogen experiments are conducted in such a field-free environment and it is therefore assumed that the normalized relative intensities of the observed emissions should be in good agreement with the A factors for these transitions. Unfortunately A factors are available for only a very small number of the transitions observed in our study (Refs 2 and 35). There is a great deal of difficulty in performing an experiment to accurately measure A factors. The most commonly accepted method of measuring A factors is with shock tube experiments. In these experiments errors of less than 50% are considered very good results. In order to do any further analysis, it is thus necessary to make several assumptions. The author feels it is justifiable to compare the ratio of relative intensities reported in the literature (obtained from discharge experiments) with the ratios of relative intensities in the He / halogen experiments, provided that certain precautions are made.

The change in the emission intensity of a transition caused by the presence of an electric field is dependent upon the extent to which the transition matrix is perturbed by the electric field. The extent to which this perturbation affects the intensity of the other possible transitions from the same energy level is dependent upon the total number of

transitions possible from that particular upper energy level. For neutral halogen atoms radiating from low energy states to the ground state there are usually only two transitions possible. If one transition matrix is greatly perturbed, the intensity of the other transition will also be affected. The ratio of the two lines can therefore be greatly affected. This is the case in the VUV region. In the visible and near infrared region, where there are many possible transitions between the higher level energy states, the perturbing of one particular transition matrix has less effect on the other possible transitions.

In such an approach, the next step is to use the computer search program in a form in which it will not only list the allowed type A transitions using the original resolution and quantum mechanical criteria, but will also list the other transitions (including their wavelengths) which are quantum mechanically allowed from the upper energy level of each of these type A transitions. These other transitions are called type B transitions in the present discussion. A sample page of the computer output from this type of search is given in Fig. 20. In Fig. 20 the A type transitions have wavelengths of 7416.16A and 7412.91A. All the other listed transitions are type B transitions. These wavelengths can now be compared with the wavelengths and intensities previously tabulated in the literature for the excited neutral atoms X I (Refs 30, 48, 55 and 68), and for the excited atomic ions X II (Refs 41, 56 and 58).

It should be noted that the optical resolution was much higher for the experiments which yielded the tabulated energy level data than the resolution in the present He⁺/halogen experiments.

The following criteria were established to aid in assignment of the transitions for the measured line wavelengths (λ_0) .

- 1. If a particular type A transition and all of its associated type B transitions were not reported in the tabulated literature data and none of the type B transitions were observed in the He⁺/halogen experiment, then that particular type A transition was eliminated. For the example shown in Fig. 20, this means that if the 7412.91Å and all of its associated type B transitions (1005.96Å, etc.) were not observed in the discharge experiment in Ref 55, and if none of the type B transitions (1005.96Å, etc.) were observed in the He⁺/halogen experiment; then the 7412.91Å wavelength of the 4p 2 S $^0_{1/2}$ + 5d 2(1) $^{1/2}$ transition would be eliminated as a possible match for the λ_0 value of 7414.00Å.
- 2. In the 400 nm to 870 nm region the additional criterion is used: If in the discharge experiment a particular type B transition was much more intense than the type A transition with which it was associated, and in the He⁺/halogen experiment that particular type B transition was less intense than the type A transition, then that particular type A transition was eliminated. For the example shown in Fig. 20, this means that if in the literature tables the

7313.78Å line of the 4p $^4S_{3/2}^0 + 5d \ 2(1)_{1/2}$ transition was much more intense than the 7412.91Å line of the 4p $^2S_{1/2}^0 + 5d \ 2(1)_{1/2}$ transition, and the 7313.78Å line was much less intense than the 7414.00Å line in the He⁺/halogen experiment, then the 7412.91Å wavelength of the 4p $^2S_{1/2}^0 + 5d \ 2(1)_{1/2}$ transition would be eliminated as a possible match for the λ_0 value of 7414.00Å.

Another criterion that was used was that if the energy dependence curve for a particular λ_0 was exothermic and only one of the type A transitions matching that λ_0 was exothermic; then that type A transition was selected as the assigned transition.

thermic and endothermic reaction energy dependence curves.

Examination of the cross section energy dependence curve can help to determine whether the reaction causing the observed radiation is endothermic or exothermic. The characteristic shape of endothermic reaction energy dependence curves is a threshold somewhere above thermal energies and the curve increases in value with an increase of energy until it reaches a leveling off point. (Actually a true endothermic reaction energy dependence curve would have a step function profile with the threshold at the value of the energy necessary to be added to thermal reactants for the endothermic reaction to occur.)

A typical example of the profile of an endothermic reaction energy dependence curve is illustrated by the 821.7 and 822.4 nm emission lines in Fig. 27. Exothermic reaction energy

dependence curves have the characteristic profile of small values at higher energies and rapidly increasing in value as thermal energies are approached. A typical example of the profile of an exothermic reaction energy dependence curve is illustrated by the 178.23 nm emission line in Fig. 54.

After applying these criteria to the total list of type A transitions for the He⁺/Cl₂ and He⁺/Br₂ experiments it was found that over 80% of the total emission lines could be assigned to specific transitions (Tables V and IX). These transition assignments are then used to construct a term diagram (Figs. 28 and 42). Next each energy level on the term diagram is individually examined to determine whether that state is predominantly directly excited or populated primarily by cascading from higher energy states (Tables VI and X).

A plot of the emission cross sections and of the direct excitation cross sections as a function of the energy levels of the populated energy states provides an indication of the energy partitioning in these reactions (Figs. 29 and 43).

Error Analysis

The accuracy of the 100 eV cross sections reported in this experiment vary. As noted before, the emission cross section is given by

$$\sigma = \frac{4\pi R_0 T_0 N_R}{P \ell N_A I \Omega_{g_L} F(\lambda)}$$
 (6)

where the symbols are defined in Table I. The maximum temperature T_{0} variation is 1% so it will be considered a constant.

Relative Cross Sections. When referring to the accuracy of relative cross sections it is necessary to consider only the variables appearing in the expression, $\frac{N_R}{PIF(\lambda)}$. accuracy of Np depends on the signal to noise ratio. For very intense peaks it is very accurate (to within ±5%) and for very weak peaks it can be accurate to within ±50%. The accuracy of N_D also depends upon how many measurements were taken. Because more measurements were taken, the cross sections measured for the energy dependence curves are generally more accurate than the cross sections calculated from the peak heights in scans. The 100 eV He ion beam crosssection measurements for the energy dependence curves have a sampling accuracy of within ±5%. Even the 5 eV He ion beam cross-section measurements for the more intense peaks generally have a sampling accuracy of within ±10% to ±15%. Occasionally the statistical error increases to 230%. Of course the cross section measurements for the weaker emissions obtained only from spectral scans, have a greater statistical error. The relative pressure P has a 5% or less error. The relative current I could have errors of 10 to 20%. The error in the relative instrument function $F(\lambda)$ in the visible region is less than 10% and as explained in Chapter II could be as high as 200% in the VUV region. The relative crosssection measurements in this experiment are consistent with

present published work using ion beam experiments for similar reactions.

Absolute Cross Sections. In absolute cross section measurements, the systematic errors no longer cancel out. Such things as the exact length of the collision region are difficult to measure. Also the beam is not uniform over the area of the collision region, although this error appears not to be large since an ion beam on the order of 1 nA is measured with the collision chamber having a 1 mm slit and an ion beam on the order of 0.1 nA is measured with the collision chamber having a 0.1 mm slit. For the stronger peaks, the accuracy is believed to be within a factor of 4 in the 400 nm to 870 nm region and a factor of 8 in the VUV. Because of the difficulties in the accurate measurements of the ion beam above 110 eV and below 20 eV the error in the measurement of absolute cross sections in these regions can be very large. The consistency of the cross section measurements is very good, even with the use of different detectors. This is illustrated in Fig. 55, where the cross section measurements for the production of the 145.7 nm iodine emission line vary up to ±40% on three separate days with two different detectors. In Fig. 56 the cross section measurements for the intense 183.0 nm iodine emission line vary generally less than ±15%. The 183.0 nm line measurements were made on two separate days using two different detectors.

V. Chlorine

Introduction

The general outline of the next three chapters follows the data analysis procedures described in Chapter IV. First the experimental data is presented in the form of the spectra obtained in the experiment and curves showing the He ion translational energy dependence of some of the measured emission cross sections. Complete listings of the measured cross sections of all of the observed emission lines are given in the tables in the appendices. These tables include the measured cross sections of each emission line and a listing of all of the allowed transition assignments for each emission line which meet the measurement uncertainty $\Delta\lambda_0$ and quantum-mechanical criteria stated in Chapter IV. Other detailed information for each allowed transition is given in these tables. A summary of the tables in the appendices is then presented in the text depicting important general features of the reaction. In the case of chlorine and bromine, further analysis is conducted resulting in term diagrams and graphs which give further insight into the reactions.

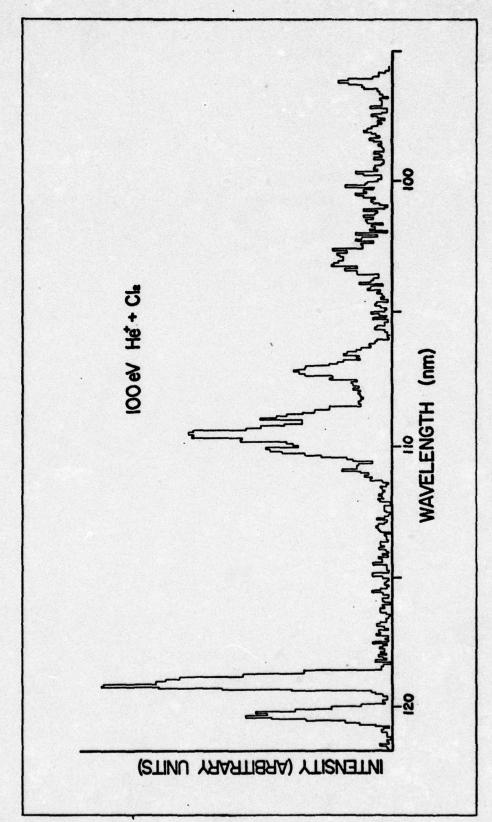
All of the spectra illustrated in this chapter and all of the cross sections listed in the tables of this chapter, were obtained from the reaction of 100 eV He⁺ ions with Cl₂ at room temperature. The translational energy of the He⁺ ions was varied only in the measurements of the energy dependence of the cross sections depicted in Figs. 26 and 27.

Spectra

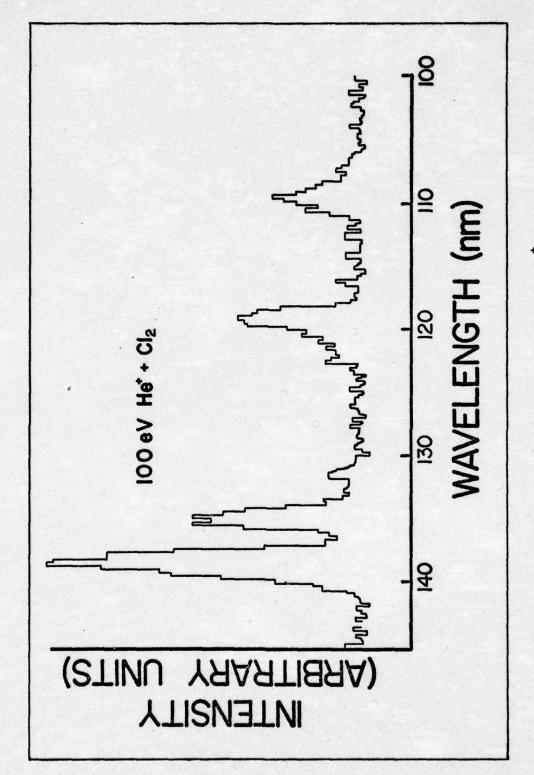
The 35 measureable chlorine emission lines observed in the 60 nm to 870 nm wavelength region are presented in Figs. 21 to 25. A high resolution spectrum of the 96 nm to 120 nm VUV region is shown in Fig. 21. Figures 22 and 23 depict examples of low and high resolution spectra of the 100 nm to 145 nm VUV region. The remaining spectra in Figs. 24 and 25 are high resolution spectra in the 720 nm to 860 nm region.

Cross Section Energy Dependence Curves

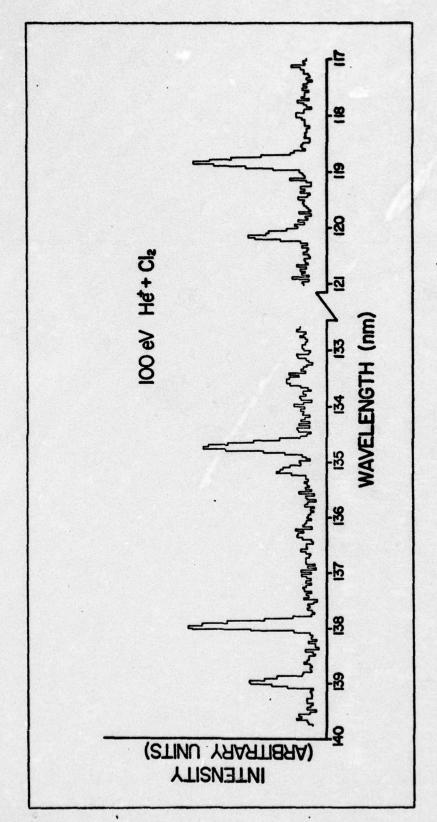
The curves in Figs. 26 and 27 depicting the energy dependence of the chlorine cross sections, were obtained from measurements made under low resolution conditions. The wavelengths assigned to each curve are the observed wavelengths at high resolution. It should be noted again that cross section measurements using this instrument are most accurate in the 100 eV region. In the 120 eV to 170 eV region not all of the ions can be collected on the ion collector so the actual cross section values are probably greater than the measured values in this energy region. In the 0 eV to 20 eV region the ion beam starts to diverge and is difficult to focus. Consequently, the size of the ion beam drops off, increasing the % error in the ion beam measurement. The curves indicate that all of the lines except the 137.93 nm, 138.98, and 139.58 nm curve are produced by endothermic processes with low thresholds in the 0 eV to 5 eV region.



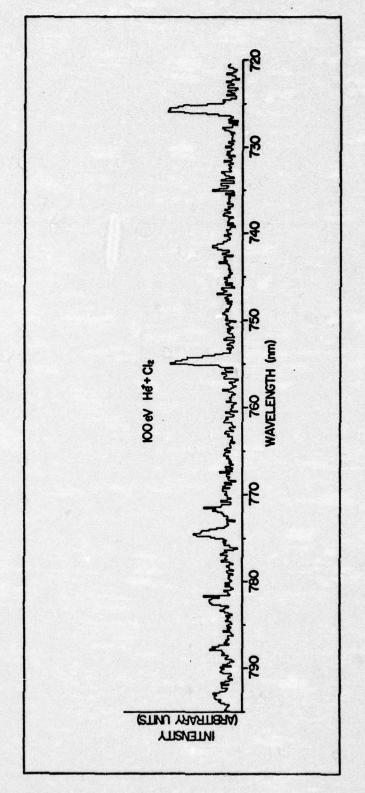
High Resolution Spectra of 100 eV He^+ Cl $_2$ Reaction in 95 nm to 122 nm Region. Fig. 21.



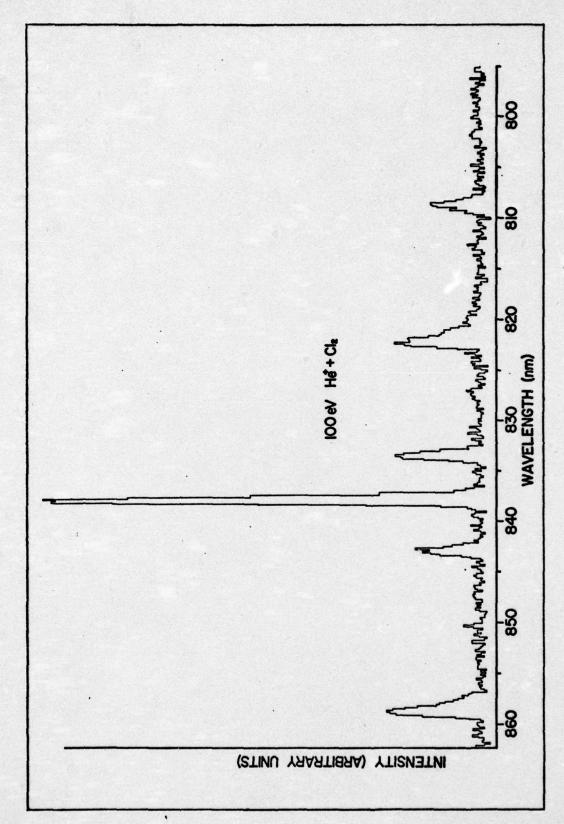
Low Resolution Spectra of 100 eV He^+ + Cl_2 Reaction in 100 nm to 145 nm Region. Fig. 22.



High Resolution Spectra of 100 eV He^+ + Cl_2 Reaction in 117 nm to 140 nm Region. Fig. 23.



High Resolution Spectra of 100 eV He $^+$ + C1 $_2$ Reaction in 720 nm to 795 nm Region. Fig. 24.



High Resolution Spectra of 100 eV He^+ + Cl_2 Reaction in 795 nm to 865 nm Region. Fig. 25.

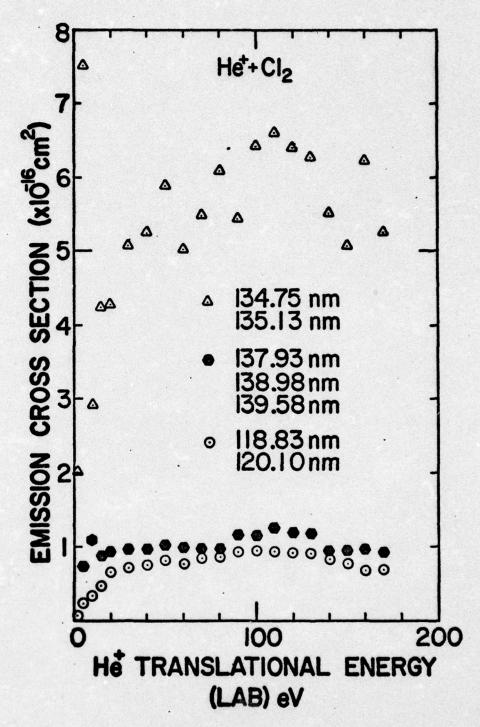


Fig. 26. The Energy Dependence of the Emission Cross Sections of Selected VUV Lines from the He⁺ + Cl₂ Reaction.

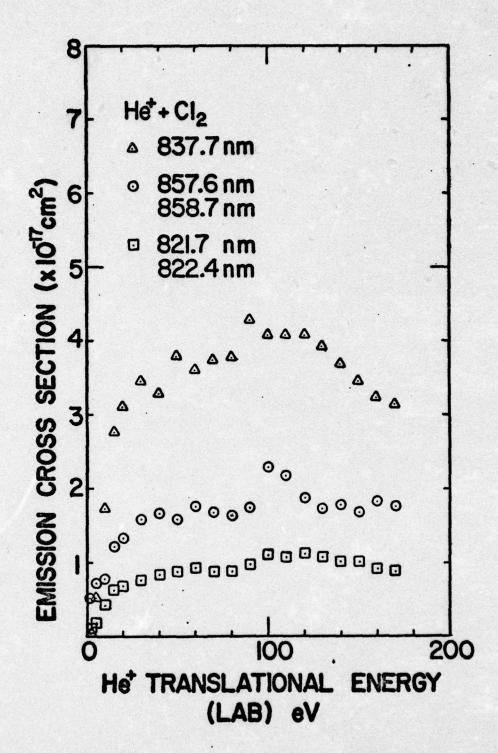


Fig. 27. The Energy Dependence of the Emission Cross Sections of Selected Lines from the He⁺ + Cl₂ Reaction.

The uncertainties listed above, plus the limited 0 eV to 170 eV energy region, preclude extensive analysis as to structure and oscillations being present in the curves. The structure and oscillations of the cross section energy dependence curves discussed in the investigations of He⁺-rare gas systems extended over the 0 eV to 10 keV energy region (Refs 5, 8, 9, 24, 38, 59, and 60). The 0 eV to 170 eV energy range is too limited to interpret separately. The data is presented here to aid in the selection of transition assignments and for completeness. As in the case of the He⁺-rare gas studies, these curves could be used in conjunction with other studies in higher energy regions for a more complete analysis of the kinetic energy behavior of the reaction.

Line Identification

A listing of all of the allowed transitions which meet the measurement uncertainty $\Delta\lambda_0$ and quantum-mechanical criteria explained in Chapter IV for each observed wavelength λ_0 in the spectra, are listed in Table XV in Appendix A. The measured cross-section for each observed wavelength is also listed. The endothermicity in eV (for thermal energy reactants) is listed for each allowed transition's upper state. This endothermicity is measured above and below the 9.09 eV energy released by the thermal energy charge exchange reaction between He $^+$ and Cl $_2$. Of course there are 100 eV of translational energy of the He $^+$ ion available in the collision process for possible conversion to excitational energy

of the product species. One goal of the present experiment is to determine if this translational energy conversion is very efficient in the 100 eV He⁺/Cl₂, Br₂, and I₂ reactions. Comparison of the energy level of the upper radiating energy states with the energy available from thermal energy charge transfer is an aid in determining whether the dominant excitation mechanism for the product species is charge exchange or conversion of translational energy. It should be noted that the 438.0 nm and 579.6 nm observed wavelengths were very weak peaks observed only on low resolution scans. They are included for completeness.

Further Analysis

Table IV is a summary of the complete listings in Table XV. It is noteworthy that the $497.0 \times 10^{-18} \text{ cm}^2$ total emission cross-section is very large and that 76% of the total cross section is accounted for by the 17 observed VUV lines. Since 23 lines match both allowed C1 I and C1 II transitions, it is evident that further analysis is necessary.

Application of the relative intensity criteria described in Chapter IV on the allowed transitions listed in Table XV revealed that the reaction yields emission arising predominantly from Cl I. The resulting Cl I transition assignments are listed in Table V. They account for 85% of the total 483.7 x 10⁻¹⁸ cm² emission cross section of the lines listed in Table XV having possible Cl I transition assignments.

A large number of the transitions which were eliminated by the relative intensity criteria violate the conservation of

Table IV

Summary of 100 eV He + Cl2 Reaction Allowed Transitions Selected by the Computer Search Program

Classification of Allowed Transitions Listed in Nur Computer of Search Lin	s Number [o of Lines (x10	ion Number σ of Lines σ	Σο Στοται ^ο	Number of VUV Lines	$\frac{\sum_{\text{VUV}^{\sigma}}}{(\text{x10}^{-18}\text{cm}^2)} \frac{\sum_{\text{VUV}^{\sigma}}}{\sum_{\text{Total}^{\sigma}\text{VUV}}}$	Σνυν ^σ Στοτα1 ^σ νυν	Number of Visible Lines	Visible (x10-18cm ²)	Σvisible Σvisible (x10 ⁻¹⁸ cm ²) Στοται ^σ visible
1 15	o	63.5	0.13	٧	56.7	0.15	ю	8.9	0.06
11 13	ю	13.3	0.03	ю	13.3	0.04	0	1	•
C1 I and C1 II	23	420.2	0.85	∞	305.9	0.81	15	114.3	0.94
Tota1	88	497.0		11	375.9		18	121.1	
					76% of			24% of	
					Total	•		Lotal	

Table V

C1 I Transition Assignments for the 100 eV He⁺ + C1₂ Reaction

a	Transition Assignmen	nt AH ^b	o ^C
^T (nm)	Lower + Upper	(eV)	$(cm^2 \times 10^{18})$
118.875	$3p^{5} {}^{2}P_{3/2}^{0} + 4s'^{2}I$	3/2 1.34	61.9
118.877		0 _{5/2} 1.34	01.5
120.135	그리고 하는데 하는데 아이들이 아니는데 그는데 하는데 하는데 하는데 하는데 하는데 하는데 하는데 하는데 하는데 하	3/2 1.34	33.4
133.573	$3p^{5} {}^{2}P_{3/2}^{0} + 4s {}^{2}P_{1}$	0.19	9.2
134.724	$3p^{5} {}^{2}P_{3/2}^{0} + 4s {}^{2}P_{3}$	0.11	45.6
135.166	$3p^{5} 2p_{1/2}^{0} \leftarrow 4s^{2}p_{1}$	0.19	11.9
136.345	$3p^{5} {}^{2}p_{1/2}^{0} \leftarrow 4s {}^{2}p_{1/2}$	0.11	13.8
137.953	- 5 2-0 . 4-	-0.10	73.0
138.969	$3p^{5} {}^{2}p_{3/2}^{0} \leftarrow 4s {}^{4}p_{3}$	5/2 -0.17	
138.996	$3p^{5} {}^{2}P_{1/2}^{0} \leftarrow 4s {}^{4}P_{1}$	-0.06	47.9
139.653	$3p^{5} {}^{2}p_{1/2}^{0} \leftarrow 4s {}^{4}p_{1}$	-0.10	5.4
725.862	4s ⁴ P _{5/2} + 4p ⁴ S	3/2 1.54	5.7
741.616	$4s^{4}P_{5/2} + 4p^{2}P_{5}$	3/2 1.50	1.6
754.915	4s ⁴ P _{3/2} + 4p ⁴ S	3/2 1.54	6.1
771.971	$4s^{4}P_{3/2} \leftarrow 4p^{2}P_{3}$	1.50	1.5
774.710	1	3/2 1.54	3.2
782.351	$4p^{4}P_{5/2}^{0} + 4d^{2}($		2.0
788.038	$4s^{4}P_{5/2} + 4p^{2}D_{5}^{2}$	5/2 1.40	1.5
821.430	$4s^{4}P_{5/2} + 4p^{4}D$	0 1.34	3.3
822.400	$4s^{4}P_{3/2} + 4p^{2}D$	5/2 1.40	7.7

Table V (continued)

C1 I Transition Assignments for the 100 eV He + C1₂ Reaction

λ _T a	Transition Assignment	ΔH ^b	$\sigma^{\mathbf{c}}$
(nm)	Lower + Upper	(eV)	$(cm^2 \times 10^{18})$
833.560	$4s^{4}P_{3/2} + 4p^{4}D_{3/2}^{0}$	1.38	7.6
837.824	$4s^{4}P_{5/2} + 4p^{4}D_{7/2}^{0}$	1.31	40.7
843.057	$4s ^4P_{1/2} + 4p ^4D_{1/2}^{\circ}$	1.41	5.6
857.760	$4s {}^{4}P_{1/2} \leftarrow 4p {}^{4}D_{3/2}^{0}$	1.38	8.9
858.834	$4s^{4}P_{3/2} + 4p^{4}D_{5/2}^{0}$	1.34	14.0
			411.5

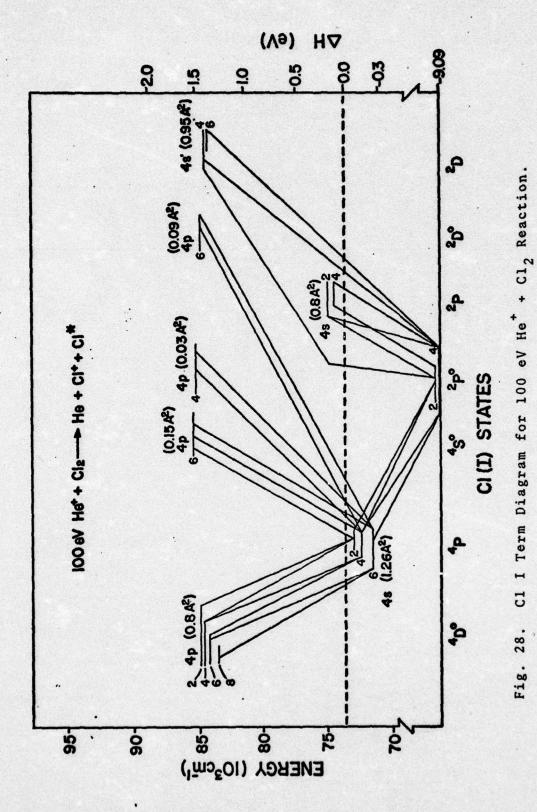
aCalculated vacuum wavelength using the energy level tables (Ref. 55).

^bEnthalpy change required to populate the upper energy state for the thermal reaction $He^+ + Cl_2 \rightarrow He + Cl^+ + Cl^*$.

 $^{^{\}mathrm{c}}$ Emission cross section for 100 $\mathrm{He}^{^{+}}$ + Cl_{2} reaction.

spin $\Delta S = 0$ and the conservation of angular momentum $\Delta L = \pm 1$, 0 selection rules of LS coupling (Ref 36:271). For example, the computer search program has listed the C1 II 4s $^3S_1^0 + 8f^5F_2$ transition as an allowed transition for the observed 137.925 nm emission line. This transition violates both the conservation of spin and conservation of momentum rules of LS coupling. Since chlorine is a relatively light atom, a large amount of LS coupling would be expected. This agreement is a further supportive check of the selection criteria.

A term diagram illustrating the assigned Cl I transitions in Table V is shown in Fig. 28. The total emission cross section of each energy state is shown in parentheses, next to the energy state designation. The small numbers next to each energy level are the 2J + 1 values for that specific energy level. The energy available from the thermal charge transfer process is indicated by a dashed line. Only the 4s 4P state is a low enough energy level to be populated exclusively by the 9.09 eV available from the thermal charge transfer process. There must be a conversion of up to 1.5 eV of the kinetic energy of the incident He ion to populate the upper states depicted on the term diagram. This explains the endothermic reaction profiles of the cross section energy dependence curves. This also explains the smaller cross sections of the high level energy states. Since the lowest energy state of C1 II is about 2.5 eV endothermic, this also explains why few ionic transitions are observed.



Another interesting observation in Fig. 28 is that there are three cases of violation of spin ($\Delta S = 0$) for LS coupling. The 4s ${}^4P + 4p {}^2P^0$ and 4s ${}^4P + 4p {}^2D^0$ transitions are explainable since they have small emission cross sections (0.03 A² and 0.09 A² respectively). Although the chlorine atom is relatively light, it is heavy enough not to be a perfect model for LS coupling. The 3p⁵ ²p⁰ + 4s ⁴P transition is at first puzzling, because this transition has the largest emission cross section on the term diagram. The most reasonable explanation is that the 4s 4P state is the lowest even energy state in the neutral chlorine atom, and the only radiative transition for decay is to the 3p⁵ ²P^o ground state. This means that is is possible the 4p 4P state has a longer lifetime than the upper states of the transitions cascading into the 4s 4P state. If the ratio of these lifetimes is a factor of ten or greater, it may be possible that a properly designed chlorine laser would radiate in the VUV at 137.953 nm, 138.969 nm, 138.99 nm or 139.653 nm.

The results of examining each energy level in the Cl I term diagram to determine its direct excitation cross section are listed in Table VI. This is done by subtracting the sum of the cross sections of the transitions having this energy level as a lower energy state, from the sum of the cross sections of transitions having this energy level as an upper energy state. The results are that the total direct formation cross section is 326.7×10^{-18} cm², which is 79% of the

Table VI

<u>Emission and Cascading Cross Sections for Cl I States</u>

<u>Observed in the 100 eV He⁺ + Cl₂ Reactions</u>

C1 I		Cross Sec	ction (cm ² x	10 ¹⁸)
State Designation	ΔH ² (eV)	Total Emission	Cascading	Direct Formation
3p ⁴ 4s ² P _{1/2}	0.19	21.1	 .	21.1
4s ² P _{3/2}	0.11	59.4	-	59.4
4s ⁴ P _{1/2}	-0.06 -0.17	47.9	70.5	-22.6
4s ⁴ P _{5/2} 4s ⁴ P _{3/2}	-0.10	78.4	36.9	41.5
4s' ² D _{3/2}	1.34	95.3		95.3
4s' ² D _{5/2}	1.34)			
4p 4s ⁰ 3/2	1.54	15.0		15.0
4p ² p ⁰ _{3/2}	1.50	3.1		3.1
4p 4po 5/2	1.19	*	2.0	-2.0
4p ² D _{5/2}	1.40	9.2		9.2
4p 4D _{1/2}	1.41	5.6		5.6
4p 4D _{3/2}	1.38	16.5		16.5
4p 4D _{5/2}	1.34	17.3		17.3
4p 4p ^o _{7/2}	1.31	40.7		40.7
4d ² (3) _{7/2}	2.78	2.0	3	2.0 b
		411.5		326.7 ^b

^{*}Note: 4p 4p0 states radiate outside wavelength range of detector.

^aEnthalpy change required to populate this energy state for the thermal reaction $\text{He}^+ + \text{Cl}_2 \rightarrow \text{He} + \text{Cl}^+ + \text{Cl}^*$ (the first radiating Cl⁺ state is 2.43 eV endothermic).

b This total does not include the negative direct formation cross sections in this column.

AIR FORCE INST OF TECH WRIGHT-PATTERSON AFB OHIO SCH--ETC F/G 20/8 EMISSION CROSS-SECTION MEASUREMENTS OF LOW ENERGY HE(+) IONS WI--ETC(U) AD-A034 035 SEP 76 K E SIEGENTHALER DS/PH/76-2 NL UNCLASSIFIED 2 OF #4 AD A034035 100

OF 2/2 34035

411.5 x 10⁻¹⁸ cm² total emission cross section of the neutral model. It should be noted that the two negative numbers in the direct formation column are neglected. Negative direct formation cross sections mean that the energy level either, (1) has a lifetime longer than 1 µsec which is the average time for an atom to stay in the collision focal region of the collision chamber, (2) decays in a radiative region outside of the 50 nm to 870 nm region, or (3) the instrument function of the apparatus used for the VUV region is too low.

A plot of the emission cross sections and the direct formation cross sections as a function of the energy levels of the C1 I atom is given in Fig. 29. The number of states available for population in each energy interval is also presented in Fig. 29. This analysis indicates that the energy of the 100 eV He⁺/C1₂ reaction is predominantly transferred to chlorine neutral atoms which are excited to their lower energy states. Formation of these states requires the addition of less than 2 eV of energy than is available from the thermal energy charge transfer process. It appears the predominant process is

As a check on the validity of using the intensity criteria stated in Chapter IV, a comparison of the relative intensities for transitions observed in discharge experiments reported in the tabulated literature data (see Ref 55), cross

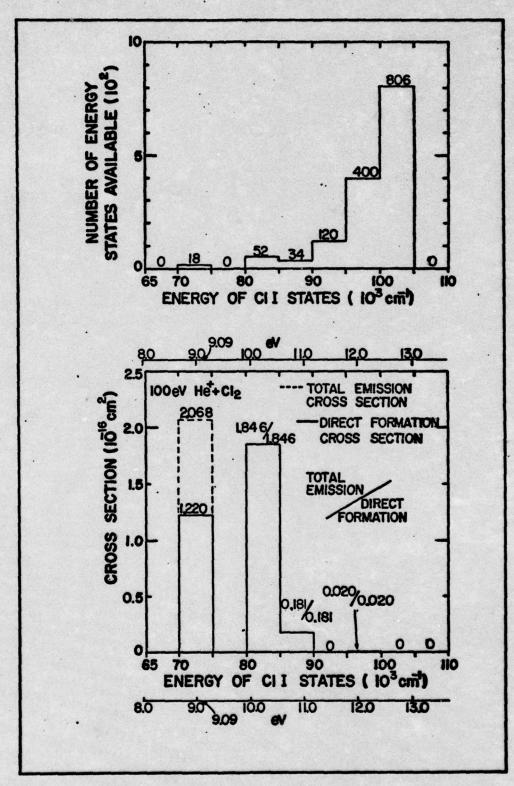


Fig. 29. Comparison of C1 I Emission Cross Sections and Direct Formation Cross Sections as a Function of the Energy Levels of the C1 I Atom.

sections measured in the present He⁺/Cl₂ reaction experiment, and A factors measured in shock tube experiments (Ref 2) are given in Table VII. It can be seen that for transitions from the same upper state the He⁺/Cl₂ experiment yields data which agrees very well with the A factors obtained in a shock tube. Both of these are relatively field free environments. The relative intensities derived from discharge experiments also agree fairly well with both the He⁺/Cl₂ reaction results and the shock tube results. It should be noted that all of these lines are in the 700 nm to 900 nm region which supports the use of the intensity criteria stated in Chapter IV for analysis in this spectral region.

Table VII

Relative Transition Probabilities for Selected Cl I Transitions in the 700 nm to 870 nm Region

Transi	Transition State	tate	e V	q.p		AA
Lower		Upper		$(cm^2 \times 10^{18})$	RIC	(10° sec + 30%
4s 4p 1/2	+	4p 4S _{3/2}	774.710	3.2	10,000	0.063
4s 4p 3/2	+	4p 4S _{3/2}	754.915	6.1	11,000	0.120
4s 4P 5/2	+	4p 4S _{3/2}	725.862	5.7	7,500	0.152
4s 4p 1/2	+.	4p 2p0	792.66	<1.0	3,000	0.021
4s 4p 3/2	+	4p 2p0 4p 3/2	171.971	1.5	7,000	0.030
4s 4p 5/2	•	4p 2po	741.616	1.6	2,000	0.047
4s 4p 3/2	٠	4p 2p _{5/2}	822.400	7.7	20,000	0.056
4s 4p 5/2	+	4p 2p0 5/2	788.038	15	3,000	0.0179
4s 4p1/2	٠	4p 4p0,1/2	843.057	5.6	15,000	0.190
4s 4p 3/2	٠	4p 4p01/2	819.67	<1.0	2,500	0.042

Table VII (continued)

Relative Transition Probabilities for Selected Cl I Transitions in the 700 nm to 870 nm Region

						P
Transition State	ion St	ate	ه ښر س	d o		A ⁻ (10 ⁸ sec ⁻¹)
Lower		Upper	(ma)	$(cm^2 \times 10^{18})$	$^{ m RI}^{ m c}$	+30%
4s 4p1/2	+	4p 4p ⁰ 3/2	857.760	8.9	20,000	0.114
4s 4p 3/2	•	4p 4p _{3/2}	833.560	7.6	18,000	0.089
4s 4p 3/2	٠	4p 4p _{5/2}	858.834	14.0	75,000	0.99
4s 4p 5/2	+	4p 4p ^o 5/2	821.430	3.3	18,000	0.055

acalculated vacuum wavelength using the energy level tables (Ref. 55).

^bEmission cross section for 100 eV He + Cl₂ reaction.

Relative intensity in discharge experiments (Ref. 55).

d-factors measured in shock tube experiment (Ref. 2).

VI. Bromine

Introduction

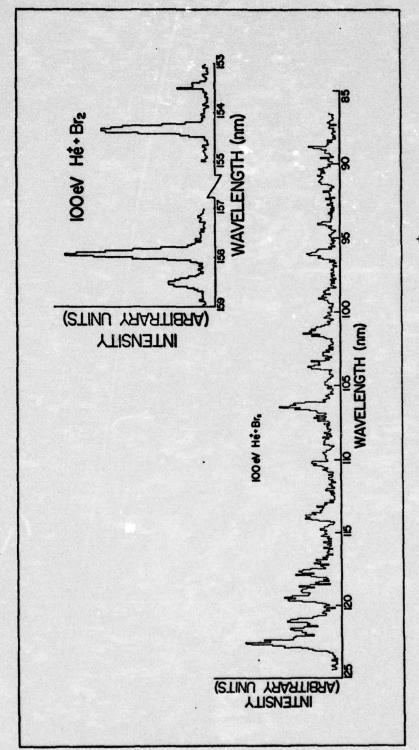
The material in this chapter is presented in the same manner as for the chlorine reaction in Chapter V. All of the spectra illustrated in this chapter and all of the cross sections listed in the tables of this chapter, were obtained from the reaction of 100 eV He⁺ ions with Br₂ at room temperature. The translational energy of the He⁺ ions was varied only in the measurements of the energy dependence of the cross sections depicted in Figs. 36 to 41.

Spectra

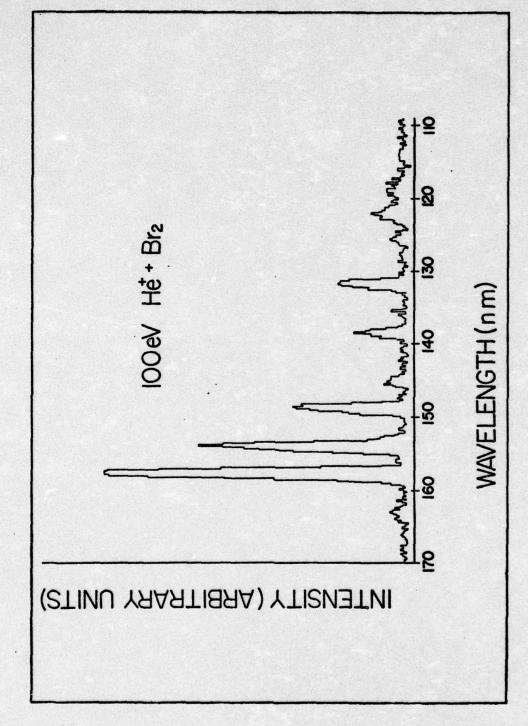
The 57 measureable bromine lines observed in the 60 nm to 870 nm wavelength region are presented in Figs. 30 to 35. A high resolution spectrum of the 85 nm to 159 nm VUV region is shown in Fig. 30. Figures 31 and 32 depict examples of low and high resolution spectra of the 110 nm to 170 nm VUV region. The remaining spectra are high resolution spectra in the 440 nm to 870 nm region.

Cross Section Energy Dependence Curves

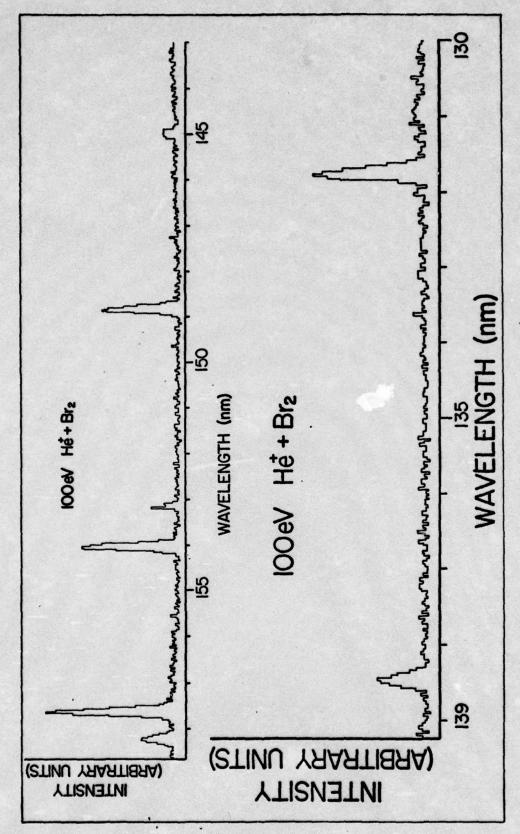
The curves in Figs. 36 to 41 depicting the energy dependence of the bromine cross sections, were obtained from measurements made under low resolution conditions. The same cross section measurement limitations apply in the 120 eV to 170 eV region and in the 0 eV to 20 eV region, as cited for chlorine in Chapter V. The curves indicate evidence of lines



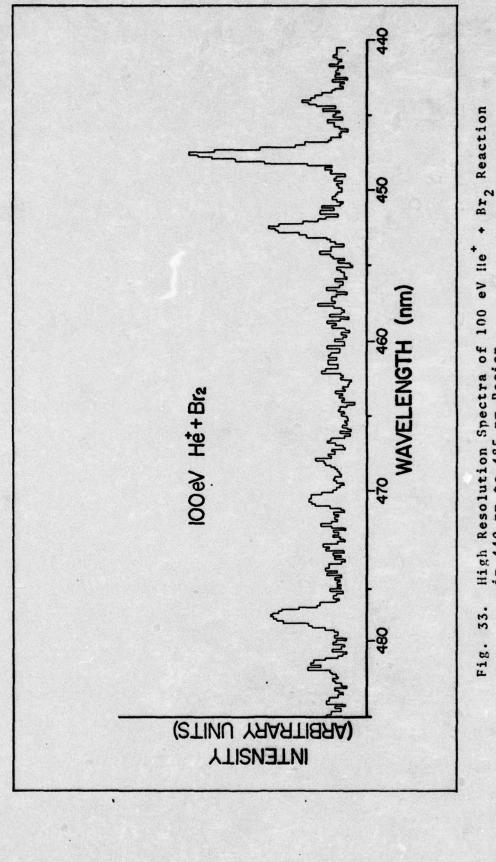
Br₂ Reaction High Resolution Spectra of 100 eV He in 85 nm to 159 nm Region. Fig. 30.



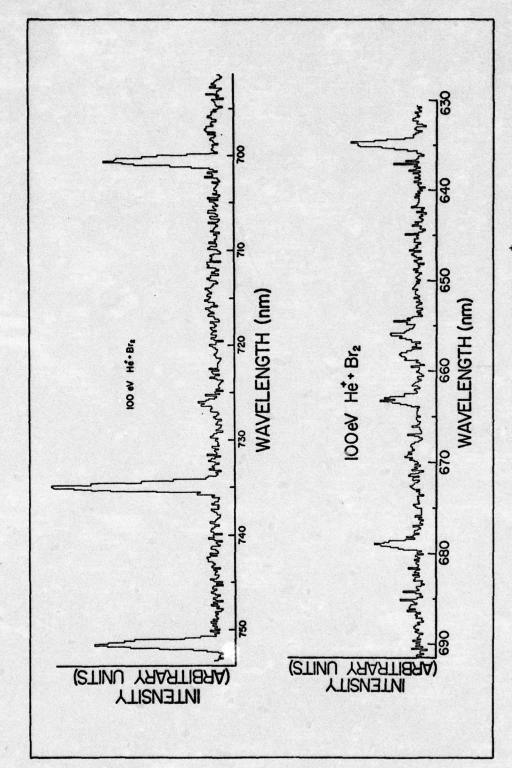
Low Resolution Spectra of 100 eV He^+ + Br_2 Reaction in 110 nm to 170 nm Region. Fig. 31.



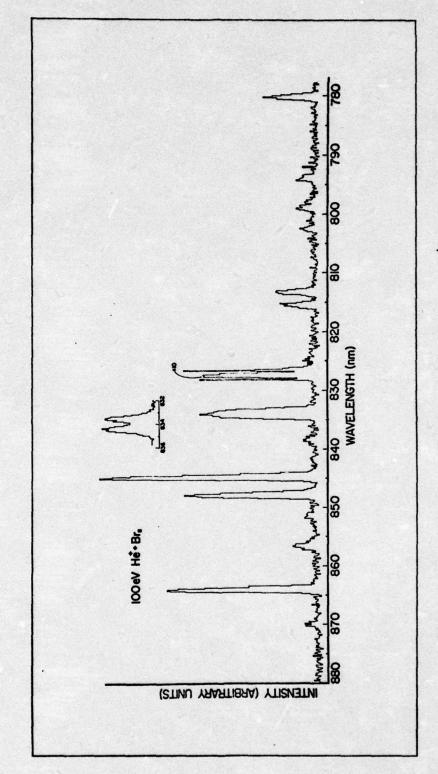
High Resolution Spectra of 100 eV He^+ + Br_2 Reaction in 130 nm to 160 nm Region. Fig. 32.



High Resolution Spectra of 100 eV He^+ + Br_2 Reaction in 440 nm to 485 nm Region.



High Resolution Spectra of 100 eV He^+ + Br_2 Reaction in 630 nm to 755 nm Region. Fig. 34.



High Resolution Spectra of 100 eV He^+ + Br_2 Reaction in 775 nm to 880 nm Region. Fig. 35.

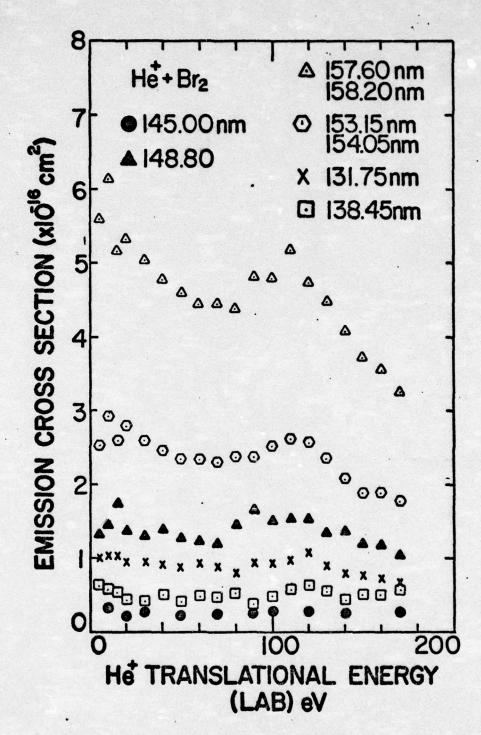


Fig. 36. The Energy Dependence of the Emission Cross Sections of Selected VUV Lines from the ${\rm He}^+$ + ${\rm Br}_2$ Reaction.

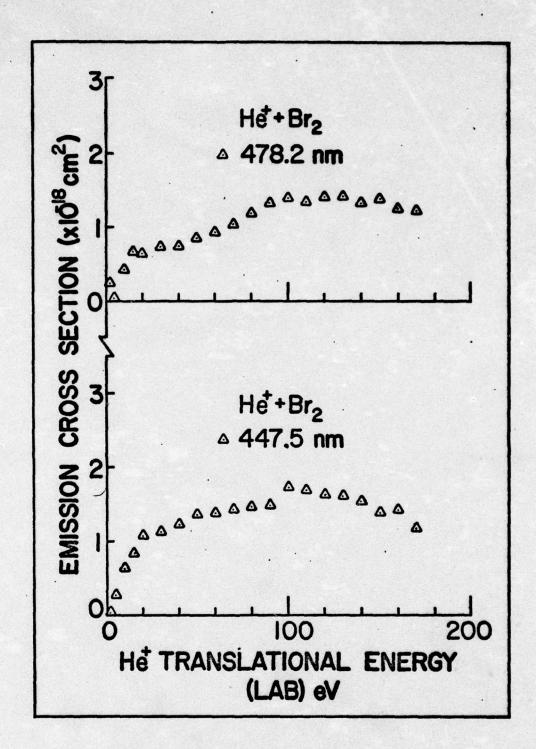


Fig. 37. The Energy Dependence of the Emission Cross Sections of the 447.5 nm and 478.2 nm Lines from the He⁺ + Br₂ Reaction.

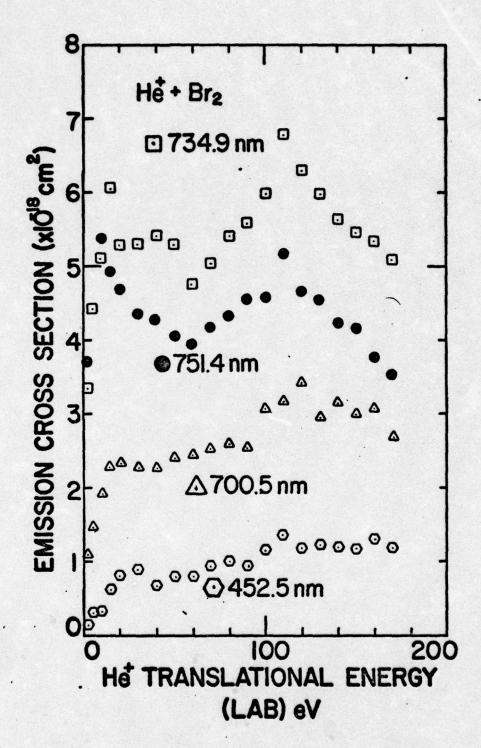


Fig. 38. The Energy Dependence of the Emission Cross Sections of Selected Visible Lines from the He⁺ + Br₂ Reaction.

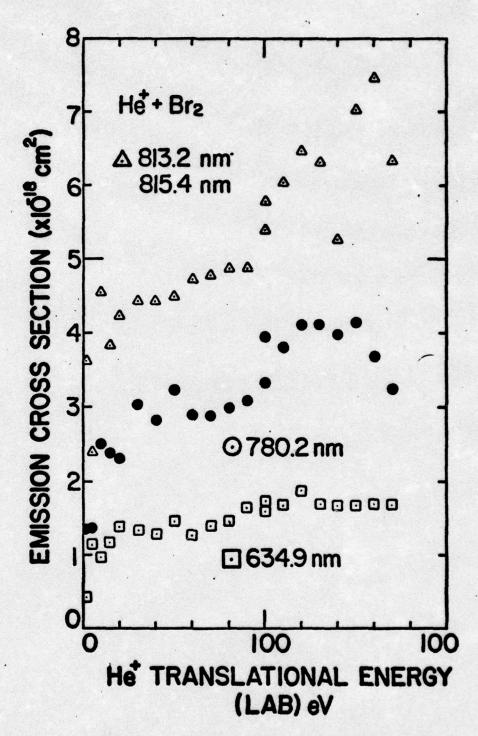


Fig. 39. The Energy Dependence of the Emission Cross Sections of Selected Lines from the He⁺ + Br₂ Reaction.

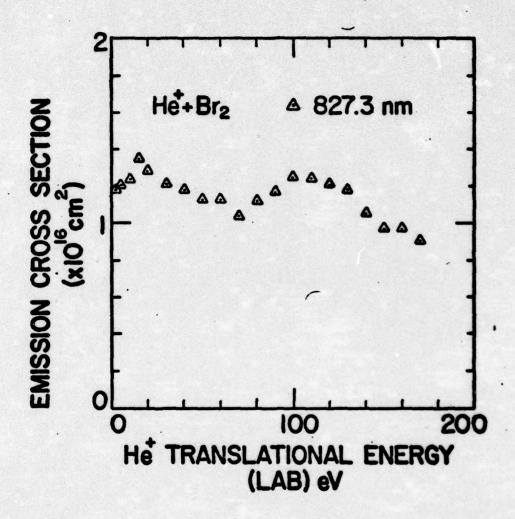


Fig. 40. The Energy Dependence of the Emission Cross Section of the 827.3 nm Line from the He⁺ + Br₂ Reaction.

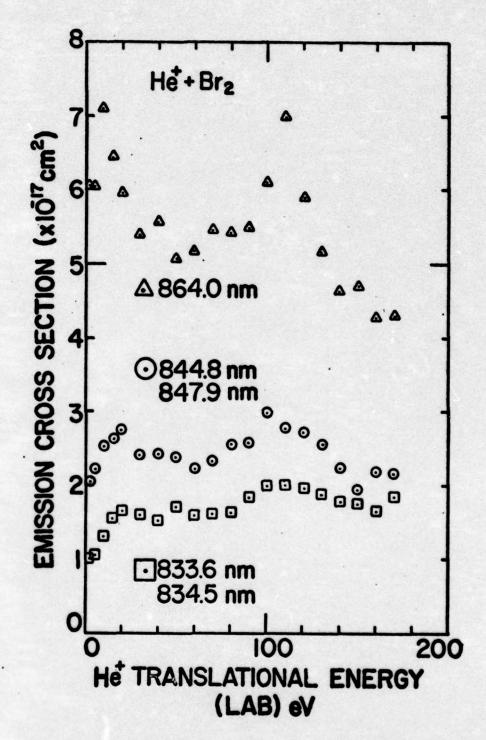


Fig. 41. The Energy Dependence of the Emission Cross Sections of Selected Infrared Lines from the He + Br 2 Reaction.

produced by both exothermic processes (such as the 157.60 nm and 158.20 nm line in Fig. 36) and endothermic processes with low thresholds in the 0 eV to 5 eV region (see Fig. 37). Again, as in Chapter V, all of the cross section energy dependence curves are presented to aid in the selection of transition assignments and for completeness.

Line Identification

A listing of all of the allowed transitions which meet the measurements uncertainty $\Delta\lambda_0$ and the quantum-mechanical criteria described in Chapter IV for each observed wavelength λ_0 in the spectra, are listed in Table XVI in Appendix B. The measured cross section for each observed wavelength is also listed. The endothermicity in eV for thermal energy reactants is listed for each allowed transition's upper state. This endothermicity is measured above and below the 10.77 eV energy released by the thermal energy charge exchange reaction between He and Br, for the same purpose discussed previously in the chlorine line identification section. A Br III transition is listed as a possible assignment for the 96.075 nm observed wavelength. This is listed because it was selected as the transition assignment in Ref 45. The author feels that if charge transfer is the predominant process in the reaction, one of the Br II transitions should be assigned to this wavelength.

Further Analysis

Table VIII is a summary of the complete listings in Table XVI. It is noteworthy that the 1493.3 x 10^{-18} cm² total emission cross section is even larger than chlorine and that 77% of the total cross section is accounted for by the 26 observed VUV lines. Using the relative intensity criteria stated in Chapter IV, it was found that the reaction yields emission arising predominantly from Br I. The resulting Br I transition assignments are listed in Table IX. They account for 86% of the total 1476.0×10^{-18} cm² emission cross section of the lines listed in Table XVI having possible Br I transition assignments.

A term diagram illustrating the assigned Br I transitions in Table IX is shown in Fig. 42. The total emission cross section of each energy state is shown in parentheses, next to the energy state designation. The small numbers next to each energy level are the 2J + 1 values for that specific energy level. The energy available from the thermal charge transfer process is indicated by a dashed line. In contrast to C1 I where only the 4s ⁴P state was low enough to be populated exclusively by the charge transfer process, Br I has many energy states which are low enough to be populated by the 10.77 eV available from the thermal charge transfer process. This is a reasonable explanation of why the total emission cross section for the bromine reaction is about three times as large as the chlorine reaction (14.7 A² versus 5.0 A²). The Br I term diagram is more complex than the

Table VIII

Summary of 100 eV He + Br Reaction Allowed Transitions Selected by the Computer Search Program

Classification of Allowed Transitions Listed in Nu Computer of Search Lis	ion Number of Lines	on Number δ^{σ} Lines (x10 ⁻¹⁸ cm ²)	Σσ Στοτα1σ	Number of VUV Lines	Σνυν ^σ (x10 ⁻¹⁸ cm ²)	$\frac{\sum_{\text{VUV}^{\text{O}}}}{(\text{x10}^{-18}\text{cm}^2)} \frac{\sum_{\text{Total}^{\text{O}}}}{\sum_{\text{Total}^{\text{O}}}\text{VUV}}$	Number S., visible Lines (Σvisible ^σ (x10 ⁻¹⁸ cm ²)	<pre>\(\lambda\text{visible}\) \(\text{visible}\) \(\text{x10}^{-18}\text{cm}^2\) \(\text{Total}\delta\text{visible}\) </pre>
Br I	83	869.8	0.58	12	593.7	0.50	11	276.1	0.91
Br 11	2	15.1	0.01	o,	14.5	0.01	-	9.0	0.005
Br I and	18	608.4	0.41	w	580.7	0.49	13	27.7	0.00
Total	52	1493.3		56	1188.9 80% of		31	304.4 20% of	
					\sum_{Total}^{σ}			[Total	

Table IX

<u>Br I Transition Assignments for the 100 eV He⁺ + Br₂ Reaction</u>

$\lambda_{\mathbf{r}}^{\mathbf{a}}$	Transition .	Assign	ment	ΔНЪ	σ ^c
(nm)	Lower		Upper	(eV)	$(cm^2 \times 10^{18})$
121.601	$4p^5 ^2p^0_{3/2}$	+	6s ⁴ P _{5/2}	-0.57	15.8
138.459	4p ³ ² p ⁰ _{1/2}	+	(1D ₂)5s 2D _{3/2}	-1.36	47.1
144.990	$4p^{5} {}^{2}p_{3/2}^{0}$	+	5s" ² P _{1/2}	-2.22	28.2
148.846	$4p^{5} {}^{2}P_{3/2}^{0}$	+	5s' ² P _{3/2}	-2.44	151.2
153.175	$4p^5 \ ^2p_{1/2}^0$	+	5s" ² P _{1/2}	-2.22	41.8
154.066	$4p^{5} {}^{2}p_{3/2}^{0}$	+	5s ⁴ P _{3/2}	-2.72	209.1
157.638	$4p^{5} ^{2}p_{3/2}^{0}$	+	5s ⁴ P _{5/2}	-2.91	384.2
158.231	$4p^{5} {}^{2}p_{1/2}^{0}$	+	5s' ⁴ P _{1/2}	-2.48	96.0
444.298	5s ⁴ P _{5/2}	+	6p 4D0	-0.11	. 0.4
447.385	5s ⁴ P _{3/2}	+	(1 _{D2})5p 2 _{P3/2}	0.05	1.8
447.898	5s ⁴ P _{5/2}	+	6p D _{7/2}	-0.14	•••
452.686	5s ⁴ P _{5/2}	+	6p 4po 5/2	-0.17	1.2
470.473	5s' ² P _{3/2}	+	$(^{1}D_{2})5p^{2}D_{3/2}^{0}$	0.20	0.6
635.248	5s ⁴ P _{5/2}	+	5p' 4s _{3/2}	-0.95	1.7
663.343	5s ⁴ P _{5/2}	+	5p' 2D° 5/2	-1.04	1.0
700.715	5s ⁴ P _{3/2}	+	5p' 4s _{3/2}	-0.95	3.1
735.056	5s 4P 3/2	+	5p' 2D° 5/2	-1.04	6.0
751.505	5s ⁴ P _{5/2}	+	5p 4D _{3/2}	-1.26	4.5
780.517	5s' ⁴ P _{1/2}	•	5p" 2p0 3/2	-0.89	3.9
799.213	5s' ² P _{3/2}	+	5p" 2p0 3/2	-0.89	1.5
813.374	5s' ⁴ P _{1/2}	+	5p' 4s° 3/2	-0.95	3.7
815.597	5p 4p ⁰ _{5/2}	•	5d ⁴ D _{5/2}	0.01	1.5

Table IX (continued)

Br I Transition Assignments for the 100 eV He + Br Reaction

λ_{T}^{a}	Transiti	on As	signment	ΔНЪ	σ ^c
(nm)	Lower		Upper	(eV)	$(cm^2 \times 10^{18})$
815.621	5s ⁴ P _{5/2}	+	5p 4D°5/2	-1.39	1.5
827.469	5s ⁴ P _{5/2}	+	5p 4DO 7/2	-1.41	123.9
833.698	5s' ² P _{3/2}	+	5p' 4s _{3/2}	-0.95	10.4
834.596	5s' ⁴ P _{1/2}	+	5p' 4D0	-0.99	10.6
838.634	5p 4p _{3/2}	+	5d ⁴ D _{5/2}	0.01	1.3
844.888	5s ⁴ P _{3/2}	+	5p 4D _{3/2}	-1.26	24.0
847.976	5s' ⁴ P _{1/2}	+	$5p'^{2}D_{3/2}^{0}$	-1.02	, 15.7
856.008	5s' ² P _{3/2}	+	5p' 4D0	-0.99	5.1
864.104	5s ⁴ P _{5/2}	+	5p 4po 3/2	-1.47	63.0
870.090	5s' ² P _{3/2}	+	5p' 2D _{3/2}	-1.02	9.6
					1269.4

aCalculated vacuum wavelength using the energy level tables (Ref. 68).

bEnthalpy change required to populate the upper energy state for the thermal reaction He⁺ + Br₂ → He + Br⁺ + Br^{*}.

^cEmission cross section for 100 eV He⁺ + Br₂ reaction.

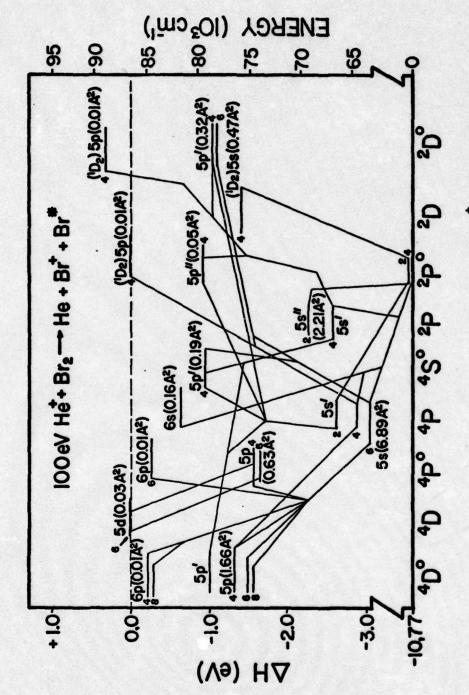


Fig. 42. Br I Term Diagram for 100 eV He + Br2 Reaction.

C1 I term diagram, with more violations of conservation of spin for LS coupling. Since bromine is a heavier atom, this is to be expected. Since the lowest energy state of Br II is about 0.75 eV endothermic, it is reasonable to expect few ionic transitions.

The results of examining each energy level in the Br I term diagram to determine its direct excitation cross section is listed in Table X. The total direct formation cross section is $973.8 \times 10^{-18} \text{ cm}^2$, which is 77% of the total emission cross section for the He^+/Br_2 reaction.

A plot of the emission cross sections and the direct formation cross sections as a function of the energy levels of the Br I atom is given in Fig. 43. The number of states available for population in each energy interval is also presented in Fig. 43. This analysis indicates that the energy of the 100 eV He⁺/Br₂ reaction is predominantly transferred to bromine neutral atoms which are excited to their lower energy states. These lower energy states are exothermic for the charge transfer process. It appears the predominant process is

100 eV He⁺ + Br₂
$$\rightarrow$$
 He + Br* + Br⁺ (12)

As a check on the validity of using the intensity criteria stated in Chapter IV a comparison of the relative intensities for transitions observed in the discharge experiments reported in the tabulated literature date (see Refs 67 and 68), cross sections measured in the present $\mathrm{He}^+/\mathrm{Br}_2$

Table X

<u>Emission and Cascading Cross Sections for Br I States</u>

<u>Observed in 100 eV He⁺ + Br₂ Reaction</u>

Br I			Cross Sec	tion $(cm^2 \times 10^1)$	8)
State	nation	ΔH ^a (eV)	Total Emission	Cascading	Direct Formation
4p4	5s ⁴ P _{3/2}	-2.72	209.1	34.0 (0.9)	175.1
	5s ⁴ P _{5/2}	-2.91	384.2	198.2 (4.1)	186.0
	5s' ⁴ P _{1/2}	-2.48	96.0	34.0	62.0
	5s' ² p _{3/2}	-2.44	151.2	24.6	126.6
	5s" ² P _{1/2}	-2.22	70.0		70.0
	$(^{1}D_{2})5s ^{2}D_{3/2}$	-1.36	47.1	'	47.1
	5p 4D _{3/2}	-1.26	28.5	<u> -</u>	28.5
	5p 4D _{5/2}	-1.39	1.5 (1.5)		1.5
	5p 4D°7/2	-1.41	123.9		123.9
	5p 4po 3/2	-1.47	63.0	1.3	61.7
	5p 4po 5/2	-1.51		1.5 (1.5)	-1.5
	5p' 4s _{3/2}	-0.95	18.9 (1.7)	-	18.9
	5p' 20°3/2	-1.02	25.3		25.3
	5p' 2D° 5/2	-1.04	7.0		7.0
	5p' ⁴ D _{1/2}	-0.99	12.2 (1.5)		12.2
	5p" ² p _{3/2}	-0.89	5.4		5.4
	$(^{1}D_{2})5p^{2}P_{3/2}^{0}$	0.05	0.9 (0.9)		0.9
	$(^{1}D_{2})5p^{2}D_{3/2}^{0}$	0.20	0.6		0.6
	5d ⁴ D _{5/2}	0.01	2.8 (1.5)		2.8
	6s ⁴ P _{5/2}	-0.57	15.8	-	15.8

Table X (continued)

Emission and Cascading Cross Sections for Br I States Observed in 100 eV He + Br Reaction

Cross Section (cm² x 10¹⁸)

Br I				
State Designation	ΔH ^a (eV)	Total Emission	Cascading	Direct Formation
6p 4p 0 5/2	-0 - 17	1.2		1.2
6p 4D _{3/2}	-0.11	0.4		0.4
6p 4D _{7/2}	-0.14	0.9 (0.9)		0.9
		1265.9		973.8 ^b

^aEnthalpy change required to populate this energy state for the thermal reaction He⁺ + Br₂ → He + Br⁺ + Br^{*} (the first radiating C1⁺ state is 0.81 eV endothermic).

bThis total does not include the negative direct formation cross section in this column.

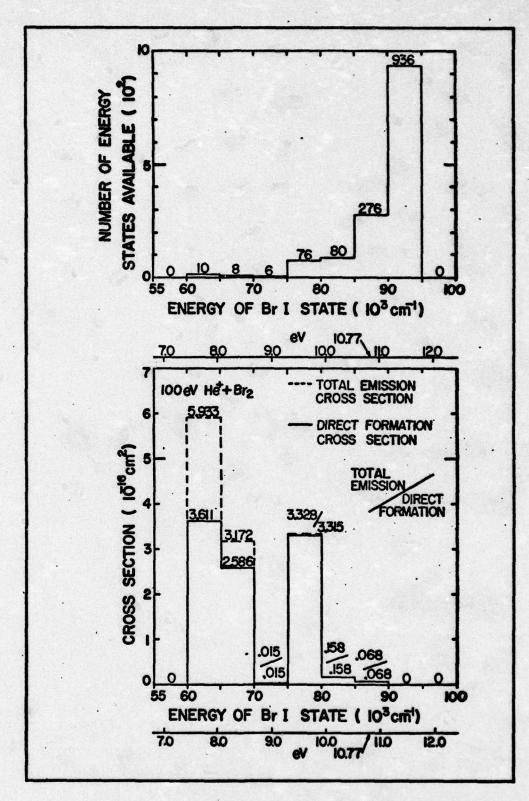


Fig. 43. Comparison of Br I Emission Cross Sections and Direct Formation Cross Sections as a Function of the Energy Levels of the Br I Atom.

reactions experiment, and A factors measured in shock tube experiments (Ref 2) are given in Table XI.

Table XI

Relative Transition Probabilities for Selected Br I Transitions in 700 nm to 870 nm Region

A-factor ^d (10 ⁸ sec ⁻¹)	0.117 +35%	0.116 +35\$	0.146 +50%	0.0379 +35%	0.123 +50%	0.139 +50%	0.119 +35%	not reported	0.219 +35\$
RIC	40,000	40,000	20,000	30,000	10,000	20,000	10,000	1,000	10,000
σ^{b} $(\mathrm{cm}^2 \times 10^{18})$	24.0	4.5	10.4	3.7	3.1	1.0	6.0	5.1	10.6
, T, (mn)	844.888	751.505	833.698	813.374	700.715	663.343	735.056	826.008	834.596
State Upper	5p 4p _{3/2}	sp 40,3/2		5p' 480,	5p' 4so 3/2	5p' 20°,2	sp' 2 ₀ ,	sp' 400,	sp' 400
Transition State Lower	5s 4p3/2	5s ⁴ P _{5/2}	5s' ² p _{3/2}	5s' 4p1/2	5s 4p3/2	5s 4p _{5/2}	5s 4 _{P3/2}	5s' ² p _{3/2}	5s' ⁴ P _{1/2}

Table XI (continued)

41	
100	
21	
0	
=	
2	
21	
d	
H	
-1	
-1	
1	
8	
PI	
0	-1
#I	EI .
8	٠ ا۲.
H	00
0	0
S	21
41	41
6	21
4	_
	2
8	201
	-
+	0
	11
=	SI
9	21
a	
9	2
2	2
6	
E	5.18
.2	
-	
-	997
S	
=	
H	
H	
-	
3	700 nm to 870 nm Region
-	100
+	
a	100
7	
2	

Tuesday and the teacher					
Iransition state		8°4.	وم		A-factor
Lower U	Upper	(mr)	(cm ² x 10 ¹⁸)	RIC	(10° sec 1)
5s' 2p _{3/2} 5j	p" 2p0,	799.213	1.5	30,000	0.0296 +509
	5p" 2po 3/2	780.517	3.9	30,000	0.0533 +354

a Calculated vacuum wavelength using the energy level tables (Ref. 68).

^bEmission cross section for 100 eV He⁺ + Br₂ reaction.

Relative intensity in discharge experiments (Refs. 67 and 68).

d-factors measured in shock tube experiment (Ref. 2).

VII. Iodine

Introduction

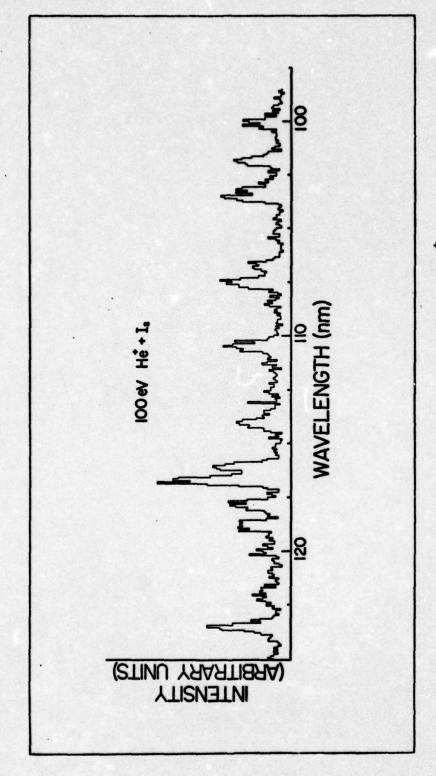
The data in this chapter is presented in the same manner as for the chlorine and bromine reactions in the two preceding chapters. All of the spectra illustrated in this chapter and all of the cross sections listed in the tables of this chapter, were obtained from the reaction of 100 eV He $^{+}$ ions with I $_{2}$ at room temperature. The translational energy of the He $^{+}$ ions was varied only in the measurement of the energy dependence of the cross sections depicted in Figs. 53 to 60.

Spectra

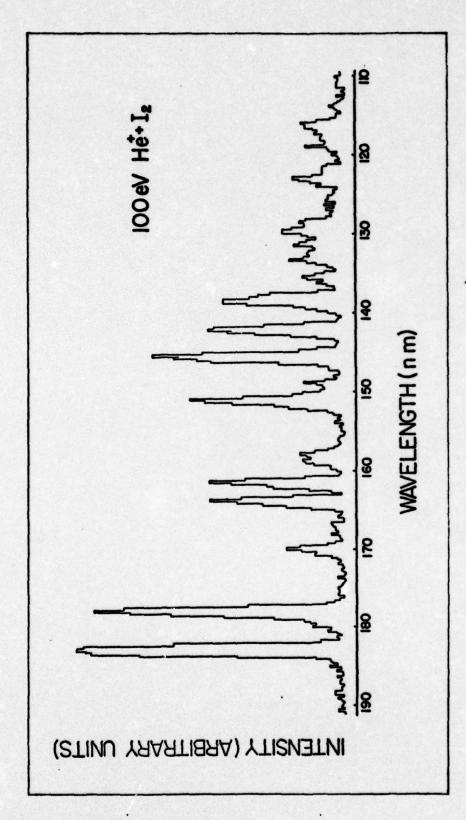
The 81 measureable iodine lines observed in the 60 nm to 870 nm wavelength region are presented in Figs. 44 to 52. A high resolution spectrum of the 98 nm to 124 nm VUV region is shown in Fig. 44. Figures 45 to 47 depict examples of low and high resolution spectra of the 110 nm to 190 nm VUV region. The remaining figures are high resolution spectra in the 400 nm to 870 nm region.

Cross Section Energy Dependence Curves

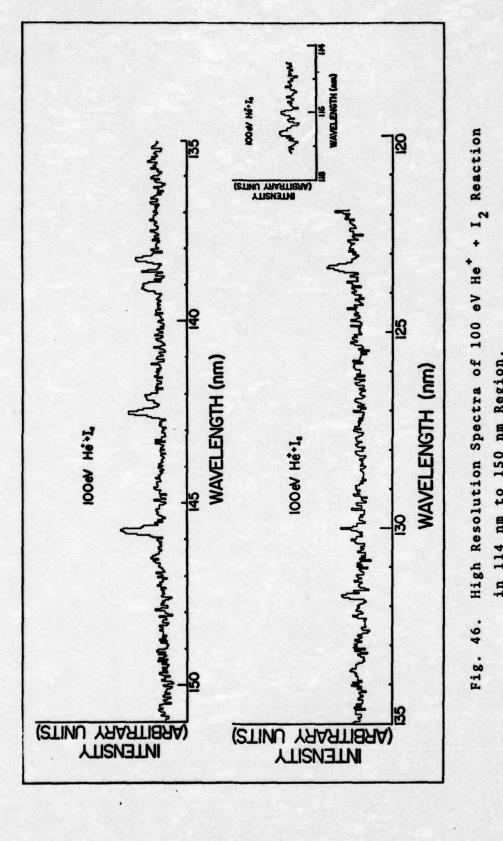
The curves in Figs. 53 to 60 depicting the energy dependence of the iodine cross sections, were obtained from measurements made under low resolution conditions. The same cross section measurement limitations apply in the 120 eV to 170 eV region and in the 0 eV to 20 eV region, as cited for chlorine and bromine in the two preceding chapters.



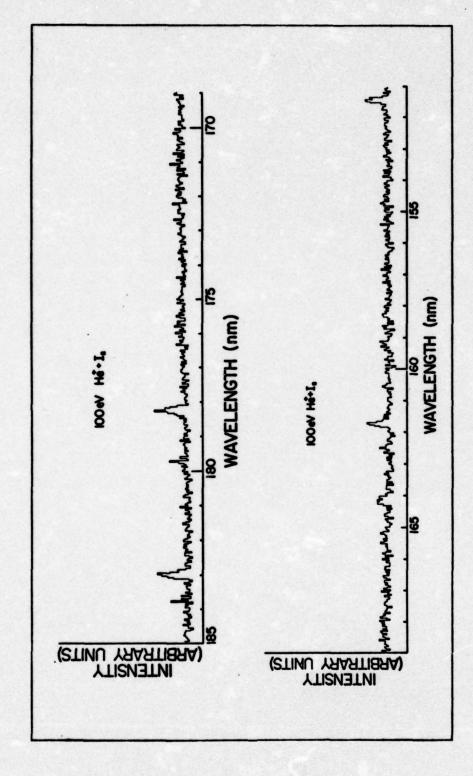
High Resolution Spectra of 100 eV He + I2 Reaction in 98 nm to 124 nm Region. Fig. 44.



Low Resolution Spectra of 100 eV He + I Reaction in 110 nm to 190 nm Region. Fig. 45.



High Resolution Spectra of 100 eV He + I Reaction in 114 nm to 150 nm Region.



High Resolution Spectra of 100 eV He + I Reaction in 150 nm to 185 nm Region. Fig. 47.

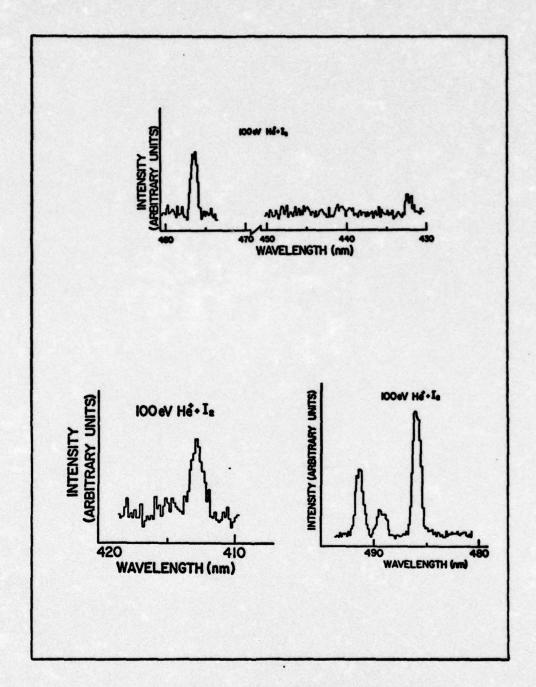
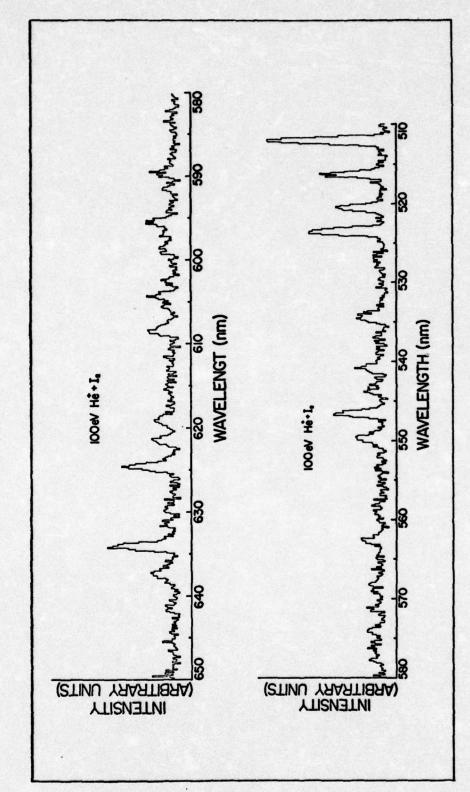
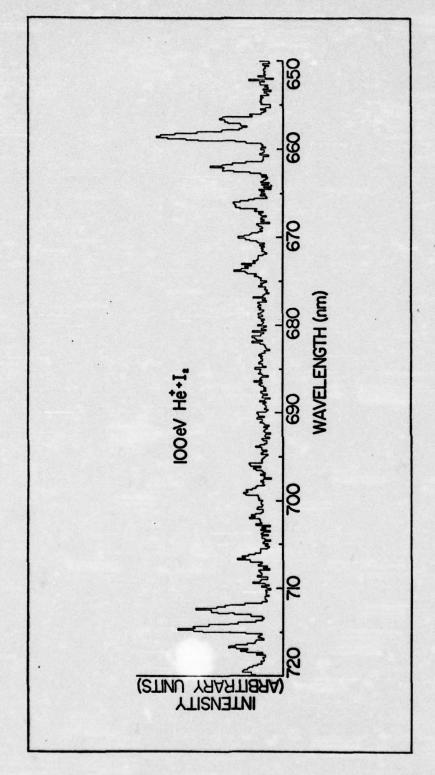


Fig. 48. High Resolution Spectra of 100 eV ${\rm He}^+$ + I $_2$ Reaction in 410 nm to 495 nm Region.



High Resolution Spectra of 100 eV He + I Reaction in 510 nm to 650 nm Region. Fig. 49.



High Resolution Spectra of 100 eV He + I2 Reaction in 650 nm to 720 nm Region. Fig. 50.

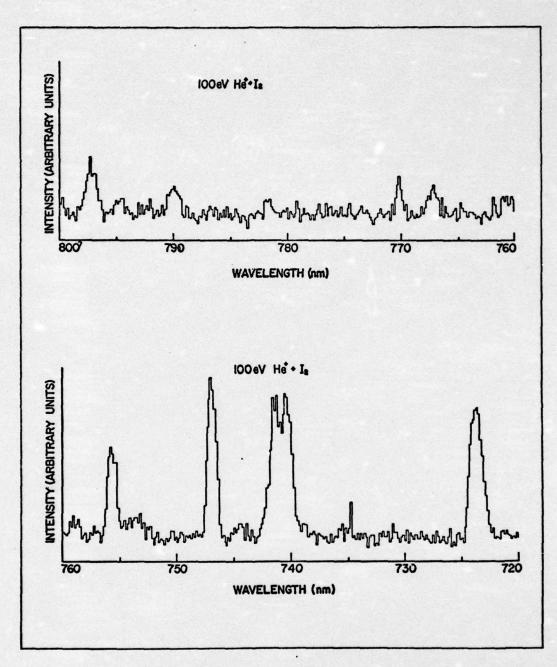


Fig. 51. High Resolution Spectra of 100 eV ${\rm He}^+$ + I Reaction in 720 nm to 800 nm Region.

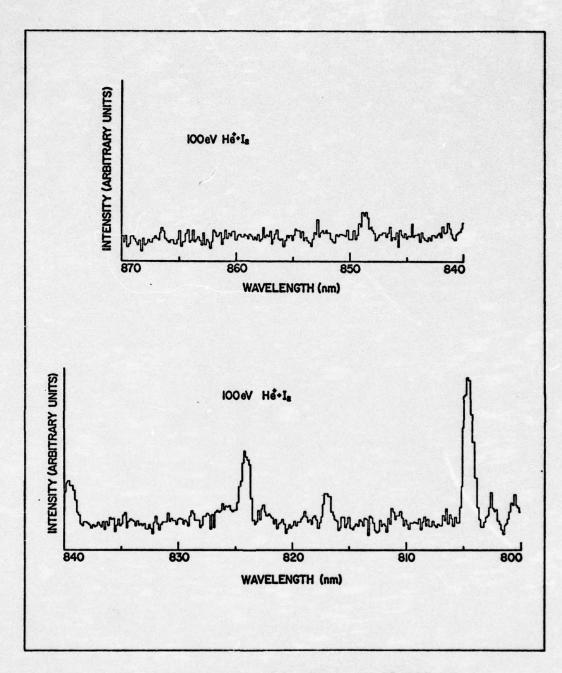


Fig. 52. High Resolution Spectra of 100 eV ${\rm He}^+$ + ${\rm I}_2$ Reaction in 800 nm to 870 nm Region.

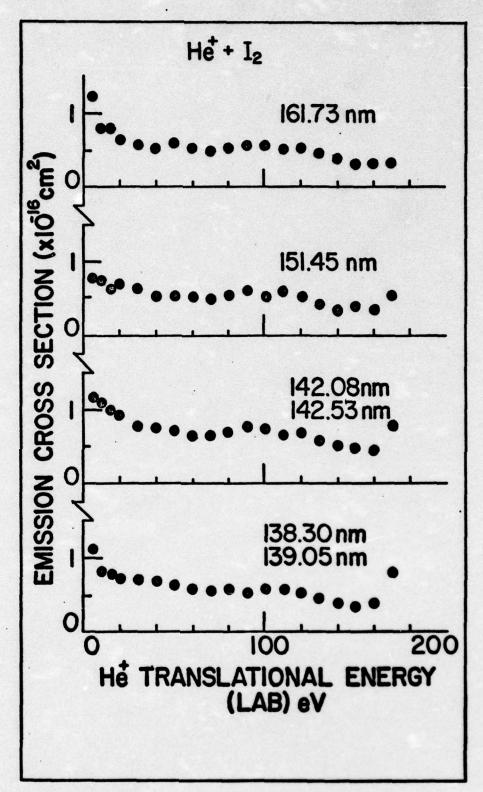


Fig. 53. The Energy Dependence of the Emission Cross Sections of Selected VUV Lines from the ${\rm He}^++{\rm I}_2$ Reaction.

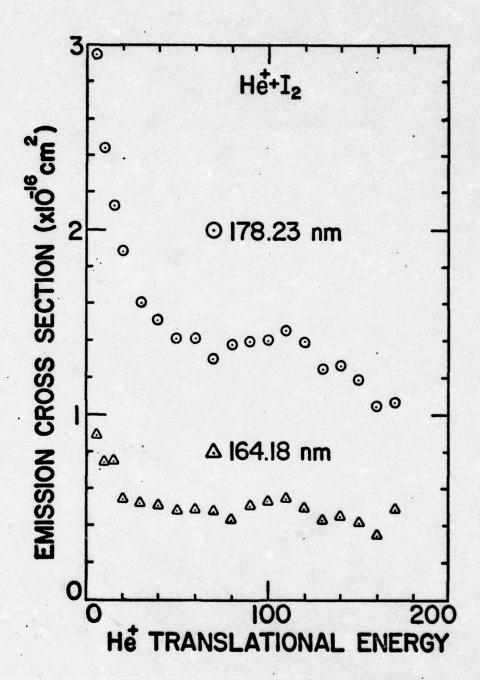
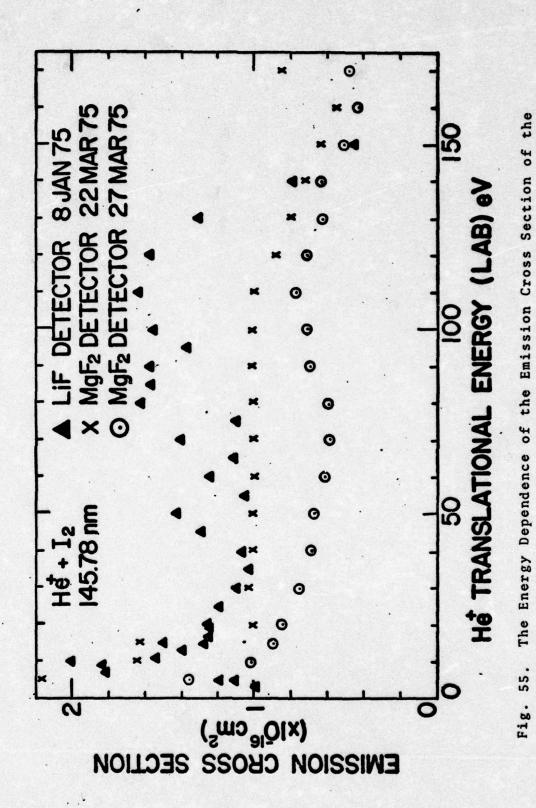
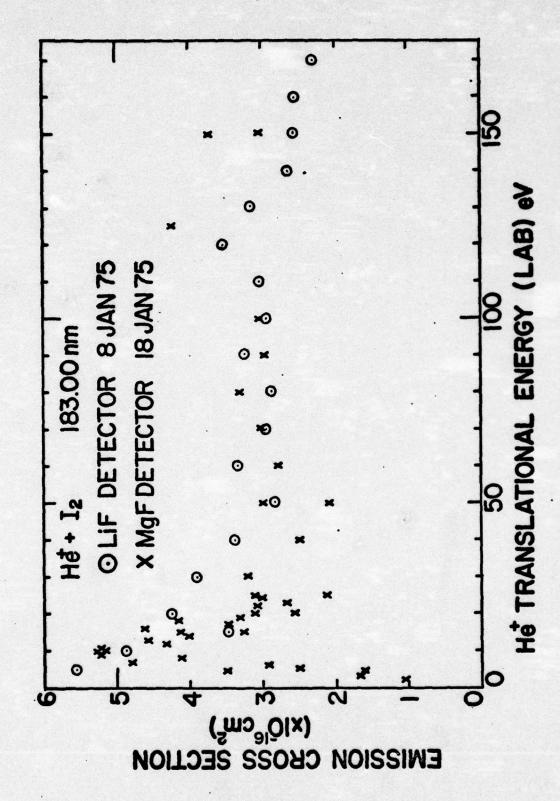


Fig. 54. The Energy Dependence of the Emission Cross Sections of the 164.18 nm and 178.23 nm Lines from the ${\rm He}^+$ + ${\rm I}_2$ Reaction.



145.78 nm Line from the $He^+ + I_2$ Reaction Using Various Detectors.

124



183.00 nm Line from the He^+ + I_2 Reaction Using Various Detectors. The Energy Dependence of the Emission Cross Section of the Fig. 56.

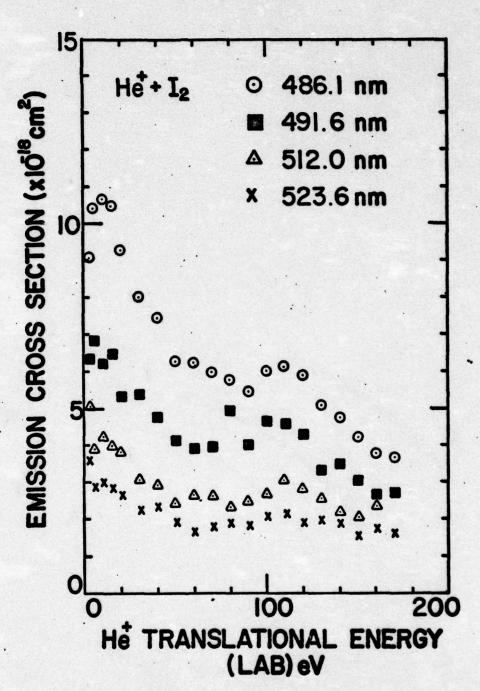


Fig. 57. The Energy Dependence of the Emission Cross Sections of Selected Visible Lines from the ${\rm He}^+$ + ${\rm I}_2$ Reaction.

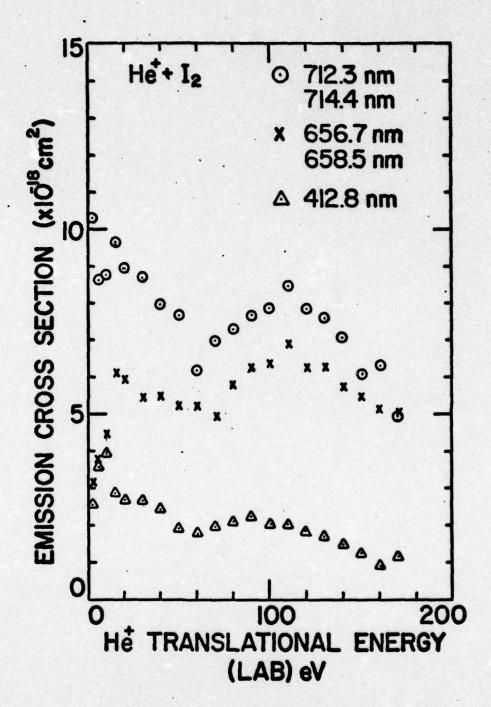


Fig. 58. The Energy Dependence of the Emission Cross Sections of Selected Lines from the ${\rm He}^+$ + ${\rm I}_2$ Reaction.

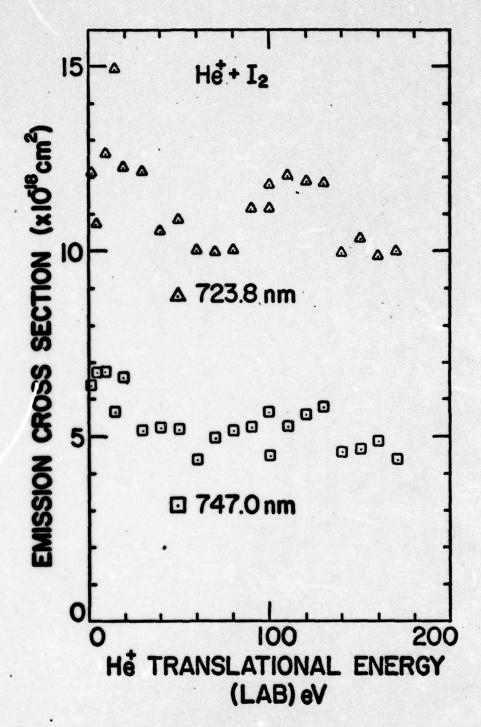


Fig. 59. The Energy Dependence of the Emission Cross Sections of the 723.8 nm and 747.0 nm Lines from the He⁺ + I₂ Reaction.

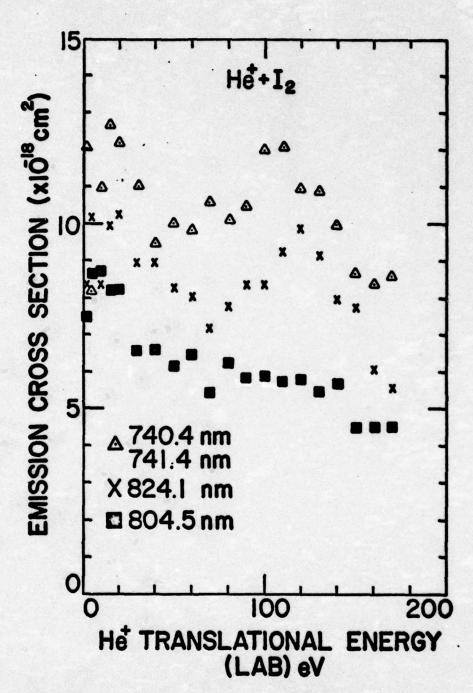


Fig: 60. The Energy Dependence of the Emission Cross Sections of Selected Infrared Lines from the ${\rm He}^+ + {\rm I}_2$ Reaction.

The curves indicate evidence of lines produced by both exothermic processes (such as in Fig. 54) and endothermic processes with low thresholds in the 0 eV to 5 eV region (such as in Fig. 56). As in Chapters V and VI, all of the cross section energy dependence curves are presented to aid in the selection of transition assignments and for completeness.

Line Identification

A listing of all of the allowed transitions which meet the measurement uncertainty $\Delta\lambda_0$ and the quantum-mechanical criteria described in Chapter IV for each observed wavelength λ_0 in the spectra, are listed in Table XVII in Appendix C. The measured cross section for each observed wavelength is also listed. The endothermicity in eV for thermal energy reactants is listed for each allowed transition's upper state. This endothermicity is measured above and below the 12.58 eV energy released by the thermal energy charge exchange reaction between He $^+$ and I $_2$ for the same purpose discussed previously in the chlorine line identification section. The search was compared with the energy levels for I I from both Ref 30 and Ref 48. Transitions which match Minnhagen's energy levels are listed in Table XVII as MI I.

Further Analysis

Table XII is a summary of the complete listings in

Table XVII. Since the energy differences between the I I

neutral iodine atom and I II ionic energy levels are not as

Table XII

Summary of 100 eV He + I2 Reaction Allowed Transitions Selected by the Computer Search Program

ple		•				
Σvisible ^σ Σvisible ^σ (x10 ⁻¹⁸ cm ²) Στοται ^σ visible	ļ	0.02	0.98			
Σvisible ^σ Σvisible ^σ (x10 ⁻¹⁸ cm ²) Στοτα1 ^σ vis	;	2.5	152.6	155.1	10% of	Σ _{Total} σ
Number of Visible Lines	0	ю	21	54		
Σνυν ^σ Στοται ^σ νυν	0.33	0.14	0.53			
$\frac{\sum_{\text{VUV}^{\sigma}}}{(\text{x10}^{-18}\text{cm}^2)} \frac{\sum_{\text{VUV}^{\sigma}}}{\sum_{\text{Total}^{\sigma}\text{VUV}}}$	472.0	200.1	765.2	1437.3	30% of	\(\text{Total}^\sigma \)
Number of VUV Lines	œ	Ħ	œ	27		
Σσ ΣTotal ^σ	0.30	0.13	0.58			
Number $\sum_{\substack{\sigma \\ \text{of}}} \frac{\sum_{\sigma}}{\sum_{\text{Total}^{\sigma}}}$	472.0	202.6	917.8	1592.4		
ion Number of Lines	∞	41	29	81		
Classification of Allowed Transitions Listed in Nu Computer of Search Lin	:	1111	I I and I II	Total		

large as in the cases of chlorine and bromine, it is difficult to apply the same analysis as was done for the chlorine and bromine data. It should be noted that although only 27 of the 81 observed lines were in the VUV, 90% of the total emission cross section was in the VUV. The total emission cross section for the 100 nm to 860 nm region was 1592.4 x 10^{-18} cm² with 1437.3 x 10^{-18} cm² in the VUV and 155.1 x 10^{-18} cm² in the visible.

The experiment has been successful in determining that iodine has a very large cross section, particularly in the VUV and has measured the cross sections of 81 emission lines. The energy dependence of many of these emission lines has been measured. Any further modeling in the form of term diagrams and the effects of cascading will require the use of a more sophisticated analysis than has been applied in this experiment.

In comparing the results of this experiment with the reported helium iodine ion laser lines it is found that only three emission lines are possible laser lines. The 540.8 nm and 562.6 nm emission lines are possible matches for the 540.736 nm and 562.569 nm laser lines. The cross sections of these emission lines were $1.0 \times 10^{-18} \text{ cm}^2$. The 658.5 nm emission line $(6.4 \times 10^{-18} \text{ cm}^2 \text{ cross section})$ is possibly the 658.521 nm laser line. The reason so few helium iodine ion laser lines were observed is probably because the metastable lifetimes of the upper energy levels of the laser lines are longer than the 1×10^{-6} sec lifetime observation

limitation of the ion-beam experiment. This is supported by Shay, et al. report that the measured lifetimes of most of the upper energy states of the I II laser lines measured were on the order of 3 x 10^{-4} sec (Ref 63).

VIII. Conclusion

Observations of the internal energy distribution of the product species of low energy He⁺/halogen reactions for Cl₂, Br₂, and I₂ were made in the present studies. The emission cross sections for 173 individually resolved emission lines in the 60 nm to 870 nm region were measured. The variation of the emission cross sections with the He⁺ translational energy was measured for the more intense lines. The excited product species from the reaction of 100 eV He⁺ ions with Cl₂, Br₂, and I₂ are predominantly produced by charge exchange processes. It was discovered that the 100 eV He⁺/halogen reaction total emission cross sections are very large and are predominantly in the VUV.

Additional analysis in the Cl₂ and Br₂ cases indicate that these emissions are predominantly from the lower energy levels of excited neutral halogen product species. Cascading is believed to account for approximately 20% of the total measured emission cross section, with the remaining 80% being produced by direct formation of excited energy states from the collision process. These findings are summarized in Tables XIII and XIV.

Figure 61 presents a reasonable explanation for the large increase in emission cross section between the chlorine system and the bromine system (5.0 A^2 to 14.9 A^2). In Fig. 61 the energy level range of all of the excited energy states of neutral and singly ionized chlorine, bromine, and iodine atoms are shown. A dashed line is drawn at the energy level

Table XIII

Summary of 100 eV He / Halogen Emission Cross Sections

Σvisible ^σ Σrotal ^σ	0.24	0.20	0.10
$\sum_{\text{Visible}^{\sigma}} (x10^{-18} \text{cm}^2)$	121.1	304.4	155.1
Number of Visible Lines	18	31	54
$\frac{\sum_{\mathbf{V}\mathbf{U}\mathbf{V}^{\mathbf{G}}}}{\sum_{\mathbf{Total}^{\mathbf{G}}}}$	0.76 18	08.0	06.0
$\frac{\sum_{\text{VUV}^{\text{G}}}}{(\text{x10}^{-18}\text{cm}^2)} \frac{\sum_{\text{VUV}^{\text{G}}}}{\sum_{\text{Total}^{\text{G}}}} v$	375.9	1188.9	1437.3
Number of VUV Lines	17	56	27
$\begin{array}{ccc} \Sigma_{\texttt{Total}}^{\texttt{Number}} & \text{Of} \\ \Sigma_{\texttt{Total}}^{\texttt{of}} & \text{of} \\ (\texttt{x10}^{-18} \text{cm}^2) & \texttt{Lines} \end{array}$	497.0	1493.3	1592.4
Total Number of Lines	35	57	81
Reaction	100 eV He ⁺ /Cl ₂	100 eV $\mathrm{He}^{+}/\mathrm{Br}_{2}$	100 eV He ⁺ /I ₂

Table XIV

Summary of Results of 100 eV He +/Halogen Investigation in 60 nm to 870 nm Spectral Region

		C1	Br	I
Total Emission Cross Section Observed	(A^2)	5.0	14.9	15.9
Total VUV Emission Cross Section Observed	(A^2)	3.8	11.9	14.4
cross section observed	(%) ^a	76	80	90
Total Cross Section	(A^2)	0.13	0.15	2.0
Identified as Definitely Ionic	(%) ^a	3	1	13
Total Emission	(A^2)	4.1	12.7	
Cross Section of Neutral Model	(%) ^a	83	85	-
Total Direct	(A^2)	3.3	9.7	
Formation Cross Section in Neutral Model	(%) ^b	79	77	
Total Cascading Cross Section in Neutral Model	(%) b	21	23	-

^aThe % of the total emission cross section observed.

bar The % of the total emission cross section of the neutral model.

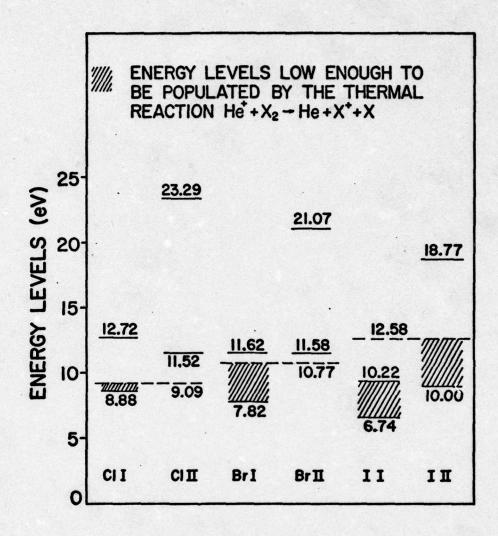


Fig. 61. Comparison of the Energy Levels of the Halogen Atoms and Ions Available for Population Exclusively by the Energy Released in Thermal Charge Transfer.

of the energy released in the thermal charge transfer process for each system (9.09 eV for chlorine, 10.77 eV for bromine, and 12.58 eV for iodine). The energy levels below the dashed line in each system are cross hatched to indicate they could be excited exclusively by the energy available in the thermal charge transfer process.

In the case of the chlorine system, only the very lowest energy states of the neutral chlorine atom can be excited exclusively by the 9.09 eV of energy available from the thermal charge transfer process. This is also illustrated in the chlorine neutral (Cl I) term diagram in Fig. 28. A direct result of this, is that the emissions observed in the chlorine system are predominantly the result of transitions from excited lower-level energy states of neutral chlorine. To be populated, the higher Cl I energy levels require the conversion of some of the kinetic energy of the He ion into internal excitation energy. Therefore the cross sections for producing emissions from transitions from the higher C1 I energy levels are generally small. This also explains the endothermic process profiles of the cross sections energy dependence curves for the chlorine system (see Figs. 26 and 27). Since even the lowest energy levels of Cl II are 2.43 eV endothermic, only weak emissions from the very lowest Cl II energy states were observed (see Table XV). This explains the small cross sections for the production of emissions from excited chlorine ions. The predominant process for the production of emissions in the 60 nm to 870 nm spectral region

by the chlorine system appears to be

In the case of the bromine system, only the very highest energy states of the neutral bromine atom can not be excited exclusively by the 10.77 eV of energy available from the thermal charge transfer process. This is also illustrated in bromine neutral (Br I) term diagram in Fig. 42, where transitions from many excited energy states of bromine neutral atoms are shown. Since so many energy states are now available for excitation by the thermal charge transfer energy, the bromine emission cross section is nearly three times larger than the chlorine emission cross section. Since even the lowest energy levels of Br II are 0.71 eV endothermic, only weak emissions from the very lowest Br II energy states were observed (see Table XVI). This explains the small cross sections for the production of emissions from excited bromine ions. The predominant process for the production of emissions in the 60 nm to 870 nm spectral region by the bromine system appears to be

In the case of the iodine system, all of the energy states of the neutral iodine atom and a large portion of the lower energy states of the singly ionized iodine atom, can be excited exclusively by the 12.58 eV of energy available from the thermal charge transfer process. This

explains the increase in the cross section for the production of emissions from excited iodine ions in the iodine system in comparison to the chlorine and bromine systems. This abundance of energy states which can be populated by charge transfer explains the exothermic process profiles of many of the cross section energy dependence curves for the iodine system (see Figs. 53 and 54). The predominant processes for the production of emissions in the 60 nm to 870 nm spectral region by the iodine system appears to be a result of both

and

100 eV
$$He^+ + I_2 \rightarrow He + I + (I^+)^*$$
 (14)

Because of the large VUV emission cross sections for the bromine and iodine systems (11.9 A^2 and 14.4 A^2), one can speculate that these systems are efficient sources of VUV radiation. The total charge transfer cross section has not been measured for the 100 eV He $^+$ + Br $_2$ and 100 eV He $^+$ + I $_2$ reactions. Comparison with similar systems, such as 100 eV He $^+$ + Ar, which have been measured, would lead one to estimate the total charge transfer value to be in the 20 A^2 to 50 A^2 region (Ref 37). If this is correct, then low energy He $^+$ /Bromine and He $^+$ /Iodine systems could be utilized as efficient sources of VUV radiation.

Bibliography

- 1. Bates, D. R. "Collisions Involving the Crossing of Potential Energy Curves". Proceedings of Royal Society (London), A257: 22-31 (27 September 1960).
- Bengtson, Roger D., et al. "Atomic Transition Probabilities of the Halogens". Physical Review A, 3: 16-24 (January 1971).
- Collins, C. B., et al. "Stimulated Emission from Charge-Transfer Reactions in the Afterglow of an e-Beam Discharge into High-Pressure Helium-Nitrogen Mixtures".
 <u>Applied Physics Letters</u>, 24: 477-478 (15 May 1974).
- 4. Collins, G. J. "Excitation Mechanisms in He-Cd and He-Zn Ion Lasers". <u>Journal of Applied Physics</u>, 44: 4633-4652 (October 1973).
- 5. DeHeer, F. J., et al. "Excitation of Ne, Ar, Kr, and Xe by He⁺ Impact (0.3 10 keV)." Physics, 41: 588-619 (27 March 1969).
- 6. Dunn, Gordon H. Private Communication.
- 7. Dunn, Gordon H., et al. "Production of Lyman Alpha Radiation in Ion-atom Collisions". Physical Review, 128: 2200-2206 (1 December 1962).
- 8. Dworetsky, S. H. and R. Novick. "Experimental Tests of the Post-Collision-Interaction Model for the He⁺ He Excitation Functions". Physical Review Letters, 23: 1484-1488 (29 December 1969(.
- 9. Dworetsky, S. H., et al. "Gross Failure of the Conventional Adiabatic Criterion; Structure and Coherence in the Low-Energy Excitation of Helium Atoms by Helium Atoms". Physical Review Letters, 18: 939-941 (29 May 1967).
- 10. EMR Photoelectric Model 541F-08-18-03900 LiF Window Serial Number 15245 Multiplier Phototube. Spectral response was calibrated on 24 February 1971 by EMR Division of Weston Instruments, Inc., Box 44, Princeton, New Jersey 08540.
- 11. EMR Photoelectric Model 541F-09-18-03900 MgF₂ Window

 Serial Number 17891 Multiplier Phototube. Spectral response was calibrated on 29 January 1975 by EMR Division of Weston Instruments, Inc., Box 44, Princeton, New Jersey 08540.

- 12. Fannery, M. R., et al. "Theoretical and Experimental Zero-Field Reduced Mobilities for Molecular Ion-Molecule Systems". Chemical Physics Letters, 27: 221-223 (15 July 1974).
- 13. Franklin, J. L. <u>Ion-Molecule</u> <u>Reactions</u>. New York: Plenum Press, 1972.
- Grating Calibrations performed by Analytical Systems
 Division, 820 Linden Avenue, Bausch and Lomb, Rochester,
 New York, 14625.
- 15. Hasted, J. B. Physics of Atomic Collisions. London: Butterworths, 1964.
- 16. Hertzberg, Gerhard. Molecular Spectra and Molecular Structure, Vol. I, Spectra of Diatomic Molecules, (Second Edition). New York: Van Nostrand Reinhold Company, 1950.
- 17. Hopper, Darrel. Private Communication.
- 18. Hughes, B. M., E. G. Jones, C. D. Miller and T. O. Tiernan. "Light Emission from Low-Energy Ion-Neutral Collisions". American Society for Mass Spectrometry Twenty-First Annual Conference on Mass Spectrometry and Allied Topics, San Francisco, California, 20-25 May 1973.
- 19. Hughes, B. M., E. G. Jones and T. O. Tiernan. Bulletin of American Physical Society, 19: 156 (1974).
- 20. Hughes, B. M., E. G. Jones and T. O. Tiernan. Abstracts of VIII International Conference on the Physics of Electronic and Atomic Collisions. Vol. I: 223. Institute of Physics, Beograd, Yugoslavia (1973).
- 21. Hughes, B. M., E. G. Jones and T. O. Tiernan. Private Communication.
- 22. Hunter, William R. Private Communication.
- 23. Interactions Between Ions and Molecules, edited by Pierre Ausloos. New York: Plenum Press, 1974.
- 24. Jaecks, D., F. J. DeHeer and A. Salop. "Excitation of Ne, Ar, Kr, and Xe by He Impact (0.3 35 keV; 3000A 6000A)". Physica, 36: 606-619 (1967).
- 25. Jensen, R. C. and G. R. Fowles. "New Laser Transitions in Iodine Inert Gas Mixtures". Proceedings of the IEEE, 52: 1350. (November 1964).

- 26. Johnson, M. C. and J. Svenson. "Absolute Quantum Efficiency of a Channeltron Photomultiplier". A Technical Paper from the Bendix Corporation, Research Laboratories Division, Southfield, Michigan.
- 27. Johnson, Raynor C. An Introduction to Molecular Spectra. London: Methuen and Co., Ltd., 1949.
- 28. Jones, E. G., B. M. Hughes and T. O. Tiernan. "Low Energy He +/H2 Interactions". American Society for Mass Spectrometry Twenty-Third Annual Conference on Mass Spectrometry and Allied Topics, Houston, Texas, 25-30 May 1975.
- 29. Kaminsky, Manfred. Atomic and Ionic Impact Phenomena on Metal Surfaces. New York: Academic Press, Inc., 1965.
- 30. Kiess, C. C. and C. H. Corliss. "Description and Analysis of the First Spectrum of Iodine". <u>Journal of Research of the National Bureau of Standards A. Physics and Chemistry</u>, 63A: 1-18 (July-August 1959).
- 31. Klein, Miles V. Optics. New York: John Wiley and Sons, Inc., 1970.
- 32. Kobayashi, N. and Y. Kaneko. "Molecular Charge Transfer Reactions in the Thermal and Suprathermal Range".

 Abstracts of VIII International Conference on the Physics of Electronic and Atomic Collisions. Vol. I: 81-82.

 Institute of Physics, Beograd, Yugoslavia (1973).
- 33. Kostkouski, H. J. and R. D. Lee. "Theory and Methods of Optical Pyrometry". National Bureau of Standards Monograph 41. 1962.
- 34. Laidler, Keith J. The Chemical Kinetics of Excited States. Oxford: Oxford University Press, 1955.
- 35. Lawrence, G. M. "Resonance Transition Probabilities in Intermediate Coupling for Some Neutral Non-Metals". The Astrophysical Journal, 148: 261-268 (April 1967).
- 36. Leighton, Robert B. Principles of Modern Physics. New York: McGraw-Hill Book Compan, Inc., 1959.
- 37. Lindholm, Einar. "Mass Spectra and Appearance Potentials Studied by Use of Charge Exchange in a Tandem Mass Spectrometer". <u>Ion-Molecule Interactions</u>, edited by J. L. Franklin. New York: Plenum Press, 1972.

- 38. Lipeles, M. R. et al. "Energy Dependence of the 4610-and 4765A Lines of Ar Excited in Low-Energy He + Ar Collisions". Physical Review Letters, 24: 799-801 (13 April 1970).
- 39. Lipeles, M., R. Novick, and N. Tolk. "Optical Excitation with Very Low Energy Ions". Physical Review Letters, 15: 815-818 (22 November 1965).
- 40. Maier, William B. "Charge Transfer and Ionization in Collisions between Atomic Ions and Rare-Gas Atoms for Primary-Ion Energy below 100 eV". Physical Review A, 5: 1256-1267 (March 1972).
- 41. Martin, William C. and Charles H. Corliss. "The Spectrum of Singly Ionized Atomic Iodine (I II)". <u>Journal of Research of the National Bureau of Standards A. Physics and Chemistry</u>, 64A: 443-479 (November-December 1960).
- 42. Martin, William C. "Energy Levels and Spectrum of Neutral Helium (4He I)". Journal of Research of the National Bureau of Standards A. Physics and Chemistry, 64: 19-28 (January-February 1960).
- 43. Marx, R. "Luminescence from Low Energy Ion Molecule Interaction". Interactions Between Ions and Molecules, edited by Pierre Ausloos. New York: Plenum Press, 1974.
- 44. Massey, H. S. W. "Collisions Between Atoms and Molecules at Ordinary Temperatures". The Physical Society (London) Reports on Progress in Physics, 12: 248-269 (1949).
- 45. McDaniel, E. W. Collision Phenomena in Ionized Gases. New York: John Wiley and Sons, Inc., 1964.
- 46. McDaniel, E. W., et al. <u>Ion-Molecule Reactions</u>. New York: Wiley-Interscience, 1970.
- 47. Miller, C. D. Private Communication.
- 48. Minnhagen, Lennart. "The Energy Levels of Neutral Atomic Iodine". Arkiv for Fysik, 21: 415-478 (1962).
- 49. Moore, Walter J. Physical Chemistry (Third Edition). Englewood Cliffs, New Jersey: Prentice-Hall, Inc., 1962.
- 50. "Nitrogen Ion Laser Pumped by Charge Transfer". Optical Spectra, 8: 29 (September 1974).
- 51. Pearse, R. W. B. and A. G. Gaydon. The Identification of Molecular Spectra (Third Edition). New York; John Wiley and Sons, Inc., 1963.

- 52. Piper, J. A. "Increased Efficiency and New CW Transitions in the Helium-Iodine Laser System". <u>Journal of Physics</u>, <u>D</u>: <u>Applied Physics</u>, <u>7</u>: 323-328 (21 January 1974).
- 53. Pretzer, Donavon, et al. "Lyman Alpha Production in Proton-Rare Gas Collisions". Physical Review Letters, 10: 340-342 (15 April 1963).
- 54. Quartz, Jerry. Private Communication.
- 55. Radziemski, Leon J., Jr., and Victor Kaufman. "Wavelengths, Energy Levels, and Analysis of Neutral Chlorine (C1 I)". The Journal of the Optical Society of America, 59: 424-443 (April 1969).
- 56. Radziemski, Leon J., Jr., and Victor Kaufman. "Wavelengths, Energy Levels, and Analysis of the Second Spectrum of Chlorine (Cl II)". The Journal of the Optical Society of America, 64: 366-389 (March 1974).
- 57. Rao, Y. Bhupala. "Structure of the Spectrum of Doubly Ionized Bromine". <u>Indian Journal of Physics</u>, 35: 386-400 (August 1961).
- 58. Rao, Y. Bhupala. "Structure of the Spectrum of Singly Ionized Bromine". <u>Indian Journal of Physics</u>, 32: 497-515 (November 1958).
- 59. Rosenthal, H. "Nonadiabatic Effects in Slow Atomic Collisions I. He⁺ + He". <u>Physical Review A</u>, <u>4</u>: 1030-1042 (September 1971).
- 60. Rosenthal, H. and H. M. Foley. "Phase-Interference Effects in Inelastic He⁺ + He Collisions". Physical Review Letters, 23: 1480-1483 (29 December 1969).
- 61. Samson, J. A. R. Techniques of Vacuum Ultraviolet
 Spectroscopy. New York: John Wiley and Sons, Inc., 1967.
- 62. Schuebel, W. K. Private Communication.
- 63. Shay, T., et al. "Excitation Mechanism of the He I Laser". Applied Physics Letters, 26: 531-534 (1 May 1975).
- 64. SSR Model 1110 Photon Counter System. SSR Instruments Co., 1001 Colorado Avenue, Santa Monica, California 90404.
- 65. Stebbins, R. F., et al. "Lyman-Alpha Production in He H (1s) Collisions". Physical Review, 138: Al312-Al316 (31 May 1965).

- 66. Stedeford, J. B. H. and J. B. Hasted. "Further Investigations of Charge Exchange and Electron Detachment".

 Proceedings of the Royal Society of London, 227: 466-486

 (8 February 1955).
- 67. Striganov, A. R. and N. S. Sventitskii. <u>Tables of Spectral Lines of Neutral and Ionized Atoms</u>. New York: Plenum, 1968.
- 68. Tech, Jack L. "Analysis of the Spectrum of Neutral Atomic Bromine (Br I)". <u>Journal of Research of the National Bureau of Standards A. Physics and Chemistry 67A: 505-531 (November-December 1963).</u>
- 69. Tolk, N. H., et al. "Phase Interference Effects in Low Energy Na Ne and Ne Ne Collisions". in Abstracts of Papers of the VIIth International Conference on the Physics of Electronic and Atomic Collisions, edited by L. M. Branscomb, et al. Amsterdam: North-Holland Publishing Co., 1971.
- 70. Tolk, N. H. et al. "Quantum-Mechanical Phase Interference and Optical Polarization in Low-Energy Na* Ne Inelastic Collisions". Physical Review A, 13 969-984 (March 1976).
- 71. Zaidel, A. N. and E. Ya. Shreider. <u>Vacuum Ultraviolet</u>
 <u>Spectroscopy</u>. Translated by Z. Lerman. Ann Arbor: Ann
 Arbor-Humphrey Science Publishers, 1970.
- 72. Zaidel, A. N., et al. Tables of Spectral Lines. New York: Plenum, 1970...
- 73. Zener, Clarence. "Non-Adiabatic Crossing of Energy Levels". The Proceedings of the Royal Society (London), A137: 696-702 (September 1932).

Appendix A

Table XV

7

Luminescence from the Reaction 100 eV He + Cl₂ + He + Cl⁺ + Cl + Energy

Explanation of Symbols

 λ_0 = Observed vacuum wavelength (nm)

 $\Delta \lambda_0$ = Search interval (nm)

= Emission cross section $(cm^2 \times 10^{18})$

X = Emitting atom or ion

 $\lambda_{\rm T}$ = Calculated vacuum wavelength in nm using the energy level tables (Refs. 42, 55 and 56).

 ΔH = Enthalpy change in eV required to populate the upper energy state for the thermal reaction He + Cl₂ + He + Cl⁺ + Cl⁺.

= Transition selected by criteria stated in Chapter IV.

Inner electron configuration designation (Refs. 55 and 56).

C1 I Unprimed =
$$\binom{3}{P}$$

C1 II Unprimed = $\binom{4}{S}$

$$= \binom{2}{0}$$

 $(a_1) = 1$

$$" = {2 \choose P}$$

Table XV (continued)

	(eV)	5.25	5.25	2.93	2.93	2.94	2.95	2.97	2.97	2.98	2.98	3.00	3.00	3.04	3.04
	$\lambda_{\rm T}^{-\lambda_{\rm o}}$	0.000	0.000	0.367	0.351	0.288	0.134	0.041	0.017	-0.066	-0.082	-0.216	-0.272	-0.559	-0.595
l + Energy	T, (mm)	96.150	96.150	103.167	103.151	103.088	102.934	102.841	102.817	102.734	102.718	102.584	102.528	102.241	102.205
2 + He + C1 + C	signment Upper State	3d' 1po	$^{3p^5}_{1p^0}$	4d 2(0) _{1/2}	4d 2(3) _{5/2}	4d 2(1) _{3/2}	4d 1(1) _{1/2}	6s 2(2) _{5/2}	4d 1(1)3/2	4d 1(3) _{5/2}	4d 1(2) _{3/2}	6s 2(2) _{3/2}	4d 1(2) _{5/2}	4d 0(2) _{5/2}	4d 0(2)3/2
from the Reaction 100 eV He ⁺ + Cl ₂ + He + Cl ⁺ + Cl + Energy	ltion As	3p ⁴ 1 _{D2} ←	+	3p ⁵ 2p ⁰ +	+	+	+	+	+	•	•	•	+	+	•
the Reaction	×	C1 11		C1 I											
Luminescence from 1	$(cm^2 \times 10^{18})$	2.2		8.1											
Lumi	Δλ _o (mm)	0.30		09.0											
	o (mm)	96.15		102.80											

Table XV (continued)

	ΗV	(ev)	3.04	3.07	3.07	3.11	2.56	2.56	2.49	2.49	. 2.56	2.56	2.61	2.61	2.56	2.56
	γ- ₁ γ	(mm)	0.335	0.120	0.062	-0.245	-0.017	-0.017	0.004	0.004	0.077	0.077	-0.306	-0.306	0.423	0.423
+ Energy	۲	(mm)	103.135	102.920	102.862	102.555	106.383	106.383	107.104	107.104	107.177	107.177	106.794	106.794	107.523	107.523
Luminescence from the Reaction 100 eV He + Cl ₂ + He + Cl ⁺ + Cl + Energy	signment	Upper State	+ 4d 0(2) _{3/2}	+ 6s 1(1)3/2	6s 1(1) _{1/2}	6s 0(0) _{1/2}	+ 3p ⁵ 3p ^o	3d' ³ p ^o	+ 3p ⁵ 3p ^o	3d' 3po	3p ⁵ 3p_0	3d' 3po	3p ⁵ 3po	3d' 3po	3p ⁵ 3p ⁰	3d' 3po
C12	ASS 1	+	+	+	+	+	+	+	+	+	+	+	+	+	+	+
100 eV He +	Transition Assignment	Lower State + Upper State	3p ⁵ 2p ⁰	•			3p ⁴ 3p ₂		3p ⁴ 3p ₂		$^{3p^4}_{^{2p}}$				3p4 3p0	
Reaction		×	C1 I				C1 11		11 13							
escence from the	b ($(cm^2 \times 10^{18})$					3.4		7.7							
Lumin	δλ _o	(mm)					0.30		0.50							
	₄ °	(mm)					106.40		107.10							

Luminescence from the Reaction 100 eV He + Cl₂ + He + Cl + Energy Table XV (continued)

Δλ_o (mm) 0.35

(mm)

				18-		
ъ		Transitio	Transition Assignment		بر - بر	HV.
$(cm^2 \times 10^{18})$	×	Lower State	+ Upper State	(mg)		(e)
13.0	1 13	3p ⁵ 2po 3/2	+ 3d ⁴ p _{5/2}	109.098	0.298	2.27
			+ 5s 2(2)3/2	109.074	0.274	2.28
			+ 3d ² F _{5/2}	108.806	900.0	2.30
			+ 5s 1(1) _{3/2}	108.530	-0.270	2.33
٠			+ 5s 1(1) _{1/2}	108.517	-0.283	2.33
			+ 3d ² p _{3/2}	108.467	-0.333	2.34
		3p ⁵ 2p ⁰ 1/2	+ 5s 0(0) _{1/2}	109.027	0.227	2.39
	C1 11	3p ⁴ 1s ₀	+ 3d 3D ₁	108.737	-0.063	5.77
			+ 3d' 3D'	108.737	-0.063	5.77
		$^{3p}_{2}$ 5 $^{9}_{2}$	+ 8f ⁵ F ₃	108.996	0.196	13.86
			+ 8f ⁵ F ₂	108.996	0.196	13.86
			+ 8f ³ F ₃	108.966	0.166	13.86
		3d' 3po	+ 8f ⁵ F ₃	108.996	0.196	13.86
			+ 8f ⁵ F ₂	108.996	0.196	13.86
			+ 8f ³ F ₂	108.966	0.166	13.86

Table XV (continued)

λ_T - λ_o
(mm)
0.357
0.287
0.231
0.027 109.244 -0.206 109.213 -0.237 109.098 -0.352 109.074 -0.376 λ_T (nm) 109.807 109.737 109.681 Luminescence from the Reaction 100 eV He + Cl2 + He + Cl + Cl + Energy Lower State + Upper State $3p^5 \, ^2p_0^0$ + $3d \, ^4p_{1/2}$ + $3d \, ^2b_{5/2}$ + $3d \, ^2b_{3/2}$ + $3d \, ^2b_{3/2}$ + 5s 2(2)_{5/2} + 3d ⁴P_{3/2} + 3d ²P_{1/2} + 3d ⁴P_{5/2} 5s 2(2)_{3/2} Transition Assignment $(cm^2 \times 10^{18}) X$ C1 I δλ_o 0.40

109.45

γ° (E

AH (eV) 2.20 2.21 2.26

2.27

2.28

2.33

0.130

109.580

5s 1(1)_{3/2}

2.33

0.116

109.566

5s 1(1)_{1/2}

0.065

109.515

+ 3d ²p_{3/2} + 8f ⁵F₂

C1 11

0.303

109.753

109.753

2.34

Table XV (continued

Luminescence from the Reaction 100 eV He + Cl2 + He + Cl + Energy

	HV	(ev)	2.16	2.19	2.20	2.26	2.26	2.28	2.19	2.20	2.21	1.34	1.34	12.91	12.92
1	λ _T - λ _o	(mm)	0.094	-0.148	-0.293	0.207	0.176	0.034	0.279	0.131	0.003	0.052	0.050	0.065	-0.034
	,	(mm)	110.194	109.952	109.807	110.307	110.276	110.134	111.029	110.881	110.753	118.877	118.875	118.890	118.791 -0.034
7	ignment	Upper State	+ 3d 4F5/2	+ 3d 4F3/2	3d 4p1/2	3d 4p3/2	3d ² P _{1/2}	5s 2(2) _{3/2}	3d 4F3/2	+ 3d 4p1/2	3d ² D _{3/2}	+ 4s', D _{5/2}	4s' ² _{D3/2}	5p' ³ D ₂	+ 5p' ³ 0;
	n Ass	+	+	+	+	+	+	+	+	+	+	+	+	+	+
	Transition Assignment	Lower State + Upper State	3p ⁵ 2p ⁰ 3/2			$^{3p^5}_{^2p_0}^{^2}$			3p ⁵ 2p ⁰ _{1/2}			3p ⁵ 2p ⁰ _{3/2}		3p ⁵ 3p ⁰	
		×	1 13						C1 1			1 13		C1 11	
	, b	$(cm^2 \times 10^{18})$	13.7						3.8		,	61.9			
1	Δλ _o	(mu)	0.30						0.30			0.100			
	۰,0	(mm)	110.10						110.75			118.825			

Table XV (continued)

رم <u>(آ</u>

31	uminescence from	the Reac	tion 100 ev He	+	Luminescence from the Reaction 100 eV He + C_{12} + He + C_{11} + C_{11} + Energy	+ CI + Ener	žá	
	b		Transition Assignment	n As	signment	۲	λ γ	ΗV
	$(cm^2 \times 10^{18})$	×	Lower State	+	Lower State + Upper State		(mu)	(e)
		C1 11	$^{3p}_{2}^{5}$ $^{3p_{0}}_{2}$	+	+ 5p' ^l p ₁	118.759 -0.066	-0.066	12.93
				+	+ 5p ¹ ³ F ₃	118.791	-0.034	12.97
				+	Sp' 3D1	118.759	-0.066	12.9
	•		3d' 3po	+		118.890	0.065	12.91
				+	5p' ³ D ₃	118.791	-0.034	12.9
				+	5p' ¹ p ₁	118.759	990.0-	12.9
				+	5p' ³ F ₃	118.791	-0.034	12.97
				+	sp. 3D1	118.759	-0.066	12.93
			3p ^{5 3} p ⁰	+	5p' ³ p ₂	118.832	0.007	13.00
				+	Sp' ³ p ₁	118.797	-0.028	13.00
				+	5p' ³ p ₀	118.782	-0.043	13.00
			3d' 3po	+	5p' ³ p ₂	118.832	0.007	13.00
				+		118.797 -0.028	-0.028	13.00

118.782 -0.043

Table XV (continued)

Luminescence from the Reaction 100 eV He + Cl₂ + He + Cl + Energy

رسا (سا)	δ. (III)	σ (cm ² x 10 ¹⁸)	×	Transition Assignment Lower State + Upper St	Transition Assignment Lower State + Upper State	, [E	ر - بر (سا)	₩ •
			C1 11	3p ^{5 3} po	- 7p ⁵ p,	118.806	-0.019	13.04
				3d' ³ po	+ 7p ⁵ p ₁	118.806	-0.019	13.04
120.125	0.100	33.4	. I		+ 4s' ² D _{3/2}	120.135	0.010	1.34
			C1 11	3p ⁵ 3po	+ 5p' 1p ₁	120.137	0.012	12.93
					+ 5p' ³ _{D₁}	120.137	0.012	12.93
				34, 3po	+ 5p' 1p ₁	120.137	0.012	12.93
					+ 5p' 3p ₁	120.137	0.012	12.93
133.550	0.100	9.2	1 13		+ 4s ² p _{1/2}	133.573	0.023	0.19
				3d ⁵ D ₄	+ 8f ³ F ₃ .	133.614	0.064	13.86
					+ 8f ³ F ₄	133.614	0.064	13.86
				3d 5po	+ 8f ³ F ₃	133.615	0.065	13.86
					+ 8f ³ F ₄	133.615	0.065	13.86
				34 ⁵ D _o	+ 8f ³ F.	133.621	0.071	13.86

Table XV (continued)

Luminescence from the Reaction 100 eV He + Cl₂ + He + Cl + Energy

	17000							
~° (ه ^ر (g d		Transition	Transition Assignment	₽ ,	λ _T - λ _o	HQ.
2		(cm_x10_)	×	Lower State	Lower State + Upper State	(M		(e)
134.700	0.100	45.6	C1 I	2	+ 4s ² p _{3/2}	134.724	0.024	0.11
			C1 11	4s ⁵ S ₂	+ 4f' ³ G ₃	134.741	0.041	13.49
5.125	135.125 0.100	11.9	. 1	3p ⁵ 2po .	+ 4s ² p _{1/2}	135.166	0.041	0.19
136.300	0.100	13.8	1 13	3p ⁵ 2po .	+ 4s ² p _{3/2}	136.345	0.045	0.11
137.925	0.100	73.0	1 13	7	+ 4s 4p _{3/2}	137.953	0.028	-0.10
			C1 11	4s ³ S ₁	+ 8f ⁵ F ₂	137.922	-0.003	13.86
138.975	0.100	47.9	1 13		+ 4s 4 _{P5/2}	138.969	-0.006	-0.17
				3p ⁵ 2p ⁰	+ 4s 4p _{1/2}	138.996	0.021	-0.06
			C1 11		+ 5p' 1 _{D2}	138.901	-0.074	13.21
					+ 4f' 3G ₅	139.026	0.051	13.50
					+ 4f' 3f4	139.013	0.038	13.50
					+ 4f' 3F	138.973 -0.002	-0.002	13.51

Table XV (continued)

E PH	13.51	13.50	13.51	13.51	13.51	13.50	13.51	13.50	13.51	13.51	13.51	13.51	13.51
λ _T - λ _o	-0.010	0.038	-0.002	-0.010	-0.042	0.039	000.0	0.039	000.0	-0.033	-0.039	-0.040	-0.039
₽ [138.965	139.013	138.973	138.965	138.933	139.014	138.975	139.014	138.975	138.942	138.936	138.935	138.936
ignment Upper State	4f' ¹ H _S	4f' 3G4	+ 4f' 3G3	4f' 3 _{H5}	8p ⁵ p ₃	+ 4f' 3 _{F4}	+ 4f' 3f3	4f' 3G4	4f' ³ G ₃	+ 8p ⁵ p ₂	4f' ³ F2	8p ⁵ P ₃	+ 4f' ³ D ₂
Ass	+	+	+	+	+	+	+	+	+	+	+	+	+
Transition Assignment Lower State + Upper State	3d ⁵ D ₄					3d ⁵ D ₃							
×	: II												
σ (cm ² x 10 ¹⁸)			-										
δλ _o													

~° [

Table XV (continued)

у (mm)

Δλ _o	b.		Transiti	on As	Transition Assignment	Ļ	λ- γ	HV
(m)	$(cm^2 \times 10^{18})$	×	Lower State	+	Lower State + Upper State	(mm)	(ma)	<u>§</u>
		C1 11	34 ⁵ D ₂	+	4f' 3F3	138.980	0.005	13.51
				+	4f' 3G3	138.980	0.005	13.51
	•			+	8p ⁵ p ₁	138.952	-0.023	13.51
				+	sp ⁵ P ₂	138.948	-0.027	13.51
				+	4f' 3F2	138.942	-0.033	13.51
				+	8p ⁵ p ₃	138.940	-0.035	13.51
				+	4f' ¹ p ₁	138.927	-0.048	13.51
				+	4f' 3 _{D2}	138.942	-0.033	13.51
				+	4f' ³ p ₁	138.927	-0.048	13.51
			3d ⁵ D ₁	+	8p ⁵ p.	138.957	-0.018	13.51
				+	8p 5p ₂	138.953	-0.022	13.51
				+	4f' 3F2	138.946	-0.029	13.51
				+	4£' 1 _P 1	138.932	-0.043	13.51
				+	4f' 3D2	138.946	-0.029	13.51

Table XV (continued)

Luminescence from the Reaction 100 eV He + Cl₂ + He + Cl + Energy

(ev)	13.51	13.51	13.51	13.51	-0.10	14.95	14.95	14.95	2.65	2.67	2.73	2.74
λ _T - λ _o (mm)	-0.043	-0.016	-0.040	-0.040	0.078	0.938	0.938	916.0	1.098	-0.723	0.113	-1.551
λ _T (mm)	138.932	138.959	138.935	138.935	139.653	438.938	438.938	438.916	439.098	437.277	438.113	436.449
Transition Assignment Lower State + Upper State	+ 4f' ³ P ₁	8p ⁵ p ₁	4f' ¹ P ₁ .	+ 4f' ³ p ₁	+ 4s 4p _{3/2}	+ 5d ³ p ₂	sd ³ D ₁	1 bs	5p 4po.	5p 2p0 5/2	5p 4p0 3/2	5p 4p _{5/2}
n Ass	+	+	+	+	+	+	+	+	+	÷	+	+
Transition Assignment Lower State + Upper St	3d ⁵ D ₁	34 40°			3p ⁵ 2p ⁰	2p 1p0			4s 4ps/2		4s 4P3/2	
×	C1 11				C1 I	He I			C1 1			
$(cm^2 \times 10^{18})$					5.4	2.4						
δλ _ο (mm)					0.100	2.0						
~° (III					139.575	438.0						

Table XV (continued)

Y° (IIII)

# 5	(ev)	2.76	2.76	2.78	3.02	3.03	3.03	10.08	10.08	10.08	10.08	10.08	10.08	10.08	11.89
λτ - λ _ο		1.164	0.879	-0.927	-0.133	-0.810	-0.816	-0.592	-0.612	-0.647	-0.372	-0.407	-0.457	-0.357	-1.627
<u>ئ</u> ئې		439.164	438.879	437.073	437.867	437.190	437.184	437.408	437.388	437.353	437.628	437.593	437.543	437.643	436.373
ignment	Upper state	5p 4 _{D1/2}	5p 4 ₃ ,2	5p 2p03/2	4f 2(2) ⁰ 3/2	4f 2(1)0 4f 2(1)1/2	4f 2(1) ⁰ 3/2	44 5p0	4d ⁵ D ₁	4d ⁵ D ₂	4d ⁵ D ₁	4d ⁵ D ₂	4d ⁵ D ₃	44 5 _D °	6s ³ S,
A ASS	+	+	+	÷	+	+	+	+	+	+	+	+	+	+	+
	LOWEr State	4s 4P1/2			4s ² P _{1/2}			4p 3p1			4p 3p ₂			4p 3p0	4p' 3D.
,		1 13						C1 11							
g g g g g g g g g g g g g g g g g g g		J						C							
مم (سر	Î														

Table XV (continued)

(am)

1

δλ _ο	b		Transit	ion As	Transition Assignment	, T	$^{\lambda_{\rm T}}$ - $^{\lambda_{\rm o}}$	₩
(mm)	$(cm^2 \times 10^{18})$	×	Lower State	+	Lower State + Upper State	(mm)	(mm)	(eV)
		C1 11	4p' 3p2	+	6s ³ S ₁	436.445	-1.555	11.89
			4p' 3F2	+	5d ⁵ D ₁	439.665	1.665	11.96
				+	5d ⁵ D ₂	439.660	1.660	11.96
				+	5d ⁵ D ₃	439.650	1.650	11.96
			4p' 1F3	+	5s' 3 _{D2}	436.115	-1.885	12.05
			4p' 3p2	¥	4d' 3Fo	439.085	1.085	12.31
				+	44' 3FO	437.592	-0.408	12.32
			Sp Sp	+	5s' 3po	436.907	-1.093	13.52
				+	5s' 3po	436.249	-1.751	13.52
			sp sp2	+	5s' 3po	436.533	-1.467	13.52
			4p" 1p1	+	5s' 3po	439.291	1.291	13.52
				+	5s' 3po	438.625	0.625	13.52
				+	5s' 3po	437.162	-0.838	13.53

13.52

Table XV (continued)

λ_o Δλ_o (nm)

+ Energy	γ - γ WH	(mu)	438.936 0.936 11.26	438.928 0.928 11.26	438.921 0.921 11.26	437.425 -0.575 11.27	437.423 -0.577 11.27	437.415 -0.585 11.27	438.928 0.928 11.26	438.921 0.921 11.26	438.915 0.915 11.26	437.425 -0.575 11.27	437.423 -0.577 11.27	439.238 1.238 14.08	439.967 1.967 14.08
He + C1 + C1	Т ,														
He ⁺ + C1 ₂ +	Transition Assignment	Lower State + Upper State	+ 4f 5F4	+ 4f 5F3	+ 4f 5F ₂	+ 4f 3F2	\leftarrow 4f 3 F ₃	+ 4f 3F4	+ 4f 5F3	+ 4f 5F2	+ 4f 5F ₁	+ 4f 3F2.	+ 4f 3F3	+ 6s' 300	+ 6s' 300
Reaction 100 eV	Transiti	Lower State	3d' 3 _{D3}						3d ³ D ₂					4f SF4	4£ 5p
Luminescence from the Reaction 100 eV He + Cl ₂ + He + Cl + Energy	, c	$(cm^4 \times 10^{18})$ X	C1 11												

Table XV (continued)

Luminescence from the Reaction 100 eV He + Cl₂ + He + Cl + Energy

A) A) (mm)

g d	•	Transition Assignment	on As:	signment	ኍ(λ _T - λ _o	HĄ (
(OI x II)	×	Lower state	+	Lower State + Upper State	Ē,		(ev)
	C1 11	4f ⁵ F ₂	+	6s' 3 ₀	439.975	1.975	14.08
			+	6s' 3 _D °	439.254	1.254	14.08
		4f ⁵ F ₁	+	6s' ³ D ₂	439.981	1.981	14.08
		4f 3F2	+	6s' 1 _{D2}	436.094	-1.906	14.11
		4f ³ F ₃	+	$6s^{1}D_{2}^{0}$	436.096	-1.904	14.11
		44 5 _D °	+	5p' ³ _{D₁}	438.084	0.084	12.91
			+	5p' ¹ p ₁	438.084	0.084	12.91
		4d ⁵ D ₁	+	sp' 3 _{D1}	438.104	0.104	12.91
			+	5p' ³ D ₂	437.445	-0.555	12.91
			+	5p' lp'	438.104	0.104	12.91
		4d 5p ₂	+	5p' · 3 _{D1}	438.140	0.140	12.91
			+	5p' ³ D ₂	437.481	-0.519	12.91
			+	5p' ³ D ₃	436.152	-1.848	12.92
			+	Sp' 1P1	438.140	0.140	12.91

Table XV (continued)

~° (E

ΔH (eV) 12.92

12.91

12.92

12.92

12.92 13.21 13.21

3.33

-0.645

578.955

-0.854

578.746

5g 2(4)_{7/2} 5g 2(3)_{5/2}

-0.855

578.745

5g 2(3)7/2

	γ - γ ₀	(mm)	-1.848	-0.470	-1.798	-1.798	-1.778	-1.778	0.694	0.694	0.853	0.040
+ Energy	Ļ	(m)	436.152	437.530	436.202	436.202	436.222	436.222	438.694	438.694	580.453	579.640
+ C1 ₂ + He + C1	signment	Upper State	+ 5p ¹ 3F ₃	5p' ³ D ₂	5p' ³ D ₃	5p1 3F3	5p' ³ D ₃	5p' ³ F ₃	5p' 1 _{D2}	5p' 1 _{D2}	5d 1(3),,,	5d 1(1) _{3/2}
Luminescence from the Reaction 100 eV He + Cl ₂ + He + Cl + Energy	Transition Assignment	ate	4d 5 _{D2} +	4d ⁵ p ₃ +	+	+	4d 5p ^o +	+	3d' 3po +	3p 3po +	4p 4p, +	7/5
from the Rea		×	11 13								1 13	
Luminescence	, b	(nm) $(cm^2 \times 10^{18})$									3.6	
	δλο	(mm)									2.0	

Table XV (continued)

Energy	1
C1 + C1 + Ener	
-	The state of the s
+ He	
e from the Reaction 100 eV He + Cl > + He +	
eV He	
on 100	1
Reacti	
m the	1
ce fro	1
Luminescence	

λ_o Δλ_o (nm)

mirites centre	TIOIII	Neaction 100 ev	distribution the reaction for evine + C12 + ne + C1 + C1 + C1 + C1 t filety	15	i k	
b (Transitio	Transition Assignment	۲,	λ _T - λ _O	HV .
(cm ² x 10 ¹⁸)	×	Lower State	Lower State + Upper State	(mu)	(mm)	(e)
	C1 I	4p 4po 5/2	+ 5g 2(2) _{5/2}	578.476	-1.124	3.33
			+ 5g 2(2) _{3/2}	578.476	-1.124	3.33
		4p 4p _{5/2}	+ 8s 2(2) _{5/2}	578.237	-1.363	3.48
•		4p 4po	+ 5d 1(2) _{5/2}	580.846	1.246	3.35
		4p 4 _{D3/2}	+ 6d 1(1) _{3/2}	580.044	0.444	3.52
		4p 4p ⁰ / _{7/2}	+ 6d 2(4) _{9/2}	580.152	0.552	3.45
			+ 3d' ² G _{7/2}	579.806	0.206	3.45
			+ 3d' ² G _{9/2}	579.791	0.191	3.45
			+ 5g 0(4) _{9/2}	578.059	-1.541	3.46
			+ 5g 0(4) _{7/2}	578.059	-1.541	3.46
		4P 2D5/2	+ 6d 1(2)3/2	581.479	1.879	3.54
			+ 6d 1(2) _{5/2}	581.028	1.428	3.54
			+ 3d' ² p _{3/2}	578.132	-1.468	3.55

Table XV (continued)

y (iii)

	Luminescence	from	the Re	action 100 eV	He+	Luminescence from the Reaction 100 eV He + Cl ₂ + He + Cl + Cl + Energy	+ C1 + Ene	rgy	
γ _o (III)	σ σ (cm ² × 10 ¹⁸)	. *		Transition Tower State	on As	Transition Assignment	ት <u>[</u>	λ _T - λ _o	# 8
	(or v m)	•		חסווסו המוסד	,	opper state			(66)
		2	C1 1	4p 4p01/2	¥	3d' ² p _{1/2}	579.490	-0.110	3.55
					+	3d' ² p _{3/2}	579.490	-0.110	3.55
					+	6d 0(2) _{3/2}	577.643	-1.957	3.56
				4p 2p03/2	+	3d' ² _{D5/2}	581.428	1.828	3.58
				4p 2po 3/2	+	8d 2(2) _{5/2}	581.264	1.664	3.64
		CI	C1 11	4p ⁵ p ₃	+	3d" ³ po	578.572	-1.028	9.01
	*				+	3d' ³ po 2	578.572	-1.028	9.01
				4s' 1 _{D2}	+	4p' ³ _{D₁}	579.213	-0.387	9.05
					+	4p' 3 _{D2}	579.086	-0.514	9.05
				4p' 1 _{D2}	+	5s' ³ Dº	579.439	-0.161	12.05
					+	5s', 3 _{D2}	578.755	-0.845	12.05
				5p 5p1	+	7s ⁵ S ₂	581.110	1.510	12.81
				4p" 3p1	+	$_{\rm 6d} ^{\rm 5p_0^o}$	579.146	-0.454	12.89
				4p" 3p2	+	44, 3 _S 0	578.697	-0.903	12.91

Table XV (continued)

Luminescence from the Reaction 100 eV He + Cl2 + He + Cl + Energy

φλ_ο (m)

(mm)

				25		al	
0 2 18	•	Transiti	on As:	Transition Assignment	, ⊢ (λ _T - λ _o	#
C N × IIO	×	Lower State	+	Lower State + Upper State		(E)	(e)
	C1 11	3d" 3F0	+	sp 3p2	578.325	-1.275	10.95
			+	sp ³ p ₁	999'22'	-1,934	10.95
			+	4p" ³ p ₂	578.325	-1.275	10.95
			+	4p" ³ p ₁	577.666	-1.934	10.95
		3d' 3F2	+	5p 3p ₂	578.325	-1.275	10.95
			+	sp 3p ₁	577.666	-1.934	10.95
			+	4p" ³ p ₂	578.325	-1.275	10.95
			+	4p" ³ p ₁	577.666	-1.934	10.95
		5p 3p	+	6d ⁵ D ₁	579.146	-0.454	12.89
		5p 3p2	+	44' ³ so	578.697	-0.903	12.91
		4£ 3F3	+	7d ⁵ D ₄	577.938	-1.662	. 13.41
		4£ 3F4	+	7d ⁵ D ₄	577.953	-1.647	13.41
		3d' ³ F ₃	+	5p' 3F;	580.288	0.688	12.95
		3d' 1F3	+	5p' 3F4	580.288	00.688	12.95

Table XV (continued)

		20	4	d	4	4	4	4	0	Σ.	4	15
1	(e) H	2.95	1.54	12.31	12.24	12.24	12.24	12.24	1.50	3.23	1.54	12.33
λ ₄ - λ ₂	(mm)	-0.142	0.262	-0.253	0.354	-0.017	0.354	-0.017	0.216	-0.109	0.115	-0.218
ţ	(mm)	725.458	725.862	725.347	725.954	725.583	725.954	725.583	741.616	741.291	754.915	754.582 -0.218
Transition Assignment λ _τ λ ₁	Lower State + Upper State	+ 4d 1(1) _{1/2}	4p 4s _{3/2}	4d' 3F2	6p ⁵ P ₁	6p ⁵ P ₂	6p ⁵ p ₁	6p ⁵ P ₂	4p 2po 4p 3/2	5d 2(1) _{1/2}	+ 4p 4so +	4d' 3Fo
on As	+	+	+	+	+	+	+	+	+	+	+	+
Transiti	Lower State	4p 4p0	4s 4p 5/2	4p" 3D3	$3d^{1} p_{2}^{0}$		3d" 1 _{D2}		4s 4p 5/2	4p 2s1/2	4s 4p 3/2	Sp Sp3
	×	C1 I		C1 11					C1 I		, C1 1	C1 11
6	$(cm^2 \times 10^{18})$	5.7							1.6		6.1	
44		0.50							0.50		0.50	
۲,	(mm)	725.60							741.40		754.80	

Table XV (continued)

	HV	(§)	15.44	15.44	15.44	1.50	14.11	14.11	14.11	14.04	1.54	3.42	3.42	15.21	15.21	15.21
rgy	λ _T - λ _o	(mm)	0.169	0.169	-0.134	0.171	0.428	0.447	0.461	-0.231	0.210	0.071	0.055	-0.470	-0.470	-0.471
- C1 + Ene	Ļ	(mm)	771.969	771.969	771.666	171.971	772.228	772.247	772.261	771.569	774.710	774.571	774.555	781.830	781.830	781.829
Luminescence from the Reaction 100 eV He + Cl2 + He + Cl + Cl + Energy	ignment	Upper State	15p ³ p ^o	15p ³ p ₀	15p ¹ p ⁰	4p 2po	6s' 1 _{D2}	6s' 1 _{D2}	6s' 1 _{D2}	9f ⁵ F ₅	4p 4S _{3/2}	5f 1(3)%	5f 1(3) _{5/2}	7p 3po	7p ³ p ^o	7p 3p0
100 eV He +	Transition Assignment	ate +	+	+	+	+	+	+	•	+	+	+	+	•	+	+
Reaction	Ţ	Lower	3s 1S0			4s 4p3/2	Sf ⁵ F ₃	Sf SF2	Sf SF	4d' 1G4	4s 4p1/2	3d 4D7/2		3s 3S1		
from the		×	He I			1 13	C1 11				1 13			He I		
Luminescence	•	(cm ² x 10 ¹⁸)	1.5								3.2			2.0		
	δλ _ο	(mm)	0.50								0.50			0.50		
	₄ °	(mr)	771.80								774.50			782.30		

Table XV (continued)

	(eV)	15.42	15.42	2.78	3.42	3.42	1.40	2.98	3.11	3.42	3.42	8.43	8.43
ZZ	λ _T - λ _ο (nm)	-0.433	-0.433	0.051	-0.153	-0.181	0.338	0.273	0.072	0.374	-0.396	0.473	0.473
- C1 + Ener	۲ [,] (آس	781.867	781.867	782.351	782.147	782.119	788.038	787.973	787.772	788.074	787.304	788.173	788.173
C1 ₂ + He + C1 ⁺	ignment Upper State	13p 3po	13p 3p0	4d 2(3) _{7/2}	Sf 1(2) ⁰ 3/2	Sf 1(2) _{5/2}	4p 2p _{5/2}	4d 1(3) _{5/2}	4f 1(2)0,2/2	7p 2(2)3/2	Sf 1(3) _{\$/2}	34' 30°	3d 3D ₂
Luminescence from the Reaction 100 eV He + Cl2 + He + Cl + Cl + Energy	Transition Assignment Lower State + Upper State	3s 1S ₀ +	+	4p 4p0 +	٠	٠	٠	+	+		•	4p 5p2 +	•
om the Reac	×	H -		1 13			1 10					n 13	
uminescence fr	g (cm ² x 10 ¹⁸)						1.5						
21	4° (II						0.50						
	γ° (m)						787.70						

Table XV (continued)

Ν	(e)	2.87	2.90	2.97	3.04	3.07	3.42	13.80	13.80	13.80	14.08	14.08	15.45	. 15.45
1 - 1°	(mm)	0.208	0.319	-0.486	0.348	0.090	-0.063	-0.081	-0.267	0.460	-0.067	-0.060	-0.051	-0.051
7	(mm)	793.608	793.719	792.914	793.748	793.490	793.337	793.319	793.133	793.860	793.333	793.340	808.649	808.649
Transition Assignment	Lower State + Upper State	4d 2(4) _{9/2}	4d 2(4) _{7/2}	4d 1(1) _{3/2}	4d 0(2)3/2	6s 1(1) _{3/2}	7p 2(2)3/2	4d" 3F0	4d" 3F0	4d" 3F0	6s' 30°	6s' 3 ₀	17d ³ D ₃	17d ³ D,
ion Ass	+					٠			٠	٠	٠	٠	٠	+
Transit	Lower Stat	4p 4p,	4p 4p.	4p 20,5/2	4p 2p0,	4p 2p0	3d 4p°	6p Sp2		6p Sp3	Sf 3F2	Sf 3F3	3p 3po	
	*	1 13						11 13					# 1	
	(cm, x 1018)	1.5											4.2	
40	(III	09.0											0.40	
ر °	(mm)	793.40											808.70	

Table XV (continued)

(E) 0,

1

49	b		Transition Assignment	n As	signment	Ļ	λ- λ	HV
	(cm ² x 10 ¹⁸)	*	Lower State	+	+ Upper State	(mg)	(mm)	(e)
		He I	3p 3po	+	17d ³ D ₁	808.649	-0.051	15.45
				+	17d ¹ D ₂	808.646	-0.054	15.45
			3p 3po	+	17d ³ D ₂	808.650	-0.050	15.45
				+	17d ³ D ₁	808.650	-0.050	15.45
				+	174 ¹ D ₂	808.648	-0.052	15.45
			3p 3p0	+	17d ³ D ₁	808.668	-0.032	15.45
	٠	1 13	4p 2p _{3/2}	+	4d 1(2) _{3/2}	808.697	-0.003	2.98
			4p 2p0	+	4d 0(2) _{5/2}	808.716	0.016	3.04
			4p 4s3/2	+	6s 1(1) _{1/2}	808.718	0.018	3.07
			4s' 2 _{D5/2}	+	4p' 2po 5/2	808.890	0.190	2.87
				+	4p' 2p0 3/2	808.673	-0.027	2.87
			4s' 2 _{D3/2}	+	4p' 2p° 4p' 25/2	808.995	0.295	2.87
				+	4p' 2p',	808.778	0.078	2.87

Table XV (continued)

		Luminescence fr	om the Rea	ction 100 eV	He+	Luminescence from the Reaction 100 eV He + Cl2 + He + Cl + Energy	+ C1 + Ener	X 3 .	
γ° (mm)	δλ _o (mm)	σ (cm ² x 10 ¹⁸) X	×	Transiti Lower State	ion As	Transition Assignment Lower State + Upper State	, [II]	$\lambda_{\rm T} - \lambda_{\rm o}$ (nm)	₽H (eV)
			11 13	4d' 3FO	+	+ 8f ⁵ F ₅	808.361	-0.339	13.86
					+	8f ⁵ F ₄	808.361	-0.339	13.86
					+	8f ⁵ F ₃	808.361	-0.339	13.86
821.20	0.40	3.3	He I	3p 3p0	+	14s ¹ S _o	821.356	0.156	15.43
			1 13	4s 4P5/2	+	4p 4p° 5/2	821.430	0.230	1.34
				4p 2s0	+	6s 1(1) _{1/2}	820.856	-0.344	3.07
			C1 11	4s" 3p0	+	4p' ³ p ₁	820.856	-0.344	9.50
822.20	0.50	7.7	He I	3p 3p ₂	+	14s ³ S ₁	822.252	0.052	15.42
				3p 3p0	+	14s ³ S ₁	822.254	0.054	15.42
				3p 3p0	+	14s ³ S ₁	822.272	0.072	15.42
			C1 I	4s 4p 3/2	+	4p ² D _{5/2}	822.400	0.200	1.40
				4s ⁴ P _{1/2}	+	4p 2p _{3/2}	822.271	0.071	1.45
				4p 2pg,	+	+ 4d 1(1), /2	822.311	0.111	2.95

Table XV (continued)

	ΔH (eV)	10.52	10.52	14.32	1.38	3.33	3.33	9.48	10.97	10.97	13.60	13.60	13.60
ZS.	λ _T - λ _o (mm)	-0.104	-0.104	0.308	0.160	0.165	0.150	0.352	0.068	0.068	-0.017	-0.017	-0.017
. C1 + Ene	λ _T (mm)	822.096	822.096	822.508	833.560	833.565	833.550	833.752	833.468	833.468	833.383	833.383	833.383
+ C1 ₂ + He + C1 +	signment Upper State	4p" ³ S ₁	4p" ³ S ₁	5p" ³ D ₂	4p 4p ^o 3/2	5f 2(2) ⁰ 3/2	Sf 2(2) ⁰ ,	4p' ³ p ₂	3d 3 _D	4d ³ D ₃	7£ ⁵ F ₄	7f ^S F ₃	7f ⁵ F ₂
Luminescence from the Reaction 100 eV He ⁺ + Cl ₂ + He + Cl ⁺ + Cl + Energy	Transition Assignment Lower State + Upper State	+	3d' 3po +	7s 5S ₂ +	4s 4p _{3/2} +	3d 4 _{D3/2} +	A	4s" ³ p° +	4p' 3p ₂ +	+	5d ³ D ₃ +	+	+
om the Reg	*	C1 11			1 13			C1 11					
uminescence fr	$(cm^2 \times 10^{18})$				7.6								
71	γγ _o (mm)				0.50								
	γ° (mm)				833.40							•	

13.60

833.267 -0.133

5d 3p2

13.60

-0.135

Table XV (continued)

Luminescence from the Reaction 100 eV He + Cl₂ + He + Cl⁺ + Cl + Energy

λ_o (nm) 837.70

۵ ^۸ ۵	b (Transition Assignment	on As	signment	۲,	Yr - Yo	ΔH
(mm)	$(cm^2 \times 10^{18})$ X	×	Lower State	+	Lower State + Upper State	(mm)	(mm)	(eV)
0.40	40.7	He I	3d ³ D ₃	+	20p 3po	838.001	0.301	15.46
			3d ³ D ₂	+	20p 3p0	838.001	0.301	15.46
				+	20p 3po	838.001	0.301	15.46
				+	20p 1p0	837.862	0.162	15.46
			34 ³ _{D1}	+	20p 3po	838.005	0.305	15.46
				+	20p 3p0	838.005	0.305	15.46
				+	20p 3po	838.005	0.305	15.46
				+	20p 1p0	837.865	0.165	15.46
		C1 I	4s 4p 5/2	+	4p 4p°7/2	837.824	0.124	1.31
			4p 2po 3/2	+	44 2(0)1/2	837.402	-0.298	2.93
		C1 11	4p' 3 _{D1}	+	3d' 1 _{D2}	837.639	-0.061	10.53
				+	3d" 1 _D °	837.639	-0.061	10.53
			4p' 3 _{D2}	+	$34^{\circ} ^{1}D_{2}^{0}$	837.906	0.206	10.53
				+	3d" 1D2	837.906	0.206	10.53

Table XV (continued)

λ_o (nm) 842.90

	Luminescence fr	om the	Reaction 100 eV	He+	Luminescence from the Reaction 100 eV He + Cl ₂ + He + Cl ⁺ + Cl + Energy	+ C1 + Ene	rgy	
Δλ _o (mm)	$(cm^2 \times 10^{18})$. ×	Transit: Lower State	ion As	Transition Assignment Lower State + Upper State	λ _T (mm)	λ _T - λ _o (mm)	∆H (eV)
0.40	5.6	He I	3d 3 _{D3}	+	18p ³ p ₂	842.594	-0.306	15.45
			3d ³ D ₂	+	$^{18p}_{2}$ $^{3p_{2}^{0}}$	842.595	-0.305	15.45
				+	18p ³ p ^o ₁	842.595	-0.305	15.45
			3d ³ D ₁	+	18p 3po	842.598	-0.302	15.45
				+	18p ³ p ^o ₁	842.598	-0.302	15.45
				+	18p ³ p ^o ₀	842.598	-0.302	15.45
			3d 1 0	+	18p ³ p ^o ₂	842.837	-0.063	15.45
				+	18p ³ p ⁰ ₁	842.837	-0.063	15.45
				+	18p ¹ p0	842.636	-0.264	15.45
		C1 1	4s ⁴ P _{1/2}	+	4p 4po 1/2	843.057	0.157	1.41
			3d ² D _{3/2}	+	7f 1(2) ⁰ ,2	843.072	0.172	3.68
				+	7f 1(2) ⁰ _{5/2}	843.063	0.163	3.68

AD-A03	SIFIED	AIR F EMISS SEP 7	ION CRO	ST OF T SS-SECT SIEGENT 76-2	ION MEA	GHT-PAT	TERSON TS OF L	AFB OH	IO SCH RGY HE(ETC +) IONS	F/G 20/ WIET	(8 (U)	
	3 OF 44 AD A034035										Parity minds		
de di ini de di ini de di ini de di ini di ini	Sincial Control of the Control of th		Affirm serion	Gilliani Grantesi Grantesi	Chillin to the description of control of the control of control of control of the		Janetti tiy Janetti tiy Janetti tiy	perference on berde in	der de Sterry Secretals	And the second			
			Account of		-			process of the second	de me deln la me e	landia ke ;	planner the	Gillian Total	N. S.
	And I		And the second s		le comment		Rossess Rossess Rossess			American Agenty and		Francis Commission (Commission Commission Co	
				Access eller	January III	Januarian Januarian J	Butturen		James Commission of the Commis	plants with the colors of the	perfect selection of the selection of th	Annual desiration of the same	
Final Property Control of the Contro			Action 100 per		printerne ka pina n k	A Common	Contestion of	Janes III	Am inimi Am		Accordance of the second	An order	
				January January Livery	Parameter Communication of the	Anti-reference	James June James June June + cold	Samuel Sa	10000000000000000000000000000000000000			de men	



Table XV (continued)

	PH (SeV)	13.86	13.86	13.86	13.86	14.32	15.44	2.79	1.38	13.50	13.50	13.50	13.50
첢	$\lambda_{\rm T} - \lambda_{\rm O}$	-0.270	-0.270	-0.270	0.292	0.211	0.298	0.438	0.160	-0.241	-0.241	0.374	0.374
C1 + Energ	, [E	842.630	842.630	842.630	843.192	843.111	857.898	858.038	857.760	857.359	857 359	857.974	857.974
C12 + He + C1 +	signment Upper State	+ 8f ⁵ F ₅	8f ⁵ F ₄	8f ⁵ F ₃	8f ³ F ₄	5p" ³ D ₂	16s ³ S	1 4d 2(2) _{5/2}	4p 4p° 2/2	4f' 3 _{D2}	4f' 1 _{D2}	4f' ³ f ₄	4f' ³ G ₄
from the Reaction 100 eV He + Cl ₂ + He + Cl + Energy	Transition Assignment Lower State + Upper State	4d, 3G, +	•		44' 3G5 +	7s ³ S ₁ +	3n 1po +	4p 4p + +++++++++++++++++++++++++++++++	4s 4p _{1/2} +	5s' 3 _D ° +	•	5s' 3 _{D3} +	
m the Read	×	n n					<u>.</u>	1 15		11 13			
Luminescence fro	σ (cm ² x 10 ¹⁸)						o «						
31	Δλ _o						0.50						
	γ° (III)						857.60						

Table XV (continued)

λ_o Δλ_o (nm) (nm) 858.70 0.50

Inescence fro	om the R	eaction 100	eV He +	Luminescence from the Reaction 100 eV He + Cl2 + He + Cl + Energy	+ C1 + Ener	, KBX	
, d		Transi	tion As:	Transition Assignment	Ļ	λ _T - λ ₀	HA.
x 10 ¹⁰)	×	Lower State +	tte +	Upper State	(max)	(mm)	(ev)
14.0	He I	3p 3p0	+	10d ³ D ₃	858.500	-0.200	15.36
			+	10d ³ D ₂	858.500	-0.200	15.36
			+	104 ³ D ₁	858.500	-0.200	15.36
			+	10d ¹ D ₂	858.486	-0.214	15.36
		3p 3po	+	10d ³ D ₂	858.501	-0.199	15.36
1			+	104 ³ D ₁	858.501	-0.199	15.36
			+	10d ¹ D ₂	858.487	-0.213	15.36
		3p 3p0	+	10d ³ D ₁	858.521	-0.179	15.36
		3d ³ D ₃	•	14p 3po	858.811	0.111	15.43
			+	14f ³ f ^o	858.422	-0.278	15.43
			+	14f ³ F ₃	858.422	-0.278	15.43
			+	14£ 3F2	858.422	-0.278	15.43
		3d ³ D ₂	٠	14p 3po	858.811	0.111	15.43
			+	14p 3po	858.811	0.111	15.43

Table XV (continued)

A (III)

~° (III

Luminescence fro	om the	Reaction 100 eV	He++	Luminescence from the Reaction 100 eV He + Cl ₂ + He + Cl + Energy	+ C1 + Ener	rgy_	
b		Transiti	ion Ass	Transition Assignment	Ļ	۸- ۲۰	HV
$(cm^2 \times 10^{18})$	×	Lower State	+	Lower State + Upper State	(mm)	(ma)	<u>6</u>
	He I	3d ³ D ₂	+	14f ³ F ₃	858.423	-0.277	15.43
			+	14f ³ F ₂	858.423	-0.277	15.43
			+	14p ¹ p ^o ₁	858.347	-0.353	15.43
		34 ³ D ₁	+	14p 3po	858.814	0.114	15.43
			+	14p ³ p ^o ₁	858.814	0.114	15.43
			+	14p 3p0	858.814	0.114	15.43
			+	14f 3F ₂	858.426	-0.274	15.43
			+	14p 1po	858.351	-0.349	15.43
		3d ¹ D ₂	٠	14p 3po	859.063	0.363	15.43
			+	14p 3po	859.063	0.363	15.43
			+	14f 3 _F ⁰	858.675	-0.025	15.43
			+	14f ³ F ₂	858.675	-0.025	15.43
			+	14p 1p0	858.599	-0.101	15.43
	1 2	4s 4p 3/2	+	4p 4p _{5/2}	858.834	0.134	1.34

Table XV (continued)

	4	(ex)	13.50	13.50	13.50	13.50
23	λ _T - λ _o		0.160	-0.185	0.160	-0.185
+ C1 + Ener) ۲۰		858.860	858.515	858.860	858.515
ce from the Reaction 100 eV He + Cl ₂ + He + Cl ⁺ + Cl + Energy	Transition Assignment	rower state + opper state	(1 5s' $^3D_2^0 + ^4f' ^3D_2$	+ 4f' ³ D ₃	+ 4f' ¹ D ₂	+ 4f' ³ F ₃
Luminescence from the	0 0 000	v (orv =)	11 15			
	a °[
	~° [Ì				

$$\sigma_{TOTAL} = 497.0 \times 10^{-18} \text{ cm}^2$$
 $\sigma_{VUV} \text{ TOTAL} = 375.9 \times 10^{-18} \text{ cm}^2$ $\sigma_{VISIBLE} \text{ TOTAL} = 121.1 \times 10^{-18} \text{ cm}^2$

Appendix B

Table XVI

Luminescence from the Reaction 100 eV He + Br + He + Br + Br + Energy

Explanation of Symbols

a = Observed vacuum wavelength (nm)

Δλ_o = Search interval (nm)

= Emission cross section $(cm^2 \times 10^{18})$

- Emitting atom or ion

= Calculated vacuum wavelength in nm using the energy level tables (Refs. 42, 58 and 68).

 ΔH = Enthalpy change in eV required to populate the upper energy state for the thermal reaction He⁺ + Br² + He + Br⁺ + Br^{*}.

= Transition selected by criteria stated in Chapter IV.

Inner electron configuration designation (Refs. 58 and 68).

Br I Unprimed =
$$\binom{3p}{2}$$
 ' = $\binom{3p}{1}$ '' = $\binom{3p}{2}$ ($^{1}D_{2}$) = $\binom{1}{2}$ ($^{1}D_{2}$) = $\binom{1}{2}$ Br II Unprimed = $\binom{4}{5}$ ' = $\binom{2}{5}$ '' = $\binom{2}{5}$

Table XVI (continued)

								á	
%	A A	° (Transition Assignment	n As	signment	ታ	۸- ۲۰	Ħ
(mm)		(nm) (cm ² x 10 ¹⁸) X	×	Lower State + Upper State	+	Upper State	(m)	(ma)	(eV)
88.925	0.3	1.5	Br 11	4p ⁴ 3p ₂	+	+ 4d 3 _D 0	88.971	0.046	3.16
					+	4d ³ D ₃	88.920	-0.005	3.17
				4p ⁴ 1s ₀	+	sd ⁵ p ₁	89.010	0.085	19.9
903.75	0.3	1.0	Br 111	4p ⁴ 3p ₂	+	5s' ³ D ₃	90.598	0.223	2.91
				$4p^4 1_{D_2}$	٠	5s" 3po	90.475	0.100	4.43
					+	44' ¹ F ₃	90.397	0.022	4.45
90.775	0.3	6.0	Br 11	4p ⁴ 3p ₂	+	+ 5s' 300	90.598	-0.177	2.91
				4p ⁴ 3p ₁	+	4p ⁵ 1po	90.741	-0.034	3.28
					÷	5s' 1 _{Do}	91.074	0.299	3.23
•				4p ⁴ 1 _{D2}	+	5s" 3po	90.475	-0.300	4.43
				4p ⁴ 1s ₀	+	+ 6s A ₁	90.702	-0.073	6.36

Table XVI (continued)

	H	(eV)	2.80	2.83	3.23	3.28	4.30	6.29	2.80	2.83	3.92	2.14	2.13	2.13	2.14
87	λ _T - λ _o	(m)	0.209	-0.003	-0.101	0.147	0.187	-0.044	0.033	-0.192	-0.075	-0.061	-0.001	0.038	-0.035
+ Br + Energy	۴	(mu)	91.384	91.172	91.074	91.322	91.362	91.131	94.083	93.858	93.975	96.014	96.074	96.113	96.04
Luminescence from the Reaction 100 eV He + Br ₂ + He + Br +	Transition Assignment	Lower State + Upper State	5s' 3 ₀	5s' 3 ₀	5s' 1 _{D2}	$4p^{5} _{1}^{p_{0}}$	5s" 3po	6s ³ S ₁	5s' ³ D ₁	5s' 3 _{D2}	44' 3FO	44 ⁵ D ₁	4d ⁵ D ₂	44 ⁵ D ₃	4p4 4p3/2
/ He +	ion Ass	+	+	+	+	+	+	+	+	+	•	•	+	+	+
ction 100 e	Transit	Lower Stat	4p4 3p2		4p4 3p1	4p4 3p0	4p4 1p2	4p ⁴ 1s ₀	4p ⁴ 3p ₁		4p4 1p2	4p4 3p2			4p3 4S0
rom the Rea		×	Br II		•				Br II			Br 11			Br 1111
uminescence f	٥,	$(cm^2 \times 10^{18})$	1.3						1.2			1.9			
-1		(<u>m</u>	0.3		÷.				0.3			0.3			
	_ح ہ	(mm)	91.175						94.050			96.075			

Table XVI (continued)

(nm) (cm ² x 10 ¹⁸) X Lower State + Upper State (nm) 0.3		440	, b		Transition	Transition Assignment	,	λ _T - λ _o
775 0.3 1.4 Br II $4p^4 ^3p_1 + 4d ^5p_0^2$ 98.944 - 4d $^5p_0^2$ 98.997		(mm)	$(cm^2 \times 10^{18})$	×	Lower State	+ Upper State	(mm)	(mm)
$\begin{array}{cccccccccccccccccccccccccccccccccccc$	98.975	0.3	1.4	Br 11	4p ⁴ 3p ₁ +		98.944	-0.031
$\begin{array}{cccccccccccccccccccccccccccccccccccc$			•		+		98.997	0.022
0.4 2.3 Br II $4p^4$ 3p_2 + $4p^5$ 1p_0 98.771 - $^4p^4$ 3p_2 + $5s^3$ 3s_0 101.547 + $4p^4$ 3p_0 + $4d^3$ 3p_0 101.100 - $^4p^4$ 3p_0 + $^4p^5$ 3p_0 106.489 0.3 6.7 Br II $^4p^4$ 3p_0 + $^4p^5$ 3p_0 106.489 + $^4p^5$ 4p_0					•	44 ⁵ D ₂	99.062	0.087
0.4 2.3 Br II $4p^4 \ ^3p_2 + 5s \ ^3s_1^0$ 101.547 $+ 4p^5 \ ^3p_0$ 101.207 $- 4p^4 \ ^4s_0 + 4d^4 \ ^3p_0$ 101.100 $- 4d^4 \ ^3p_0 + 4d^4 \ ^3p_0 + 4d^4 \ ^3p_0$ 103.692 $- 6.7$ Br II $4p^4 \ ^3p_2 + 4p^5 \ ^3p_0^2$ 106.489 $+ 8s^4 \ ^4p_{1/2} + 8s^4 \ ^4p_{1/2} + 8s^4 \ ^4p_{1/2} + 6d^4 \ ^2p_{5/2} + 6d^4 \ ^2p_$			(C) 149.				177.86	-0.204
0.4 2.3 Br II $4p^4 \ ^3p_2 + 5s \ ^3S_1^0$ 101.547 + $4p^5 \ ^3p_0$ 101.207 - $4p^4 \ ^1S_0 + 4d^4 \ ^3p_1$ 101.100 - 0.4 3.0 Br II $4p^4 \ ^3p_2 + 4p^5 \ ^3p_2$ 103.692 - 0.3 6.7 Br I $4p^5 \ ^2p_0 + 8s^4 \ ^4p_{1/2}$ 106.489 + $8s^4 \ ^4p_{1/2}$ 106.489 + $6d^{11} \ ^2p_{5/2}$ 106.282 -						5s' 1p ^o ₂	99.166	0.191
$\begin{array}{cccccccccccccccccccccccccccccccccccc$	101.325	0.4	2.3	Br 11			101.547	0.222
0.4 3.0 Br II $4p^4$ $^{1}S_{0}$ + $4d^{1}$ $^{3}P_{0}$ 101.100 - 0.4 3.0 Br II $4p^4$ $^{3}P_{2}$ + $4p^5$ $^{3}P_{2}$ 103.692 - 0.3 6.7 Br I $4p^5$ $^{2}P_{3/2}$ + $8s^{1}$ $^{2}P_{3/2}$ 106.489 + $8s^{1}$ $^{4}P_{1/2}$ 106.282 - $+$ 6d" $^{2}P_{5/2}$ 106.282 -					•	4p ⁵ 3po	101.207	-0.118
0.4 3.0 Br II $4p^4 \ ^3p_2 + 4p^5 \ ^3p_2^0$ 103.692 - 0.3 6.7 Br I $4p^5 \ ^2p_3^0 + 8s' \ ^4p_{1/2}$ 106.489 + 8s' $^4p_{1/2}$ 106.282 - 106.282 -						4d' 3p ₁	101.100	-0.225
0.3 6.7 Br I $4p^5 ^{2}p_{3/2}^{0} + 8s' ^{2}p_{3/2}$ 106.489 $+ 8s' ^{4}p_{1/2}$ 106.402 - $+ 6d'' ^{2}p_{5/2}$ 106.282 -	725	0.4	3.0	Br 11			103.692	-0.033
8s' ⁴ p _{1/2} 106.402 6d" ² p _{5/2} 106.282	.425	0.3	6.7	Br I		8s' ² p _{3/2}	106.489	0.064
6d" ² _{5/2} 106.282					•	8s' ⁴ P _{1/2}	106.402	-0.023
					•		106.282	-0.143

AH (eV) 2.15 2.15 2.13 3.28 3.23 1.44 1.48 4.95

0.88 0.90

Table XVI (continued)

~° €

X	λ _T - λ _O	(mm)	-0.135	0.167	0.160	0.297	0.040	-0.079	-0.090	0.192	0.168	0.226	-0.075	-0.079
· Br + Ener	Ļ	(mm)	106.290	106.592	106.585	106.722	106.465	110.146	110.135	110.417	110.393	110.451	110.150	110.146
· Br ₂ + He + Br +	signment	Upper State	6d" ² D _{3/2}	10d ⁴ D _{5/2}	10d ⁴ D _{3/2}	$(^{1}D_{2})^{4d}$ $^{2}S_{1/2}$	5s ⁵ S ₂	8s ⁴ P _{5/2}	8s ⁴ p _{3/2}	5d' ² F _{5/2}	5d' ⁴ P _{5/2}	5d' 4p 3/2	(¹ D ₂)6s ² D _{3/2}	5s ⁵ S ₂
Luminescence from the Reaction 100 eV He + Br 2 + He + Br + Br + Energy	Transition Assignment	Lower State + Upper State	4p ^{5 2po} +		+		4p ⁴ 3p ₂ +	4p ⁵ 2p ⁰ +	•	•	+	•	4p ⁵ 2p ⁰ +	4p ⁴ 3p ₁ +
rom the R		×	Br I				Br 11	Br I						Br 11
Luminescence f	, ,	$(cm^2 \times 10^{18})$				•		3.7						
	Δλ _o							0.3						

ΔH (eV) 0.89 0.86 0.85 0.85

0.49 0.46 0.45 0.94 0.88

Table XVI (continued)

		Luminescence fr	om the Res	Luminescence from the Reaction 100 eV He + Br + He + Br + Energy	+ He + Br +	Br + Energ	Ы	
_م ہ	440	ъ,		Transition Assignment	ment	ئ	λ- λ	ΗV
(mm)		$(cm^2 \times 10^{18}) \times$	×	Lower State + Upper State		(mm) (mm)	(mm)	(e)
113.925	0.4	6.4	Br 1	4p ⁵ 2p ⁰ _{3/2} + 5d 4F _{5/2}	⁴ F _{5/2}	113.954	0.029	0.11
				+ 5d 4F _{3/2}	4F3/2	113.934	0.009	0.11
•			•	+	sd ⁴ P _{1/2}	113.955	0.030	0.11
				$4p^5 2p_0^0 + 7s^1$	7s' ² p _{3/2}	114.157	0.232	0.55
	•			+	7s' 4 _{p1/2}	114.074	0.149	0.56
				÷ 7d	7d ⁴ D _{1/2}	113.629	-0.296	09.0
117.725	0.3	12.8	Br I	$^{4p}_{3/2}$ $^{2}_{1/2}$ $^{4p}_{3/1}$	5 2 _{51/2}	117.889	0.164	-0.25
				+ 4d" ² D _{S/2}	" ² _{D5/2}	117.723 -0.002	-0.002	-0.24
118.925	0.3	10.1	Br I	+	4d' ⁴ P _{3/2}	118.938	0.013	-0.35
				+	sd 4F _{3/2}	118.928	0.003	0.11
				+ 5d ⁴ P _{1/2}	4 _{P1/2}	118.950	0.025	0.11

Table XVI (continued)

Luminescence from the Reaction 100 eV He + Br + He + Br + Br + Energy

λ _T - λ _o ΔH (nm) (eV) -0.034 -0.39 0.173 -0.41	0.000 -0.52	0.076 -0.57	0.066 -0.64			0.315 -0.21
λ _T (nm) 119.441 119.648 119.637	120.975	121.601	122.441	122.805	122.113	122.690
Transition Assignment Lower State + Upper State $4p^{5} ^{2}p_{3/2}^{o} + 4d' ^{2}F_{5/2}$ $+ 4d' ^{2}p_{3/2}$ $+ 4d' ^{2}p_{3/2}$ $4p^{5} ^{2}p_{0}^{o} + 5d ^{4}p_{1/2}$	+ 6s ⁴ P _{3/2} + 6s" ² P _{1/2}	+ 6s 4p _{5/2}	+ 4d ⁴ F _{5/2} + 4d ⁴ F _{+,12}	3/2 + 4d ⁴ P _{1/2} + 6e' ² P	+ 6s' ² p _{1/2}	+ 4d" ² D _{3/2}
ion Ass :e + + + + + + + + + + + + + + + + + + +						+
Transiti Lower State $4p^5$ 2 2 2 2 2 2 2 4 5 2 2 0	$4p^5 2p_0^0$ $4p^5 2p_0^0$	4p ⁵ 2p ⁰ 3/2	4p ^{5 2po} 3/2	7.5 2.0	τρ '1/2	
X X Br I	Br I	Br 1	Br I			
cm ² x 10 ¹⁸)	. 8. 	15.8	34.9			
Δλ _ο (nm) 0.3	0.3	0.3	0.5			
λ _o (nm) 119.475	120.975	121.525	122.375			

-0.21

Table XVI (continued)

	(eV)	0.88	2.80	-1.36	-1.36	-0.90	-1.36	-2.22	-2.44	9.21	9.21	-2.22
787	λ _T - λ _o (nm)	-0.170	0.246	0.019	-0.012	-0.077	0.009	-0.010	0.046	-0.083	-0.002	0.025
Br + Ener	۲ [,] (آآآ	122.205	122.621	131.769	131.738	131.673	138.459	144.990	148.846	148.717	148.798	153.175
+ Br ₂ + He + Br ⁺ +	signment Upper State	+ 5s ⁵ S ₂	ss' 3 _D °	(¹ b ₂)5s ² b _{5/2}	(¹ b ₂)5s ² b _{3/2}	4s ⁴ D _{3/2}	(¹ D ₂)5s ² D _{3/2}	5s" ² p _{1/2}	5s', ² P _{3/2}	4f' ³ D ₂	4f' A ₂	5s" ² P _{1/2}
Luminescence from the Reaction 100 eV He + Br ₂ + He + Br + Br + Energy				4p ⁵ 2po +	,	4p ⁵ 2p ⁰ _{1/2} +	4p ⁵ 2po +	4p ⁵ 2po +	4p ⁵ 2p ⁰ +	5s 5s ₂ +	•	4p ⁵ 2p ⁰ +
from the Re	×	Br 11		Br I			Br I	Br I	Br I	Br 11		Br I
Luminescence	$(cm^2 \times 10^{18})$			93.4			47.1	28.2	151.2			41.8
	δλ _o (mm)			0.1			0.1	0.1	0.1			0.1
	o (mm)			131.75			138.45	145.00	148.80			153.15

Table XVI (continued)

Energy
+ Br +
+ Br +
Br ₂ + He +
He + Br ₂
100 eV He + B
on 10
Reaction
the I
e from
Luminescence

o' (mm)	φ. (III)	$(cm^2 \times 10^{18})$	*	Transition Assignment Lower State + Upper State	signment Upper State	_ተ ረ (መ)	λ _T - λ _o (mm)	(eV)
154.05	0.1	209.1	Br I	4p ^{5 2po} + 5s ⁴ p _{3/2}	5s ⁴ P _{3/2}	154.066		-2.72
157.60	0.12	384.2	Br 1	4p ⁵ 2po +	5s ⁴ P _{5/2}	157.638	0.038	-2.91
			Br II	$^{4p}_{1/2}$ $^{+}_{3/2}$ $^{+}_{3/2}$ $^{5s}_{3_1}$ $^{+}_{4f'}$ $^{1b}_{2}$	58' ⁷ 3/2 4f' ¹ D ₂	157.679	0.079	9.30
158.20	0.1	96.0	Br I	4p ⁵ 2po +	+ 5s' ⁴ P _{1/2}	158.231	0.031	-2.48
444.05	0.5	0.4	He I	+	5s ¹ S ₀	443.880	-0.170	13.24
			Br I		6p 4p _{3/2}	444.298	0.248	-0.11
•			Br 11	+ +	5d 5D ₃	443.914	-0.136	6.62
447.55	0.5	1.8	He I	2p 3po +	+ 4d 3 _{D3}	447.273 -0.277	-0.277	12.97
					2			

Table XVI (continued)

	# 5	(6)	12.97	12.97	12.97	12.97	12.97	12.97	0.02	-0.14	0.33	0.33	09.9	-0.17	9.35
χ	$\lambda_{\rm T} - \lambda_{\rm o}$		-0.278	-0.317	-0.276	-0.276	-0.315	-0.256	-0.165	0.348	-0.428	-0.260	-0.241	0.136	0.119
Br + Ener	٦٠ آ]	447.272	447.233	447.274	447.274	447.235	447.294	447.385	447.898	447.122	447.290	447.309	452.686	452.669
$Br_2 + He + Br^+$	ignment Imner State	oppor orace	44 'D ₁	4d ¹ D ₂	44 ³ _{D2}	44 ³ D ₁	44 ¹ D ₂	4d ³ D ₁	(102)5p 2p0,3/2	6p 4p ^o _{7/2}	7p 4po 5/2	7p 4po 3/2	sd ³ D ₂	60 4po	4f' ³ F ₂
Luminescence from the Reaction 100 eV He + Br + Br + Br + Energy	Transition Assignment		2p 'P2' +	+	2p ³ p ⁰ +	+	+	+	+	+	5s' ² P _{3/2} +	+	5p ³ p ₂ +	5s 4p +	+
om the Reac	>	· •	ie I		**************************************				Br I				Br II	Br 1	Br 11
uminescence fr	σ σ (cm ² × 10 ¹⁸)		•											1.2	
ᆁ	δλ _ο (III)														
	ر° [[)					452.55	

Table XVI (continued)

		Luminescence fro	om the Rea	action 100 eV He	Luminescence from the Reaction 100 eV He + Br + He + Br + Energy	+ Br + Ene	rgy	
ر°	AA _o	, b		Transition Assignment	ssignment	٠	٨- ١٠	HV
(mu)	(mu)	$(cm^2 \times 10^{18})$	×	Lower State + Upper State	Upper State	(III)	(ma)	(e _V)
470.55	0.5	9.0	Br I	5s' ² p _{3/2} +		470.473	-0.077	0.20
				+	4f (1)%	470.768	0.218	0.19
				•	4f (1) ⁰ _{1/2}	470.781	0.231	0.19
			Br 111	5s 5S ₂ +	Sp Sp3	470.617	0.067	3.51
				5d 5D ₀ +	4f' 1 _{G4}	470.989	0.439	9.26
				5d 5D ₄ +	4f' 1 _{G4}	470.936	0.386	9.26
478.20	9.0	1.4	Br I	5s 4p3/2 +	6p 4 _D 6/2	478.164	-0.036	-0.13
				•	6p 4p0	478.652	0.452	-0.13
				5s" ² P _{1/2} +	6p" 2po 1/2	477.654	-0.546	0.38
			Br 111	5s 5s +	Sp Sp2	478,684	0.484	3.47
				5p' 3F2 +	6s' 3 _D °	478.643	0.443	8.01
				5s' 30° +	5p' 3F2	477.842	-0.358	5.42
				5s' 30° +	5p' 3F2	477.772	-0.428	5.51

Table XVI (continued)

Luminescence from the Reaction 100 eV He + Br 2 + He + Br + Br + Energy

						•			
~°	۵γ	, b		Transition Assignment	n Ass	signment	۲,	λ _T - λ ₀	ΑΛ
(mm)		$(cm^2 \times 10^{18})$	×	Lower State	+	Upper State	(mar.)	(mm)	(eV)
			Br 11	5p" ³ p ₁	+	6s" A ₂	478.799	0.599	9.87
				$5d^5 D_1^0 + 4f' A_2$	+	4f' A ₂	478.238	0.038	9.21
481.55	0.5	9.0	Br 11		+	sp ^S p ₁	481.805	0.255	3.45
					+	6s' ³ 0	481.976	0.426	8.00
					+	5d' 300	481.649	0.099	8.74
				5d 3p ^o ₂	+	+ 4f' ³ G ₃	481.672	0.122	9.18
634.95	9.0	1.7	Br I	5p 4po 5/2	+	+ 5d' ² F _{7/2}	634.706	-0.244	0.44
					+	+ 6d 4F3/2	635.158	0.208	0.44
				5s 4p5/2	+	+ 5p' 45°,	635.248	0.298	-0.95
				5p' 2s0,	+	+ 10d ⁻⁴ D _{3/2}	635.103	0.153	0.86
				$(^{1}p_{2})$ 5s $^{2}p_{3/2}^{+}$ 8p $^{4}p_{3/2}^{0}$	+n	8p 4p _{3/2}	634.556	-0.394	0.59
			Br 11	5s' 1 _D °	+	5p' ³ _{D1}	635.453	0.503	5.18

Table XVI (continued)

Luminescence from the Reaction 100 eV He + Br + He + Br + Br + Energy

_ر ه	440	; ه ور		Transiti	on As	Transition Assignment	Ļ	γ- ۳-	H
(mm)	(mm)	$(cm^2 \times 10^{18})$	×	Lower State	+	Upper State	(mm)	(mu)	(e)
654.50	0.5	.0.4	Br I	5p 4p°,	+	$5p^{4}p_{7/2}^{\circ} + 8s^{4}p_{5/2}$	654.990		0.49
				5p 4po	+	6d ⁴ D _{5/2}	654.637	0.137	0.38
				5p 4po	+	5d' ² p _{1/2}	654.313	-0.187	0.42
				5p' 2p° 5/2	+	10d ⁴ D _{7/2}	654.144	-0.356	0.86
			Br 111	5p" 3 _{D1}	+	5d' 3p0	654.690	0.190	8.74
					+	+ 5d' 1 _{D2}	654.189	-0.311	9.18
655.90	9.6	0.7	Br I	5s 4P _{5/2}	+	$+$ $sp'^2 p_{3/2}^0$	626.159	0.259	-1.02
					+	9d ⁴ D _{3/2}	655.338	-0.562	08.0
658.80	9.0	0.5	Br I	5p 4po 5/2	+	6d ⁴ D _{7/2}	658.398	-0.402	0.37
					+	7d 4F3/2	658.597	-0.203	0.63
				5p 4p0	+	5d" ² D _{3/2}	658.443	-0.357	0.51
				5p' 2p° 2/2	+	4d ² F _{7/2}	659.143	0.343	0.85

Table XVI (continued)

Luminescence from the Reaction 100 eV He + Br + He + Br + Energy

ر ه	4	b		Transition Assignment	on As	signment		۰۲ - ۲	¥
(mm)	1	(nm) (cm ² x 10 ¹⁸)	*	Lower State	+	Upper State	(mm)		· 6
			Br II	4d' 3 _{D2}	+	44' $^{3}D_{2}^{0}$ + 5p" $^{3}D_{2}$	659.352	0.552	9.94
663.15	0.5	1.0	Br. I	5p 4 _{D3/2}	+	7d 4 _{P1/2}	663.092	-0.058	0.61
					+	5p' 2p° 5/2	663.343	0.193	-1.04
				4d 4 _{D3/2}	+	5f" (3) ⁰ 5/2	663.581	0.431	0.97
			Br II		+	+ 5d C ₂	663.143	-0.007	9.12
678.95	0.5	1.4	He I	3s ³ S ₁	+	18p ³ p ^o ₂	678.755	-0.195	13.77
					+	18p 3p0	678.755	-0.195	13.77
					+	18p 3p0	678.755	-0.195	13.77
					+	18p ¹ p ₁ 0	678.625	-0.325	13.77
			Br I	5p 4p°7/2	+	6d 4F9/2	679.191	0.241	0.42
				5p 4po 5/2	+	5d' 2F7/2	678.859	-0.091	0.44
					+	6d 4F3/2	679.376	0.426	0.44

Table XVI (continued)

Luminescence from the Reaction 100 eV He + Br + He + Br + Br + Energy

	(eV)	0.35	0.45	0.79	0.81	0.87	0.88	0.88	0.88	-0.95	0.82	0.82
1	(mm)	0.385	0.235	-0.190	-0.029	0.015	-0.239	0.054	0.089	0.165	0.003	990.0
	(ma)	679.335	679.185	678.760	678.921	678.965	678.711	679.004	679.029	700.715	700.553	700.616
, mont	Upper State	6d ⁴ D _{1/2}	5d' 4p _{3/2}	6d' ² F _{7/2}	9d ⁴ D _{5/2}	8s' ² p _{3/2}	5f' (4)0,	5f' (2) ⁰ 5/2	5f' (2) ⁰ 3/2	5p' 4s',,	6d' ⁴ P _{3/2}	9d ⁴ P _{1/2}
Transition Assimm	Lower State + Upper State	+	+	5p' 2p° +	+	+	+	+	•	+		+
	×	Br I	·	,						Br I		
	$(cm^2 \times 10^{18})$									3.1		
	(mr.)									0.5		
	(mm)									700.55		

Table XVI (continued)

Luminescence from the Reaction 100 eV He + Br₂ + He + Br + Br + Energy

ΔH (eV)	-1.02	0.82	0.84	0.35	0.76	0.76	0.76	0.77	0.76	0.77	0.17	0.43	-1.04
λ _T - λ _o (mm)	0.245	-0.199	-0.433	-0.244	0.440	0.347	0.347	-0.018	0.001	-0.402	0.223	-0.246	0.156
, (m)	726.245	725.801	725.567	725.756	726.440	726.347	726.347	725.982	726.001	725.598	735.123	734.654	735.056
Transition Assignment Lower State + Upper State	5s ⁴ P _{3/2} + 5p' ² D _{3/2}	5p" 2p0 + 6d' 4p5/2		5/2	$^{4d}^{4}D_{5/2} + ^{7f} (4)^{0}_{7/2}$	+	+ 7f (3) ⁰ _{5/2}	+ 7f (2) ⁰ _{5/2}	+ 7f (2) ⁰ _{3/2}	+ 7f (1) ⁰ _{3/2}	5p 4po + 7s 4pz/2		
×	Br 1										Br I		
$(cm^2 \times 10^{18})$	9.0										6.0		
δλ _o (mm)	0.5										4.0		
(mm)	726.00										734.90		

Table XVI (continued)

Luminescence from the Reaction 100 eV He + Br₂ + He + Br + Br + Energy

ΔH (eV)	-1.26	0.76	0.80	-0.89	0.70	0.74	0.20	99.0	99.0	99.0	0.67	0.67
λ _T - λ _o (nm)	0.055	0.434	-0.299	0.267	-0.281	0.210	0.136	-0.169	0.247	0.274	-0.451	-0.426
بر (mn)	751.505	751.884	751.151	780.517	696.621	780.460	794.086	793.781	794.197	794.224	793.499	793.524
Transition Assignment Lower State + Upper State			$^{4d}^{4}D_{1/2} + ^{10p}^{4}D_{3/2}^{0}$	5s' ⁴ p _{1/2} + 5p" ² p _{3/2}			5/2	$4d^4D_{3/2} + 4f''(3)_{5/2}^0$	+ 6f (2) ⁰ _{5/2}	+ 6f (2) ⁰ _{3/2}	+ 6f (1) ⁰ _{3/2}	+ 6f (1)0,2
×	Br I	•		Br 1			Br I					
o (cm ² x 10 ¹⁸)	4.5			3.9			1.4					
δλ _o (mm)	0.5			0.5			9.0				•	
ر (العالم) م	751.45			780.25			793.95					

Table XVI (continued)

Luminescence from the Reaction 100 eV He + Br + He + Br + Br + Energy

(eV)	09.0	-0.89	0.58	0.19	0.19	90.5	0.03	0.17	0.45	99.0	0.18	0.18
λ _T - λ _o (mm)	0.144	0.163	0.144	-0.133	-0.095	0.215	0.061	-0.078	-0.080	-0.340	-0.031	-0.011
(II)	799.194	799.213	799.194	718.917	798.955	799.265	802.611	802.472	802.470	802.210	802.519	802.539
ignment Upper State	7d ⁴ D _{1/2}	5p" 2p0 3/2	8p 4p _{5/2}	4f (1)%	4f (1)0,	44' 3po	+ 5d 4 _{D3/2}	+ 7s 4p3/2	+ 5d' 4p3/2	9s 4p _{5/2}	4f (3)0,2	+ 4f (3) ⁰ _{5/2}
Transition Assignment Lower State + Upper State	5p' 4s _{3/2} +	5s' 2p3/2 +	4d 4D7/2 + 8p 4D5/2	(1 _{D2})5s 2 _{D3/2} +	٠	5p 5p ₃ + 4d' 3 _{D2}			5p' 2s0 +	5p" 2po +	$(^{1}p_{2})5s^{2}p_{5/2}^{+}$ 4f $(3)_{7/2}^{0}$	•
×	Br I					Br 11	Br I					
$(cm^2 \times 10^{18})$	1.5						1.3					
Δλ _o (mm)	9.0						9.0					
y (iii)	20.66						802.55					

Table XVI (continued)

Luminescence from the Reaction 100 eV He + Br + He + Br + Br + Energy

. (₩)	0.19	0.19	0.57	0.57	0.97	0.97	13.76	13.76	13.76	-0.95	0.58	8.47
γ - γ° (mi)	-0.161	0.312	0.551	0.493	-0.243	-0.255	-0.222	-0.221	-0.203	0.224	0.109	0.262
, <u>(m</u>	802.389	802.862	803.101	803.043	802.307	802.295	812.928	812.929	812.947	813.374	813.259	813.412
gnment Ipper State	4f (2) ⁰ 5/2	4f (2) ⁰ 3/2	4f' (4)%	4f' (4)%	5f" (3)%	5f" (3) ⁰ _{5/2}	16s ³ S ₁	+ 16s ³ S ₁	16s ³ S ₁	5p1-4503/2	8p 4p _{5/2}	5d' ¹ p ⁰
Transition Assignment Lower State + Upper State	$(^{1}D_{2})5s^{2}D_{3/2} + 4f^{2}(^{2})_{5/2}^{0}$	+	4d ⁴ D _{7/2} +	•	6s ⁴ P _{5/2} +	•	3p 3po +				4d 4 _{D5/2} +	
	н						He I			Br I		Br 111
$\sigma (cm^2 \times 10^{18}) \times$							3.7					
Δλ _o (mm)							0.5					
°° (III)							813.15					

Table XVI (continued)

Luminescence from the Reaction 100 eV He + Br + He + Br + Br + Energy

λ_o (nm) 815.35

# []	13.7	13.7	13.7	13.7	13.7	13.7	13.7	13.7	-1.3	0.0	0.0	9.0	0.5	8.7
λ ₁ - λ ₀ (mi)	0.427	0.427	0.427	0.423	0.428	0.428	0.425	0.446	0.271	0.247	0.138	0.267	-0.242	0.124
بر (mn)	815.777	815.777	815.777	815.773	815.778	815.778	815.775	815.796	815.621	815.597	815.488	815.617	815.108	815.474
Transition Assignment Lower State + Upper State	15d ³ D ₃	15d ³ D ₂	15d ³ D ₁	15d 1 0	3 ₀	15d ³ D ₁	1 15d 1 0	15d ³ D ₁	5p 40,5/2	5d 4D5/2	5d ⁴ D _{1/2}	7d 4F5/2	8p 4po 3/2	5d' 3D ₂
on As:	↓ .	+	+	+	+	+	٠+	+	+	+	+	+	+	+
Transiti Lower State	3p 3po				3p 3p0			3p 3p0	5s 4p 5/2	5p 4po 5/2	5p 4po 3/2	5p" 2po 3/2	4d 4D _{S/2}	5p" 1 _{D2}
×	He I								Br I					Br 111
σ	3.1													
Δλ _o (mm)	0.5	,												

Table XVI (continued)

Br. I	Rr 7	5c1 2p	+ 5n' 4so.	833.698	0.148
**************************************	I II I	5p' '3/2 5p' '53/2 5p'' ² p' ₀ 5p'' ¹ b ₂ 5p'' ³ p 5p'' ¹ p	+ 5d" 2 _{5/2} + 7d 4 _{01/2} + 5d' 3 ₀ + 5d' 1 ₀ + 5d' 3 ₀ + 5d' 3 ₀		

λ_o (nm) 827.30

ΔH (eV) 113.73 113.73 -1.41

5p" 2p3/2
5p" 2p3/2
5p" 1p2
5p" 3p
5p" 1p 3p 3po Br II He I 9.01 834.45 833.55 202

0.53 0.60 8.74 8.47 8.63

0.127 -0.196 -0.210 0.165

13.72 13.72 13.72

0.013 0.013 0.004

834.463 834.463 834.463

12d 3_D
12d 3_D
12d 3_D
12d 1_D

Table XVI (continued)

Luminescence from the Reaction 100 eV He + Br, + He + Br + Energy	
Br	
+	١
→ He	
T	ì
B	
. +	
He	
eV	-
100	-
Reaction	
the	The state of the s
from	
Luminescence	CONTRACTOR OF THE PROPERTY OF

	(ev)	4 13.7;	4 13.7.	5 13.7	3 13.7	8 13.79	8 13.79	8 13.79	1 13.79	1 13.79	1 13.79	6.0- ·	9 13.78	9 13.7
λ _T - λ ₀	(mm)	0.014	0.014	0.005	0.033	0.188	0.188	0.188	0.191	0.191	0.191	0.146	-0.449	-0.449
Ļ	(mm)	834.464	834.464	834.455	834.483	834.638	834.638	834.638	834.641	834.641	834.641	834.596	838.001	838.001
ssignment	Upper State	12d ³ D ₂	12d ³ D ₁	12d ¹ D ₂	12d ³ D ₁	22d ³ p ₂	$22d ^3p_2^0$	$22d \frac{3p^0}{1}$	22d 3po	22d 3p0	22d 3p0	5p' 4 _D 0	20p 3p2	20p 3p2
Transition Assignment	Lower State +	$^{3p}^{3p_0}$ 4 $^{12d}^{3}$ 3	4	•	3p 3po +	3d ³ D ₃ +	3d ³ D ₂ +	+	3d ³ D ₁ +	+•	Ψ	5s' ⁴ p _{1/2} +	3d ³ D ₃ +	3d 3D ₂ +
	×	He I										. Br I	He I	
, b	$(cm^2 \times 10^{18})$												1.3	
δλ _ο	(mm)												9.0	
₄ °	(mm)												838.45	

Table XVI (continued)

da or

•	Luminescence from the Reaction 100 eV He + Br ₂ + He + Br + Energy	the Reac	tion 100 eV	+ + + +	Br ₂	+ He + Br +	Br + Ener	, ,	
	$(cm^2 \times 10^{18})$	×	Iransition Assignment Lower State + Upper State	on As	Uppe	ent r State	τ. (E	راة) (اق)	(e)
		He I	34 3 _{D2}	+	$^{20p}_{}^{3p^o_{1}}$	3 _{po}	838.001	-0.449	13.78
				+	$^{20p}_{1}^{1}_{P_{1}^{0}}$	$^{1}_{P_1}^{0}$	837.862	-0.588	13.78
	,		34 ³ _{D1}	+	$^{20p}_{2}$ $^{3}p_{2}^{0}$	3 _p o	838.005	-0.445	13.78
				+	20p 3p0	$\frac{3p_0}{p_1}$	838.005	-0.445	13.78
				+	20p 3p0	3 _P 0	838.005	-0.445	13.78
				+	20p 1p0	1 _p o	837.865	-0.585	13.78
			3d ¹ D ₂	+	20p 3p2	$^{3}_{P_2}^{o}$	838.242	-0.208	13.78
				+	$^{20p}_{1}^{3p_{0}^{0}}_{1}$	$^{3p_0}_{1}$	838.242	-0.208	13.78
				`	20p 1p0	$^{1p_0}_{p_1}$	838.102	-0.348	13.78
		Br I	Sp 40,7/2	+	5d 4	5d 4F7/2	839.030	-0.580	0.0
			5p 4po	+	5d 4	5d 4 _{D5/2}	838.634	0.184	0.0
			5p' 4p0	+	8s 4	8s ⁴ P _{3/2}	838.094	-0.356	0.49
			5p" 2p0 1/2	+	74 4	74 4 _{D3/2}	838.074	-0.376	0.61
			4d 4D3/2	+	8р 4	8p 4p _{5/2}	838.473	0.023	0.58

0.58

Table XVI (continued)

	¥	(e)	13.70	13.70	13.70	13.70	13.70	13.70	13.70	13.70	-1.26	13.78	13.78	-1.02	0.37
22	٨- ١٠	(mm)	-0.121	-0.121	-0.121	-0.132	-0.119	-0.119	-0.130	-0.100	0.088	-0.247	-0.247	9.000	0.155
Br + Energ	Ļ	(mm)	844.679	844.679	844.679	844.668	844.681	844.681	844.670	844.700	844.888	847.653	847.653	847.976	848.055
Br ₂ + He + Br +	ignment	Upper State	11d ³ D ₃		11d ³ D ₁	11d ¹ D ₂	11d ³ D ₂	11d ³ D ₁	11d ¹ D ₂		5p 4 _{D3/2}	19d ³ D ₂	19d ³ D ₁	5p' 2p _{3/2}	6d 4D3/2
Luminescence from the Reaction 100 eV He + Br ₂ + He + Br + Br + Energy	Transition Assignment	ate +	3p 3p ^o +	+	•	+	3p 3po +	•	+	+	5s 4p3/2 +.	3p 1po +	•	+	+
om the Rea		×	He I		•						Br I	He I		Br I	
uminescence fr	ъ,	$(cm^2 \times 10^{18})$	24.0									15.7			
	440	(mm)	0.4									4.0			
	ر°	(nm)	844.80									847.90			

Table XVI (continued)

I

(eV)	13.76	13.76	13.76	0.04	0.43	-0.99	0.46	0.73	0.80	-1.47	0.59
λ _T - λ _o (mm)	0.162	0.162	0.162	0.314	-0.260	-0.542	0.216	0.002	0.566	0.054	0.071
(mm)	856.712	856.712	856.712	856.864	856.290	826.008	856.766	856.552	857.116	864.104	864.121
Transition Assignment Lower State + Upper State	16d ³ D ₂	16d ³ D ₁	16d ¹ D ₂	5d 4F9/2	6d 4F _{5/2}	5p' 4p0	5d' 4p3/2	7p. 2p. 7p.	10p 4po 3/2	5p 4po 3/2	8p 4po,
n Ass	+	+	+	+	+	+	+	+	٠,	+	+
Transition Assignment Lower State + Upper St	3p 1p0			5p 4p07/2	5p' 2p° 3/2	5s' 2p3/2	5p' 4p° 1/2	4d 4F7/2	4d 4F5/2	5s ⁴ P _{5/2}	4d 4D.
×	He I			Br I						Br I	
$(cm^2 \times 10^{18})$. 5.1									. 63.0	
δλ _o (mri)	9.0									0.4	
γ° (mu)	856.55									864.05	

Table XVI (continued)

I

Energy
+
+ Br
Br, + He + Br +
+
운
, 1
Br
. 1
운
9
100 eV He + Br,
from the Reaction
the
from
Luminescence

NS AS	(e)	-1.02	0.80
۸- ۲	(mm)	0.190	-0.130
۲,	(mu)	870.090 0.190	869.770
Transition Assignment	Lower State + Upper State	$5s'^{2}p_{3/2} + 5p'^{2}p_{3/2}^{0}$	4d 4F3/2 + 10p 4D0 3/2
	×	Br I	
5	(cm ² x 10 ¹⁸))	9.6	
δλ _ο	(mm)	0.5	
ر°	(mm)	869.90	

$$^{\circ}$$
TOTAL = 1493.3 x 10⁻¹⁸ cm² $^{\circ}$ VUV TOTAL = 1188.9 x 10⁻¹⁸ cm²

 $\sigma_{\text{VISIBLE TOTAL}} = 304.4 \times 10^{-18} \text{ cm}^2$

Appendix C

I

Table XVII

1

Luminescence from the Reaction 100 eV He + I 2 + He + I + I + Energy

Explanation of Symbols

 λ_0 = Observed vacuum wavelength (nm)

Δλ_o = Search interval (nm)

 σ = Emission cross section $(cm^2 \times 10^{18})$

= Emitting atom or ion

 $\lambda_{\rm T}$ = Calculated vacuum wavelength in nm using the energy level tables (Refs. 30, 41, 42 and 48). ΔH = Enthalpy change in eV required to populate the upper energy state for the thermal reaction He⁺ + I₂ + He + I⁺ + I^{*}.

Inner electron configuration designation (Refs. 30, 41, 42 and 48).

NOTE: MI I indicates use of Minnhagen's energy level tables (Ref. 48).

Table XVII (continued)

6у (•)	-0.19	0.57	1.48	1.48	1.51		-0.41	0.46	0.38	1.30	3.28		-0.60	1.11
γ γ (m)	-0.018	0.271	0.260	0.286	-0.004		-0.017	0.047	0.064	-0.078	-0.238		0.041	-0.046
\. [II]	100.057	100.346	100.335	100.361	100.001		101.858	101.922	101.939	101.797	101.637		103.466	103.379
ignment Upper State	Sd' 3Fo	6s" 3po	Sd' 1Fo	5d" 1p0	5d" 3 _D °	6	sd' 'D's	6s" 3po	Sd' 3po	6s" 1p0	5d" 1p0	3.0	6s' D3	6s" 3po
Transition Ass.	5p4 3p2 +	+	٠	٠	•		+	+	•	٠	٠		+	+
×	(II) I						(II) I							
om ² x 10 ¹⁸)	5.3						8.1					1	7.0	
	-						0.300						0.400	
ر (شار) (شار)	100.075						101.875					1	103.425	
	$\Delta\lambda_{\rm o}$ σ Transition Assignment $\lambda_{\rm T}$ $\lambda_{\rm T}-\lambda_{\rm o}$ (nm) (cm ² x 10 ¹⁸) X Lower State + Upper State (nm) (nm)	$\Delta\lambda_{o}$ σ Transition Assignment λ_{T} $\lambda_{T}-\lambda_{o}$ (nm) (cm ² x 10 ¹⁸) X Lower State + Upper State (nm) (nm) (nm) (75 0.300 5.3 I (II) $5p^{4}$ 3 2 $+ 5d^{1}$ 3 6 100.057 -0.018	$\Delta\lambda_0$ o Transition Assignment λ_T $\lambda_T - \lambda_0$ (nm) (cm ² x 10 ¹⁸) X Lower State + Upper State (nm) (nm) (nm) (nm) (75 0.300 5.3 I (II) $5p^4$ 3p_2 + $5d^4$ 3p_0 100.346 0.271	(nm) (cm ² x 10 ¹⁸) X Lower State + Upper State (nm) (nm) (nm) (nm) (nm) (nm) (nm) (nm)	(nm) (cm ² x 10 ¹⁸) X Lower State + Upper State (nm) (nm) (nm) (nm) (nm) (nm) (nm) (nm)	(nm) (cm ² × 10 ¹⁸) X Lower State + Upper State (nm) (nm) (nm) (nm) (nm) (nm) (nm) (nm)	(nm) (cm ² x 10 ¹⁸) X Lower State + Upper State (nm) (nm) (nm) (nm) (nm) (nm) (nm) (nm)	(nm) (cm ² x 10 ¹⁸) X Lower State + Upper State (nm) (nm) (nm) (nm) (nm) (nm) (nm) (nm)	(nm) (cm ² x10 ¹⁸) X Lower State + Upper State (nm) (nm) (nm) (nm) (nm) (nm) (nm) (nm)	(nm) (cm ² x10 ¹⁸) X Lower State + Upper State (nm) (nm) (nm) (nm) (nm) (nm) (nm) (nm)	(nm) (cm ² x 10 ¹⁸) X Lower State + Upper State (nm) (nm) (nm) (nm) (nm) (nm) (nm) (nm)	(nm) (cm ² x 10 ¹⁸) X Lower State + Upper State (nm) (nm) (nm) (nm) (nm) (nm) (nm) (nm)	(nm) (cm ² x 10 ¹⁸) X Lower State + Upper State (nm) (nm) (nm) (nm) (nm) (nm) (nm) (nm)	(mm) (cm ² x 10 ¹⁸) X Lower State + Upper State (nm) (nm) (nm) (nm) (nm) (nm) (nm) (nm)

Table XVII (continued)

		Luminescence f	rom the Re	eaction 100 eV	He+	Luminescence from the Reaction 100 eV He + I2 + He + I + I + Energy	I + Energy		
(mm)	679 (III)	σ (cm ² x 10 ¹⁸) x	×	Transiti Lower State	on As	Transition Assignment Lower State + Upper State	٠ ٦. [الآ	λ _T - λ _o (nm)	δH (eV)
106.775	0.300	6.2	I (II)		•	6s' 3 _D °	106.733	-0.042	96.0-
				9p		5d' ³ Go 5d' ³ Go	106.498	-0.148	0.75
107.575	0.300	13.7	1 (11)	5p ⁴ 3p ₂ 5p ⁴ 1s ₀	+ +	+ 5d ³ D ₃ + 6d ⁵ D ₁	107.520 -0.055 107.826 0.251	-0.055	-1.05
110.475	0.300	15.4	(II)	5p ⁴ 3p ₂ 5p ⁴ 3p ₁ 5p ⁴ 1s ₀	+ + + +	+ 5d 3 _{D2} + 6s' 1 _{D2} + 7s 3 _D	110.499 0.024 110.358 -0.117 110.635 0.160	0.024	-1.36
114.025	0.300	15.8	(II) I	5p ⁴ 3p ₂ 5p ⁴ 3p ₁	+ +	+ 5d ⁵ D ₁ + 6s' ³ D ₁	113.975 -0.050	-0.044	-1.70

Table XVII (continued)

Luminescence from the Reaction 100 eV He + I, + He + I + I + Energy

						19		
ر°		5		Transiti	Transition Assignment	Ţ	۸- ۲۰	¥
(mm)	(mm)	(cm ² x 10 ¹⁸)	×	Lower State	Lower State + Upper State	(mm)	(mm)	. §
116.000	0.100	29.0	(II) I	5p4 3p2	+ 5d 5D ₂	116.057	0.057	-1.9
				5p4 1p2	+ 5d' 3FO	115.988	-0.012	-0.19
116.600	0.100	. 53.5	(II) I		+ 5d ⁵ D ₃	116.648	0.048	-1.9
				Sp4 3p0	+ 5d 3D ₁	116.707	0.107	-1.1
117.850	0.100	24.3	I (II)	sp ^{4 3} p ₂	+ 6s ³ S ₁	117.865	0.015	-2.00
118.700	0.100	21.8	I (II)	5p4 3p2	+ 5p ^{5 3} p ^o	118.734	0.034	-2.1
122.075	0.500	38.6	1 (3)	5p ⁵ 2po 3/2	+ 11s 4 _{5/2}	121.841	-0.234	-2.40
					+ 8d 4p5/2	122.405	0.330	-2.4
					+ nd 31.1 _{3/2}	122.408	0.333	-2.4
					+ nd 30 _{1/2}	122.450	0.375	-2.4
					+ nd 31 _{3/2}	122.486	0.411	-2.4

-2.46

Table XVII (continued)

~° (E

	(ev)	-2.45	-2.44	-2.41	-2.40	-2.39	-2.38	-2.40	-2.40	-2.40	-2.41	-2.38	-2.39	-2.41	-2.45
	λ _T - λ _o (nm)	0.268	0.257	-0.166	-0.263	-0.361	-0.473	-0.234	-0.263	-0.338	-0.185	-0.473	-0.361	-0.166	0.330
I + Energy	رس (سر) السر)	122.343	122.332	121.909	121.812	121.714	121.602	121.841	121.812	121.737	121.890	121.602	121.714	121.909	122.405
+ I ₂ + He + I ⁺ +	signment Upper State	nd 32 _{3/2}	nd 32.1 _{1/2}	nd 32.2 _{1/2}	nd 33 _{1/2}	nd 34 _{1/2}	nd 35 _{1/2}	11s[2] _{5/2}	11s[2]3/2	(¹ 0 ₂)54[3] _{5/2}	(¹ 0 ₂)5d[2] _{5/2}	$\binom{1}{2}$ 54[2]3/2	64'[1]3/2	64'[1]1/2	94[3]5/2
Reaction 100 eV He	Transition Assignment Lower State + Upper St	5p ^{5 2po} +	•	•	•	•	+	sp ⁵ 2po +	+	*	+	+	+	•	
Luminescence from the Reaction 100 eV He + I + He + I + I + Energy	$(cm^2 \times 10^{18})$ X	(I) I						M I(I)							
	δλ _o (mm)														

,

Table XVII (continued)

>	1
1 100 eV He + I, + He + I + I + Energy	
+	l
-	۱
+	۱
٠,	۱
+	۱
He	١
+	I
I	ì
+	۱
+ 0	۱
H	I
ev	I
00	1
_	ı
_	
Reaction	-
the Reaction	-
Luminescence from the Reaction	

	₩	(eV)	-2.46	-2.45	-2.45	-2.45	-2.46	-2.46	-2.43	-0.68	-2.53	-2.53	-2.53	-0.82
	λ _T - λ _o	(mm)	0.411	0.333	0.268	0.257	0.375	0.375	0.013	-0.463	-0.004	-0.004	0.057	-0.043
	λŢ	(mm)	122.486	122.408	122.343	122.332	122.450	122.450	122.088	121.612	123.346	123.346	123.407	123.307
•	ignment	Upper State	94[2] _{5/2}	94[2]3/2	94[1]3/2	94[1]1/2	nd B _{1/2}	nd B _{3/2}	5p ⁵ 3p ^o ₂	$_{\rm 5p^{5}}^{\rm 1p^{0}}_{\rm 1}$	nd 28.2 _{3/2}	$\binom{1}{2}$ 54[1]3/2	6s ⁵ S ₂	+ 6s' 30°
	n Ass	+	+	+	+	+	+	+	+	+	+	+	+	+
	Transition Assignment	Lower State + Upper State	M I (I) $5p^5 2p_0^0$						5p ⁴ 3p ₂	sp^4 p_2		5p ⁵ 2p ⁰ 3/2		5p ⁴ 1 _{D2}
		×	M 1 (I)						1 (11)		(I) I	M I (I)	(11)	
	, b	(cm ² x 10 ¹⁸)									50.4			
	δλ _o	(mm)									0.100			
	%,	(mm)									123.350			

Table XVII (continued)

Luminescence from the Reaction 100 eV He + I2 + He + I + I + Energy

ΔH (ev)	-3.05	-3.05	-3.06	-3.06	-1.36	-3.17	-3.17	2 63	70.6-	2.67	-3.62	-2.67
$\lambda_{\rm T} - \lambda_{\rm O}$ (mm)	0.033	0.034	-0.002	-0.002	-0.043	0.004	0.004	600	0.022	-0.072	0.023	-0.072
λ _T (mm)	130.033	130.034	130.298	130.298	130.257	131.754	131.754	170 777	136.322	138.228	138.323	138.228
Transition Assignment Lower State + Upper State	+ nd 21 _{5/2}	+ 6d[2] _{5/2}	+ nd 20 _{1/2}	64[2]3/2	+ 5d 3D ₂	nd 17 _{5/2}	54'[2] _{5/2}	7. 2.	15 F3/2	9s ² P _{3/2}	+ 7s[2] _{3/2}	+ 9s[2] _{3/2}
on Ass	+	+	+_	+	+	+	+.		ŀ	+	+	+
Transition Assignment Lower State + Upper St	5p ⁵ 2po 3/2	5p ⁵ 2po 3/2	5p ⁵ 2po 3/2	5p ⁵ 2p ⁰ 3/2	$5p^4 p_2$	5p ⁵ 2p ⁰ /3/2	5p ⁵ 2po 3/2	5 2,0	op r3/2	5p ⁵ 2p ⁰	5p ⁵ 2po 3/2	5p ⁵ 2p ⁰
*	I (I)	M I (I)	I (I)	M I (I)	(II)	I (I)	M I (I)	9	3 .		M I (I)	
σ (cm ² x 10 ¹⁸)	43.7		40.1			61.8			7.60			
δλ _o (mm)	0.100		0.100			0.100			0.100			
γ° (mm)	130.00		130.300			131.750		001	138.300	•		

Table XVII (continued)

Luminescence from the Reaction 100 eV He + I2 + He + I + I + Energy

(mm)	(m)	$ \Delta \lambda_o \qquad \sigma \\ (nm) \qquad (cm^2 \times 10^{18}) $	×	Transition Assignment Lower State + Upper State	ssignment Upper State	T, (mr)	λ _T - λ _o (mm)	ΦH (eV)
139.050		30.7	(I) I	5p ⁵ 2p ⁰ _{3/2} + 7s 4p _{5/2}	7s 4p5/2	139.075	0.025	-3.67
			M I (I)	5p ^{5 2po} +	7s[2] _{5/2}	139.075	0.025	-3.67
142.075	0.150	6.98	1 (3)	5p ⁵ 2po +	nd 5.1 _{3/2}	142.136	0.061	-3.86
			M I (I)	5p ^{5 2} p ⁰ +	54[2]3/2	142.137	0.062	-3.86
142.525	0.100	73.9	1 (1)	5p ⁵ 2po +	nd 5 _{5/2}	142.549	0.024	-3.88
			M I (I)	5p ⁵ 2p ⁰ +	5d[2] _{5/2}	142.549	0.024	-3.88
145.775	0.100	119.4	I (I)	5p ⁵ 2po +	nd 2 _{3/2}	145.879	0.104	-4.08
				+	nd 3 _{5/2}	145.798	0.023	-4.08
				•	nd 43/2	145.747	-0.028	-4.07
				+	nd 4.12,	145.739 -0.036	-0.036	-4.07

Table XVII (continued)

+ He + I + I + Energy
He $+ I_2$
ev He
61 61 61
Reaction 100 eV He + I ₂ + He +
ce from the R
from
Luminescence from t

	ΔH (eV)	-4.08	-4.08	-4.07	-4.39	-3.45	-4.39	-3.45	5.76	5.76	6.04	6.05	6.05	5.65
	λ _T - λ _o (nm)	0.023	0.104	-0.036	0.018	-0.018	0.018	-0.018	-0.014	-0.014	0.071	-0.066	-0.066	0.016
	, T, (mm)	145.798	145.879	145.739	151.468	151.432	151.468	151.432	151.436	151.436	151.521	151.384	151.384	151.466
•	Transition Assignment Lower State + Upper State	$(^{1}_{D_{2}})6s[2]_{5/2}$	$\binom{1}{D_2} 6s[2]_{3/2}$	Sd[0] _{1/2}	$(^{1}_{D_{2}})^{6s}$ $^{2}_{D_{5/2}}$	nd 83/2	54[3]5/2	5d"[2] _{3/2}	5f' 3 ₂	5f' 3 ₃ .	5f''10 ₂	sf' 12 ₁	5f' 12 ₂	8f ³ F ₃
	n Ass	+	+	+	+	+	+	+	*	+	+	+	+	+
	Transition Assignment Lower State + Upper St	5p ⁵ 2po 3/2			5p ⁵ 2p ⁰ 3/2	5p ^{5 2po} 1/2	5p ⁵ 2p ⁰ 3/2	5p ⁵ 2p ⁰ 1/2	$^{5p}_{2}^{5}$ $^{3p_{0}}_{2}$		5p ^{5 3po}			6s ⁵ S ₂
	×	M I (I)			I (I)		M I (I)		I (II)					
	$\Delta\lambda_o$ σ σ (nm) $(cm^2 \times 10^{18})$			•	73.4									
	βλ _ο (mm)				0.100									
	ر (سر)				151.450									

Table XVII (continued)

Luminescence from the Reaction 100 eV He + I + He + I + I + Energy

δH (eV)	-4.92	-4.92	-5.03	-4.08	-5.03	-4.08	5.64	5.64	5.64	5.64	5.65
λ _T - λ _o (nm)	0.035	0.036	0.039	-0.097	0.039	-0.097	-0.070	0.067	0.024	0.034	0.057
τ' (mm)	161.760	161.761	164.214	164.078	164.214	164.078	164.105	164.242	164.199	164.209	164.232
Transition Assignment Lower State + Upper State	+ 6s 4p _{3/2}	+ 6s'[1] _{3/2}	6s ⁴ P _{1/2}	nd 2 _{3/2}	6s"[0] _{1/2}	$\binom{1}{0}_2 \log[2]_{3/2}$	5f' 2 ₃	8f ⁵ F ₅	8f ⁵ F ₄ .	+ 8f ⁵ F ₃	8f ³ F ₃
n As	+	+	+	+	+	+	+	+	+	+	+
Transitic Lower State	5p ⁵ 2po 3/2	5p ⁵ 2po 3/2	5p ⁵ 2po 3/2	5p ⁵ 2p ⁰ 1/2	5p ⁵ 2po 3/2	5p ⁵ 2po 1/2	5d ⁵ D ₄				5d 5p ₂
×	I (I)	M I (I)	(E) I		M I (I)		I (II)				
$ \begin{array}{ccc} \Delta\lambda_o & \sigma \\ \text{(nm)} & (\text{cm}^2 \times 10^{18}) \end{array} $	66.4		70.3								
δλ _o (mm)	0.100		0.150								
γ° (mu)	161.725		164.175								

Table XVII (continued)

Luminescence from the Reaction 100 eV He + I2 + He + I + I + Energy

¥	(e)	-4.35	-4.35	4.77	5.35	5.38	5.37	5.39	5.58	5.92	5.92	5.94	5.94
λη - λο	(mm)	0.107	0.107	-0.259	-0.298	0.167	0.044	-0.271	0.181	0.239	0.239	-0.231	-0.231
ځ	(mm)	170.207	170.207	169.841	169.802	170.267	170.144	169.829	170.281	170.339	170.339	169.869	169.869
signment	Upper State	$(^{1}_{D})6s^{2}_{3/2}$	Sd[1] _{3/2}	7p' 3F ₂	7f 5 _{F4}	7f ³ F ₂	7f ³ F ₃	7f 3F ₄	5f' 1 ₂	5f' 7 ₂	5f' 7 ₃ .	5f''81	5f' 8 ₂
n Ass	+	+	+	+	+	+	+	+	+	+	+	+	+
Transition Assignment	Lower State	5p ⁵ 2p ⁰ _{1/2}	5p ⁵ 2p ⁰ _{1/2}	6s 5 _S °	sd ⁵ D ₃	sd ⁵ D ₂	5d 5p ⁰ ₀		sd ⁵ D ₁	sd ³ D ₂			
	×	I (I)	M I (I)	I (II)									
b	$(cm^2 \times 10^{18})$	29.0											
۵۸۵	(mm)	0.30											
	(mm)	170.10											

Table XVII (continued)

he Reaction 100 eV He + I + He + I + I + Energy	
He + I	
00 eV	1
Reaction 10	-
from the	
Luminescence f	-

ΔH (eV)	-5.63	-5.63	4.82	5	-3.01	-5.81	4.35	4.78	4.83	4.82	2.80	-2.80	-2.80
λ _T - λ _o (mm)	0.051	0.051	0.010	020	0.030	0.038	0.086	-0.026	-0.048	-0.037	0.058	0.237	0.060
, (mm)	178.276	178.276	178.235	107 020	103.030	183.038	183.086	182.974	182.952	182.963	412.858	413.037	412.860
Transition Assignment Lower State + Upper State	6s ² p _{3/2}	6s[2] _{3/2}	+ 7p' ³ p ₀	6. 4n	5/2	6s[2] _{5/2}	4f' 3F2	4f' ³ D ₁	4f' 1F ₃	+ 7p' ³ F ₃	8p ² D _{5/2}	+ 8p[3] ⁰ / _{7/2}	8p[3] ^o _{5/2}
n Ass	+	+	+		ŀ	+	+	+	٠.	+	+	+,	+
Transition Assignment Lower State + Upper St	5p ⁵ 2p ⁰ 3/2	5p ⁵ 2p ⁰ _{3/2}	$5p^5$ $3p_0$	5 2 ₀ 0	3P 5/2	5p ⁵ 4p ⁶ 3/2	5p ⁵ 3p ⁰ ₂	sd ⁵ D ₀	sd Spo	Sd Spo	6s 4p5/2	6s[2] _{5/2}	
×	I (I)	M I (I)	(II) I	5	3	M I (I)	(II) I				I (I)	M I (I)	
$ \frac{\Delta\lambda_0}{\text{(nm)}} \frac{\sigma}{\text{(cm}^2 \times 10^{18})} $	161.0			702	302.4						2.0		
δλ _o (mm)	0.100			6							0.50		
γ° (mm)	178.225			182 000	183.000						412.80		

Table XVII (continued)

₹0 (E

	ΗV	(e _V)	2.74	4.06	4.36	4.36	4.77	5.95	60.9	80.9	80.9	4.19	4.48	4.31	5.58
	λ- γ	(mm)	-0.478	-0.075	0.192	0.172	-0.420	-0.500	0.358	-0.435	-0.435	0.378	-0.395	-0.389	0.135
+ I + Energy	Ļ	(ma)	412.322	412.725	412.992	412.972	412.380	412.300	413.158	412.365	412.365	413.178	412.405	412.411	412.935
ence from the Reaction 100 eV He + I2 + He + IT +	Transition Assignment	Lower State + Upper State	⁵ P ₂ + 5d" ¹ F ₃	+	+	+	$^{3}P_{2}$ + 98 $^{5}S_{2}^{0}$	+	$^{5}P_{2} + 13d^{5}D_{3}^{0}$	⁵ P ₁ + 6d" 47 ⁰	÷	+	$^{1}_{F_3}$ + 4f' $^{3}_{P_2}$	$^{1}p_{1}^{0} + ^{7}p' ^{3}p_{1}$	b ₀ + 5f' 1 ₂
Luminescence from the Reaction	o	(cm ² x 10 ¹⁸) X Lower	I (II) 6p ⁵ P ₂	6p' ³ 0 ₁	. 6p' ³ F ₃		6p' ³ p ₂	4f ³ F ₃	7p ³ p ₂	7p 3		24' 150	5d' 1F0	6s" ^{1po}	6d ⁵ D ₀
	δλο	(mm)													

Table XVII (continued)

Δλ_o (mm) 0.60

λ_o (nm) 432.20

1

	۸- ۳	E	0.103	0.509	0.105	-0.115	-0.531	0.196	-0.148	0.105	-0.054	0.472	-0.156	0.167	0.104	-0.497
+ I + Energy	_ት	(mr)	432.303	432.709	432.305	432.085	431.669	432.396	432.052	432.305	432.146	432.672	432.044	432.367	432.304	431.703
Luminescence from the Reaction 100 eV He + I + He + I + I + Energy	signment	+ Upper State	8p 4po 3/2	8p 4p0	8p[1] ^o 3/2	7d ⁵ D ₃	7d ³ D ₃	6p' 1 _{D2}	6d" 36 ₂	12s ³ S ₁	6d" 33 ⁰	6d" 33 ⁰	6d"-34°	6d" 35 ⁰	6d" 37 ⁰	6d" 45 <mark>0</mark>
+ 9	n As:		+	+	+	+	+	+	+	+	+	+	+	+	+	+
eaction 100 eV	Transition Assignment	Lower State	6s ² p _{3/2}		6s[2] _{3/2}	6p' 3F2	6p' 3F3	$_{5p^{5}}^{1p^{0}}_{1}$	6p" ³ p ₁	6p" 3 _{D2}	4f ⁵ F ₄	4f 5F3	4f ⁵ F ₁	7p ⁵ p ₁	4f ³ F ₂	7p 3p0
the R			(E) I		M I (I)	(II) I										
from 1		×	H		× .	-										
Luminescence	b ($(cm^2 \times 10^{18})$	0.8			•										

ΔH (eV) -2.76 -2.76 4.09 4.23 2.18 5.81

5.75

5.77

-0.156

>

0.167

5.85

0.104

-0.497

Table XVII (continued)

1

	(eV)	4.35	4.35	4.38	4.48	4.91	4.91	5.38	5.39	-3.20	-3.20	3.72	5.50	5.50
	λ _T - λ _o (mm)	0.065	-0.401	-0.159	-0.390	-0.150	-0.396	0.365	-0.063	0.064	0.064	0.114	-0.118	-0.118
I + Energy	بر (mg)	432.265	431.799	432.041	431.810	432.050	431.804	432.565	432.137	476.464	476.464	476.514	476.282	476.282
Luminescence from the Reaction 100 eV He + I ₂ + He + I + I + Energy										7p 4pg,			6d" 20° 4	6d" 20 ⁰ 4
eV He +	Transition Assignment er State + Upper S	+ 4£	+ 4f	+ 4f	+ 4£	+ 6f	+ 6f	+ 7£	+ 7£	4 7p	+ 7p	4 6p	p9 +	P9 +
action 100	Transition Assignment Lower State + Upper State	5d' 1F0	5d" 1D2	5d" 3 _D 0	5d' 3po	5d" 3po		6d 5 _D ⁰		6s 4pc,7	5/2 6s[2] _{5/2}	6s" 3po	4f ⁵ F ₁	
from the Re	*	I (II)								1 (3)	M I (I)	(11) 1		
Luminescence	$(cm^2 \times 10^{18})$									2.2				
	δλ _o (mm)									0.50				
	γ° (mm)									476.40				

Table XVII (continued)

Luminescence from the Reaction 100 eV He + I2 + He + I + I + Energy

ر,	δλο	۵۸۵ م		Transit	ion As	Transition Assignment	λ_T $\lambda_T - \lambda_0$	λ _T - λ ₀	₩
(mm)	(mm)	(cm ² x 10 ⁴)	×	Lower Stat	+	Lower State + Upper State	(ma)	(mm)	(e)
			(II) I	7p 5p3	. +	+ 6d" 24 ⁰	476.245	-0.155	5.58
				5d' 300	+	4f ³ F ₂	476.681	0.281	2.98
				7p 3p2	+	+ 8g 5 _G ⁹	476.199	-0.201	5.70
					+	+ 8g 5G ₂	476.100	-0.300	5.7
					+	8g 3G	476.069	-0.331	5.70
				7p 3p1	+	+ 6d" 30 ⁰	476.041	-0.359	5.68
486.10	0.50	0.9	I (3)	6s 4P _{5/2}	+	7p 2p _{5/2}	486.431	0.331	-3.26
					+	7p 4p°7/2	486.366	0.266	-3.26
			M I (I)	M I (I) 6s[2] _{5/2}	+	7p[3] ⁰ _{5/2}	486.431	0.331	-3.26
					+	7p[3] ⁰ / _{7/2}	486.367	0.267	-3.26
			(II) I	6p 5p ₂	+	7s 3S ₁	486.343	0.243	2.28
				6p' 3 _{D2}	+	5d" ³ p ⁰	486.489	0.389	3.88
				6p, 1p,	+	74 Spo .	486.459	0.359	4.08

Table XVII (continued)

Luminescence from the Reaction 100 eV He + I, + He + I + I + Energy	
-	
+ He +	
1,	
+	
He	
ev	
100	-
K	
Reacti	
the	-
from	-
Luminescence	

y (mm)

۵γ	, b		Transition Assignment	on Ass	ignment	۲,	λ- λ ₀	ΑH
(mm)	(cm ² x 10 ¹⁸)	×	Lower State	+	Lower State + Upper State	(mm)	(mm)	<u>§</u>
		(11)	6p' 1 _{D2}	+	6d' 14°	486.587	0.487	4.73
			6p" 3p2	+	6d" 44 ^o	486.586	0.486	90.9
				+	6d" 44°	486.586	0.486	90.9
	•		6p" ³ D ₃	+	6d" 42 <mark>0</mark>	486.105	0.005	6.02
			6p" 3p2	+	6d" 45 <mark>0</mark>	486.069	-0.031	90.9
				+	6d" 45°	486.069	-0.031	90.9
			4f SF3	+	7g 5G4	486.114	0.014	5.43
				+	7g 5G ₃	486.052	-0.048	5.43
				į	7g 5G ₂	485.895	-0.205	5.43
				+	7g ³ G ₄ .	486.068	-0.032	5.43
				+	7g ³ G ₃	485.867	-0.233	5.43
			5d" 3D2	+	7p, 3F2	485.666	-0.434	4.77

Table XVII (continued)

>	
H	
ne	١
Ш	
+	
-	
+	
τ,	
+	
0	
Ĭ	
+	-
(
-	1
+	
+	
Fe	
_	1
e	
0	
10	
_	
=	į
·	
tic	
actic	
leactic	
Reactic	_
he Reactic	
the Reactic	The state of the s
om the Reactic	
rom the Reactic	
from the Reactic	
ce from the Reactic	
nce from the Reactic	
cence from the Reactic	
escence from the Reactic	
Inescence from the Reactic	
minescence from the Reactic	
Luminescence from the Reaction 100 eV He + I + He + I + I + Energy	

H ((ev)	-3.28	-3.28	3.89	4.06	00.9	00.9	6.04	6.04	5.63	4.82		3.29	-2.51	-2.51
λ _T - λ _o	(mm)	0.309	0.311	0.259	0.140	-0.152	-0.152	-0.413	-0.413	-0.407	-0.244		0.228	0.290	0.257
, F (489.809	489.811	489.759	489.640	489.348	489.348	489.087	489.087	489.093	489.256		491.828	491.890	491.857
signment	upper state	7p 4S3/2	7p[2] ⁰ _{3/2}	8s ⁵ S ₂	6d' 4 <mark>0</mark>	6d" 41 ⁰	6d" 41°	6d" 43°	6d" 43 <mark>0</mark>	6d" 26 <mark>0</mark>	7p' ³ p ₀		7p 4po 5/2	6f 5 <mark>0</mark>	6f 62/2
on Ass	ŀ	+	+	+	+	+	+	+	+	į	+		+	+	+
Transiti	הסאפו סומנפ	6s 4ps/2	6s[2] _{5/2}	6p' 3F3	6p' 1p ₁	6p" ³ D ₃		6p" ³ p ₂		7p 3p ₂	7s ³ S ₁		6s 4p5/2	6s 4p1/2	
>	<	I (I)	M I (I)	I (III)							-		1 (1)		
Cm2 2 1018	(OT V III)	1.6											4.6		
۲۹° و]	0.50											0.50		
° (E]	489.50											491.60		
	λ_{Λ_0} o iransition Assignment λ_{Γ} $\lambda_{\Gamma} - \lambda_{0}$	ton Assignment λ_{T} $\lambda_{\mathrm{T}} - \lambda_{\mathrm{O}}$ (e + Upper State (nm) (nm) ((nm) (cm ² x 10 ¹⁸) X Lower State + Upper State (nm) (nm) (nm) (nm) (nm) (nm) (nm) (nm)	(nm) (cm ² x 10 ¹⁸) X Lower State + Upper State (nm) (nm) (nm) (nm) (nm) (nm) (nm) (nm)	(nm) (cm ² x 10 ¹⁸) X Lower State + Upper State (nm) (nm) (nm) (nm) (nm) (nm) (nm) (nm)	(nm) (cm ² x 10 ¹⁸) X Lower State + Upper State (nm) (nm) (nm) (nm) (nm) (nm) (nm) (nm)	(nm) (cm ² x 10 ¹⁸) X Lower State + Upper State (nm) (nm) (nm) (nm) (nm) (nm) (nm) (nm)	(nm) (cm ² x 10 ¹⁸) X Lower State + Upper State (nm) (nm) (nm) (nm) (nm) (nm) (nm) (nm)	(nm) (cm ² x10 ¹⁸) X Lower State + Upper State (nm) (nm) (nm) (nm) (nm) (nm) (nm) (nm)	(nm) (cm ² x10 ¹⁸) X Lower State + Upper State (nm) $^{\Lambda}_{T}$	(nm) (cm ² x 10 ¹⁸) X Lower State + Upper State (nm) (nm) (nm) (nm) (nm) (nm) (nm) (nm)	(nm) (cm ² x 10 ¹⁸) X Lower State + Upper State (nm) (nm) (nm) (nm) (nm) (nm) (nm) (nm)	(nm) (cm ² x10 ¹⁸) X Lower State + Upper State (nm) (nm) (nm) (nm) (nm) (nm) (nm) (nm)	(nm) (cm ² x10 ¹⁸) X Lower State + Upper State (nm) (mm) (nm) (nm) (nm) (nm) (nm) (nm)	(nm) (cm ² x ₁ 0 ¹ 8) X Lower State + Upper State (nm) (nm) (mm) (nm) (nm) (nm) (nm) (nm)

Table XVII (continued)

	٨- ١٠	(mm)
I + Energy	٦	(mn)
uminescence from the Reaction 100 eV He $^+$ + I $_2$ \rightarrow He + I $^+$ + I + Energy	Transition Assignment	Lower State + Upper State
rom the		×
Luminescence f	5	$(cm^2 \times 10^{18})$
	δλο	(mm)

~° (E

b		Transition Assignment	A As	signment	٦	٨٠ - ١٨	ΗV
$(cm^2 \times 10^{18})$	×	Lower State + Upper State	+	Upper State	(mn)	(mm)	(e)
	M I (I)	6s[2] _{5/2}	+	7p[2] ⁰ _{5/2}	491.832	0.232	-3.29
		6s"[0] _{1/2}	+	6f[1] ⁰ _{3/2}	491.859	0.259	-2.51
			+	6f[1] ⁰ _{1/2}	491.892	0.292	-2.51
	I (II)	6p' l _{F3}	+	7d ⁵ D ₄	491.517	-0.083	4.10
		6p' ³ p ₁	+	6d' 6 <mark>0</mark>	491.195	-0.405	4.34
			+	64' 62	491.195	-0.405	4.34
		6p" ³ S ₁	+	6d" 38°	491.744	0.144	5.88
		7p ⁵ p ₁	+	7g 5 _{G2}	491.603	0.003	5.43
		7p 5p3	+	6d" 20 ⁰	491.298	-0.302	5.50
		7p ³ p ₁	+	11s ⁵ S ₂	491.605	0.005	5.59
			+	11s ³ S ₁	491.318	-0.282	5.59
		5d' 1p0	+	sf ⁵ F ₂	492.025	0.425	4.18
			+	Sf ⁵ F ₁	491.538	-0.062	4.19
		5d" 3F0	+	6f ³ F ₄	491.779	0.179	4.97

Table XVII (continued)

Luminescence from the Reaction 100 eV He + I2 + He + I + I + Energy

ΗV	(ev)	-3.20	-3.20	5.16	5.36	5.78	90.9	90.9	90.9	5.37	-2.51	2.51	-2.34	-2.34
γ- ₁ γ	(mm)	0.071	0.071	-0.398	0.414	0.393	0.269	0.269	-0.272	0.244	-0.353	-0.354	-0.223	-0.332
ኍ	(mu)	512.071	512.071	511.602	512.414	512.393	512.269	512.269	. 511.728	512.244	515.847	515.846	515.977	515.868
Transition Assignment	Lower State + Upper State	7p 4po 3/2	7p[1] ⁰ _{3/2}	7s" 3po	8s' ³ D ₂	6d" 35 ⁰	6d" 45 <mark>0</mark>	6d" 45 ₂	6d" 46 <mark>2</mark>	7£ ³ F ₃	6f 10,2	6f[3] ⁰ _{5/2}	8f[2] ⁰ 3/2	8f[1] ⁰ ,2
on As	+	+	+	+	+	+	+	+	+	÷	+	+	+	+
Transiti	Lower State	6s ² P _{3/2}	6s[2] _{3/2}	6p" 3 _{D1}	6p" ³ p ₁	6p" 3s1	6p" 1p1			6d ³ D ₃	6s 4P3/2	65'[1]3/2	68'[1]1/2	
	×	I (I)	M I (I)	I (II)							(E) I .	M I (I)		
2 38	(cm × 10 -)	2.7									1.6			
δλ _ο		0.50									0.50			
~° ∫	(mu)	512.00									516.20			

Table XVII (continued)

	ΔH (ev)	2.13	-0.13	5.35	5.35	5.35	5.35	-3.24	-3.24	2.52	4.15	5.74	5.85	5.36	4.96
a	λ _T - λ _o (nm)	-0.416	0.063	0.180	902.0	0.211	-0.279	0.055	0.059	0.194	0.184	-0.466	-0.348	0.498	-0.409
+ I + Energ	بر (ست)	515.784	516.263	516.380	516.506	516.411	515.921	520.555	520.559	520.694	520.684	520.034	520.152	520.998	520.091
Luminescence from the Reaction 100 eV He + I + He + I + I + Energy	Transition Assignment er State + Upper State	+ 7s 5so	+ 6p ⁵ P ₃	+ 9d ⁵ D ₃	+ 9d ⁵ D ₃	+ 9d ⁵ D ₄	+ 7f ⁵ F ₃	$^{+}$ 7p 4 po 0	÷ 7p[1] ⁰ ,	+ 6d ⁵ D ₂ .	+ 6d'.50	+ 6d" 32°	+ 6d" 37°	+ 8s' 3 _{D2}	+ 6f ³ F ₂
Reaction 100 eV	Transition Lower State						6d ³ D ₂	6s ² P _{3/2}	6s[2]3/2	бр ³ Р ₂			6p" ³ D ₃		
from the	×	I (II)	<i>y</i> .					I (I)	M I (I)	I (II)					
Luminescence	$(cm^2 \times 10^{18})$							1.3							
	(mm)							0.50							
	ره (آس (آس)							520.50							

Table XVII (continued)

Luminescence from the Reaction 100 eV He + I2 + He + I + I + Energy

ΗV	(e)	-3.26	-3.26	4.08	4.09	5.88	5.88	5.88	5.30	5.35	5.35	5.35	5.35	5.35	5.56
۸- ۳	(mm)	0.002	0.002	-0.086	0.296	0.460	0.366	0.341	0.016	-0.157	-0.255	-0.333	-0.431	-0.499	-0.315
۲,	(mu)	523.602	523.602	523.514	523.896	524.060	523.966	523.941	523.616	. 523.443	523.345	523.267	523.169	523.101	523.285
Transition Assignment		7p $^{2}p_{5/2}^{0}$	7p[3] ⁰ _{5/2}	7d ⁵ D ₂	7d 5 _D °	9g 5 _G 3	9g 5G ₂	9g ³ G ₃	$^{3}S_{1}^{0}$	9d ⁵ D ₃	9d ⁵ D ₄ .	9d ⁵ D ₃	9d ⁵ D ₄	8s' 300	6d" 210
on As	+	+	+	+	+	+	+	+	+	÷	+	+	+	+	+
Transiti	Lower State	6s ² P _{3/2}	6s[2] _{3/2}	6p' 3 _{D3}	6p' 3F4	6p" 3p2			7p 5p ₂	7p 5p3		4£ 3F4		4f 3F2	7p 3p0
	×	I (I)	M I (I)	(11)											
ρ,	(cm [*] x 10 ⁺⁸)	2.1													
۵ ^۸ ه	(mu (L)	0.50													
ر °	(mm)	523.60										-			

Table XVII (continued)

	ΔH (eV)	4.80	5.64	2.04	1.36	4.03	1.72	4.09	3.07	4.84	4.36	4.77	4.96
	$\lambda_{\rm T} - \lambda_{\rm o}$ (nm)	-0.410	0.433	-0.192	-0.531	0.612	0.162	-0.690	-0.430	-0.140	-0.438	-0.192	0.468
I + Energy	λ, (mm)	523.190	524.033	534.308	533.969	535.112	534.662	533.810	534.070	534.360	534.062	534.308	534.968
Luminescence from the Reaction 100 eV He $^+$ + I ₂ + He + I $^+$ + I + Energy	Transition Assignment Lower State + Upper State	\leftarrow 7p' 1 _{D2}	+ 5f' 2 ₂	+ 5d" ³ po	+ 6p' 3 _{F3}	+ 6d' 2°	+ 6p' 3F ₄	+ 7d 5 _D °	\div 7p 3 _p	+ 4f' ¹ D ₂	+ 7p' ³ p ₁	+ 7p' 3F ₂	+ 6f ³ F ₂
action 100 eV	Transition Lower State	5d" 3 _D 0	5d" 1p0	6p ⁵ P ₁	6s' ³ D ₂	6p' 3 _{D3}	6s' 3 _D °	6p' 3p ₂	5d' 3F0	6d ⁵ D ₃	5d" 3po	5d" 3Fo	5d" 3F2
from the Re	×	I (II)		I (II)									
Luminescence	$(cm^2 \times 10^{18})$			6.0					•				
	δλ _ο (mm)			0.70									
	ره (الا (الاس)			534.50									

Table XVII (continued)

λ_T - λ_o (nm) 0.351 -0.109 0.087 -0.133 Luminescence from the Reaction 100 eV He + I2 + He + I + I + Energy 540.691 λ_T (nm) 541.151 540.887 540.569 540.667 Lower State + Upper State nd 30_{1/2}
6p ⁵P₃
6p' ³D₂
10s ⁵S₂
4f' ³G₃ Transition Assignment 6s ²p_{1/2} 5p⁵ ³p⁶ 6s' ³D⁶ 4f ³F₂ 5d" ³F⁶ (II) I 1 (E) $\Delta \lambda_{\rm o}$ σ σ (nm) $(cm^2 \times 10^{18})$ 1.0 0.50

540.80

(mm)

ΔH (eV) -2.45 -0.13

1.33 5.28 4.74

		•	6d ⁵ D ₂	+	+ 7p' 1 _{b2}	544.347 0.447	0.447	4.80
0.50	2.0	1 (3)	6s 4 _{P1/2}	+	8p 4po	546.244 -0.356	-0.356	-2.76
			6s ⁴ p _{3/2} + np 4 ^o _{5/2}	+	np 4°,	546.276 -0.324	-0.324	-2.65

546.60

5.75

-0.211

543.689

1.81

0.050

543.950

0.14

-0.166

543.734

+ 6p 3p₂ + 6p' 3p₁

5p⁵ 3p⁰ 6s' 1p⁰ 6p" 3p₃

(II) I

0.7

0.50

Table XVII (continued)

	HĄ.	(e)	-2.65	-0.27	1.22	3.98	4.08	5.78	5.78	5.18	4.72	4.79	4.91	-2.28
	λ _T - λ _o		-0.322	0.014	0.083	0.365	0.306	-0.351	-0.351	-0.020	-0.271	0.387	-0.229	-0.005
I + Energy	۲٠.		546.278	546.614	546.683	546.965	546.906	546.249	546.249	546.580	546.329	546.987	546.371	549.595
Luminescence from the Reaction 100 eV He $^+$ + I $_2$ + He + I $_+$ + I + Energy	ignment	Upper State	(¹ D ₂)6p[2] ^o 5/2	6p ⁵ P ₂	6p' 3F2	7s' 3 _D °	7d 5 _{D2}	6d" 35 <mark>0</mark>	6d" 35°	7s" 3po	4f' 3F ₄	7p' 3F4	6f ⁵ F ₃	12d[4]7/2
He+	on Ass	+	+	+	+	+	+	+	+	+	+	+	+	+
action 100 eV	Transition Assignment	Lower State + Upper State	6s'[1] _{3/2}	6s ⁵ S ₂	$5d^{3}D_{3}^{0}$	6p' 3 _{D3}	6p' 3p ₁	6p" ³ p ₂		7p ⁵ p ₁	5d" 3F0	6d 5 _D ^o	5d" ³ F ₂	M I (I) 6p[2] ⁰ _{5/2}
from the Reg		~	M I (I)	1 (11)	•									M I (I)
Luminescence	0 0 18,	(cm × 10)				•								1.1
	8													09.0
	ر م													549.60

Table XVII (continued)

Luminescence from the Reaction 100 eV He + I₂ + He + I + I + Energy

o (mu)

₩	(e)	-0.28	2.13	3.61	1.71	3.98	1.81	5.77	5.97	5.35	5.87	5.87	5.87
٠٠- ٢٠	(mm)	0.246	-0.297	-0.105	0.318	-0.047	0.140	-0.596	-0.143	0.346	-0.596	-0.525	-0.525
ታ	(mu)	549.846	549.303	549.495	549.918	549.553	549.740	549.004	549.457	549.946	549.004	549.075	. 549.075
signment	+ Upper State	+ 6p ⁵ P ₁	7s 5S ₂	7s' 300	6p' ³ D ₃	7s' 3 _D °	6p' ³ p ₁	6d" 34°	12d ³ D ₃	94 ⁵ D ₃	5f' 5 ₂ .	5f'.52	5f' 5 ₃
n As:	+	+	+	+	+	+	+	+	+	+	+	+	+
Transition Assignment	Lower State	6s ⁵ S ₂	6p ⁵ P ₃	6p' 3F3	5d' 3 _{D2}	6p' 3F4	5d' 3po	6p" ³ p ₂	6p" 1 _{D2}	7p 3p2	7s' 3 ₀	7s' 302	
	×	(II) I								•			
2 18	(cm x 10-')												
δλ.													

,

Table XVII (continued)

Luminescence from the Reaction 100 eV He + I2 + He + I + I + Energy

	14	•		Theresis		•			
(EE)	° E	(nm) $(cm^2 \times 10^{18})$	×	Lower State + Upper St	A HC	Lower State + Upper State	Ļ (∰	رسا (سا)	(eV)
562.60	0.50	6.0	I (II)	6s ³ S ₁	+	+ 6p 3p ₂	562.726	0.126	0.14
				5d" ³ D ₃	+	6p" ¹ D ₂	562.160	-0.440	3.72
				7p 3p ₂	+	10s 3S ₁	562.489	-0.111	5.30
		•		7p 3p ₁	+	10s 5s ₂	562.187	-0.413	5.28
				5d" 3po	+	5f ³ F ₂	562.101	-0.499	4.25
				5d" 3F2	+	4f' ¹ p ₁	562.359	-0.241	4.85
574.00	0.50	0.7	I (I)	6p 4 _{3/2}	+	nd 36 _{5/2}	574.461	0.461	-2.36
					+	nd 36.1 _{1/2}	573.504	-0.496	-2.36
			(I) I W	6p[3] ⁰ _{7/2}	+	12d[4] _{9/2}	573.728	-0.272	-2.28
					+	124[4]7/2	573.673	-0.327	-2.28
				6s'[1] _{1/2}	+	9p[2] ⁰ ,2	573.744	-0.256	-2.59
				6p[2] ⁰ _{3/2}	+	6d"[2] _{5/2}	574.465	0.465	-2.36
					+	6d"[2] 1/2	573.505	-0.495	-2.36

Table XVII (continued)

15

							•		
۰,°	o Y	9,		Transition Assignment	on As	signment	ب	٠٠- ٢٠	A4
(mm)	(mm)	(cm ² x 10 ⁴)	×	Lower State	+	Lower State + Upper State	(mm)	(mm)	(eV)
			I (II)	5p ^{5 3po}	+	6p ⁵ P ₂	574.076	920.0	-0.2
				5p ⁵ 3po	+	6p ³ p ₁	573.986	-0.014	0.0
				6s" 3po	+	6p" ³ D ₁	574.137	0.137	2.7
				6p" ³ D ₃	+	6d" 26°	574.089	0.089	5.6
				6p" ¹ D ₂	+	9g 5go	574.387	0.387	5.8
					+	9g 5 _{G2}	574.274	0.274	5.8
					+	9g 3G	574.244	0.244	5.8
				5d" 3po	+	5f ³ F ₃	574.475	0.475	4.20
				7s 5so	+	8p ⁵ p ₂	573.502	-0.498	4.28
				5d" 3F0	+	7p' ¹ D ₂	574.351	0.351	4.80
				8s ⁵ S ₂	+	5f'.11 ₃	574.249	0.249	6.0
591.60	0.50	8.0	1 (3)	6p 4p°,2	+	nd 38.1 _{5/2}	591.206	-0.394	-2.34
				6s 4p3/2	+	8p 4p ₀ 5/2	591.279	-0.321	-2.8

Table XVII (continued)

1	
N	
H	
9	
田	
+	
+	
t_	
+	
9	
-	
1	
3	1
+	
+	
위	
-	
) 	
100	
0	
- !	
E	
-	
5	
8	
2	
ol	
4	
-:	
8	
from the Reaction	
-	
8	
Ĕ	
3	
S	
F	
F	
3	
-1	

λ_ο Δλ_ο (nm)

(cm ² x 10 ¹⁸)	. ×	Transition Assignment Lower State + Upper State	n As:	signment Upper State	بر (mr)	λ ₁ - λ ₀ (mm)	(eV)
	M I (I)	6p[3]°,	+	12s[2] _{5/2}	591.206	-0.394	-2.34
		6s'[1] _{3/2}	+	8p[2]%	591.280	-0.320	-2.82
	·	54[3]7/2	+	9f[5]9/2	591.168	-0.432	-2.30
			+	9f[4]9/2	591.360	-0.240	-2.30
			+	9f[4]°,	591.341	-0.259	-2.30
		54[3]5/2	+	9f[4]°,	591.532	-0.068	-2.30
		54[3]7/2	+	9f[3]0,	591.312	-0.288	-2.30
		54[3]5/2	+	9f[3]°,	591.504	960.0-	-2.30
			+	9f[3]°,	591.369	-0.231	-2.30
			+	9f[1]°,	591.219	-0.381	-2.30
	I (II)	sd ⁵ D ₃	+	6p ³ p ₂	592.223	0.623	0.14
		6р ³ Р ₀	+	7s 3so	592.251	0.651	2.28
		6p" 1 _{D2}	+	12s ³ S ₁ ^o	591.390	-0.210	5.81
		5d" 3F2	+	4f' 3G3	591.263	-0.337	4.74
		5d" 1F0	+	4£' 1D;	591.286	-0.314	4.84

Table XVII (continued)

Luminescence from the Reaction 100 eV He + I2 + He + I + I + Energy

H	(e)	-2.45	-2.45	-2.45	-3.54	-2.36	-2.45	-2.45	-2.45	-2.33	-2.33	0.05	3.61	3.61	5.03
بر - بر	(mm)	0.352	0.103	0.169	0.346	0.371	0.351	0.103	0.167	0.298	0.298	-0.309	-0.348	-0.432	-0.287
Ļ	(mu)	595.852	595.603	595.669	595.846	595.871	595.851	595.603	295.667	595.798	595.798	595.191	595.152	890.265	595.213
Transition Assignment	Upper State	8d ⁴ D _{7/2}	+ 8d ⁴ P _{5/2}	nd 31.1 _{3/2}	np 10/3/2	6d"[2] _{3/2}	94[3]7/2	94[3]5/2	94[2]3/2	nd C _{1/2}	nd C _{3/2}	6р ³ р ₁	7s' 3 _D °	7s' 3D ₂	+ 6g 5G ₃ .
n Ass	+	+	+	+	+	+	+	+	+	+	+	+	+	+	+
Transitio	Lower State	6p 4p ₀ + 8d 4 _{D7/2}		,	6s ² p _{3/2}	6p[3] ⁰ _{5/2}	6p[2] _{5/2}			6p[1] ⁰ _{1/2}		6s ³ S ₁	6p' 1p ₁		6p" ³ D ₂
	×	1 (3)				M I (I)						(11)			
D C	(cm x 10-7)	1.4			•										
Αλ,		0.50													
؍° ڔٛ	(mm)	595.50													

Table XVII (continued)

+ I + I + Energy	1
er	1
En	۱
1 + I +	١
H	۱
+	I
+	١
+	۱
He	١
+	١
Ľ	ì
+	I
+	١
H	١
ev	I
0	1
7	1
on	۱
ti	١
eac	I
R	Į
Luminescence from the Reaction 100 eV He + I, + He + I + I	1
E	١
fre	١
0	1
en	۱
SC	١
ne	I
IMI	١
H	1

<u>ر</u> ۰	δλ _ο	96		Transition Assignment	n As	signment	, ,	γ - ¹ γ	HA.
	(mm)	(cm ² x 10 ¹⁰)	×	Lower State	+	Lower State + Upper State	(mm)	(mm)	(eV)
			(II) I	6p" ³ p ₂	+	11s ⁵ s ₂	595.072	-0.428	5.59
			•	4f ³ F ₃	+	6g ⁵ G ₄	595.533	0.033	5.03
					+	6g ⁵ G ₃	595.380	-0.120	5.03
					+	6g ³ G ₄	595.376	-0.124	5.03
				Sf ⁵ F ₃	+	6d" 50°	595.975	0.475	6.25
					+	6d" 50°	595.975	0.475	6.25
				5d" 1F0	+	7p' 3F3	595.099	-0.401	4.82
				6d ³ D ₂	+	7p' ³ b ₂	595.511	0.011	5.03
604.40	0.50	1.2	M I (I)	5d[3] _{7/2}	+	8f[5] ⁰ _{9/2}	604.161	-0.239	-2.34
					+	8f[4] ⁰ _{9/2}	604.438	0.038	-2.34
					+	8f[4] ⁰ 7/2	604.410	0.010	-2.34
				Sd[3] _{5/2}	+	8f[4] ^o _{7/2}	604.610	0.210	-2.34
				Sd[3] _{7/2}	+	8f[3]°,	604.364	-0.036	-2.34

Table XVII (continued)

Luminescence from the Reaction 100 eV He + I 2 + He + I + I + Energy

Δλ_o (mm)

γ° (mg)

σ (cm ² × 10 ¹⁸) ×	Transition Assignment	on As	signment	٢.[λ _T - λ ₀	₩.
M I (I)		+ +	8f[3] ⁰	(mm) 604.563	0.163	(ev)
	54[3]7/2	+	8f[2] ⁰ _{5/2}	604.091	-0.309	-2.34
	54[3] _{5/2}	+	8f[2] ⁰ _{5/2}	604.291	-0.109	-2.34
		+	8f[2] ^o _{3/2}	604.340	-0.060	-2.34
		+	8f[1] ⁰ ,	604.190	-0.210	-2.34
(II) I .	5d' 1p0	+	6p" ¹ D ₂	604.330	-0.070	3.72
	6p" 1 _{D2}	+	6d" 34 <mark>0</mark>	604.490	0.090	. 5.77
	5d' 1 _{D2}	+	7p ⁵ p ₂	604.346	-0.054	2.93
	7p 5p ₂	+	8d ³ D ₃	604.233	-0.167	4.98
	7p 5p3	+	6g ⁵ G ₄	604.774	0.374	5.03
		+	6g ⁵ G ₃	604.616	0.216	5.03
		+	6g 5 _{G2}	604.221	-0.179	5.03
		+	6g ³ G ₄	604.612	0.212	5.03
		+	6g 3G.	604.170	-0.230	5.03

Table XVII (continued)

Luminescence from the Reaction 100 eV He + I₂ + He + I + I + Energy

7	(§	5.03	5.03	5.03	5.03	5.03	5.03	-2.40	-3.59	-2.40	-2.40	-3.59	0.14	2.06
٨- ١٠	(mm)	0.146	0.139	-0.018	-0.300	-0.023	-0.465	0.157	-0.090	0.156	-0.572	-0.090	-0.548	0.147
۲	(mg.)	604.546	604.539	604.382	604.100	604.377	603.935	608.657	608.410	959.809	607.928	608.410	607.952	608.647
Transition Assignment	Lower State + Upper State	6g ⁵ G ₅	6g ⁵ G ₄	6g ⁵ G ₃	6g ³ G ₅	6g ³ G ₄	6g ³ G ₃	11s ⁴ p _{5/2}	6p 4 _D _{5/2}	11s[2] _{5/2}	11s[2] _{3/2}	6p'[2] ⁰ 5/2	6p ³ p ₂	54' ³ p ⁰
on Ass	+	+	+	+	+	+	+	+	+	+	+	+	+	+
Transiti	Lower State	4f 3F4						6p 2p _{5/2}	6s ² P _{3/2}	6p[3] _{5/2}		6s[2] _{3/2}	5d 5p ₂	6p ³ p ₁
	×	I (II)						(I) I		M I (I)			(II) I	
۵۲۰ و ۱	(cm ² x 10 ¹⁸)							1.5						
840	(mu)							09.0						
ب °	(mm)			•				608.50						

Table XVII (continued)

	λ _Τ ν	per State (nm) (nm)	5 5 ₂ 608.376 -0.124	6d" 30° 609.106 0.606	6d" 33.5° 609.040 0.540	8d ³ D ₁ 608.415 -0.085	4f' ³ P ₂ 608.074 -0.426
1	Assign	idn +	+ 9s 5s2	P9 .	P9 .	P8 .	. 4£
Designation and the real parties of the real p	Transition Assignment	Lower State + Upper State	6p" ³ D ₁ •	6p" ¹ p ₁ +	6p" 1 _{D2} +	7p ⁵ P ₂ ◆	5d" 3Fo
ITOM THE		×	I (III)				
raminescence	0 18	(cm x 10)				•	
	δλο	(mm)					

(mm)

, b		Transitio	n As	Transition Assignment	ታ	٨٠ - ٨٥	ΥΥ
" x 1010)	×	Lower State	+	Lower State + Upper State	(mu)	(mm)	(e)
	I (III)	6p" ³ D ₁	+	9s ⁵ S ₂	608.376	-0.124	4.77
		6p" 1p1	+	6d" 30°	609.106	909.0	2.68
		6p" 1 _{D2}	+	6d" 33.50	609.040	0.540	5.75
•		7p 5p ₂	+	8d ³ D ₁	608.415	-0.085	4.97
		5d" 3F0	+	4f' ³ p ₂	608.074	-0.426	4.48
		7s' 3 _{D2}	+	8f ³ F ₃	608.395	-0.105	5.65
1.0	I (I)	6p 4p0 5/2	+	nd 28.2 _{3/2}	618.575	-0.525	2.53
	M I (I)	6p[3] ⁰ _{5/2}	+	94[4]7/2	619.359	0.259	-2.44
		6p[2] ⁰ _{5/2}	+	$\binom{1}{2}$ 54[1]3/2	618.572	-0.528	-2.53
	(II) I	4f ⁵ F ₅	+	8d 5D ₄	619.292	0.192	4.89
		4f SF3	+	8d ⁵ D ₂	618.861	-0.239	4.89
			+	8d ⁵ D ₃	618.532	-0.568	4.89
		7p 5p ₃	+	8d ³ D ₃ .	619.168	0.068	4.98

0.70

Table XVII (continued)

c (mg)

	¥	(e)	4.98	4.29	6.29	6.29	6.29	4.74	4.45	4.95	5.89	5.89	6.10
SI.	٨- ١٠	(mm)	-0.179	-0.116	-0.086	-0.086	-0.086	0.513	-0.469	0.064	0.668	0.668	0.260
I + Energy	Ţ	(mm)	618.921	618.984	619.014	619.014	619.014	619.613	618.631	619.164	619.768	619.768	619.360
Luminescence from the Reaction 100 eV He + I2 + He + I + I + Energy	Transition Assignment	Lower State + Upper State	+ 8d ³ D ₃	+ 8p ⁵ p ₂	+ 64" 510	+ 6d" 51 ⁰	+ 64" 51°	+	+	+ 6f ³ F ₃	+ 5f' 6 ₂	+ 5f' 6 ₃	+ 5f' 13 ₃
from the Reaction 10	Trans	X Lower Sta	I (II) 4f ³ F ₄	7s ³ S ₁	8p ⁵ P ₂			5d" 1Fo	5d" 3F0	6d ³ p ₂	8s ⁵ S ₂		74 Sp4
Luminescence	, b	(cm ² x 10 ¹⁰)											
	64م	(mu)											

Table XVII (continued)

Luminescence from the Reaction 100 eV He + I + He + I + I + Energy

₹	(e) ii	-2.53	-2.45	-2.44	-2.44	-2.44	-2.53	5.35	4.89	4.89	4.89	6.29	6.29	5.87	6.10
γ - ۲	(mm)	0.393	-0.010	0.082	0.082	-0.014	0.391	0.560	-0.445	0.202	-0.130	-0.367	-0.367	-0.093	-0.327
Ļ	(mu)	621.793	621.390	621.482	621.482	621.386	621.791	621.960	620.955	621.602	621.270	621.033	621.033	621.307	621.073
Transition Assignment	Upper State	nd 28.2 _{3/2}	nd 32 _{3/2}	8d ⁴ F _{9/2}	94[4] _{9/2}	94[1]3/2	$\binom{1}{2}$ 54 $\binom{1}{3}$ 2	8s' ³ D ₁	$^{8d}_{D_1}$	8d ⁵ D ₂	8d ⁵ D ₃	6d" 51 <mark>0</mark>	6d" 51 <mark>0</mark>	5f' 5 ₂	5f' 13 ₂
on As	+	+	+	+	+	+	+	+	+	+	+	+	+	+	+
Transiti	Lower State +	6p 4S _{3/2}	6p 2p _{5/2}	6p 4p ^o _{7/2}	6p[3] ^o 7/2	6p[3] ⁰ _{5/2}	6p[2] ^o 3/2	6p" 3s1	4f 5 _{F2}			4f' 3F3		5d" 3po	74 5p°
	×	I (I)			M I (I)			(II) I							
Δλ _ο , ,	$(cm^2 \times 10^{18})$	1.2			•										
۵λ	(mm)	09.0													
~°	(mm)	621.40													

Table XVII (continued)

Luminescence from the Reaction 100 eV He + I₂ + He + I + I + Energy

λ_o (nm) 624.60

4	b		Transition Assimment	Ase	si onment			
° (iii	$(cm^2 \times 10^{18})$	×	Lower State + Upper State	+	Upper State	F (E	راس) (اسا)	PH (
0.50	2.7	I (I)	6p 2 ₀	+	+ nd 31 _{3/2}	625.088	0.488	-2.46
				+	+ 8d ⁴ D _{7/2}	624.258	-0.342	-2.45
			$(^{1}_{D})6s^{2}_{D_{5/2}} + ^{7p}_{P_{5/2}}$	+	7p 4po 5/2	624.486	-0.114	-2.41
			6s ² P _{1/2}	+	8p 4po	624.362	-0.238	-2.76
			(¹ b)6s ² b _{5/2} ⁺	+	10p 4po	624.440	-0.160	-2.41
				+	7f 1 ⁰ _{5/2}	624.783	0.183	-2.41
				+	7£ 20/2	624.621	0.021	-2.41
		M I (I)	6p[3] ⁰ _{7/2}	+	94[3]7/2	624.257	-0.343	-2.45
			6p[3] ⁰ _{5/2}	+	9d[2] _{5/2}	625.087	0.487	-2.46
				+	nd B _{3/2}	624.166	-0.434	-2.45
			54[3]7/2	+	7f[5] ⁰ _{9/2}	624.179	-0.421	-2.41
				+	7f[4]°,2	624.621	0.021	-2.41
				+	7f[4] ⁰ / _{7/2}	624.573	-0.027	-2.41
			54[3] _{5/2}	+	7f[4]°.	624.786	0.186	-2.41

Table XVII (continued)

γ° Œ

	HV	(e)	-2.41	-2.41	-2.41	-2.41	-2.41	2.73	4.88	4.20	6.23	6.23	6.29	6.29
	٠٠ - ٣	(mm)	-0.158	0.055	-0.104	0.109	-0.110	0.050	-0.445	-0.439	-0.309	-0.309	0.331	0.331
I + Energy	Ļ	(mm)	624.442	624.655	624.496	624.709	624.490	624.650	624.155	624.161	624.291	624.291	624.931	624.931
+ I ₂ + He + I ⁺ + I + Energy	ignment	Upper State	7f[3] ^o /2	7f[3] ^o _{7/2}	7f[3] ^o _{5/2}	7f[3] ^o _{5/2}	7f[2] ⁰ _{3/2}	6p" ³ ₀₁	8d ⁵ D ₀	Sf ³ F ₃	6d" 49 <mark>0</mark>	6d" 49 <mark>0</mark>	6d" 51 <mark>°</mark>	6d" 51 <mark>0</mark>
+ <u>+</u>	n Ass	+	+	+	+	+	+	+	+	+	+	+	+	+
action 100 eV	Transition Assignment	Lower State + Upper State	54[3]7/2	54[3] _{5/2}	54[3]7/2	54[3]5/2		5d' 3F2	4f ⁵ F ₁	5d" ³ D ₂	5f 3F2		8p ⁵ p ₃	
rom the Re		×	M I (I)					I (II)						
Luminescence from the Reaction 100 eV He	, c	(cm ² x 10 ¹⁸)												
	۵۸ه	(mr)												

Table XVII (continued)

Luminescence from the Reaction 100 eV He + I₂ + He + I + I + Energy

۰×°	δλ _o	5		Transition	Transition Assignment	Ļ	رد - ار	ş
(mm)	(mm)	(nm) (cm ² × 10 ¹⁸)	×	Lower State	Lower State + Upper State	(E)	(mm)	<u></u>
634.10	0.50	3.7	He I		+ 3s 1 _{S0}	633.794	-0.306	10.34
			I (I)		+ 7d ⁴ D _{7/2}	634.122	0.022	-2.58
					- 74 4 _{DS/2}	633.963	-0.137	-2.58
			M I (I)	6p[2] ⁰ 5/2	+ 8d[3] _{7/2}	634.121	0.021	-2.58
					+ 8d[3] _{5/2}	633.962	-0.138	-2.58
			(II) I		+ 6p' ³ F ₃	634.176	0.076	1.36
					+ 6p' 3p ₂	634.302	0.202	1.77
					+ 6p" ³ b ₃	633.910	-0.190	3.47
				6p" 1 _{P1} 4	+ 11s 3so	634.343	0.243	5.59
				6s" 3po	- 7p ³ p ₁	633.835	-0.265	3.07
				74 ⁵ D ₃ •	. Sf' 10 ₂	633.795	-0.305	6.04
					+ 5f' 10 ₃	633.795	-0.305	6.04
				74 ⁴ D ₀ •	+ 5f' 12 ₁	633.791	-0.309	6.05

Table XVII (continued)

HV	(e)	-2.58	-2.58	-2.58	-2.41	-2.45	-2.45	-2.58	-2.58	-2.58	-2.45	-2.45	-2.45	-2.45
٨- ١٠	(mm)	0.044	-0.397	-0.519	0.512	-0.452	0.581	0.044	-0.395	-0.518	-0.455	0.362	0.476	0.584
۲۶	(mu)	637.344	636.903	636.781	637.812	636.848	637.881	637.344	636.905	636.782	636.845	637.662	637.776	637.884
signment	Upper State	+ 7d 4p _{S/2}	nd 26 _{3/2}	nd 26.1 _{1/2}	7p 4p _{5/2}	7p 4p ₀ ,2	10p 4po 5/2	8d[3] _{5/2}	84[1]3/2	8d[1] _{1/2}	7p"[1] ⁰ ,	10p[3] ^o 7/2	10p[3] ⁰ _{5/2}	10p[3] ⁰ / _{7/2}
Transition Assignment		6p 45° +		•	$(^{1}D)6s^{2}D_{3/2} + ^{7}P_{5/2}^{4}$	$(^{1}_{D})6s^{2}_{S/2} + ^{7}_{P} ^{4}_{3/2}^{0}$	•	M I (I) $6p[2]_{3/2}^{0}$ +	+	•	5d[3] _{5/2} +	54[3]7/2 +	•	54[3] _{5/2} +
	×	I (I)		•				M I (I)						
۵۸۰ م	(cm ² x 10 ¹⁸)	1.3												
٥٨٥	(mm)	09.0												
~°	(mm)	637.30												

Table XVII (continued)

	-	Ź	۱
	-	10	١
			ı
			ı
			ı
	-	•	ı
	4	٠	ı
+			į
			ı
			ı
	i	=	ı
	1	1	I
	-		ļ
	-	4	Į
	4	ŀ	
+			
	j	Ę	
	1	>	1
	(D	
	2	3	ı
	-	1	
	5	=	1
		7	ı
	*	֖֖֭֭֭֭֭֭֡֡֡	ı
	0	G	ı
	٥	4	I
	5	D	
	+	3	ı
	1	Į	1
		4	
	4	-	
	0	3	I
	2	5	ı
	4	2	I
	9	Ď	١
	-	3	Į
	Timingsconce from the Decetion 100 of Us + I + Us + I + Enemy	3	ı
	-	1	1

γ° (mu)

					7			
βγ°	, b		Transition Assignment	n As	signment	Ļ	λ λο	HV.
(mg)	(cm ² x 10 ¹⁸)	×	Lower State	+	Lower State + Upper State	(mm)	(mm)	(e)
		M I (I)	5d[1] _{3/2}	+	+ 7f[1] ⁰ _{3/2}	637.337	0.037	-2.4]
				+	$+ 7f[2]_{3/2}^{0}$	637.819	0.519	-2.4]
		(11) 1	6p 5p	+	5d' 1 _p o	637.844	0.544	1.67
			6p" ³ P ₁	+	8d ⁵ D ₀	636.885	-0.415	4.88
			6p" 1 _{D2}	+	10d ³ D ₂	637.055	-0.245	5.66
			8p ⁵ P ₂	+	6d" 49 <mark>0</mark>	636.954	-0.346	6.23
				+	6d" 49°	636.954	-0.346	6.23
			6d 5 _D 0	+	4f' ³ p ₁	637.295	-0.005	4.45
			7d 3 _{D2}	+	5f' 13 ₂	637.432	0.132	6.10
)			+	5f' 13 ₃	637.432	0.132	6.10
			8s ⁵ S ₂	+	+ 9f ⁵ F ₃	637.664	0.364	5.83

Table XVII (continued)

	ergy	1
1	E	I
	+	I
	+	I
+		ı
	+	۱
	+ He +	I
	+	١
,	ן,	ì
	+	
+	He	-
	6	1
	100 eV He + 1, +	-
	the Reaction	sections or sections or sections
	the	-
	from	-
	Luminescence	-

VH	(e)	-2.55	-2.55	-2.86	-2.55	-2.55	-2.86	4.98	4.96	3.19	90.9	6.23	6.23	4.41	4.85
λ - γ	(mm)	0.133	-0.445	-0.041	0.129	-0.437	-0.037	-0.104	0.017	0.316	-0.019	0.456	0.456	-0.360	0.265
,	(mm)	656.833	656.255	629.929	626.829	656.263	656.663	965.599	656.717	657.016	656.681	657.156	657.156	656.340	656.965
Transition Assignment	Lower State + Upper State	nd 28 _{7/2}	nd 28.1 _{5/2}	$(^{1}_{0})^{6p} ^{2}_{3/2}^{0}$	8d[4] _{7/2}	84[2]5/2	$(^{1}b_{2})6p[1]_{3/2}^{0}$	8d ³ D ₃	8d ³ D ₂	7p 3p _o	6d" 46 <mark>0</mark>	6d" 49 <mark>0</mark>	6d" 49 <mark>0</mark>	4f' 3 _{D2}	4f' ¹ p ₁
on Ass	+	+	+	+	+	+	+	+	+	+	+	+	+	+	+
Transiti	Lower State	6p 2p _{5/2}		6s ² P _{1/2}	6p[3] _{5/2}		6s'[1] _{1/2}	7p 3p ₂	7p 3p ₁	6s" 1p0	Sf ⁵ F ₃	4f' 3F2		6d ⁵ D ₃	6d 3 _D 0
	×	1 (1)			M I (I)			I (II)		1					
ь С	(cm ² x 10 ⁴)	2.7			•										
δλ _ο	(mg)	0.50													
°	(mg)	656.70													

Table XVII (continued)

+ Energy	
1++	
+ He + I	
le + I,	
ev H	-
Luminescence from the Reaction 100 eV He + I + He + I + I + Energy	
from the	
Luminescence	

	(eV)	6.25	-2.56	-2.51	-2.51	2.51	-2.56	-2.51	-2.51	-2.51	-2.51	-2.51	-2.51	-2.51	-2.51
	ر (سر)	0.452	0.211	0.055	-0.028	-0.437	0.214	0.056	-0.027	-0.264	-0.189	0.210	-0.027	0.049	-0.440
	Υ. (E)	657.152	658.711	658.555	658.472	658.063	658.714	658.556	658.473	658.236	658.311	658.710	658.473	658.549	658.060
	Iransition Assignment Lower State + Upper State	+ 6d" 50 ⁰	nd 27.1 _{5/2}	6f 1 ⁰ _{5/2}	6f 2 ⁰ / _{7/2}	6f 30,2	nd A _{3/2}	6f[4] ⁰ _{9/2}	6f[4]°,2	6f[3]°,2	6f[3] ⁰ _{5/2}	6f[4] ⁰ / _{7/2}	6f[3] ⁰ / _{7/2}	6f[3] ⁰ 5/2	6f[2]0,
	10n AS:	+	+	5/2	+	+	+	+	+	+	+	+	+	٠	+
í	Iransit Lower Stat	8p ³ p ₂	6p 2p _{5/2} +	(¹ D)6s ² D			6p[3] ^o _{5/2}	54[3]7/2				54[3]5/2			
	×	I (II)	. (E) I				M I (I)								
,	(cm ² x 10 ¹⁸)		6.4												
4	S (III)		0.50												

658.50

o (mu)

Table XVII (continued)

Luminescence from the Reaction 100 eV He + I₂ + He + I + I + Energy

(nm)

~° (E

b		Transition Assignment	n As:	signment	Ļ	۸- ۲۰	*
$(cm^2 \times 10^{18})$	×	Lower State + Upper State	+	Upper State	(ma)	(mar)	<u>§</u>
	(II) I	$6s' \frac{3_0^0}{1_1}$	+	6p' ³ D ₁	658.702	0.202	1.06
		5d" 1po	+	+ 6p" ³ S ₁	658.105	-0.395	3.36
		6p" 3p2	+	9d ³ D ₃	658.235	-0.265	5.39
		4f 5F2	+	9s ⁵ S ₂	688.889	0.489	4.77
		7p ⁵ p ₁	+	9s ³ S ₁	658.990	0.490	4.79
		5d' 1S0	+	7p 3p ₁	658.031	-0.469	3.07
		Sf SF4	+	6d" 44°	658.625	0.125	90.9
		Sf SF3	+	6d" 44 ⁰	628.819	0.019	90.9
			+	6d" 44 ⁰	628.819	0.019	90.9
		6d 5p ^o ₂	+	4f' 3D2	658.081	-0.419	4.41
		4f' 3D2	+	6d" 51°	628.829	0.059	6.29
			+	6d" 512	628.829	0.059	6.29
			+	6d" 51°	628.839	0.059	6.29

Table XVII (continued)

Luminescence from the Reaction 100 eV He + I + He + I + I + Energy

λ_o (nm) ... 662.10

HA (Ve)	-2.39	-2.57	-2.57	-2.39	-0.27	1.33	90.9	90.9	90.9	90.9	6.16	6.16	4.83	4.82
λ ₁ - λ ₀ (mm)	0.258	0.049	0.049	0.253	-0.065	0.319	0.041	0.041	-0.035	-0.035	0.071	0.362	0.198	0.342
₹- (E)	662.358	662.149	662.149	662.353	662.035	662.419	662.141	662.141	662.065	662.065	662.171	662.462	662.298	662.442
ignment Upper State	nd 34 _{1/2}	7d 4F9/2	8d[4] _{9/2}	64'[1]3/2	6p ⁵ p ₂	6p' 3 _{D2}	6d" 44 ⁰	6d" 44°	6d" 45 <mark>0</mark>	6d" 45°	$14d_{3}^{3}_{0}^{0}$	14d ³ D ₃	4f' ¹ F ₃	+ 7n' 3F.
ASS:	+	+	+	+	+	+	+	+	+	+	+	+	+	+
Transition Assignment Lower State + Upper State	6p 4po	6p 4p° 7/2	6p[3] ^o 7/2	6p[1] ^o 3/2	5p ⁵ 3p ⁰	5d' 3 _{D2}	sf ⁵ F ₂		Sf ⁵ F ₁		4f' 3G4	4f' 3F3	6d 3 _{D3}	
×	1 (1)		M I (I)		I (II)									
$\Delta\lambda_o$ σ σ (nm) $(cm^2 \times 10^{18})$	2.7			•										
λο (mm)	0.50													

Table XVII (continued)

Luminescence from the Reaction 100 eV He + I2 + He + I + I + Energy

ş		5.76	5.76	5.85	5.85	2.67	-2 40	04.7-	-2.66	-2.58	-2.58	-2.58	-2.58	-2.67	-2.40
۸ - ۳۸	(m)	-0.076	-0.076	0.350	0.350	-0.004	165	601.0-	-0.164	0.093	-0.083	0.092	-0.083	-0.005	-0.168
ţ	(ma)	662.024	662.024	662.450	662.450	666.296	321 999	661.000	666.136	666.393	666.217	666.392	666.217	666.295	666.132
Transition Assignment	Upper State	5f' 3 ₂	5f' 3 ₃	$7s'^{3}D_{3}^{0} + 5f'^{4}$	5f' 4 ₄	9s 4p		113 F5/2	nd 25.1 _{1/2}	7p 4D7/2	7d ⁴ P _{S/2}	84[3]7/2	84[3]5/2	9s[2] _{5/2}	11s[2] _{5/2}
on As:	+	+	+	+	+	•			+	+	+	+	+	٠	+
Transiti	Lower State	8s ⁵ S ₂		7s' 3 _{D3}		6p 4p0	6n 4po	op '3/2	6p ⁵ 3/2	6p 4p0		6p[3] ⁰ _{7/2}		6p[2] _{5/2}	6p[1] ⁰ 3/2
	×					9 1						M I (I)			
6	(cm ² x 10 ¹⁸)				•	2.0									
٥٤٩						0.50									
ر °	(mm)					666.30									

Table XVII (continued)

Cam (mm)

	Ą	<u></u>	-0.28	5.50	5.50	4.77	6.04	6.04	6.04	6.04	90.9	4.31	4.81	5.94	5.94
	۸- ۲	(mu)	0.481	-0.200	-0.200	0.055	0.451	0.451	0.480	0.480	0.216	0.292	0.035	0.476	0.476
I + Energy	٢	(mm)	666.781	666.100	666.100	666.355	666.751	666.751	082.999	666.780	666.516	666.592	666.335	922.999	922.999
Luminescence from the Reaction 100 eV He + I + He + I + I + Energy	gnment	+ Upper State	6p ⁵ p ₁	6d" 20 <mark>0</mark>	6d" 20 ⁰	9s ⁵ S ₂	sf' 10 ₂	5f' 10 ₃	6d" 43°	6d" 43 <mark>0</mark>	6d" 45 <mark>°</mark>	8p ⁵ p ₃	7p' ¹ p ₁	5f' 8 ₁	5f' 8 ₂
eV He +	Transition Assignment		+	+	+	+	+	+	+	+	+	+	+	+	+
action 100	Transi	Lower State	5p ⁵ 3p ⁰	6p" 1p1		7p Sp	Sf SF2				Sf 3F3	5d" 3F0	6d 3 _{D2}	7d ⁵ D ₂	
from the Re	-	×	(II) I												
Luminescence	, ,	$(cm^2 \times 10^{10})$				•									
	δλο	(mm)													

Table XVII (continued)

	ΔH (ev)	-2.68	-2.56	-2.67	-2.54	-2.39	-3.06	-2.67	-2.56	4.73	60.9	4.38	4.80	4.81	4.37
×	$\lambda_{\rm T}^{-\lambda}$ (mm)	-0.149	-0.007	0.032	0.026	0.439	-0.081	0.031	-0.006	0.145	0.065	-0.040	0.415	0.423	0.141
+ I + Energ	λ _T (mm)	669.851	669.993	670.032	670.026	670.439	669.919	670.031	669.994	670.145	670.065	096.699	670.415	670.423	670.141
Luminescence from the Reaction 100 eV He + I ₂ + He + I + I + Energy	Transition Assignment er State + Upper State	+ 5f 1 ⁰ ,	$+$ nd $27_{3/2}$	+ 9s 4p _{5/2}	+	+ np 6 _{5/2}	+ nd 20 _{1/2}	+ 9s[2] _{5/2}	+ 8d[2] _{3/2}	+ 6d' 14°	$+ 13d ^{3}D_{3}^{0}$	+ 4f' ³ H ₅	+ 7p' 1 _{F3}	+ 7p' ¹ p ₁	+ 8p 3p.
Reaction 100 eV	Transition Lower State	6p 4p0 5/2	6p 4po	6p 4so	(¹ D)6s ² D _{5/2}	nd 1 _{3/2}	6s ⁴ p _{3/2}	6p[2] ⁰ _{3/2}	6p[1] ⁰ _{1/2}	4f ⁵ F ₃	Sf 3F4	6d ⁵ D ₄	6d ³ D ₂	6d ³ D ₁	6d 5 _D ⁰
from the	×	1 (3)						M I (I)		(11)					
Luminescence	$(cm^2 \times 10^{18})$	1.6													
	Δλ _o (mm)	0.50													
	γ (mm)	670.00		•											

Table XVII (continued)

nergy
H H
+
-
He +
+
1 + 1
위
9
의
Reaction 100 eV He + I ₂ + He + I
the
from
Luminescence from the Reaction 100 eV He + I + He + I + I + Energence

_م ہ	640	:		Transition Assignment	Assignment	٢		ر الم الم	3
(mu)	(mm)	(cm ² x 10 ¹⁸)	×	Lower State + Upper State	- Upper St	ate (nm)		(mm)	e (
			I (II)	7s' 1 _{D2}	+ 5f' 6 ₂		669.557	-0.443	5.89
					+ 5f' 63	699	669.557	-0.443	5.89
				7d ⁵ D ₃ .	+ 5f' 8 ₂	079	670.001	0.001	5.94
673.80	09.0	1.7	He I	3s ³ S,	+ 22d ³ P ₂		673.582	-0.218	11.98
					+ 22d ³ p ^o ₁		673.582	-0.218	.11.98
					+ 22d ³ p ₀		673.582	-0.218	11.98
			1 (1)	6p 4p0	+ nd 26 _{3/2}		674.126	0.326	-2.58
					+ nd 26.1 _{1/2}		673.989	0.189	-2.58
				$(^{1}_{D})6s^{2}_{D_{3/2}} + 6f^{0}_{5/2}$	+ 6f 1 ⁰ _{5/2}		673.393	-0.407	-2.51
			M I (I)	6p[1] ⁰ _{1/2} +	F 8d[1]3/2		674.128	0.328	-2.58
					+ 8d[1] _{1/2}		673.990	0.190	-2.58
				5d[1] _{3/2}	+ 6f[3] ⁰ _{5/2}		673.388	-0.412	-2.51

Table XVII (continued)

Luminescence from the Reaction 100 eV He + I, + He + I + I + Energy

(mm)

	PΑ	(eV)	-2.34	-2.34	-2.34	-2.34	4.57	5.56	4.72	4.73	4.29	4.36	6.29	6.29	4.80	5.92	5.92
7	λ _T - λ ₀	(mm)	0.039	0.030	0.376	0.340	-0.097	-0.276	0.063	-0.440	-0.341	000.0	0.113	0.113	-0.411	0.266	0.266
T T THEIRY	Ļ	(mm)	673.839	673.830	674.176	674.140	673.703	673.524	673.863	673.360	673.459	673.800	673.913	673.913	673.389	674.066	674.066
1	ssignment	Upper State	+ 8f[5] ⁰ _{11/2}	+ 8f[5] ⁰ _{9/2}	+ 8f[4] ⁰ _{9/2}	+ 8f[4] ⁰ / _{7/2}	+ 64' 110°	6d" 21 <mark>0</mark>	. 6d' 13 <mark>0</mark>	+ 6d' 14 ⁰	+ 8p ⁵ p ₂	. 7p' ³ p ₁	. 6d" 51 <mark>0</mark>		. 7p' ¹b ₂		+ 5f' 7 ₃
cence iron the heartion ion by he + 12 + he	Transition Assignment		5d[4] _{9/2} +	1	*			6p" ¹ D ₂ +	4f ⁵ F ₃ +			6d ⁵ D ₂ +	7p' ³ b ₃ +	+	6d 3 _D ⁰ +	7d 5p ₂ +	*
roll cité r		×	M I (I)				(II) I										
raminescence	, ,	(cm ² x 10 ¹⁰)															
	δλ _ο	(mm)															

Table XVII (continued)

λ_ο Δλ_ο (mm) (mm) (599.10 0.50

rgy	λη - λο	(mm)	0.039	0.039	0.039	-0.379	-0.457	-0.397	0.433	0.068	0.147
+ I + Ene	Υ ^τ	(mm)	699.139	699.139	699.139	698.721	698.643	698.703	699.533	699.168	699.247
Luminescence from the Keaction 100 eV He + 1_2 + He + 1 + 1 + Energy	signment	Upper State	$^{3}P_{2}^{0}$	12p ³ p ^o	12p ³ p ₀	12f ³ f ^o	$^{12p}_{1}^{1p_0}_{1}$	nd 29 _{3/2}	7s ² p _{1/2}	9s ² p _{3/2}	nd 40 _{5/2}
음 1년	n Ass	+	+	+	+	+	+	+	+	+	+
Reaction 100 e	Transition Assignment	Lower State + Upper State	3s ³ S ₁					6p 4po	6p 4 _S 0 _{3/2}	6p 2po 5/2	nd 2 _{3/2}
the			H					Ξ			
trom		×	He I					(E) I			
Luminescence	9	(cm x 10 10)	1.4								

ΔH (eV) 11.91 11.91 11.91 .11.91 -2.49

-2.67

-2.67 -2.75 -2.49 -2.46

0.070 0.434 -0.397 -0.117 0.009

698.703

9s[2]_{3/2}
7s[1]_{1/2}
10s[2]_{3/2}
7p"[1]₀
9p[3]_{5/2}

6p[3]₅/₂ 6p[2]₃/₂ 6p[1]₃/₂ 5d[1]₁/₂ 5d[1]₃/₂

699.170

M I (I)

699.534

-2.58

Table XVII (continued)

1	
60	
4	
01	
č	
i iii	
+1	
_	
+	
-1	
4	
-	
He +	
7	
-	
4	
T	
4	2
-17	
. 1	
+1	
-	
ना	
五	
2	
01	
01	
8	
100	
100 eV H	
100	
lo 100	
ion 100	
tion 100	
ction 100	
action 100	
eaction 100	
Reaction 100	
Reaction 100	
e Reaction 100	
he Reaction 100	
the Reaction 100	
the Reaction 100	
m the Reaction 100	
om the Reaction 100	
rom the Reaction 100	
from the Reaction 100	
from the Reaction 100 eV He + I2 + H	
escence from the Reaction 100	

Ą		-2.41	-2.41	-2.41	-2.41	-2.41	5.97	90.9	90.9	4.29		10.14	10.14	10.14
۸- ۳۸	(mm)	-0.257	-0.272	0.281	0.221	0.057	0.109	0.118	0.118	-0.376		0.212	0.216	0.266
ځ	(mm)	698.843	698.828	699.381	699.321	699.157	699.209	699.218	699.218	698.724		706.712	706.716	706.766
signment	Upper State	7f[5] ⁰ 111/2	7f[5] ^o _{9/2}	7f[4] ⁰ _{9/2}	7f[4] ⁰ / _{7/2}	7f[3] ⁰ / _{7/2}	12d ³ D ₃	6d" 45 <mark>0</mark>	6d" 45°	4f' ³ G ₄	٧	3s ³ s ₁	+ 3s ³ S ₁	3s ³ S ₁
n Ass	+	+	¥	+	+	+	+	+	+	+		+	+	+
Transition Assignment	Lower State + Upper State	5d[4] _{9/2}					Sf 3F3	8p 5p ₂		6d ⁵ D ₃	0	2p 2p2	2p ³ p ⁰ ₁	2p 3p0
	×	M I (I)					(11) 1					He I		
	(cm ² x 10 ¹⁸)											1.6		
δ _o	(mm)											0.50		
~°	(mm)											706.50		

Table XVII (continued)

Luminescence from the Reaction 100 eV He + I2 + He + I + I + Energy

γ° (mg)

	λ _T - λ _O	(nm) (eV)		-0.077 11.89	-0.077 11.89	0.464 -2.66	0.049 -3.27	0.051 -3.27	0.295 1.48	0.186 4.73	-0.135 4.73	0.422 4.18	0.362 4.20	0.277 6.06	-0.033 6.06	
	Ļ	(mu)	706.423	706.423	706.423	706.964	706.549	706.551	706.795	706.686	706.365	706.922	706.862	706.777	706.467	
	Transition Assignment	Upper State	$3s^{5}s_{1} + 11p^{5}p_{2}^{0}$	11p ³ p ⁰ ₁	11p 3p0	nd 25.1 _{1/2}	7p 4so 3/2	7p[2] ⁰ _{3/2}	5d" 1 _{D2}	6d" 14 ⁰	6d' 14 ⁰	5f ⁵ F ₂	5f ³ F ₃	6d" 45 ⁰	6d" 44 ⁰	•
	on As:	+	+	+	+	+	+	+	+	+	+	+	+	+	+	
	Transiti	Lower State	3s ⁵ S ₁			6p 4p0	6s 4 _{P1/2}	6s"[0] _{1/2}	6p ⁵ p ₁	7p 5p3	4f 3F4	5d" 3 _D 0	5d" 3F0	8p 5p ₃	4f' 3D3	
٠		×	He I		ŕ	I (I)		M I (I)	(11)							
	,	(cm x 10 10)														
	٥γ٥															

Table XVII (continued)

Luminescence from the Reaction 100 eV He + I2 + He + I + I + Energy

ΔH (eV) 6.06	5.03	5.83	-2.79	2.78	-2.34	-2.79	-2.78	1.48	2.96	6.04	6.10	6.10	6.10
$\lambda_{\rm T}^{-} \lambda_{\rm o}$ (nm) -0.154	0.235	0.216	0.101	-0.099	0.568	0.101	-0.098	-0.092	960.0-	0.323	0.219	0.219	-0.695
λ _T (nm) 706.346	706.735	706.716	712.401	712.201	712.868	712.401	712.202	712.208	712.204	712.623	712.519	712.519	711.605
ent r State 462	3D_2	π 3	6d 4ps/2	nd 22 _{3/2}	3/2	74[3]5/2	74[1]3/2	1 _{D2}	D ₀ .	102	132	13,	13 ₃
ssignme Upper	7p*	9£ 5	+ 6d 4	+ nd 2	np 7°,2					5f' 10 ₂	5f' 13 ₂	+ 5f' 13 ₃	+ 5f' 13 ₃
tion A	+	+	+	+	+	+	+	+	+	+	+	+	+
Transition Assignment Lower State + Upper State $^7\mathrm{P}^1$ $^3\mathrm{D}_1$ + $^6\mathrm{d}^{11}$ $^4\mathrm{G}_2^0$	5d" 1po	7d ⁵ p ₂ ^o	6p 4po 5/2	6p 4so	nd 3 _{5/2}	6p[2] ⁰ _{5/2}	6p[2] ⁰ 3/2	6p ⁵ P ₂	6p' 3F2	7d ³ D ₁	5g 5G3		5g 3G
× × (II) 1		Ž/	1 (1)			M I (I)		I (II).					
° (cm ² × 10 ¹⁸)			4.4										
Δλ _o (mm)			0.50										
(mm)			712.30										

Table XVII (continued)

Luminescence from the Reaction 100 eV He + I2 + He + I + I + Energy

ΑA	(eV)	-2.80	-2.34	-2.34	-2.80	-2.34	-2.34	-2.34	-2.34	-2.34	2.95	1.33	5.38	5.81
٨- ١٠	(mm)	0.003	-0.309	-0.114	0.002	-0.114	-0.491	-0.104	-0.143	-0.208	0.386	-0.305	-0.473	0.356
Ļ	(mrl)	714.403	714.091	714.286	714.402	714.286	713.909	714.296	714.257	714.192	714.786	714.095	713.927	714.756
Ignment	Jpper State	+ 6d ⁴ D _{7/2}	$+ \text{ np } 7_{3/2}^{0}$	np 7°,	74[3] _{7/2}	7p'[1] ^o 1/2	8f[5] ⁰ _{9/2}	8f[4] ^o 2	8f[4] ^o 7/2	8f[3] ^o 5/2	6d ³ D ₃	6p' ³ D ₂	9d ³ D ₂	+ 12s ³ s ₁
n Assi	+	+	+	+	+	+	+	+	+	+	+	+	+	+
Transition Assignment	Lower State + Upper State	6p 4p0 5/2	nd 4 _{3/2}	nd 4.1 _{3/2}	6p[2] ⁰ _{5/2}	54[0]1/2	5d[4] _{7/2}				6p' 3F2	5d' 3 _D °	6p" 1p1	6p" 180
	×	I (I)			M I (I)					•	I (II)			
σ σ 18	(cm x 10)	5.6												
٥٨,	(mu	0.50												
, ۲۰		714.40												

Table XVII (continued)

Luminescence from the Reaction 100 ev He + I + He + I + I + Energy

λ_o (nm) 716.60

	•		•					
° [2 .,18,	•	Iransition Assignment	n AS	Signment	Ļ	γ _T - γ ₀	Н
	(cm × 10)	×	Lower State	+	Lower State + Upper State	(mm)	(E)	(e _V)
09.0.	2.5	He I	3s ³ S ₁	÷	$10p \frac{3p_0^0}{2}$	716.258	-0.342	11.87
				+	10p 3p0	716.258	-0.342	11.87
				+	10p 3p0	716.258	-0.342	11.87
	•	I (I)	6p 4so 53/2	+	6d ⁴ P _{5/2}	716.673	0.073	-2.79
		M I (I)	6p[2] ^o 3/2	+	74[3] _{5/2}	716.674	0.074	-2.79
			54[0]1/2	+	8f[2] ⁰ _{3/2}	716.758	0.158	-2.34
				+	8f[1] ⁰ ,2	716.547	-0.053	-2.34
		I (II)	6p' 3F ₂	+	6d 3p ₂	716.876	0.276	2.95
			5d" 3F0	ŧ	Sf ⁵ F ₄	717.083	0.483	4.17
			Sf 3F4	+	$^{3}D_{3}^{0}$	716.312	-0.288	5.97
			6d ⁵ D ₃	+	Sf ³ F ₂	716.975	0.375	4.25
			8p 5p ₂	+	6d" 42 ⁰	716.400	-0.200	6.02
			4f' 3F ₂	+	6d" 47°	716.364	-0.236	6.08
				+	6d" 47°	716.364	-0.236	6.08

Table XVII (continued)

	(eV)	6.29	4.31	90.9		-2.80	-2.80	-2.51	-2.80	-2.80	0.02	2.91	4.65	4.24	4.25
	λ _T - λ _o (mm)	-0.400	-0.558	-0.173		0.065	0.151	-0.235	0.065	0.151	-0.400	-0.489	0.460	-0.173	-0.246
+ Energy	بر (mg)	716.200	716.042	716.427		719.365	719.451	719.065	719.365	719.451	718.900	718.811	719.760	719.127	719.054
Luminescence from the Reaction 100 eV He + I ₂ + He + I + I + Energy	Transition Assignment Lower State + Upper State	+ 6d" 510	$+$ 7p' 3D_1	+ 6d" 462		+	+ nd 21.2 _{1/2}	+ 6f 1 _{5/2}	+ 7s'[1] _{3/2}	+	+ 6p ³ p ₁	+ 7p ⁵ p ₁	+	+ 5f ³ F ₄	+ 5f ³ F ₂ .
tion 100	Transi Lower Sta	4f' 3p0	6d 5p0	8p ³ p ₁	4.0	6p 53/2		nd 1 _{3/2}	6p[2] ⁰ 3/2	6p[2] ⁰ _{3/2}	sd ⁵ D ₁	5d' 1S0	7p 5p2	6d 5p ⁰ ₃	6d 5p ^o ₂
rom the Read	×	(II) I				(E) I			M I (I)		I (II)				
Luminescence f	$(cm^2 \times 10^{18})$	•				1.8									
	φ, (mm.)					09.0									
	, (mr)					719.30									

Table XVII (continued)

Luminescence from the Reaction 100 eV He + I + He + I + I + Energy

2	(e)	6.02	6.10	60.9	60.9	60.9	5.76	5.76	-2.55	-2.36	-2.36	-2.36	-2.36
% - }	(ma)	-0.195	-0.259	0.465	0.465	-0.260	-0.153	-0.153	-0.229	0.200	0.400	-0.168	-0.032
ţ	(mm)	719.105	719.041	719.765	719.765	719.040	719.147	719.147	723.571	724.000	724.200	723.632	723.832
gnment	pper State	6d" 42 ⁰	11g 5G6	6d" 48 <mark>0</mark>	6d" 48 <mark>2</mark>	13d ³ D ₃	5f' 3 ₂	5f' 3 ₃ .	nd 28.1 _{5/2}	7p 2p _{3/2}	7p 2p _{3/2}	7p 2po 3/2	7p 2po 7p 3/2
Assign	5 +	4	+	4	9	+	+ 5	+	+	+	+ 1	+	+ 1
Transition Assignment	Lower State + Upper State	4f' 3F3	4f' 3Hs	8p 3p ₂			$7s^{1}D_{2}^{0}$		6p 4po 5/2	nd 43/2	nd 4.13/2	nd 43/2	nd 4.13/2
	×	I (III)							I (E)				
b	(nm) $(cm^2 \times 10^{18})$				•				11.5				
84	(mm)								0.50				
٧°	(mm)								723.80				

Table XVII (continued)

y (mg)

	¥		-2.68	-2.68	-2.55	-2.36	-2.36	-2.68	-2.68	-2.68	-2.68	-2.68	-2.68	-2.68	4.65	5.35
	٠٠- ١٠	(mm)	0.083	-0.417	-0.221	0.030	0.397	0.077	-0.102	-0.479	0.185	-0.420	-0.193	0.081	0.007	-0.020
+ Energy	ţ	. (M	723.883	723.383	723.579	723.830	724.197	723.877	723.698	723.321	723.985	723.380	723.607	723.881	723.807	723.780
I ₂ + He + I + I	ignment	Upper State	5f 1 ^o _{3/2}	5f 3 ⁰ _{5/2}	8d[2] _{5/2}	7p'[2] ^o 3/2	7p'[1] ^o _{3/2}	Sf[4] ⁰ _{9/2}	Sf[4] ⁰ / _{7/2}	5f[2] ⁰ _{5/2}	5f[4] ⁰ 7/2	sf[3] ⁰ _{5/2}	sf[2] ⁰ 5/2	Sf[2] ⁰ _{3/2}	6d' 12 <mark>°</mark>	8s' ³ 0.
tion 100 eV He +	Transition Assignment	Lower State + Upper State	$(^{1}D)6s^{2}D_{5/2}$ $^{+}$	+	M I (I) $6p[1]_{3/2}^{0}$ +	54[0]1/2 +	•	54[3]7/2 +	•	+	5d[3] _{5/2} +	•	•	•	6p" ³ p ₁ +	+
Luminescence from the Reaction 100 eV He + I_2 + He + I + I + Energy		(cm ² x 10 ⁴) X	E 1		M I (I)										(II) I	
	δλο	(mm)														

Table XVII (continued)

	ΑH	(eV)	00.9	9.00	00.9	90.9	90.9	6.16	6.04	6.04	-2.77	-2.56	-2.77	-2.56
	γ - γ ₀	(mm)	-0.335	-0.335	-0.335	-0.162	-0.162	-0.155	0.283	0.283	0.008	0.368	0.008	0.371
I + Energy	Ļ	(mm)	723.465	723.465	723.465	723.638	723.638	723.645	724.083	724.083	740.408	740.768	740.408	740.771
from the Reaction 100 eV Het + I2 + He + I + I + Energy	ignment	Upper State	6d" 410	6d" 41 ⁰	6d" 41 ⁰	6d" 45 <mark>0</mark>	6d" 45 ⁰	$14d \frac{3}{5} D_{3}^{0}$	6d" 43°	6d" 43 <mark>0</mark>	nd 23_,,	9p ² D _{5/2}	74[4]7/2	9p[1] ^o ,2
+ +: 	n Ass	+	+	+	+	+	+	+	+	+	+	+	+	+
ction 100 eV	Transition Assignment	Lower State + Upper State	8p ⁵ p ₂			4f' 3F2		7p' 3p ₂	8p ³ p ₁		6p 2p,	nd 1 _{3/2}	6p[3] ^o 5/2	54[1]1/2
om the Rea		×	(II) I								. (E) I		M I (I)	
Luminescence fr	, d	(cm x 10 ")							•		8.6			
	δλ _ο	(mg									0.50			
	ر ° ((mu)									740.40			

Table XVII (continued)

σ Transition Assignment $\lambda_{\rm T}$ (cm ² x 10 ¹⁸) X Lower State + Upper State (nm)
(II) I ·
4f' ³ p ₀
7d S _D ^o ₃
7s' ³ D ₃
8.1 I (I) 6p 4p ⁰ _{7/2}
6s ⁴ P _{3/2}
nd 2 _{3/2}

Table XVII (continued)

Luminescence from the Reaction 100 eV He + I + He + I + I + Energy

~° (E)

ΔH (eV) -2.68	-2.68	268	-2.77	-3.24	-2.68	-2.68	-2.68	-2.51	-2.51	-2.51	-2.41	-2.41
λ _T - λ _o (nm) 0.450	0.164	-0.076	0.408	0.261	-0.076	0.163	0.450	-0.146	-0.172	0.397	0.231	-0.420
λ _T (nm) 741.850	741.564	741.324	741.808	741.661	741.324	741.563	741.850	741.254	741.228	741.797	741.631	740.980
Assignment - Upper State + 5f 13/2	$+ 5f 2_{1/2}^{0}$	+ 5f 35/2	+ 7d[4]7/2	$^{+}$ $^{7p[1]}_{1/2}^{\circ}$	+ 5f[3] ⁵ /2	+ 5f[2] ⁵ /2	$+ 5f[2]_{3/2}^{0}$	+ 6f[5] _{11/2}	+ 6f[5] ⁹ /2	+ 6f[3]7/2	+ 7f[2] ⁰ 3/2	+ 7f[1] ⁰ _{3/2}
Transition Assignment Lower State + Upper State $\binom{1}{0}$ 6s $\binom{2}{0}_{3/2}$ + 5f $\binom{0}{3/2}$		0[2]	op[5]7/2		5d[1] _{3/2}			5d[4] _{9/2}			$(^{1}D_{2})6s[2]_{3/2}$	
X E I			(I) W									
Δλ _ο σ (mm) (cm ² x 10 ¹⁸) x		•										
(mm)												

Table XVII (continued)

Luminescence from the Reaction 100 eV He + I + He + I + I + Energy

Ş	(e)	5.86	4.25	6.04	-2.78	2.78	-2.78	-2.78	5.38	5.95	5.95	4.30	5.76
بر - بر	(mg)	0.480	0.317	0.095	0.021	0.104	0.104	0.022	-0.025	-0.229	0.142	-0.221	-0.481
ţ	(mar)	741.880	741.717	741.495	747.021	747.104	747.104	747.022	746.975	746.771	747.142	746.779	746.519
ignment	Upper State	11d $^{3}_{D_{3}^{0}}$	+ 5f ³ F ₂	5f' 10 ₃	nd 22 _{3/2}	6d 4F9/2	74[4]9/2	74[1]3/2	9d ³ D ₂	6d" 40°	6d" 40 <mark>0</mark>	4f' ³ D ₃	+ 5f' 3 ₂
n Ass	+	+	+	+	+	+	+	+	+	+	+	+	+
Transition Assignment	Lower State + Upper State	sf ⁵ F ₂	6d ⁵ D ₁	6d' 8 ⁰	6p 2p _{5/2}	6p 4p ^o _{7/2}	6p[3] ^o ,	6p[3] ⁰ _{5/2}	6p" 1 _{D2}	4f' 3G4	4f' 3F3	5d" 3F0	74 ⁵ 0 ₁
	× .	(II)		•	I (I)		M I (I)		I (II)				
b ((nm) (cm ² x 10 ¹⁸) x				5.1								
هم م	(mm)				0.50								
%	(mm)				747.00								

Table XVII (continued)

	(eV)	5.89	5.89	5.89	5.64	5.64	-2.80	-3.28	-2.80	-3.28	5.36	4.57	4.73	60.9	60.9
	λ _T - λ _o (nm)	-0.027	-0.027	-0.027	-0.036	0.165	0.027	0.272	0.027	0.273	0.100	0.134	0.263	0.047	-0.024
I + Energy	, T (mm)	746.973	746.973	746.973	746.964	747.165	755.627	755.872	755.627	755.873	755.700	755.734	755.863	755.647	755.576
Luminescence from the Reaction 100 eV He + I ₂ + He + I + I + Energy	ignment Upper State	5f' 6 ₂	5f' 6 ₃	5f' 6 ₄	8f ⁵ F ₄	8f ⁵ F ₃	6d ⁴ D _{7/2}	7p 4so	74[3]7/2	7p[2] ^o _{3/2}	8s' 30°	6d' 10 ⁰	6d' 14°	6d" 48 ⁰	13d ³ D ₃
He+	n Ass +	+	+	+	+	+	+	+	+	+	+	+	+	+	+
action 100 eV	Transition Assignment Lower State + Upper Si	7d ³ D ₃			7s' 300		6p 4 _D 0,2	6s 4P _{3/2}	6p[3] ⁰ 7/2	6s[1] _{3/2}	6p" ¹ D ₂	7p 5p ₂	7p 3p ₂	7p' 3p ₃	7p' 3p2
from the Re	×	(II)		٠			(E) I		M I (I)		I (II)				
Luminescence	$(cm^2 \times 10^{18})$						4.6								
	Δλ _o (mm)						0.50								
	γ° (mm)						755.60								

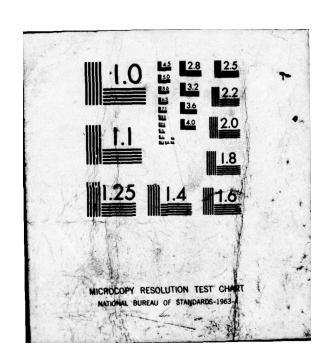


Table XVII (continued)

~
2
21
21
삪
F
ш!
+
1
H
+1
+
-
2
-
1
C
Inescence from the Reaction 100 eV He + I2 + He + I + I + Energy
+1
+ 1
0
7
~1
7
41
91
0
7
51
0
اند
10
~
0
2
H
-
2
4
41
E
0
H
441
01
Ö
2
3
2
21
9
01
2
1
81
31
1

	44,	ь		Transition Assignment	Assign	ment	ل	, , ,	
(mu)	(mm)	(nm) (cm ² x 10 ¹⁸)	×	Lower State + Upper State	ddn +	er State	(F)	° (E	(ev)
767.20	09.0	1.8	I (I)	6p 4po	+ 7s 4p3/2	4 _{P3/2}	767.212	0.012	-2.80
					pu +	nd 21.2 _{1/2}	767.310	0.110	-2.80
			M I (I)	M I (I) $6p[1]_{1/2}^{0}$	+ 7s'	7s'[1] _{3/2}	767.213	0.013	-2.80
					p/ +	74[1]1/2	767.311	0.111	-2.80
					+ 10f	10f[4] ^o / _{7/2}	767.124	-0.076	-2.27
			1 (11)		+ 6p'	$^{3}_{\mathrm{F_{3}}}$	766.779	-0.421	1.36
				6p" ³ D ₁	.p9 +	7 <mark>0</mark>	766.809	-0.391	4.35
					. p9 +	70	766.809	-0.391	4.35
				5d" 1 _{D2}	+ 7p 3p ₂	3 _{P2} .	960.792	-0.104	3.09
770.10	0.50	2.2	13	6p 4po 3/2	₽ +	30,2	770.545	0.445	-2.66
				$(^{1}_{D})6s^{2}_{5/2} + ^{4}_{P}^{0}_{7/2}$	+ 8p	4 _D 0,7/2	770.234	0.134	-2.79
			M I (I)	54[3]7/2	- 1 +	2)6p[3]0,2	906.692	-0.194	-2.79
				5d[3] _{5/2}	-	2)6p[3]0	770.230	0.130	-2.79

Table XVII (continued)

	₩ (%)	-2.46	1.48	2.18	2.91	4.18	6.02	90.9	90.9	5.76	5.76	-2.96	-2.51	-2.51
	λ _T - λ _o (mm)	-0.223	-0.292	0.346	-0.238	0.435	-0.196	-0.021	-0.487	0.180	0.180	0.649	0.263	-0.446
I + Energy	۲ [,] (ست)	769.877	769.808	770.446	769.862	770.535	769.904	770.079	769.613	770.280	770.280	790.549	790.163	789.454
from the Reaction 100 eV He + I2 + He + I + I + Energy	signment Upper State	7p"[1] ⁰ _{1/2}	5d' 1F0	6p' 1 _{D2}	7p ⁵ p ₁	Sf ⁵ F ₂	6d" 42 ⁰	6d" 45 ⁰	6d" 462	5f' 3 ₂	Sf' 3 ₃	8s ² P _{3/2}	6£ 1°,2	6f 3°,2
n 100 eV He +	Transition Assignment Lower State + Upper State	5d[0] _{1/2} +	+	+	6s" 1po +	•	4f' 3 _{D2} +	7p' 3 _{D3} +	•	7d 3p ₂ +	•	6p 4po +	nd 23/2 +	+
om the Reactio	X	M I (I) Sd	1 (11) бр	s9	s9 .	P9	4£	7p	4 7	P7		I (I) 6p	P	
Luminescence fr	(cm ² × 10 ¹⁸)				•							2.0		
31	(m) 64°											0.70		
	, (mu)											789.90		

-2.51

789.295 -0.605

Table XVII (continued)

₹°

5.88

0.170

790.070

-0.114

789.786

Table XVII (continued)

Luminescence from the Reaction 100 eV He + I2 + He + I + I + Energy

~°	ชื			Transition Assignment	n As	signment	Ţ	ر الم الم	¥
(mu)		$(cm^2 \times 10^{18})$	×	Lower State	+	Upper State	. (mg	(mm)	§
			I (II)	5d" 1po	+	4f' ^l P ₁	789.247	-0.653	4.85
				7p' ³ p ₁	+	7p' ³ p ₁ + 9g ⁵ G ₂	790.593	0.693	5.88
797.20	09.0	. 3.1	. He I	3s ¹ S ₀	+	+ 11p 1p0	797.381	0.181	11.89
			1 (1)	6p 4p0 6p 5/2	+	8s ⁴ P _{5/2}	797.167	-0.033	-2.98
				nd 1 _{3/2}	+	+ 5f 1 ⁰ _{3/2}	797.666	0.466	2.68
					+	+ 5f 20,	797.335	0.135	-2.68
					+	+ 5f 3 ⁰ _{5/2}	797.059	-0.141	-2.68
			M I (I)	6p[2] ⁰ _{5/2}	+	+ 8s[2] _{5/2}	797.167	-0.033	-2.98
				54[1]1/2	+	+ 5f[2] ⁰ _{3/2}	797.666	0.466	-2.68
			(II) I	Sf ^S F ₁	+	+ 6d", 32°	796.752	-0.448	5.74
				74 ⁵ D ₄	+	+ 8f ³ F ₃	796.693	-0.507	5.65

Table XVII (continued)

Luminescence from the Reaction 100 eV He + I + He + I + I + Energy

ช	b		Transition Assignment	Ass	sionment			
) [i	nm) (cm ² x 10 ¹⁸)	×	Lower State + Upper State	+	Upper State	r [€ ¥
09.0	1.9	He I	3p 3po	+	21d ³ D ₃	800.151	-0.249	11.98
				+	21d ³ D ₂	800.151	-0.249	11.98
		•		+	21d ³ D ₁	800.151	-0.249	11.98
			3p 3p0	+	21d ³ D ₂	800.152	-0.248	11.98
				+	21d ³ D ₁	800.152	-0.248	11.98
			3p 3p0	٠	21d 3D1	800.169	-0.231	11.98
		1 (1)	6s 4p1/2	+	6p 4p ₀	800.582	0.182	-3.48
			(¹ p)6s ² p _{3/2}	+	8p ² p _{5/2}	800.022	-0.378	-2.80
		M I (I)	6s"[0] _{1/2}	+	6p'[1]0,	800.582	0.182	-3.48
			5d[1] _{3/2}	+	8p[3] ^o _{5/2}	800.021	-0.379	-2.80
		(II) I	4f' 3D3	+	6d" 37 ⁰	800.816	0.416	5.85
			7p' 3p ₂	+	6d" 41 <mark>0</mark>	800.411	0.011	6.00
				+	6d" 41 ⁰	800.411	0.011	6.00
	•			+	6d" 41°	800.411	0.011	6.00

~° (E

Table XVII (continued)

Luminescence from the Reaction 100 eV He + I2 + He + I + I + Energy

λ _T - λ _o ΔH (m) (eV) 0.211 5.88	0.064 5.64	0.042 '-2.81 -0.223 -2.34	0.021 -2.98	-0.151 4.19 -0.206 4.29	0.121 5.85	-0.189 5.93 -0.369 5.95	
λ _T λ _T (rum) (rum) (rum) (σ. 800.611 0. 800.233 -0.	800.464 0.	802.542 0. 802.277 -0.	802.521 0. 802.546 0.	802.294 -0.	802.621 0.	802.311 -0.	
signment Upper State 6d" 381 8f ⁵ F	+ 8f ⁵ F ₃ + 8s ⁴ P _{5/2}	+ 8p 4s ⁰ / _{3/2} + np 7 ⁰ / _{3/2}	+ 8s[2] _{5/2} + 8p[2] _{3/2}	5f ⁵ F ₁ 8p ^{\$p} ,	6d" 37 ⁰	+ 6d" 394 + 6d" 40°	6d" 50 ⁰
Transition Assignment Lower State + Upper State 8p ³ p ₁ + 6d" 38 ⁰ 7d ⁵ p ₃ + 8f ⁵ F ₄	6p ⁴ S _{3/2} +	$(^{1}D)6s^{2}D_{3/2} + ^{4}S_{3/2}^{0}$ $nd^{5}S_{5/2} + ^{0}D^{7}O_{3/2}^{0}$	+ +		+		4f' ³ _G +
* E	. E 1		M I (E)	(II) 1			
(cm ² × 10 ¹⁸)	1.7						
4 E	0.50						
~°Œ	802.50						

Table XVII (continued)

Luminescence from the Reaction 100 eV He + I2 + He + I + I + Energy

, م	% °	P 6		Transition Assignment	ASS 1	ignment	Ļ	ئر- بر	#
		(cm × 10 - ')	×	Lower State + Upper State	+	Upper State	(mu)	(mm)	(e)
	0.50	5.9	1 (3)		+	6p 4p0	804.592	0.092	-4.27
				6s ² P _{1/2}	+	7p 4pg/2	804.204	-0.296	-3.20
					+	2^{+} 7^{p} 2^{p_0}	804.840	0.340	-2.81
			M I (I)	6s[2] _{\$/2}	+	6p[1] ⁰ _{3/2}	804.594	0.094	-4.27
				6s'[1] _{1/2}	+	7p[1] ⁰ _{3/2}	804.204	-0.296	-3.20
				Sd[1] _{3/2}	+	8p[1]0,	804.830	0.330	-2.81
			I (II)	5d" 1p0	+	7p' ³ P ₀	804.006	-0.494	4.82
				7s' 10°	+	5f' 1 ₂	804.934	0.434	5.58
					+	5f' 1 ₃	804.934	0.434	5.58
				7d 5p ₀	+	Sf' 2 ₂	804.760	0.260	5.64
				7d ⁵ D ₄	+	8f ⁵ F ₄	804.138	-0.362	5.64
					+	8£ ⁵ F ₃	804.371	-0.129	5.64

Table XVII (continued)

Luminescence from the Reaction 100 eV He + I₂ + He + I + I + Energy

λ_ο (nm) 816.90

4A _o	•	<i>r</i>	Transition Assignment	Assignment	Ļ	λ λ.	
(E)	(nm) (cm ² x 10 ¹⁸)	*	Lower State + Upper State	. Upper State	(E)		§ §
0.50	2.5	He I		+ 15s ³ S ₁	817.096	0.196	11.94
			3p 3po +	+ 15s ³ S ₁	817.097	0.197	11.94
		·	3p 3p0 +	+ 15s ³ S ₁	817.115	0.215	11.94
		1 (3)	$(^{1}_{D})6s^{2}_{3/2}$		817.158	0.258	-2.84
			nd 2 _{3/2}	. 9p ² D _{5/2}	816.448	-0.452	-2.56
		M I (I)	5d[1] _{3/2} +		817.164	0.264	-2.84
			$(^{1}D_{2})6s[2]_{3/2}^{+}$		816.458	-0.442	-2.56
		(II) I	6p' 3 _{D1} +		817.202	0.302	2.58
			5d' 3Fo +		817.234	0.334	1.33
			6p" 1p1 +	. 7s" ³ p ₀	816.846	-0.054	5.16
			7p' 3p ₁ +	. 6d" 38°	817.056	0.156	5.88
				+ 6d" 37 ⁰	816.462	-0.438	5.85
			5g ³ G ₄ +	. 5£' 5 ₃	817.349	0.449	5.87

Table XVII (continued)

Luminescence from the Reaction 100 eV He + I2 + He + I + I + Energy

~	4	b		Trancition Accimment	Ace	e i ammen t			
(mu)	e (mu	(nm) (cm ² x 10 ¹⁸)	×	Lower State + Upper State	+	Upper State	£.[j	رالة) (الق)	€ ¥
824.10	0.50	8.4	1 (3)	nd 3 _{5/2}	+	9p 4s _{3/2}	824.209	0.109	-2.57
			M I (I)	5d[4] _{9/2}	+	5f[5] ⁰ _{9/2}	824.189	0.089	-2.68
					+	Sf[5]0	824.231	0.131	-2.68
			(II) I	5d' 1F0	+	+ 4f 3F ₂	824.292	0.192	2.98
				7p ³ p ₁	+	+ 6d' 1100 +	824.527	0.427	4.57
				Sf 3F4	+	6d" 33 ⁹	823.720	-0.380	5.75
				5f 3F2	+	6d" 33.50	823.849	-0.251	5.75
				4f' 3D3	+	6d" 36 ⁰	823.846	-0.254	5.81
				4f' 3F2	+	6d" 37 ⁰	824.436	0.336	5.83
839.50	0.50	3.8	He I		+	+ 19p 1p0	839.943	0.443	11.97
					+	+ 19p ¹ p ^o ₁	839.947	0.447	11.97
			1 (3)		+	nd 21 _{5/2}	839.400	-0.100	-3.05
					+	+ 8s ² p _{3/2}	839.540	0.040	-2.96

839.564

6s 4p_{1/2} + 6p 2p_{3/2}

Table XVII (continued)

		Luminescence	from the Re	action 100 eV	He+	cence from the Reaction 100 eV He + I2 + He + I + I + Energy	I + Energy	~1	
۳۰		•		Transition Assignment	on As	signment	ţ	۸- ۴	7
(mm)	E	(cm ² x 10 ¹⁸)	×	Lower State	+	Lower State + Upper State	(ma)	(mu)	6
			M I (I)	6p[3] ^o 5/2	+	8s[2] _{3/2}	839.538	0.038	-2.96
				6p[2] ⁰ _{3/2}	+	6d[2] _{5/2}	839.402	-0.098	-3.05
			•	6s"[0] _{1/2}	+	6p'[2] ^o _{3/2}	839.567	0.067	-3.55
			(H)	4f ⁵ F ₄	+	5g 3G4	839.521	0.021	4.36
				7p 3p ₂	+	6d' 10 ⁰	839.466	-0.034	4.57
				4f' 3D3	+	6d" 35 ⁰	839.612	0.112	5.78
					+	6d" 35°	839.612	0.112	5.78
				7p' 3 _{D3}	+	6d" 39 ⁰	839.925	0.425	5.93
				74 5 _D °	+	Sf' 1 ₂	839.383	-0.117	5.58
				5g 3G	+	9f ⁵ F ₄	839.055	-0.445	5.83
	•			5g 5 _{G3} .	+	9£ ⁵ F ₃	839.906	0.406	5.83
848.70	0.50	2.5	He I	3p 3p2	+	11s ³ S ₁ .	848.303	-0.397	11.89
				3p 3p0	+	11s ³ S ₁	848.305	-0.395	11.89
		a		3p 3p0	+	11s ³ S ₁	848.324	-0.376	. 11.89

Table XVII (continued)

o (me

4	b		Transition Assignment	n As	signment	٢	Y - 47	7
(mg)	$(cm^2 \times 10^{18}) \times$	*	Lower State	+	Lower State + Upper State	(mu)		(§)
		He I	3d 3 _D 0	+		849.109	0.409	11.95
			3d 3 _{D2}	+	16p 3po	849.110	0.410	11.95
		·		+	16p ³ p ^o ₁	849.110	0.410	11.95
				+	16p ¹ p0	848.812	0.112	11.95
			3d ³ D ₁	+	16p ³ p ₂	849,113	0.413	11.95
				+	16p ³ p ₀	849.113	0.413	11.95
				+	16p ³ p ₀	849,113	0.413	11.95
				+	16p ¹ p ₀	848.815	0.115	11.95
			3d ¹ D ₂	+	16p 1p0	849.058	0.358	11.95
		I (I)	6p 4p,	+	8s ⁴ P _{5/2}	848.842	0.142	-2.98
		M I (I)		+	8s[2] _{5/2}	848.842	0.142	-2.98
		1 (11)	4£ ⁵ F ₂	+	6d' 70	848.997	0.297	4.35
				+	. 62 .P9	848.997	0.297	4.35

Table XVII (continued)

4	44,	b		Transition Assignment	n Assign	ment		A - A	4
(mn)) (E	$(cm^2 \times 10^{18})$	×	Lower State + Upper State	4	er State	(mg)	(mm)	(e)
			I (II)	sf ^S F ₁	+ 6d" 290	" 29°	848.992	0.292	5.65
				8p 5p ₂	+ 6d" 33 ⁰	" 33 ⁰	848.907	0.207	5.75
			•	4f' 3F2	+ 6d" 36 ⁹	" 362	848.865	0.165	5.81
				7p' ³ D ₁	+ 6d" 34 ⁰	" 34°	849.018	0.318	5.77
OTOTAL.	= 1592.4	$\sigma_{\text{TOTAL}} = 1592.4 \times 10^{-18} \text{ cm}^2$. AIIA _D	$\sigma_{\rm VIV} \ _{\rm TOTAL} = 1437.3 \times 10^{-18} \ _{\rm cm}^2$	× 10-18		σ _{VISIBLE} TOTAL = 155.1 × 10 ⁻¹⁸ cm ²	AL = 155.1	c 10 ⁻¹⁸ cm ²

Kenneth Eugene Siegenthaler, son of Paul Alfred and Ruth Elizabeth Siegenthaler, was born 10 March 1939 in Huron, South Dakota. In 1957 he was appointed to the United States Military Academy where in 1961 he was graduated and was commissioned in the United States Air Force. He received a Bachelor of Science Degree in Physics from the University of Utah in 1962 and was elected to Sigma Pi Sigma. was graduated from aircraft navigator training. From 1963 to 1971 he flew over 6000 hours as a Military Airlift Command Navigator in C-124 and C-133 aircraft. He entered the Air Force Institute of Technology in 1971, where he was elected to Tau Beta Pi. In 1973 he was graduated from the Air Force Institute of Technology Resident School and awarded the Master of Science Degree in Engineering Physics. He then entered the AFIT Resident School Doctoral Program. Following completion of the academic portion of this program in 1974, he was assigned to the Aerospace Research Laboratories Gaseous Excitation and Ionization Processes Group as a laser research engineer. In 1975 with the disestablishment of the Aerospace Research Laboratories, he was assigned to the Air Force Materials Laboratory as a laser development engineer.

Permanent address: 1421 East Pecan Street

Gainesville, Texas 76240

REPORT DOCUMENTATION PAGE	READ INSTRUCTIONS BEFORE COMPLETING FORM
DS/PH/76-2	. 3. RECIPIENT'S CATALOG NUMBER
4. TITLE (and Subtitle) EMISSION CROSS-SECTION MEASUREMENTS OF LOW ENERGY He IONS WITH C12, Br2, I2 REACTIONS	5. Type of Report & PERIOD COVERED Dissertation 6. Performing org. Report Number
7. AUTHOR(*) Kenneth E. Siegenthaler Major USAF	8. CONTRACT OR GRANT NUMBER(*)
PERFORMING ORGANIZATION NAME AND ADDRESS Air Force Institute of Technology (AU) Wright-Patterson AFB OH 45433	10. PROGRAM ELEMENT, PROJECT, TASK AREA & WORK UNIT NUMBERS
11. CONTROLLING OFFICE NAME AND ADDRESS (12. REPORT DATE September 1976
	43. NUMBER OF PAGES 285
14. MONITORING AGENCY NAME & ADDRESS(il different from Controlling Office)	15. SECURITY CLASS. (of this report) Unclassified 15a. DECLASSIFICATION/DOWNGRADING SCHEDULE

Approved for public release; distribution unlimited.

17. DISTRIBUTION STATEMENT (of the abstract entered in Block 20, if different from Report)

18. SUPPLEMENTARY NOTES

Approved for public release IAW AFR 190-17.

JERAL F. GUESS, Capt, USAF

Director of Information Air Force Institute of Tech.

19. KEY WORDS (Continue on reverse side if necessary and identify by block number)

Charge Transfer, Charge Exchange, Atomic Spectroscopy, Ultraviolet Spectroscopy, Low Energy Ion-Neutral Collisions, Low Energy Ion Beam Experiment, Helium Ion/Halogen Reactions, Helium Ion/Chlorine Molecule Collisions, Helium Ion/Bromine Molecule Collisions, (continued on reverse)

20. ABSTRACT (Continue on reverse side if necessary and identify by block number)

The cross sections for production of emission lines in the 60 nm to 870 nm region were measured for the collision of 100 eV He^+ ions with Cl_2 , Br_2 , and I_2 . These cross section measurements were made with an ion beam apparatus. Only emissions from

transitions from excited electronic states with lifetimes shorter than a usec were measured. The dependence of the cross sections on the kinetic energy of the He ions between 2 to 170 eV was determined by use of the more intense emission lines. The total cross section obtained for emissions between 90 nm and 870 nm for chlorine is 5.0A; of this, 3.8 A² is for emissions in the VUV region. Emissions from excited neutral chlorine atoms account for at least 85% of the total cross section. Of the cross section for production of emission from excited neutral chlorine atoms, 80% is caused by direct excitation with the remainder resulting from cascading. The total cross section obtained for emissions between 80 nm and 870 nm for bromine is 14.9 A²; of this, 11.9 A² is for emissions in the VUV region. Emissions from excited neutral bromine atoms account for at least 85% of the total cross section. Of the cross section for production of emission from excited neutral bromine atoms, 75% is caused by direct excitation with the remainder resulting from cascading. The total cross section obtained for emissions between 100 nm and 870 nm for iodine is 15.9 A²; of this, 14.4 A² is for emissions in the VUV region. The proportion of the total cross section for the production of emissions from singly-ionized iodine atoms is much larger than for either the chlorine or bromine reactions.

Item 19 Continued: Helium Ion/Iodine Molecule Collisions, Emission Cross Sections, Chlorine, Bromine, Iodine, VUV Emissions, Visible Emissions, Near IR Emissions, Halogens